Integro-differential models for evolutionary dynamics of populations in time-heterogeneous environments

Susely Figueroa Iglesias

THÈSE

En vue de l'obtention du

DOCTORAT DE L'UNIVERSITÉ DE TOULOUSE

Délivré par : *l'Université Toulouse 3 Paul Sabatier (UT3 Paul Sabatier)*

Présentée et soutenue le *30/09/2019* **par :**

Susely Figueroa Iglesias

Integro-differential models for evolutionary dynamics of populations in time-heterogeneous environments

---

JURY

Jean-Michel ROQUEJOFFRE	Université Paul Sabatier	Examinateur
Delphine SALORT	Sorbonne Université	Examinatrice
Stéphane MISCHLER	Université Paris Dauphine	Examinateur
Grégoire NADIN	CNRS, Sorbonne Université	Rapporteur
Matthieu ALFARO	Université de Montpellier	Rapporteur
Sepideh MIRRAHIMI	CNRS, Université Paul Sabatier	Directrice de Thèse

---

École doctorale et spécialité :
MITT : Domaine Mathématiques : Mathématiques appliquées
Unité de Recherche :
Institut de Mathématiques de Toulouse
Directeur de Thèse :
Sepideh MIRRAHIMI
Rapporteurs :
Grégoire NADIN et *Matthieu ALFARO*

A mi esposo Ale...
el amor que podemos ver reflejado
en nuestras vidas a través de otras personas
es simplemente hermoso.

Remerciements

***

Tout d'abord, je tiens à remercier ma directrice de thèse Sepideh Mirrahimi pour m'avoir pris sous son aile et pour m'avoir proposé ce sujet passionnant que j'ai aimé depuis le début. Durant ces années sous sa direction, elle m'a enseigné beaucoup de concepts et de techniques avec beaucoup de dévouement et de patience, surtout les plus difficiles en tenant toujours compte de mes intérêts. Je la remercie surtout de m'avoir inculquée la capacité de travailler avec indépendance et rigueur. Au-delà du travail au laboratoire, je la remercie également pour avoir consacré une partie de son précieux temps pour m'aider dans les tâches administratives en France, et ses conseils pour la suite de ma carrière professionnelle.

Je remercie Grégoire Nadin et Mathieu Alfaro pour avoir bien voulu accepter le rôle de rapporteurs de ma thèse et tous les conseils qu'ils m'ont donné afin de parfaire le travail accompli durant ces trois années. Merci également au reste du jury Jean-Michel Roquejoffre et Delphine Salort pour leur travail impeccable tout au long du processus de lecture et de soutenance. Un merci particulier à Stéphane Mischler également pour son travail en tant que membre du jury et surtout pour m'avoir fait confiance dans le cadre de l'échange Cuba-France mais aussi pour m'avoir fortement recommandé pour la bourse de la Fondation de Sciences Mathématiques de Paris (FSMP), à laquelle je suis très reconnaissante pour l'opportunité qui m'a été offerte.

Pendant mes études de master à Dauphine, j'ai eu l'occasion d'échanger avec des professeurs tels que Jacques-Fejoz et Jean-Pierre Marco qui ont supervisé mon rapport de fin d'études et m'ont introduit dans le monde de la recherche française en me proposant un sujet sur lequel je n'avais aucune connaissance précédent et que j'ai découvert avec passion. Je suis également reconnaissante de l'aide (surtout administrative) que m'a apportée ma tutrice Daniela Tonon durant cette période, sans laquelle mon adaptation en France n'aurait pas été possible, et je remercie tout particulièrement Otared Kavian pour son aide dans les premiers mois du Master sans laquelle je n'aurais pu réussi cette année difficile. En ce qui concerne ma carrière, je ne peux manquer de mentionner mon cher professeur de premier cycle et de master à Cuba, Mariano Rodriguez Ricard qui m'a fait découvrir le monde fascinant des équations différentielles et de la recherche mathématique appliquée, ainsi que Giani Egaña pour son aide pendant mes premières recherches et sa compagnie et son soutien dans mes premiers mois à Paris.

Pendant ma thèse, j'ai eu l'opportunité de travailler un été avec les thésards Anna Melnykova et Samuel Nordmann dans le cadre d'un projet de recherche du CEMRACS'18 supervisé par Vincent Calvez et Sylvie Méléard et avec la grande collaboration de Hélène Hivert. Ensemble, nous avons pu réaliser un travail très intéressant qui a transformé un été de travail en plaisir. Je suis sincèrement reconnaissante d'avoir eu l'occasion de travailler avec eux tous, ce fut pour moi une expérience inoubliable et enrichissante qui m'a fait toucher de

plus près le monde de la recherche qui se cache derrière les industries.

Ma thèse s'est déroulée principalement à l'Institut de Mathématiques de Toulouse (IMT) où j'ai eu l'occasion de me lier à l'enseignement dans la faculté des sciences de l'Université Paul Sabatier-Toulouse III puis à l'INSA de Toulouse, comme une première expérience d'enseignement en France que j'ai beaucoup apprécié. C'est pourquoi je remercie Franck Barthe pour l'accueil chaleureux qu'il m'a réservé dans leur équipe de travail et ses conseils pour ma recherche. J'en suis infiniment reconnaissante à Olivier Mazet pour l'aide et la méthodologie apportées ainsi que pour m'avoir proposé gentiment de faire une "proofreading" de ma thèse afin de rendre ce manuscrit plus beau et ses conseils lors de ma première répétition. Également un remercierment très special pour Simona Grusea pour tous les moments de convivialité passés ensemble pendant mes séjours à l'INSA.

Je remercie également mes collegues thésards à l'IMT. À Baptiste pour les moments des répresentants des doctorants partagés, à Alexis mon co-thésard et aux autres, Joachim, Mathias, Phuong, Michèle, Kuntal pour les déjeuners, séminaires et cafés partagés ensemble. Je remercie tout particulièrement mes co-bureaux, en particulier Kamilia Dahmani, qui est devenue une amie très proche, pour toutes les heures de soutien et les larmes que nous avons partagées pendant ces années stressantes. Non moins important, bien sûr, Anthony Mur pour avoir été si amusant et enthousiaste, ce qui a rendu notre séjour au bureau vraiment agréable. Merci également à Guillaume pour ses conseils de langue et administratifs. Co-bureaux plus anciens mais non moins importants, je remercie Sourav, un petit enfant à qui il a fallu tout apprendre et très cordialement à Victor pour une année pleine de coopération et des conseils (numériques aussi).

Un mot en espagnol pour mes amis cubains en France à qui je dois de grandes heures de détente dans ma vie en France : a Miraine muchas gracias por tu decisiva ayuda en mis primeros tiempos en Paris y por convertirte en una amiga muy cercana ayudándome con la nostalgia por nuestra tierra...muchas felicidades por tus logros y tu familia tan especial. A Willy muchas gracias por sus ocurrencias y divertidos consejos y a Yeny por hacerme entenderte la mayoría de la veces. A Armandito muchas gracias por las horas de tu tiempo dedicadas a mis códigos poco eficientes de MatLab y tu sabiduría para enseñarme y a tu pequeñita esposa Anaisy por poder contar con su alegría avileña en mi vida. Por último y no menos importante muchas gracias Josué por tu compañía y amistad incondicional, por pasar de ser un alumno a ser un gran amigo y por llegar de último a Math-France para convertirte en su principal protagonista. Gracias a todos por el tiempo dedicado en PhD & Beyond a todas mis preguntas.

Au-delà du laboratoire je remercie tous les amis que j'ai fait en France, en commençant par mes premiers voisins Isabelle et Bernard pour tous les repas dont on a profité ensemble et plus spécialement à Laura et Guillaume pour avoir rendu nos soirées tellement amusantes, merci de nous avoir inclus dans votre cercle le plus proche.

Par ailleurs mes chères TATICAS, un gros merci à toutes pour rendre ma vie plus heureuse depuis plus de 15 ans. Je vous aime tellement : GRACIAS POR VUESTRA AMISTAD.

Merci de tout mon cœur à mes parents pour leur soutien pendant toutes ces années de vie : à ma mère d'être toujours là sans me laisser grandir et en même temps de m'aider à le faire par les moyens de vie les plus simples, GRACIAS MAMITA ! et à mon père pour son courage et sa confiance dans la réussite dans mes études, pour ne laisser personne me faire penser autrement GRACIAS PAPI ! En général à toute ma famille pour leur affection et leur soutien, en particulier à ma tante Yolanda qui m'a compris plus que quiconque. Ma gratitude familiale s'adresse aussi à mon autre famille, à mes beaux-parents et à Dania pour son amour et son soutien pendant

toutes ces années, surtout à ma belle-mère pour m'avoir fait sa fille (avant d'avoir pris son nom de famille), GRACIAS EDE !

Mes derniers remerciements vont à celui qui est devenu la personne la plus spéciale dans ma vie : mon mari Ale. Je comprends qu'il n'est pas facile de supporter une thésarde, son stress et ses sauts d'humeur et j'apprécie beaucoup tout ton soutien durant ces années et toutes les années où nous avons été ensemble, merci d'avoir rendu ma vie plus belle et douce et pour inclure la petite Nasha dans notre quotidien.

Susely FIGUEROA IGLESIAS

ABSTRACT

This thesis focuses on the qualitative study of several parabolic equations of the Lotka-Volterra type from evolutionary biology and ecology taking into account a time-periodic growth rate and a non-local competition term. In the initial part we first study the dynamics of phenotypically structured populations under the effect of mutations and selection in environments that vary periodically in time and then the impact of a climate change on such population considering environmental conditions which vary according to a linear trend, but in an oscillatory manner. In both problems we first study the long-time behaviour of the solutions. Then we use an approach based on Hamilton-Jacobi equations to study these long-time solutions asymptotically when the effect of mutations is small. We prove that when the effect of mutations vanishes, the phenotypic density of the population is concentrated on a single trait (which varies linearly over time in the second model), while the population size oscillates periodically. For the climate change model we also provide an asymptotic expansion of the mean population size and of the critical speed leading to the extinction of the population, which is closely related to the derivation of an asymptotic expansion of the Floquet eigenvalue in terms of the diffusion rate. In the second part we study some particular examples of growth rates by providing explicit and semi-explicit solutions to the problem and present some numerical illustrations for the periodic model. In addition, being motivated by a biological experiment, we compare two populations evolved in different environments (constant or periodic). In addition, we present a numerical comparison between stochastic and deterministic models modelling the horizontal gene transfer phenomenon. In a Hamilton-Jacobi context, we are able to numerically reproduce the evolutionary rescue of a small population that we observe in the stochastic model.

Keywords: Nonlocal reaction-diffusion equations, Mutation-selection models, Asymptotic study and long time behavior, Hamilton-Jacobi equations, Dirac concentrations.

RÉSUMÉ

Cette thèse porte sur l'étude qualitative de plusieurs équations paraboliques de type Lotka-Volterra issues de la biologie évolutive et de l'écologie, équations qui prennent en compte un taux de croissance périodique en temps et un phénomène de compétition non locale. Dans une première partie nous étudions d'abord la dynamique des populations phénotypiquement structurées sous l'effet des mutations et de la sélection dans des environnements qui varient périodiquement en temps, puis nous étudions l'impact d'un changement climatique sur ces populations, en considérant que les conditions environnementales varient selon une tendance linéaire, mais de manière oscillatoire. Dans les deux problèmes nous commençons par étudier le comportement en temps long des solutions. Ensuite nous utilisons une approche basée sur les équations de Hamilton-Jacobi pour l'étude asymptotique de ces solutions en temps long lorsque l'effet des mutations est petit. Nous prouvons que lorsque l'effet des mutations disparaît, la densité phénotypique de la population se concentre sur un seul trait (qui varie linéairement avec le temps dans le deuxième modèle), tandis que la taille de la population oscille périodiquement. Pour le modèle de changement climatique nous fournissons également un développement asymptotique de la taille moyenne de la population et de la vitesse critique menant à l'extinction de la population, ce qui est lié à la dérivation d'un développement asymptotique de la valeur propre de Floquet en fonction du taux de diffusion. Dans la deuxième partie, nous étudions quelques exemples particuliers de taux de croissance en donnant des solutions explicites et semi-explicites au problème, et nous présentons quelques illustrations numériques pour le modèle périodique. De plus, étant motivés par une expérience biologique, nous comparons deux populations évoluant dans des environnements différents (constants ou périodiques). En outre, nous présentons une comparaison numérique entre les modèles stochastiques et déterministes pour le phénomène de transfert horizontal des gènes. Dans un contexte Hamilton-Jacobi, nous parvenons à reproduire numériquement le sauvetage évolutif d'une petite population que nous observons dans le modèle stochastique.

Mots clés: Équations de réaction-diffusion non locales, Modèles de sélection-mutation, Étude asymptotique et comportement à long terme, Équations de Hamilton-Jacobi, Concentrations de Dirac.

Contents

***

INTRODUCTION

***

1 Motivation biologique et état de l'art

Dans cette thèse on s'intéresse à l'étude des équations intégro-différentielles de type Lotka-Volterra avec un terme de compétition non local, en décrivant la dynamique évolutive des populations. Nous nous intéressons particulièrement aux populations phénotypiquement structurées dans un environnement qui varie en temps. Au niveau de la population, les processus fondamentaux de la naissance et de la mort relient la sélection naturelle et la dynamique des populations. Nous considérons l'évolution d'une population asexuée dont la taille peut varier avec le temps. La dynamique évolutive de cette population est basée sur trois mécanismes d'évolution : **l'hérédité, les mutations et la sélection naturelle**. Si l'hérédité permet de transmettre l'information génétique au fil des générations, les mutations sont l'une des principales sources de variation sur lesquelles agit la sélection naturelle, permettant ainsi l'évolution des organismes vivants. Les individus sont en **compétition** pour des ressources, ce qui mène à la sélection des meilleurs traits phénotypiques en temps long. Nous explorons, en particulier, le rôle des **fluctuations environnementales** sur l'évolution de la densité phénotypique d'une telle population. Les fluctuations de l'environnement peuvent être, par exemple, dues aux facteurs climatiques (comme la température, l'humidité et les précipitations), ou à l'administration dépendant du temps de médicaments pour tuer des cellules cancéreuses ou des bactéries [67, 83, 12, 91].

Les études de l'adaptation des populations aux environnements qui changent, remontent par exemple à Lande et Shanon, 1996 [69]. Ils décrivent comment les changements dans l'environnement affectent différemment le trait phénotypique moyen de la population, si l'environnement change de façon directionnelle, où il suit le trait optimal avec un retard, ou dans le cas d'un environnement cyclique où le trait moyen oscille avec la même période que le trait optimal, mais avec une amplitude moindre. Au cours des dernières années, une attention croissante a été portée dans la littérature biologique ainsi que mathématique aux effets des fluctuations sur l'adaptation et la démographie d'une population ([60, 66, 74, 83, 91, 6]).

Une motivation naturelle et d'importance croissante concerne l'étude de l'impact d'un changement climatique (*Global Warming*) sur la dynamique d'une espèce biologique, ([87, 28, 57]), notamment le fait que de nombreuses populations naturelles sont sujettes à la fois à des changements directionnels de l'optimum phénotypique et à des fluctuations aléatoires de l'environnement.

Du côté medical, il est connu que des nombreux processus pharmacothérapeutiques, dans les thérapies anticancéreuses, antivirales ou antibiotiques, peuvent faillir à contrôler la prolifération, car la population cible (virus, cellule, parasite) devient résistante. L'apparition d'une résistance aux médicaments est donc un obstacle majeur au succès du traitement. Pour pouvoir décrire l'émergence de la résistance aux médicaments il est important de considérer un environnement dépendant du temps pour prendre en compte une administration de médicaments qui varie avec le temps. Parmi des

études de ce type on peut citer la comparaison d'efficacité entre l'application cyclique et le mélange des antibiotiques [12], ou l'étude des modèles de sélection-mutation en considérant une population structurée par des cellules saines/-cancéreuses avec un niveau de résistance génique pour chaque cellule [75, 31]. Un autre phénomène important à prendre en compte lors de l'étude de l'émergence de résistance notamment pour les bacteries est le transfert horizontal de gènes (transmission de matériel génétique entre deux organismes vivants, contraire à la transmission verticale d'un parent à sa progéniture) qui a un role important dans ces processus [20, 19].

Quelques définitions biologiques

Tout au long de cette thèse nous abordons certains concepts biologiques qui sont ensuite décrits. Nous avons enoncé précédemment le fait que l'on étudie des populations *phénotypiquement structurées* sous l'effet de la *sélection* et des *mutations*. Tout d'abord précisons ces terminologies.

Définition 1

- *Génotype : désigne l'ensemble des gènes constituant l'ADN (identité et constitution génétique) d'un organisme ou d'une population. Chaque gène, individuellement et/ou en coopération, contribue de manière différente au développement, à la physiologie et au maintien fonctionnel de l'organisme.*
- *Phénotype : est un ensemble de caractères qui se manifestent visiblement chez un individu et qui expriment l'interaction entre son génotype et son milieu, les effets de son environnement. Il précise l'apparence physique ou externe d'un organisme (morphologie) en contraste avec sa constitution génétique (biométrie).*
- *Trait Phénotypique : est un sous-ensemble du phénotype d'un individu.*
- *Mutation : est une modification spontanée ou artificielle de la structure génétique (du gène ou du chromosome) qui produit habituellement un effet observable sur l'individu concerné. C'est aussi une modification brusque et héréditaire qui apparaît chez les êtres vivants, et se produit au hasard. Il s'agit d'un accident génétique au niveau du patrimoine de l'espèce : la disparition d'un gène sur un chromosome, défaut dans le positionnement, échange d'une partie de chromosome.*
- *Sélection Naturelle : qualifie le processus par lequel les individus présentant les adaptations les plus appropriées connaissent une meilleure réussite que d'autres, et parviennent à survivre et proliférer. Les caractères qui font la force d'une espèce étant transmissibles, ils se propagent au sein de la population.*

Nous avons également mentionné que l'on considère une *compétition non locale* au sein de la population. La compétition est une interaction négative qui se produit lorsque des organismes de la même espèce ou d'espèces différentes utilisent les mêmes ressources en même temps et que leur taux de croissance est réduit. Nous nous concentrons ici sur les interactions des individus d'une même espèce (compétitions intraspécifiques).

Principales questions abordées

Dans un premier temps on s'intéresse à l'étude de la dynamique des populations phénotypiquement structurées sous l'effet de la sélection et des mutations qui font face aux fluctuations périodiques de l'environnement. Il y a plusieurs questions que l'on peut formuler dans ce contexte : la population survivra-t-elle dans un environnement fluctuant ? Quel sera l'impact des variations de l'environnement sur la distribution phénotypique de la population ? Comment la taille de la population sera-t-elle affectée ?

Dans un second temps, nous incluons l'effet d'un changement climatique dans l'étude de la dynamique évolutive des populations structurées par un phénotype. Nous considérons ici un environnement qui varie avec une tendance linéaire par rapport au trait mais d'une façon oscillante. Nous cherchons à répondre à des questions suivantes : la population pourrait-elle suivre le changement climatique ? Existe-t-il une vitesse maximale du changement climatique à partir

de laquelle la population ne pourra pas survivre ? Quel sera l'impact de ces changements sur la démographie et la distribution phénotypique de la population ?

Dans la dernière section nous étudions également un modèle issu du phénomène de transfert horizontal de gènes, motivé par la résistance aux antibiotiques de certaines bactéries. En effet, on aborde ce problème du point de vue numérique en faisant une comparaison entre les modèles stochastiques et déterministes qui décrivent ce phénomène.

2 Préliminaires sur les modèles d'évolution

Plusieurs cadres ont été utilisés pour étudier la dynamique des populations sous l'effet de la sélection et des mutations. L'une des premières approches pour étudier la dynamique évolutive a été la *Théorie des jeux* [92, 54]. De même la *Dynamique Adaptative* classique basée sur la stabilité des systèmes dynamiques a permis d'étudier l'évolution sous des mutations rares [35, 36]. Par ailleurs, les outils probabilistes permettent d'étudier des populations de petite taille [26], et aussi de dériver des modèles déterministes dans la limite de grandes populations [27]. D'autre part, les modèles intégro-différentiels sont utilisés pour étudier la dynamique évolutive de grandes populations [78, 24, 34, 33].

Nous faisons ensuite un tour d'horizon sur des modèles utilisés dans la littérature pour décrire la dynamique évolutive des populations. On commence par décrire quelques modèles stochastiques de base en décrivant des populations de petite taille puis nous montrons des modèles déterministes plus pratiques utilisés dans le cas d'une population plus importante dans un environnement constant. Nous présentons ensuite quelques résultats connus pour ces modèles en utilisant une approche basée sur des équations de Hamilton-Jacobi.

2.1 Modèles Stochastiques

Les modèles stochastiques de dynamique de populations les plus simples sont les *processus de naissance et de mort*. Soit N_t une taille de population à l'instant t, on dit que ce nombre évoluera comme un processus de naissance et de mort si

- N_t est une chaîne de Markov à valeurs dans $\{0, 1, 2, ...\}$
- $P[N_{t+\Delta t} = n + i | N_t = n] = \begin{cases} \lambda_n \Delta t + o(\Delta t), & \text{si } i = 1 \\ \mu_n \Delta t + o(\Delta t), & \text{si } i = -1 \\ o(\Delta t), & \text{si } |i| > 1 \\ 1 - \lambda_n \Delta t - \mu_n \Delta t + o(\Delta t), & \text{si } i = 0. \end{cases}$
- les taux de naissance $\lambda_0, \lambda_1, \lambda_2, ...$, et de mort $\mu_0, \mu_1, \mu_2, ...$ sont tels que $\lambda_i \geq 0$, $\mu_i \geq 0$, et $\mu_0 = 0$.

Ces modèles peuvent s'étendre afin de prendre en compte les característiques des individus, (position, age, phenotype,...) on parle alors des modèles individu-centré (IBM pour son sigle en anglais : *Individual Based Models*). Ces modèles sont très utilisés par les biologistes théoriques (mais également pour faire des simulations numériques, voir par exemple [70, 21, 63, 37].) Plus récemment en [43], (voir aussi par exemple [25, 79]) une population asexuée et isolée est étudiée, où chaque individu est caractérisé par un trait phénotypique appartenant à l'espace des traits $X \subset \mathbb{R}^d, d \geq 1$, que l'on suppose fermé. On décrit l'évolution de la population structurée par phénotype pour chaque t par la mesure ponctuelle

$$\nu_t^K(dx) = \frac{1}{K} \sum_{i=0}^{N_t^K} \delta_{X_i(t)}(dx), \tag{1}$$

où le paramètre K est un paramètre d'échelle, appelé capacité de charge (*carrying capacity*). Il représente le nombre maximal d'individus que l'environnement est capable d'héberger (K peut représenter, par exemple, le montant des

ressources disponibles). $N_t^K = K \int \nu_t^K(dx)$ est la taille de la population au temps t, et $X_i(t) \in X$ est le trait du $i-$ème individu vivant à l'instant t. La démographie d'une telle population est d'abord régulée par la naissance et la mort. Un individu avec le caractère x donne naissance à un nouvel individu à un taux $b(x)$. Le caractère y de la progéniture est distribué selon une mesure de probabilité appelée noyau de mutation. Un individu avec le trait x meurt à un taux de mortalité $d(x, \nu)$ qui prend en compte la mortalité intrinsèque et parfois l'effet de tous les individus vivants. On obtient ainsi un processus de Markov à valeurs mesure.

Ces modèles permettent être simulés numériquement de façon exacte mais ces expérimentations peuvent être couteuses notamment pour une échelle de temps et une population de grande taille. Dans ce cas, on utilisera des approximations déterministes ou stochastiques sous forme d'EDO, EDP, EDS, ([27, 40]).

2.2 Modèles Déterministes de sélection-mutation dans des environnements constants

Les équations déterministes de sélection-mutation décrivent l'action de ces deux phénomènes sur la composition génétique d'une population de grande taille. Parmi les premiers travaux importants l'on peut citer Crow et Kimura (1964), [62] et Kimura (1965), [61], qui ont introduit le modèle des allèles continus ("the continuum-of-alleles model"). Ils considèrent un modèle avec un *locus*[1] haploïde isolé et des allèles continus, et ils introduisent le modèle suivant :

$$\frac{\partial p(x,t)}{\partial t} = [m(x) - \bar{m}(t)]\, p(x,t) + \mu \left[\int_{-\infty}^{\infty} u(x-y) p(y,t) dy - p(x,t) \right], \tag{2}$$

où p représente la densité des effets alléliques, u est une distribution de mutation avec taux μ et $m(x)$ une function de *fitness*[2] avec $\bar{m}(t) = \int_{-\infty}^{\infty} m(x) p(x,t) dx$ qui modélise la fitness moyenne. De cette manière le premier terme à droite décrit les changements dus à la sélection et le deuxième ceux dus aux mutations.
Le principal intérêt ici étaient les solutions stationnaires $p = p(x)$. En considérant la fonction de fitness particulière $m(x) = -sx^2$, et après une transformation de type $y \mapsto y + x$ suivi d'un développement de Taylor pour $p(x + y)$, ils obtiennent formellement une équation en fonction des moments de la distribution de mutation u. En supposant que la moyenne est nulle et que la variance est donnée par γ^2 et les termes d'ordre supérieur sont négligeables (comme pour une gaussienne avec petite variance γ^2), ils arrivent alors à l'équation suivante

$$s \left(x^2 - \int_{-\infty}^{\infty} y^2 p(y) dy \right) p(x) = \frac{1}{2} \mu \gamma^2 \frac{d^2 p(x)}{dx^2}. \tag{3}$$

Notons que la fonction gaussienne avec moyenne zero et variance

$$\sigma^2 = \sqrt{\frac{\mu}{s} \frac{\gamma^2}{2}},$$

est solution de l'équation (3).
Ces résultats ont été ensuite développés par Lande 1975 [68], en les généralisant au cas des plusieurs *loci* liés ou pas, puis par Fleming 1979 [42] qui prend en compte une version temps-discrète du modèle de Kimura et Crow et fournit des approximations d'ordre deux pour la solution.

Au cours des dernières années la dynamique évolutive des populations en milieu constant a été largement étudiée (voir par exemple [78, 24, 34, 33, 3]). En particulier des modèles sous la forme fréquence dépendant, (comme (2) et (3)) ont

[1] Emplacement précis d'un gène sur le chromosome qui le porte.
[2] La fitness, dans un contexte biologique, aussi appelée la "*fitness darwinienne*" est liée à la théorie évolutionniste de Charles Darwin sur la sélection naturelle. La fitness darwinienne décrit à quel point un organisme a réussi à transmettre ses gènes. Plus un individu a de chances de survivre et de vivre plus longtemps pour se reproduire, plus sa fitness est élevée.

été beaucoup étudiés, ([3, 47, 4, 5]). Dans certains cas des solutions explicites sont fournies ([3]).

Dans le cadre de l'étude des modèles intégro-différentiels l'on peut également remarquer le développement d'un point de vue asymptotique. Cette approche a été introduite pour la première fois par O. Diekmann, P. Jabin, S. Mischler et B. Perthame dans [34], puis les premiers résultats rigoureux sont données dans [88]. Cette méthode, qui est bassée sur des équations de Hamilton-Jacobi, a été développée pour étudier les solutions asymptotiques des équations de sélection-mutation, en supposant un petit effet des mutations. Les solutions des modèles de sélection-mutation se concentrent en générale comme des masses de Dirac, lorsque l'effet des mutations sont petits et en temps long. Dans tous ces travaux, l'idée principale de la méthode asymptotique est de partir d'un modèle intégro-différentiel avec compétition non-locale, où les mutations sont souvent représentées par un Laplacien, et de caractériser la solution lorsque les mutations ont des petits effets. Pour cela, on considère que l'effet d'une mutation est de l'ordre d'un petit paramètre que l'on appelle ε et après une transformation logarithmique de la solution on en déduit un problème limite lorsque $\varepsilon \to 0$. Ce problème limite est en effet une équation de Hamilton-Jacobi avec contrainte. Une étude de cette équation permet ensuite de décrire la densité phénotypique de la solution du problème original, lorsque $\varepsilon \to 0$.

2.2.1 Modèles Integro-Différentiels et heuristiques sur l'approche Hamilton-Jacobi

Un modèle typique des équations intégro-différentielles peut être écrit de la manière suivante :

$$\partial_t n - \sigma \Delta n = nR(x, I(t)), \quad I(t) = \int_{\mathbb{R}} \psi(x) n(t,x) dx, \tag{4}$$

où $n(t,x)$ représente la densité d'individus ayant le trait x à l'instant t. Les mutations sont représentées par le terme de Laplace avec le taux σ. Le terme intégral signifie la consommation totale de ressources. Nous supposons qu'il y a un seul nutriment dans l'environnement que les individus consomment avec un taux $\psi(x)$. De plus, le terme $R(x,I)$ correspond au taux de croissance qui dépend du trait et de l'environnement, et prend en compte les compétitions entre les individus. Notons que la différence principale avec le modèle de Kimura est que l'on prend en compte la démographie. Nous citons ci-dessous quelques exemples et variantes de ce modèle :

(i) On obtient un modèle simple lorsqu'on prend

$$R = \kappa \left(r(x) - I(t) \right),$$

pour $\kappa > 0$, et r étant le taux de croissance, que l'on peut considérer constant ([46, 48]) ou pas.

(ii) On peut considérer une variante du modèle précédent en prenant le terme intégral comme une convolution, c'est à dire

$$I(t,x) = \int_{\mathbb{R}} \psi(x-y) n(t,y) dy,$$

qui prend en compte une compétition plus importante pour les traits les plus proches (voir [48, 17] et leurs références).

(iii) Encore une autre variante du modèle apparaît si dans l'équation (4) on considère les mutations modélisées par un noyau intégral, au lieu du laplacien, comme ci-dessous

$$\int_{\mathbb{R}} [n(t,x+h) - n(t,x)] K(h) dh. \tag{5}$$

Pour le modèle (4) habituellement on procède à un changement d'échelle pour passer de l'échelle microscopique à l'échelle macroscopique. D'une part, on considère le cas des petites mutations : pour un petit paramètre $\varepsilon > 0$, on

substitue $\sigma = \varepsilon^2$. Cependant, lorsque ε est petit, l'effet des mutations ne peut être observé que sur une plus grande échelle de temps. Ainsi, on rééchelle le temps avec $t \mapsto \frac{t}{\varepsilon}$. Le modèle (4) alors devient

$$\varepsilon \partial_t n_\varepsilon - \varepsilon^2 \Delta n_\varepsilon = n_\varepsilon R(x, I_\varepsilon(t)), \quad I_\varepsilon(t) = \int_{\mathbb{R}^d} \psi(x) n_\varepsilon(t,x) dx. \tag{6}$$

Ensuite, le but est d'étudier le comportement de la solution lorsque $\varepsilon \to 0$. Le résultat qualitatif intéressant est que les solutions se concentrent en masses de Dirac.
Pour obtenir ce résultat généralement, on impose les hypothèses suivantes au modèle (4) :

- Il existent des constants ψ_m et ψ_M telles que la fonction ψ vérifie

$$0 < \psi_m \leq \psi \leq \psi_M < \infty, \qquad \psi \in W^{2,\infty}(R^d).$$

- On choisit $R \in C^2$, et l'on suppose qu'il existe des constantes positives I_M, C_1 et C_2 telles que

$$\max_{x \in \mathbb{R}^d} R(x, I_M) = 0 = R(0, I_M),$$

$$-C_1 \leq \frac{\partial R}{\partial I} \leq -C_2,$$

avec I_M qui vérifie également,

$$I_\varepsilon(0) = \int_{\mathbb{R}^d} \psi(x) n_\varepsilon(0,x) dx < I_M.$$

La première étape dans l'approche Hamilton-Jacobi introduite dans [34, 88] est de considérer le changement de variable suivant

$$n_\varepsilon(t,x) = e^{\frac{u_\varepsilon(t,x)}{\varepsilon}},$$

pour n_ε solution de (6). Ce type de changement est appelé la transformation de Hopf-Cole, et vient du fait qu'avec un tel changement d'échelle, la solution n_ε aura naturellement cette forme. Alors, la fonction u_ε vérifie l'équation suivante

$$\partial_t u_\varepsilon - \varepsilon \Delta u_\varepsilon = |\nabla u_\varepsilon|^2 + R(x, I_\varepsilon). \tag{7}$$

En faisant tendre ε vers 0, (voir par exemple [34, 33, 88]), on obtient que u_ε converge vers une solution de viscosité u d'une équation de Hamilton-Jacobi avec contrainte

$$\begin{cases} \partial_t u = |\nabla u|^2 + R(x, I(t)), \\ \max\limits_{\mathbb{R}^d} u(t,x) = 0, \end{cases} \tag{8}$$

où I est la limite de I_ε, lorsque ε tend vers 0. Notons que la contrainte peut être déduite à partir de la *propriété de saturation*. C-à-d, soit $\rho_\varepsilon(t) = \int_{\mathbb{R}^d} n_\varepsilon(t,x) dx$ alors il existent des constants ρ_m et ρ_M telles que :

$$0 < \rho_m \leq \rho_\varepsilon(t) \leq \rho_M \quad \forall t. \tag{9}$$

Cette propriété peut être obtenue en faisant une intégration dans (6) par rapport à x après quelques calculs.
De plus nous pouvons montrer la propiété suivante, [88] :

$$\text{supp } n(t,x) \subset \{(t,x) | u(t,x) = 0\} \subset \{(t,x) | R(x,I) = 0\},$$

où $n(t,x)$ est la limite faible de $n_\varepsilon(t,x)$ lorsque $\varepsilon \to 0$.

Enfin, pour comprendre comment ces résultats peuvent aider à déterminer la limite de n_ε et obtenir le phénomène de concentration nous pouvons citer deux cas :

1. La concentration de n_ε peut être obtenue d'une façon simple, [88], lorsque la dimension d est égale à 1 et que la fonction $R(x, I)$ est monotone par rapport à x, alors pour tout t, l'ensemble de $\{R(x, I) = 0\}$ a un seul point et donc
$$n_\varepsilon \rightharpoonup \rho(t)\delta(x - \bar{x}(t)), \tag{10}$$
avec
$$u(t, \bar{x}(t)) = R(\bar{x}(t), I(t)) = 0, \tag{11}$$
où $\rho(t) = \lim_{\varepsilon\to 0} \rho_\varepsilon(t)$ et (u, I) vérifie l'équation (8).
2. Supposons en outre que $R(\cdot, I)$ est strictement concave, uniformément pour I borné. Ensuite, pour tout u_0, condition initiale pour (8), uniformément concave également, toute solution de (8) est strictement concave et donc l'ensemble $\{u = 0\}$ a un unique point, [76]. On en déduit que n est une masse de Dirac :
$$n_\varepsilon \rightharpoonup n(t, x) = \rho(t)\delta(x - \bar{x}(t)).$$

3 Dynamique des populations phénotypiquement structurées dans des environnements variables en temps

Dans cette thèse nous nous intéressons à la dynamique évolutive des populations dans des environnements variables en temps. C'est à dire que l'on considère le taux de croissance R en (4) comme étant aussi une fonction du temps : $R(t, x, I(t))$, en particulier on suppose la fonction R comme étant périodique par rapport à son premier argument, pour analyser l'impact de ces fluctuations dans la distribution phénotypique de la population. Pour les modèles variables en temps l'on peut citer le travail dans [30], où les auteurs montrent que les fluctuations environnementales peuvent amener la population à entrer dans un état épigénétique instable et fluctuant et que cela peut déclencher l'émergence d'oscillations dans la taille de la population. Par ailleurs, dans [83], un modèle similaire au notre est étudié, en utilisant également une approche basée sur l'équation de Hamilton-Jacobi mais avec une échelle différente. Plus récemment, dans [6], les auteurs étudient une population mixte de cellules cancéreuses structurées par le niveau d'expression d'un gène lié à la fois au taux de prolifération cellulaire et au niveau de résistance pharmaco-cytotoxique. Ils considèrent alors une forme particulière de taux de croissance temps-dépendant $R = R(x, \rho(t), u(t))$ et des solutions semi-explicites sont fournies, en fonction de la taille de la population $\rho(t)$ et la dose de médicaments $u(t)$.

Nous étudierons également une population qui fait face à un changement climatique en plus des fluctuations périodiques $R(t, x - ct, I(t))$. L'intérêt ici est d'abord de déterminer des conditions sur la vitesse "c" du changement climatique qui conduit à l'extinction ou à la survie de la population. Nous étudions ensuite la distribution phénotypique et la taille de la population. Des modèles similaires, mais avec un terme de réaction locale et sans fluctuations, ont été largement étudiés (voir par exemple [14, 16, 15, 13]). Ces modèles sont introduits pour étudier la dynamique des populations structurées par une variable spatiale négligeant l'évolution. De plus, dans [2], la dynamique spatiale et évolutive d'une population est étudiée dans un environnement dont l'optimum est en mouvement linéaire.

Dans ces deux types de problèmes nous utilisons une approche basée sur des équations de Hamilton-Jacobi pour étudier asymptotiquement la population lorsque l'effet des mutations est petit mais non nul. Nous présentons ci-dessous nos résultats pour les modèles de sélection-mutation dans des environnements variables en temps.

3.1 L'effet des fluctuations périodiques sur la distribution phénotypique de la population

Un premier modèle que nous étudions est le suivant

$$\begin{cases} \partial_t n(t,x) - \sigma\Delta n(t,x) = n(t,x)[a(t,x) - \rho(t)], \quad (t,x) \in [0,+\infty) \times \mathbb{R}^d, \\ \rho(t) = \displaystyle\int_{\mathbb{R}^d} n(t,x)dx, \\ n(t=0,x) = n_0(x). \end{cases} \tag{12}$$

Ce modèle est du type de celui décrit dans (4) en prenant la fonction de croissance $R = R(t,x,\rho(t)) = a(t,x) - \rho(t)$. Dans ce modèle le terme intégral ρ correspond à la taille totale de la population et sa présence dans l'équation représente la compétition non-locale des individus. La densité initiale des individus $n_0(x)$ présentant de grands traits est exponentiellement petite. Par ailleurs, la fonction a est supposée $T-$périodique en temps et l'on condidère que la fonction moyennée

$$\bar{a}(x) = \frac{1}{T}\int_0^T a(t,x)dt,$$

atteint son maximum et celui-ci est positif, ce qui signifie qu'ils existent au moins quelques traits avec un taux de croissance moyen strictement positif. Concernant le comportement en temps long de la population, le premier résultat à noter est le suivant

Proposition 2 *([F.I., Mirrahimi, 2018]. Convergence en temps long 1)*
Soit la fonction $a(t,x)$ dans l'équation (12) *"suffisamment petite à l'infini" qui vérifie* $\max_{\mathbb{R}^d} \bar{a}(x) > 0$. *On suppose de plus que σ est assez petit. Alors*

$$\|n(t,\cdot) - \tilde{n}(t,\cdot)\|_{L^\infty} \to 0, \qquad \textit{lorsque } t \to \infty,$$

où $\tilde{n}(t,x)$ est la seule solution périodique du problème (12).

Rémarque 3

(i) Nous avons mis entre guillemets que la fonction "a" doit être suffisamment petite, c'est-à-dire qu'elle doit prendre des valeurs négatives pour des valeurs de x grandes. Nous clarifierons cela plus tard.

(ii) La solution périodique $\tilde{n}(t,x)$ peut s'écrire de la manière suivante

$$\tilde{n}(t,x) = \tilde{\rho}(t)\frac{p(t,x)}{\int_{\mathbb{R}^d} p(t,x)dx},$$

avec $\tilde{\rho}(t)$ la seule solution périodique de l'EDO

$$\begin{cases} \dfrac{d\tilde{\rho}}{dt} = \tilde{\rho}(t)\left[\dfrac{\int_{\mathbb{R}^d} a(t,x)p(t,x)dx}{\int_{\mathbb{R}^d} p(t,x)dx} - \tilde{\rho}(t)\right], \quad t \in (0,+\infty) \\ \tilde{\rho}(0) = \tilde{\rho}(T), \end{cases}$$

et $p(t,x)$ la seule fonction propre périodique (sauf multiplication par un scalaire) associée à la valeur propre λ dans le problème linéaire suivant

$$\begin{cases} \partial_t p(t,x) - \sigma\Delta p(t,x) = p(t,x)[a(t,x) - \lambda], \quad (t,x) \in [0,+\infty) \times \mathbb{R}^d, \\ 0 < p(0,x) = p(T,x), \quad x \in \mathbb{R}^d. \end{cases}$$

(iii) L'unicité d'une telle paire (p,λ) solution du problème ci-dessus peut être établie à partir des résultats classiques

pour des domaines bornés dans [53] et en utilisant des résultats plus récents dans [56], (voir également [84, 85] où cette unicité est généralisée au cas périodique en temps et en espace).

Alors que l'on connait l'existence d'une seule solution périodique pour l'équation (12), on s'intéresse à son comportement asymptotique lorsque les mutations sont petites ou rares. Avec un changement de notation pour prendre en compte les hypothèses de la Proposition 2, on note $\sigma = \varepsilon^2$ et on s'intéresse à la solution $n_\varepsilon(t,x)$ du problème périodique suivant

$$\begin{cases} \partial_t n_\varepsilon(t,x) - \varepsilon^2 \Delta n_\varepsilon(t,x) = n_\varepsilon(t,x)[a(t,x) - \rho_\varepsilon(t)], \quad (t,x) \in [0,+\infty) \times \mathbb{R}^d, \\ \rho_\varepsilon(t) = \displaystyle\int_{\mathbb{R}^d} n_\varepsilon(t,x)dx, \\ n_\varepsilon(0,x) = n_\varepsilon(T,x). \end{cases} \tag{13}$$

Nous introduisons la transformation de Hopf-Cole en vue d'utiliser l'approche Hamilton-Jacobi pour cette étude asymptotique. On note

$$n_\varepsilon(t,x) = \frac{1}{(2\pi\varepsilon)^{d/2}} \exp\left(\frac{u_\varepsilon(t,x)}{\varepsilon}\right), \tag{14}$$

et nous montrons la convergence de la densité n_ε vers une masse de Dirac via le Théorème suivant.

Théorème 4 *([F.I., Mirrahimi, 2018]. Comportement Asymptotique 1)*
Soit n_ε solution de (13) et on suppose en plus des hypothèses de la Proposition 2 que le maximum de $\bar{a}$ est atteint en un seul point noté x_m. Alors,

(i) lorsque $\varepsilon \to 0$, on a :

$$\|\rho_\varepsilon(t) - \tilde{\varrho}(t)\|_{L^\infty} \to 0, \quad \text{et} \quad n_\varepsilon(t,x) - \tilde{\varrho}(t)\delta(x - x_m) \rightharpoonup 0, \tag{15}$$

ponctuellement en temps, faiblement en x dans le sens des mesures, avec $\tilde{\varrho}(t)$ donné par

$$\tilde{\varrho}(t) = \frac{1 - \exp\left[-\displaystyle\int_0^T a(s,x_m)ds\right]}{\exp\left[-\displaystyle\int_0^T a(s,x_m)ds\right] \displaystyle\int_t^{t+T} \exp\left[\int_t^s a(\theta,x_m)d\theta\right] ds}. \tag{16}$$

(ii) Par ailleurs, lorsque $\varepsilon \to 0$, u_ε converge localement uniformément vers une fonction $u(x) \in C(\mathbb{R}^d)$, la seule solution de viscosité de l'équation suivante :

$$\begin{cases} -|\nabla u|^2 = \dfrac{1}{T}\displaystyle\int_0^T (a(t,x) - \tilde{\varrho}(t))dt, \quad x \in \mathbb{R}^d, \\ \max\limits_{x \in \mathbb{R}^d} u(x) = u(x_m) = 0. \end{cases} \tag{17}$$

Dans le cas où $x \in \mathbb{R}$, u est en effet une solution classique donnée par

$$u(x) = -\left|\int_{x_m}^x \sqrt{-\bar{a}(y) + \overline{\varrho}}\, dy\right|, \tag{18}$$

où $\overline{\varrho} = \frac{1}{T}\int_0^T \tilde{\varrho}(t)dt$.

Pour prouver ce théorème, nous prouvons d'abord quelques estimations de régularité sur u_ε et passons ensuite à la limite au sens de viscosité en utilisant la méthode des fonctions de test perturbées. Notons que pour prouver des estimations de régularité sur u_ε, une difficulté vient du fait que u_ε étant périodique en temps, on ne peut pas utiliser les bornes de la condition initiale et plus de travail est requis, (voir par exemple [10, 76] où un travail de régularité similaire est effectué

mais en utilisant dans ce cas des bornes sur la condition initiale pour obtenir des bornes pour tout le temps).
Les résultats dans le Théorème 4 peuvent être mieux compris à partir des heuristiques suivantes qui suggèrent également une approximation pour la densité phénotypique de la population n_ε, lorsque ε est petit mais non nul. En remplaçant u_ε dans (13), on note que u_ε est solution de

$$\frac{1}{\varepsilon}\partial_t u_\varepsilon - \varepsilon\Delta u_\varepsilon = |\nabla u_\varepsilon|^2 + a(t,x) - \rho_\varepsilon(t), \quad (t,x) \in [0,+\infty)\times\mathbb{R}^d. \tag{19}$$

Nous écrivons alors formellement un développement asymptotique en puissances de ε avec des coefficients périodiques en temps pour u_ε et ρ_ε comme ci-dessous

$$u_\varepsilon(t,x) = u(t,x) + \varepsilon v(t,x) + \varepsilon^2 w(t,x) + o(\varepsilon^2), \quad \rho_\varepsilon(t) = \rho(t) + \varepsilon\kappa(t) + o(\varepsilon). \tag{20}$$

En substituant dans (19) on obtient

$$\partial_t u(t,x) = 0 \Leftrightarrow u(t,x) = u(x),$$

et

$$\partial_t v(t,x) = |\nabla u|^2 + a(t,x) - \rho(t).$$

On intègre pour $t \in [0,T]$ et l'on utilise la $T-$périodicité de v pour obtenir :

$$-|\nabla u|^2 = \frac{1}{T}\int_0^T (a(t,x) - \rho(t))dt. \tag{21}$$

Pour les termes d'ordre ε on a :

$$\partial_t w - \Delta u = 2\nabla u\cdot\nabla v - \kappa(t),$$

et en intégrant en $[0,T]$ à nouveau on en déduit

$$-\Delta u = \frac{2}{T}\nabla u\int_0^T \nabla v dt - \overline{\kappa}, \qquad \text{avec} \quad \overline{\kappa} = \frac{1}{T}\int_0^T \kappa(t)dt,$$

et l'on obtient les équations suivantes pour v

$$\left\{\begin{array}{rcl} \partial_t v &=& a(t,x) - \overline{a}(x) - \rho(t) + \overline{\rho}, \\ -\Delta u &=& \dfrac{2}{T}\displaystyle\int_0^T \nabla u\cdot\nabla v dt - \overline{\kappa}. \end{array}\right. \tag{22}$$

Ces développements formels peuvent être utilisés pour approcher la densité phénotypique de la population de la façon suivante :

$$n_\varepsilon(t,x) = \frac{1}{(2\pi\varepsilon)^{d/2}}\varepsilon^{\frac{u(x)}{\varepsilon} + v(t,x) + \varepsilon w(t,x)}, \tag{23}$$

ce qui permet d'estimer les moments de la distribution de la population (plus de détails pour les calculs ci-dessus peuvent être trouvés dans le Chapitre 1, voir aussi [81, 45] où ces approximations ont été utilisées dans l'étude de la distribution phénotypique d'une population dans un environnement hétérogène en espace).

Application biologique

Le travail dans le Chapitre 1 a été motivé par une expérience biologique dans [60], où une population bactérienne a été étudiée. Dans cette expérience, plusieurs populations de *Serratia marcescens* ont été maintenues dans des milieux à

température constante ou fluctuante pendant plusieurs semaines. Ensuite, leurs taux de croissance ont été mesurés dans différents environnements. En particulier, on a observé qu'une population de bactéries évoluée dans des températures fluctuantes périodiquement (variation quotidienne entre 24°C et 38°C, moyenne 31°C) est plus performante que les souches qui ont évolué dans des températures constantes (31°C), lorsque les deux populations sont placées dans un environnement constant avec la température 31°C. Il est à noter que cet effet est surprenant, car on s'attend à ce que la population évoluée dans un environnement constant aurait déjà sélectionné le meilleur trait dans un tel environnement. Nos approximations dans les equations (20)-(23) permettent d'estimer, pour deux exemples de taux de croissance, les moments de la distribution phénotypique et la *fitness* moyenne de la population dans un environnement constant. Ces estimations permettent, en fait, de capturer le phénomène observé dans l'expérience de [60] sous quelques conditions sur le taux de croissance choisi.

Les détails peuvent être trouvés dans le Chapitre 1.

3.2 L'impact d'un changement climatique sur la densité phénotypique de la population

On étudie ensuite le modèle suivant qui prend en compte un changement climatique

$$\begin{cases} \partial_t \tilde{n} - \sigma \partial_{xx} \tilde{n} = \tilde{n}[a(t, x - \tilde{c}t) - \tilde{\rho}(t)], \quad (t,x) \in [0, +\infty) \times \mathbb{R}, \\ \tilde{\rho}(t) = \displaystyle\int_{\mathbb{R}} \tilde{n}(t,x)dx, \\ \tilde{n}(t=0,x) = \tilde{n}_0(x). \end{cases} \tag{24}$$

Cette équation modélise la dynamique d'une population qui est structurée par un trait phénotypique $x \in \mathbb{R}$ et qui doit faire face à un changement climatique. Le terme $-\tilde{c}t$ a été introduit dans le taux de croissance intrinsèque d'un individu $a(t, x-\tilde{c}t)$ pour considérer une variation du trait optimal avec une tendance linéaire. À nouveau, la dépendance du terme a par rapport à la première variable est supposée être périodique pour tenir compte des fluctuations de l'environnement, qui peuvent faire varier le trait optimal ou d'autres paramètres de la sélection. Le reste des termes dans le modèle ont une signification similaire au modèle (12). Pour éviter le changement dans le taux de croissance a, nous introduisons $n(t,x) = \tilde{n}(t, x + \tilde{c}t)$ solution de :

$$\begin{cases} \partial_t n - \tilde{c}\partial_x n - \sigma \partial_{xx} n = n[a(t,x) - \rho(t)], \quad (t,x) \in [0, +\infty) \times \mathbb{R}, \\ \rho(t) = \displaystyle\int_{\mathbb{R}} n(t,x)dx, \\ n(t=0,x) = \tilde{n}_0(x), \end{cases} \tag{25}$$

et l'on obtient un résultat de convergence pour cette équation analogue au résultat dans la Proposition 2 en supposant la vitesse $\tilde{c}$ plus petite qu'une vitesse critique que l'on appelle $\tilde{c}^*_\sigma$.

Proposition 5 *(Convergence en temps long 2)*
Soit $n(t,x)$ solution de (25). On suppose que la fonction $a(t,x)$ est "suffisamment petit à l'infini" et en plus vérifie $\max_{\mathbb{R}} \bar{a}(x) > 0$. Pour σ assez petit et $\tilde{c} < \tilde{c}^*_\sigma$ on obtient

$$\|n(t,\cdot) - \widehat{n}(t,\cdot)\|_{L^\infty} \to 0, \qquad \textit{lorsque } t \to \infty,$$

où $\widehat{n}(t,x)$ est la seule solution périodique du problème (25). De plus si $\tilde{c} \geq \tilde{c}^*_\sigma$ la population s'éteint, plus précisément

$$\|n(t,\cdot)\|_{L^\infty} \to 0, \qquad \text{lorsque } t \to \infty.$$

Rémarque 6

(i) La valeur de la vitesse critique dépend de σ et il s'agit en effet d'une vitesse critique du changement climatique au-dessus de laquelle la population s'éteint.

(ii) Similairement à la Remarque 3-(ii) la fonction $\widehat{n}(t,x)$ peut s'écrire

$$\widehat{n}(t,x) = \widehat{\rho}(t)\frac{p_c(t,x)}{\int_{\mathbb{R}} p_c(t,x)dx},$$

avec $\widehat{\rho}(t)$ la seule solution périodique de l'EDO

$$\begin{cases} \dfrac{d\widehat{\rho}}{dt} = \widehat{\rho}(t)\left[\dfrac{\int_{\mathbb{R}} a(t,x)p_c(t,x)dx}{\int_{\mathbb{R}} p_c(t,x)dx} - \widehat{\rho}(t)\right], \quad t \in (0,+\infty), \\ \widehat{\rho}(0) = \widehat{\rho}(T), \end{cases}$$

et $p_c(t,x)$ la seule fonction propre périodique (sauf multiplication par un scalaire) associée à la valeur propre $\lambda_{\tilde{c},\sigma}$ dans le problème linéaire suivant

$$\begin{cases} \partial_t p_c(t,x) - \tilde{c}\partial_x p_c - \sigma\partial_{xx}p_c(t,x) = p_c(t,x)\big[a(t,x) - \lambda_{\tilde{c},\sigma}\big], \quad (t,x) \in [0,+\infty)\times\mathbb{R}, \\ 0 < p_c(0,x) = p_c(T,x), \quad x \in \mathbb{R}. \end{cases} \tag{26}$$

On s'intéresse maintenant à l'analyse asymptotique de la solution périodique lorsque les mutations sont petites. On pose $\sigma = \varepsilon^2$, $\tilde{c} = c\varepsilon$, et l'on définie $c^*_\varepsilon := \dfrac{\tilde{c}^*_{\varepsilon^2}}{\varepsilon}$ avec $\tilde{c}^*_{\varepsilon^2}$ la vitesse critique $\tilde{c}^*_\sigma$ pour $\sigma = \varepsilon^2$. On étudie la solution $n_\varepsilon(t,x)$ du problème :

$$\begin{cases} \partial_t n_\varepsilon(t,x) - c\varepsilon\partial_x n_\varepsilon(t,x) - \varepsilon^2\partial_{xx}n_\varepsilon(t,x) = n_\varepsilon(t,x)[a(t,x) - \rho_\varepsilon(t)], \quad (t,x) \in [0,+\infty)\times\mathbb{R}, \\ \rho_\varepsilon(t) = \displaystyle\int_{\mathbb{R}} n_\varepsilon(t,x)dx, \\ n_\varepsilon(0,x) = n_\varepsilon(T,x), \end{cases} \tag{27}$$

via l'approche Hamilton-Jacobi. Pour cela on fait à nouveau un changement de Hopf-Cole comme ci-dessous

$$n_\varepsilon(t,x) = \frac{1}{\sqrt{2\pi\varepsilon}}\exp\left(\frac{\psi_\varepsilon(t,x)}{\varepsilon}\right),$$

et l'on obtient le résultat suivant :

Théorème 7 *(Comportement Asymptotique 2)*

Soit $n_\varepsilon(t,x)$ solution de (27) et l'on suppose en plus des hypothèses de la Proposition 5 que $c < \liminf_{\varepsilon\to 0} c^*_\varepsilon$. Alors,

(i) lorsque $\varepsilon \to 0$, on a $\|\rho_\varepsilon(t) - \tilde{\varrho}(t)\|_{L^\infty} \to 0$, avec $\tilde{\varrho}(t)$ une fonction $T-$périodique.

(ii) Par ailleurs, lorsque $\varepsilon \to 0$, $\psi_\varepsilon(t,x)$ converge localement uniformément vers une fonction $\psi(x) \in C(\mathbb{R})$, solution au sens de viscosité de l'équation:

$$\begin{cases} -\left|\partial_x\psi + \dfrac{c}{2}\right|^2 &= \overline{a}(x) - \overline{\rho} - \frac{c^2}{4}, \quad x \in \mathbb{R}, \\ \max\limits_{x\in\mathbb{R}} \psi(x) &= 0, \\ -A_1|x|^2 - \frac{c}{2}x - A_2 \leq \psi \leq & c_1 - c_2|x|, \end{cases} \tag{28}$$

avec

$$\bar{\rho} = \int_0^T \tilde{\varrho}(t)dt,$$

et certaines constantes positives A_1, A_2, c_1 *and* c_2.

Le théorème ci-dessus est étroitement lié au Théorème 4 mais une nouvelle difficulté vient du terme de "dérive". Par ailleurs, la question d'unicité de la solution de viscosité de (28) n'est pas abordée dans ce théorème. Au contraire du Théorème 4, il est nécessaire d'ajouter à l'équation une condition d'encadrement en plus de la contrainte de négativité, et plus de travail est requis.

Pour présenter notre résultat principal pour le modèle (27), nous avons besoin de définir le problème à valeurs propres suivant :

$$\begin{cases} \partial_t p_{c\varepsilon} - \varepsilon c \partial_x p_{c\varepsilon} - \varepsilon^2 \partial_{xx} p_{c\varepsilon} - a(t,x) p_{c\varepsilon} = p_{c\varepsilon} \lambda_{c,\varepsilon}, \quad (t,x) \in [0,+\infty) \times \mathbb{R}, \\ 0 < p_{c\varepsilon}(0,x) = p_{c\varepsilon}(T,x), \qquad\qquad x \in \mathbb{R}, \end{cases} \tag{29}$$

où on a noté $\lambda_{c,\varepsilon}$ la valeur propre principale $\lambda_{\tilde{c},\sigma}$ pour $\tilde{c} = c\varepsilon$ et $\sigma = \varepsilon^2$.

Théorème 8 *(Unicité et développement asymptotique)*
Soit $\lambda_{c,\varepsilon}$ *la valeur propre principale du problème* (29). *On suppose en plus des hypothèses du Théorème 7 que* x_m *est le seul point où* $\bar{a}$ *atteint son maximum. Par ailleurs, on suppose qu'il existe un seul point* $\bar{x}$ *tel que* $\bar{x} < x_m$ *et* $\bar{a}(x_m) - \frac{c^2}{4} = \bar{a}(\bar{x})$. *Alors,*

(i) On obtient les développements asymptotiques suivants

$$\overline{\rho}_\varepsilon = -\lambda_{c,\varepsilon} = \overline{a}(x_m) - \frac{c^2}{4} + \varepsilon\sqrt{-\overline{a}_{xx}(x_m)} + o(\varepsilon), \tag{30}$$

$$c^*_\varepsilon = 2\sqrt{\overline{a}(x_m)} - \varepsilon\sqrt{-\overline{a}_{xx}(x_m)/2} + o(\varepsilon), \tag{31}$$

avec $\overline{\rho}_\varepsilon = \frac{1}{T}\int_0^T \rho_\varepsilon(t)dt$.

(ii) Par ailleurs la solution de viscosité de (28) *est unique et elle est (en effet) une solution au sens classique donnée par*

$$\psi(x) = \frac{c}{2}(\overline{x} - x) + \int_{\overline{x}}^{x_m} \sqrt{\overline{a}(x_m) - \overline{a}(y)}dy - \left| \int_{x_m}^{x} \sqrt{\overline{a}(x_m) - \overline{a}(y)}dy \right|, \tag{32}$$

où $\overline{x} < x_m$.

(iii) En outre, soit n_ε *solution de* (27), *alors*

$$n_\varepsilon(t,x) - \tilde{\varrho}(t)\delta(x - \overline{x}) \rightharpoonup 0, \qquad \textit{quand } \varepsilon \to 0, \tag{33}$$

ponctuellement en temps, faiblement en x *dans le sens des mesures, avec* $\tilde{\varrho}$ *la seule solution périodique de l'équation suivante*

$$\begin{cases} \dfrac{d\widetilde{\varrho}}{dt} = \widetilde{\varrho}\left[a(t,\bar{x}) - \widetilde{\varrho}\right], \quad t \in (0,T), \\ \widetilde{\varrho}(0) = \widetilde{\varrho}(T). \end{cases} \tag{34}$$

Rémarque 9

(i) L'énoncé (iii) dans le Théorème 8 implique que la solution du problème initial (24) *avec* $\sigma = \varepsilon^2$ *et* $\tilde{c} = c\varepsilon$ *vérifie*

$$\tilde{n}_\varepsilon(t,x) - \tilde{\varrho}(t)\delta(x - \overline{x} - ct) \rightharpoonup 0, \qquad \textit{quand } \varepsilon \to 0, \tag{35}$$

ponctuellement en temps, faiblement en x *dans le sens des mesures.*

L'idée principale afin de prouver le résultat d'unicité est d'introduire une nouvelle fonction vérifiant une équation de Hamilton-Jacobi similaire à (28) et d'utiliser le fait que ses solutions dans un domaine borné Ω peuvent être déterminées de façon unique par ses valeurs sur les points de la frontière de Ω, et par ses valeurs aux points maximum du RHS de cette nouvelle équation. Notons également que le développement asymptotique fourni pour la vitesse critique c_ε^* et la taille moyenne de la population $\bar{\rho}_\varepsilon$ est en effet lié à l'approximation de la valeur propre de Floquet et par conséquent à l'approximation harmonique de l'état fondamental de l'énergie de l'opérateur de Schrödinger ([49]). Cependant, nous avons ici un opérateur parabolique, non auto-adjoint.

Les détails sur les résultats présentés dans cette sous-section peuvent être trouvés dans le Chapitre 2.

4 Quelques exemples biologiques et simulations numériques

La deuxième partie de cette thèse est consacrée à l'étude de quelques modèles biologiques et leurs simulations numériques. Dans le Chapitre 3 nous étudions d'un point de vue numérique les modèles étudiés dans le Chapitre 1 pour quelques exemples de taux de croissance. Dans le Chapitre 4, nous proposons une étude numérique du phénomène du Transfert Horizontal de Gènes où notre objectif est de comprendre dans quelle mesure le modèle de Hamilton-Jacobi reproduit le comportement qualitatif du modèle stochastique et en particulier le phénomène du sauvetage évolutif.

4.1 Exemples des taux de croissance périodiques

Dans le Chapitre 3, nous étudions les modèles présentés dans la section précedénte pour certains exemples de taux de croissance a. Dans les modèles paraboliques étudiés dans la section précédente, où les taux de croissance sont pris périodiques en temps, on observe une convergence à long terme vers une solution périodique qui conduit en général à un phénomène de concentration autour du trait dominant lorsque l'effet des mutations est petit, tandis que la taille de la population varie périodiquement. Afin d'illustrer les résultats théoriques précédents, nous étudions d'abord deux exemples où les fluctuations agissent différemment sur le taux de croissance :

$$a_1(t,x) = r - g(x-\theta(t))^2, \qquad a_2(t,x) = r - g(t)(x-\theta)^2.$$

Dans les deux exemples, r représente le taux de croissance maximal, g modélise la pression de sélection (constante pour a_1 et $T-$périodique pour a_2) et θ modélise le trait optimal qui est (contrairement à g), $T-$périodique pour a_1 et constante pour a_2. Ces taux de croissance sont considérés comme ayant des fluctuations sur le trait optimal et sur la pression de sélection respectivement.

Pour ces taux de croissance, il est possible en effet de calculer des solutions (explicite pour a_1 et semi-explicite por a_2) du problème périodique (13). Nous fournissons également des simulations numériques. La solution (semi-)explicite proposée a le profil d'une Gaussienne centrée autour d'un trait dominant avec une taille de population qui oscille périodiquement, ce qui est observable également à partir des simulations obtenues. Ces calculs confirment les résultats du Chapitre 1, mais permettent de plus de comprendre, pour ces exemples, ce qui se passe quand le taux de mutation croit. Par ailleurs, des exemples avec des taux de croissance en dehors des hypothèses des théorèmes enoncés précédemment sont également analysés, en particulier avec deux maximums pour $\bar{a}$, ce qui peut amener à des distributions dimorphes.

Plus de résultats analytiques et numériques en prenant d'autres taux de croissance sont détaillés dans le Chapitre 3.

4.2 Comparaison entre les modèles pour le Transfert Horizontal de Gènes

Le transfert horizontal de génes (HGT pour son sigle en anglais : *Horizontal Gene Transfer*) est la transmission de matériel génétique entre deux organismes vivants, contrairement à la transmission verticale qui désigne le transfert d'ADN d'un parent à sa progéniture. Il est connu que ce phénomène joue un rôle important dans l'évolution de certaines bactéries, notamment pour le développement d'une résistance aux antibiotiques. Plusieurs modèles mathématiques ont été proposés dans la littérature pour décrire l'impact du HGT sur la dynamique écologique avec deux types de modèles différents (stochastiques ou déterministes) [71, 59, 52, 19]. Des expériences numériques montrent que l'effet d'un HGT peut conduire à un comportement cyclique de la population [20]. C'est-à-dire que si l'HGT pousse les individus vers un phénotype non adapté et, par conséquent, vers l'extinction, très peu d'individus non affectés par l'adaptation au transfert peuvent éventuellement repeupler l'environnement. C'est ce qu'on appelle le "sauvetage évolutif d'une petite population" (voir Figure 1).

Nous considérons d'abord un modèle stochastique du type individu-centré, décrivant l'évolution d'une population structurée par phénotype, qui est écrit à chaque instant t par la mesure ponctuelle décrite dans (1). Comme on a déjà enoncé dans la section 2.1, la démographie d'une telle population est d'abord régulée par la naissance et la mort. Un individu avec le trait x donne naissance à un nouvel individu avec le taux $b(x)$. Avec la probabilité $1 - p_K$, le nouvel individu porte le trait x et avec la probabilité p_K, il y a une mutation sur le trait. Le trait z du nouvel individu est choisi selon une distribution de probabilité $m(x, dz)$ appelée le noyau de mutation. La mortalité est modélisée par un taux de mortalité intrinsèque $d(x)$ pour un individu de trait x plus un taux de mortalité représentant la compétition $C\frac{N_t^K}{K}$.

Enfin, un individu avec le trait x peut induire un transfert horizontal *unilatéral* à un individu avec le trait y au taux $h_K(x, y, \nu)$, de sorte que la paire (x, y) devient (x, x). Pour simplifier, nous supposons que $h_K(x, y, \nu)$ est sous la forme particulière

$$h_K(x, y, \nu) = h_K(x - y, N) = \tau_0 \frac{\alpha(x - y)}{N/K}, \tag{36}$$

où $N = K \int_{\mathbb{R}^d} \nu(dx)$ est le nombre d'individus, $\tau_0 > 0$ est une constante et α est, soit une fonction Heaviside, soit une fonction regulière (plus utile dans les modèles EDPs), tout en imitant la nature binaire de la fonction Heaviside, telle que pour une petite constante $\delta > 0$,

$$\alpha(z) = \begin{cases} 0 & \text{if } z < -\delta \\ 1 & \text{if } z > +\delta \end{cases}, \quad \alpha'(0) = \frac{1}{2\delta}. \tag{37}$$

Pour une population $\nu = \frac{1}{K}\sum_{i=1}^N \delta_{x_i}$ et une fonction générique mesurable bornée F, le générateur du processus est alors donné par :

$$\begin{aligned} L^K F(\nu) = \sum_{i=1}^N b(x_i) \int_{\mathbb{R}^d} \left(F\left(\nu + \frac{1}{K}\delta_y\right) - F(\nu)\right) m(x_i, dy) \\ + \sum_{i=1}^N \left(d(x_i) + C\frac{N}{K}\right)\left(F\left(\nu - \frac{1}{K}\delta_{x_i}\right) - F(\nu)\right) \\ + \sum_{i,j=1}^N h_K(x_i, x_j, \nu)\left(F\left(\nu + \frac{1}{K}\delta_{x_i} - \frac{1}{K}\delta_{x_j}\right) - F(\nu)\right). \end{aligned}$$

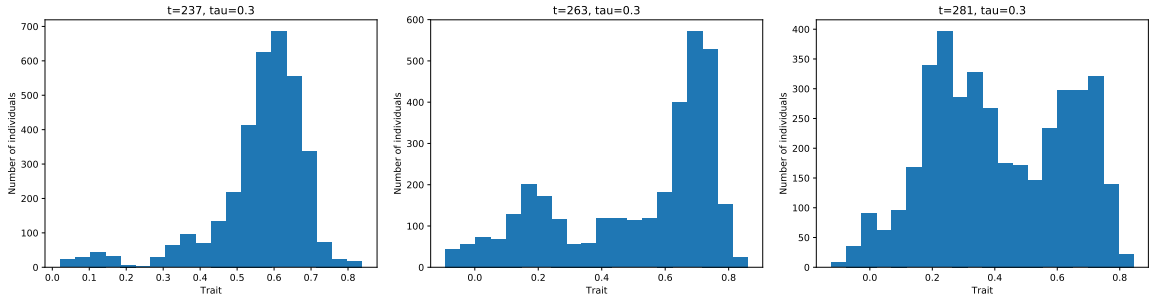

(a) (b) (c)

Figure 1 – Histogrammes pour des valeurs de t différentes montrant le sauvetage évolutif dans le modèle stochastique qui modélise le HGT. De (a) à (c) on observe une petite population non affectée pour le HGT qui devient importante avec le temps et qui repeuple l'environnement.

Pour fixer les idées on prend

$$b(x) = b_r > 0, \tag{38}$$

$$d(x) = d_r x^2, \quad d_r > 0, \tag{39}$$

$$m(z) = \frac{1}{\sqrt{2\pi}\sigma} e^{-\frac{z^2}{2\sigma^2}}. \tag{40}$$

Notons ici, que si l'on part d'une population initiale centrée sur le maximum de m les transferts élevés convertissent d'abord les individus à des traits plus grands (à droite) et, dans le même temps, la population diminue, vu que le trait dominant devient moins adapté. À un moment donné, la taille de la population est si petite que le transfert ne joue plus aucun rôle, ce qui entraîne la résurgence d'une souche quasi-invisible, issue de quelques individus bien adaptés et présentant de petits traits (à gauche); ceux ici pouvant envahir la population résidente.

Cependant, dans un cadre de processus de sauts stochastiques, il est difficile de définir et d'étudier avec précision les phénomènes cycliques observés. Ainsi, dans le cas d'une population importante, il est plus pratique de travailler avec un modèle EDP déterministe, obtenu comme limite pour un système stochastique (voir [40, 19]). Nous étudions alors l'équation non linéaire integro-différentielle, donnée par :

$$\begin{cases} \varepsilon \partial_t f_\varepsilon(t,x) = -(d(x) + C\rho_\varepsilon(t)) f_\varepsilon(t,x) + \displaystyle\int_{\mathbb{R}^d} m(z) b(x+\varepsilon z) f_\varepsilon(t, x+\varepsilon z) dz + f_\varepsilon(t,x) \int_{\mathbb{R}^d} \tau(x-y) \frac{f_\varepsilon(t,y)}{\rho_\varepsilon(t)} dy, \\ \rho_\varepsilon(t) = \displaystyle\int_{\mathbb{R}^d} f_\varepsilon(t,x) dx, \\ f_\varepsilon(0,x) = f_\varepsilon^0(x) > 0, \end{cases} \tag{41}$$

avec $f_\varepsilon(t,x)$ la densité de la population avec trait x au temps t. Les fonctions, $b(x)$, $d(x)$ et C représentent les taux de naissance, mort et compétition respectivement (tout comme dans le modèle stochastique précédent). De plus, m est le noyau de mutation et τ

$$\tau(y-x) := \tau_0 \left[\alpha(x-y) - \alpha(y-x)\right], \tag{42}$$

est le flux de transfert. Enfin, ρ_ε modélise la taille totale de la population. Cette équation a été déjà normalisée avec le petit paramètre $\varepsilon > 0$ pour ne considérer que les mutations petites ainsi que rééchelée par rapport au temps ($t \to \frac{t}{\varepsilon}$) pour tenir compte d'un temps beaucoup plus long qu'une échelle de génération.

Ensuite, nous dérivons le problème limite lorsque $\varepsilon \to 0$. Dans certains contextes, (comme dans les modèles précédents) la densité phénotypique se concentre, à la limite de $\varepsilon \to 0$, comme une masse de Dirac. Dans ce cas, on peut appliquer l'approche Hamilton-Jacobi en passant par une transformation de type Hopf-Cole.

En effet, soit $u_\varepsilon(t,x) = \varepsilon \ln f_\varepsilon(t,x)$, elle vérifie

$$\partial_t u_\varepsilon = -(d(x) + C\rho_\varepsilon(t)) + \int_{\mathbb{R}^d} m(z) b(x+\varepsilon z) \exp\left\{ \frac{u_\varepsilon(t, x+\varepsilon z) - u_\varepsilon(t,x)}{\varepsilon} \right\} dz + \int_{\mathbb{R}^d} \tau(x-y) \frac{f_\varepsilon(t,y)}{\rho_\varepsilon(t)} dy. \tag{43}$$

Formellement, dans la limite $\varepsilon \to 0$, u_ε converge vers une fonction continue u, solution de viscosité de l'équation de Hamilton-Jacobi suivante

$$\partial_t u = -(d(x) + C\rho(t)) + b(x) \int_{\mathbb{R}^d} m(z) e^{z \cdot \nabla_x u} dz + \tau(x - \overline{x}(t)), \tag{44}$$

où $\lim_{\varepsilon \to 0} \rho_\varepsilon(t) = \rho(t) \geq 0$ et $\bar{x}(t) = \text{argmax } u(t,\cdot)$.

L'approche Hamilton-Jacobi est utilisée avec succès pour comprendre les phénomènes de concentration en biologie évolutive (voir par exemple [88, 76, 80]). Nous cherchons à comprendre dans cette étude, si ce cadre est également bien adaptée pour décrire le phénomène de sauvetage évolutif qui repose essentiellement sur une description précise des petites populations. Les simulations du modèle de Hamilton-Jacobi illustrées dans la Figure 2 montrent explicitement comment le cycle apparaît dans sa solution : la croissance des individus "bien adaptés" que l'on voit dans les simulations stochastiques (voir les histogrammes dans la Figure 1) est reproduite dans ce cas par un changement du point maximum de u.

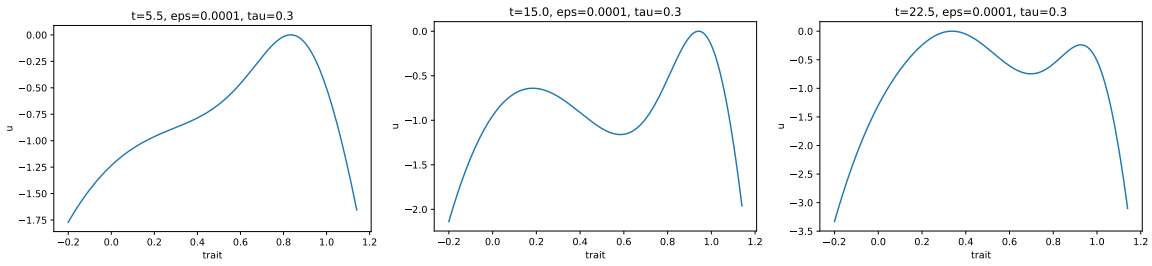

(a) (b) (c)

Figure 2 – Solution de l'équation de Hamilton-Jacobi modélisant le HGT pour des valeurs différentes de t. De (a) à (c) on observe le changement du point maximum.

On précise que les simulations dans la Figure 2 ne sont pas tout à fait comparables avec les histogrammes de la Figure 1, vu que la solution de l'équation Hamilton-Jacobi est en fait la limite dans les petites mutations du logarithme de la solution du modèle EDP (obtenu comme limite pour les grandes populations). Cependant elles permettent d'avoir une première idée du comportement de la densité phénotypique réelle de la population. Une comparaison plus exhaustive des résultats de chaque modèle peut être trouvée dans le Chapitre 4.

5 Perspectives

Dans cette section nous explorons brièvement quelques questions qui émergent naturellement à la suite de cette thèse.

Termes d'ordre supérieur dans l'approximation de la solution

Lorsque nous utilisons la transformation Hopf-Cole (14) pour étudier asymptotiquement la solution périodique $n_\varepsilon(t,x)$ du problème (13) nous faisons formellement un développement asymptotique de la fonction $u_\varepsilon(t,x)$ dans lequel on retrouve naturellement la fonction $u = \lim_{\varepsilon\to 0} u_\varepsilon$, solution de viscosité de l'équation Hamilton-Jacobi (17) ainsi que des fonctions périodiques correspondant au termes d'ordres supérieurs en ε, notamment $v(t,x)$ (voir (20)). Alors une question naturelle à se poser serait si l'on pouvait prouver la convergence de $\frac{u_\varepsilon - u}{\varepsilon}$ vers une certaine fonction v pour écrire rigoureusement un développement asymptotique de u_ε comme suit

$$u_\varepsilon(t,x) = u(x) + \varepsilon v(t,x) + o(\varepsilon).$$

Plus précisément, soit u_ε solution $T-$périodique de l'équation suivante

$$\frac{1}{\varepsilon}\partial_t u_\varepsilon - \varepsilon\Delta u_\varepsilon = |\nabla u_\varepsilon|^2 + a(t,x) - \rho_\varepsilon(t),$$

et $u(x)$ solution de (17). On défini $v_\varepsilon(t,x) = \frac{1}{\varepsilon}\left(u_\varepsilon(t,x) - u(x)\right)$ et l'on veut prouver que lorsque $\varepsilon \to 0$ la fonction v_ε tend vers v solution du système

$$\begin{cases} \partial_t v = a(t,x) - \bar{a}(x) - \varrho(t) - \bar{\rho} \\ -\Delta u = \frac{2}{T}\nabla u \int_0^T \nabla v(t,x)dt - \Delta u(x_m), \end{cases}$$

où $\bar{\rho} = \frac{1}{T}\int_0^T \varrho(t)dt$.

Taux de croissance avec plusieurs maximums

Dans le Chapitre 3 de cette thèse on fait une étude numérique des solutions de l'équation (13) pour différents taux de croissance $a(t,x)$. En particulier, nous allons au delà des hypothèses du Chapitre 1 et prenons des taux de croissance qui atteignent leurs maximums deux fois dans une période de deux manières différentes. En effet, dans un cas on considère que le taux de croissance est symétrique par rapport à un certain hyperplan, (c-à-d, les derivées sont égales aux points de maximum) et dans l'autre cas nous prenons un taux de croissance non-symétrique. Il est intéressant de noter que dans ce dernier exemple, lorsque ε est petit la population se concentre autour du point du maximum le plus plat de $\overline{a}$ tandis que dans le cas symétrique on obtient une population dimorphe, (voir Figure 3).

Ce phénomène est lié au fait que l'état fondamental d'un opérateur de Schrödinger se concentre sur le point de minimum global le plus plat du potentiel [50, 51]. Dans le cas de l'environnement constant et pour le modèle de réplication-mutation, (donné dans la Section 2.2), une étude du caractère uni-modal ou multi-modal de la distribution phénotypique de la population en fonction du taux de croissance et du taux de mutation est fournie dans [5]. Je suis intéressée par étendre ces résultats au cas d'un environnement fluctuant.

Noyau des mutations plus générales

Les variations phénotypiques peuvent également être modélisées en remplaçant l'opérateur de diffusion linéaire par un noyau intégral de la forme

$$\int_{\mathbb{R}^d} (M(x,y)n(t,y) - M(y,x)n(t,x))dy, \tag{45}$$

où le noyau $M(x,y)$ modélise la mutation d'un phénotype y vers le phénotype x. Il est en effet plus réaliste de modéliser les mutations par un noyau intégral plutôt qu'une diffusion (voir Section 2.2 et [25]). Le modèle avec le noyau intégral est en effet dérivé sous des hypothèses moins restreintes.

L'approche Hamilton-Jacobi pour des modèles avec des environnements constants a été déjà développée pour étudier

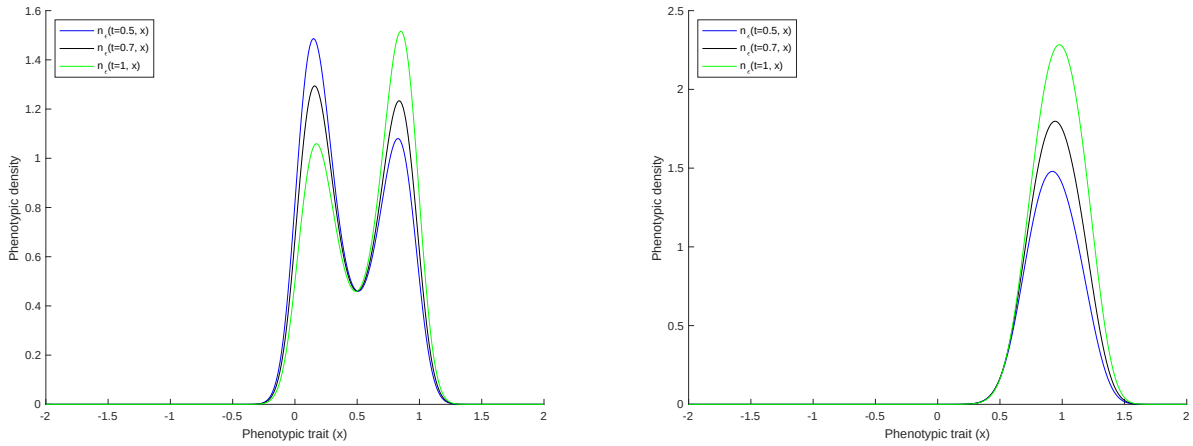

(a) (b)

Figure 3 – Densité phénotypique $n_\varepsilon(t,x)$ de la population pour t fixé : (a) pour un taux de croissance avec deux maximums symétriques ; (b) pour un taux de croissance avec deux maximums non symétriques. Dans la figure (a) la solution est dimorphe et oscille périodiquement autour des traits dominants alors que dans la figure (b) la population est monomorphe et le trait sélectioné est celui autour du quel $\bar{a}$ est le plus plat, ($\varepsilon = 10^{-2}$).

un terme de mutation de type (45), [10]. Je suis alors intéressée par la généralisation de ces résultats au cas des environnements fluctuants.

Dérivation rigoureuse de l'équation de Hamilton-Jacobi pour le modèle de Transfert Horizontal de Gènes : existence, unicité et périodicité de la solution

L'équation (43) obtenue à partir de la transformation Hopf-Cole de f_ε solution de (41) converge formellement vers l'équation (44) lorsque $\varepsilon \to 0$. Dans le Chapitre 4, la dérivation formelle de cette équation limite permet en effet d'effectuer les analyses numériques. Cependant la dérivation rigoureuse de cette convergence reste à établir.

Par ailleurs, dans les simulations numériques on observe une certaine "périodicité" (phénomène cyclique décrivant le sauvetage évolutif) en fonction du taux de transfert τ_0. Il est intéressant de vérifier si la solution de l'équation (44), est en effet périodique pour certains valeurs de τ_0 et dans ce cas déterminer les conditions sur τ_0 pour avoir ce type de comportement.

Part I

DYNAMIQUE ÉVOLUTIVE DES POPULATIONS PHÉNOTYPIQUEMENT STRUCTURÉES

Chapter 1

Approche Hamilton-Jacobi pour décrire la dynamique évolutive des populations dans des environnements fluctuants

***

Les espèces qui survivent ne sont pas les espèces les plus fortes, ni les plus intelligentes, mais celles qui s'adaptent le mieux aux changements–
Charles DARWIN

Résumé

Nous étudions le comportement à long terme d'une équation parabolique de type Lotka-Volterra en considérant un taux de croissance périodique en temps et avec une competition non locale. Une telle équation décrit la dynamique d'une population phénotypiquement structurée sous l'effet de mutations et de sélection dans un environnement fluctuant. Nous prouvons d'abord que, en longtemps, la solution converge vers la solution périodique unique du problème. Ensuite, nous décrivons cette solution périodique asymptotiquement lorsque l'effet des mutations disparaît. En utilisant une théorie basée sur les équations de Hamilton-Jacobi avec contrainte, nous prouvons que lorsque l'effet des mutations disparaît, la solution se concentre sur une seule masse de Dirac, alors que la taille de la population varie périodiquement dans le temps. Lorsque l'effet des mutations est faible mais non nul, nous fournissons quelques approximations formelles des moments de la distribution de la population. Nous montrons ensuite, à l'aide de quelques exemples, comment ces résultats peuvent être comparés à des expériences biologiques. Les résultats dans ce chapitre ont été publiés en colaboration avec Sepideh Mirrahimi, [41].

1.1 Introduction

1.1.1 Model and motivations

The purpose of this chapter is to study the evolutionary dynamics of a phenotypically structured population in a time-periodic environment. While the evolutionary dynamics of populations in constant environments are widely studied (see for instance [34, 27, 33, 90, 80]), the theoretical results on varying environments remain limited (see however [74, 83]). The variation of the environment may for instance come from the seasonal effects or a time varying administration of medications to kill cancer cells or bacteria. Several questions arise related to the time fluctuations. Could a population survive under the fluctuating change? How the population size will be affected? Which phenotypical trait will be selected? What will be the impact of the variations of the environment on the population's phenotypical distribution?

Several frameworks have been used to study the dynamics of populations under selection and mutations. Game theory has been one of the first approaches to study evolutionary dynamics [54, 92]. Adaptive dynamics which is a theory based on the stability of dynamical systems allows to study evolution under rare mutations [35, 36]. Integro-differential models are used to study evolutionary dynamics of large populations (see for instance [24, 33, 34, 78]). Probabilistic tools allow to study populations of small size [26] and also to derive the above models in the limit of large populations [27].
Here, we are interested in the integro-differential approach. We study in particular the following Lotka-Volterra type model

$$\begin{cases} \partial_t n(t,x) - \sigma \Delta n(t,x) = n(t,x)[a(t,x) - \rho(t)], \quad (t,x) \in [0,+\infty) \times \mathbb{R}^d, \\ \rho(t) = \displaystyle\int_{\mathbb{R}^d} n(t,x)dx, \\ n(t=0,x) = n_0(x). \end{cases} \tag{1.1}$$

Here, $n(t,x)$ represents the density of individuals with trait x at time t. The mutations are represented by a Laplace term with rate σ. The term $a(t,x)$ is a time-periodic function, corresponding to the net growth rate of individuals with trait x at time t. We also consider a death term due to competition between the individuals, whatever their traits, proportional to the total population size $\rho(t)$.

A main part of our work is based on an approach using Hamilton-Jacobi equations with constraint. This approach has been developed during the last decade to study asymptotically the dynamics of populations under selection and small mutations. There is a large literature on this approach. We refer for instance to [80, 88] where the basis of this approach for problems coming from evolutionary biology were established. Note that related tools were already used to study the propagation phenomena for local reaction-diffusion equations [39, 44].

Our work follows an earlier article on the analysis of phenotype-structured populations in time-varying environments [83]. In [83], the authors study a similar equation to (1.1) using also the Hamilton-Jacobi approach, but with a different scaling than in this work. They indeed obtain a homogenization result by simultaneously accelerating time and letting the size of the mutations vanish. In this chapter, we study first a long time limit of this equation and next we describe asymptotically such long time solutions as the effect of the mutations vanishes. Our scaling, being motivated by biological applications (see Section 1.6), leads to a different qualitative behavior of solutions and requires a totally different mathematical analysis.

1.1.2 Assumptions

To introduce our assumptions, we first define

$$\overline{a}(x) = \frac{1}{T}\int_0^T a(t,x)dt.$$

We then assume that $a(t,x)$ is a time-periodic function with period T, and C^3 with respect to x, such that

$$a(t,x) = a(t+T,x),\ \forall\ (t,x) \in \mathbb{R}\times\mathbb{R}^d, \quad \text{and } \exists\ d_0 > 0 : \|a(t,\cdot)\|_{L^\infty(\mathbb{R}^d)} \le d_0 \quad \forall\ t \in \mathbb{R}. \tag{H1}$$

Moreover, we suppose that there exists a unique x_m which satisfies for some constant a_m,

$$0 < a_m = \max_{x\in\mathbb{R}^d} \overline{a}(x) = \overline{a}(x_m). \tag{H2}$$

In order to guarantee that the initial condition do not explode, we make the following assumption

$$0 \le n_0(x) \le e^{C_1 - C_2|x|}, \quad \forall x \in \mathbb{R}^d, \tag{H3}$$

for some positive constants C_1, C_2.
Furthermore, only for the proof of Proposition 1.1 in Section 1.2, that is the case with $\sigma = 0$, we assume additionally that

$$H = \left(\frac{\partial^2 \overline{a}}{\partial x_i \partial x_j}(x_m)\right)_{i,j} \quad \text{is negative definite,} \tag{H4}$$

i.e., its eigenvalues are all negative. Also, let us suppose that there exist some positive constants δ and R_0 such that

$$a(t,x) \le -\delta, \quad \text{for all } t \ge 0,\ \text{and } |x| \ge R_0. \tag{H5}$$

Finally, let M and d_1 be positive constants, it is assumed again for the case of no mutations, that

$$\|n_0\|_{W^{3,\infty}} \le M, \qquad \|a\|_{W^{3,\infty}} \le d_1. \tag{H6}$$

1.1.3 Main results

We begin the qualitative study, with a simpler case, where $\sigma = 0$, which means there is no mutation. The model reads as follows

$$\begin{cases} \partial_t n(t,x) = n(t,x)[a(t,x) - \rho(t)], \quad (t,x) \in [0,+\infty)\times\mathbb{R}^d, \\ \rho(t) = \displaystyle\int_{\mathbb{R}^d} n(t,x)dx, \\ n(t=0,x) = n_0(x). \end{cases} \tag{1.2}$$

Our first result is the following.

Proposition 1.1 *(case $\sigma = 0$)*
Assume (H1)-(H6). *Let n be the solution of* (1.2). *Then,*

(i) as $t \to +\infty$, $\|\rho(t) - \widetilde{\varrho}(t)\|_{L^\infty} \to 0$, where $\widetilde{\varrho}(t)$ is the unique positive periodic solution of equation

$$\begin{cases} \dfrac{d\widetilde{\varrho}}{dt} = \widetilde{\varrho}(t)\left(a(t,x_m) - \widetilde{\varrho}(t)\right), \quad t \in (0,T), \\ \widetilde{\varrho}(0) = \widetilde{\varrho}(T), \end{cases} \tag{1.3}$$

given by

$$\widetilde{\varrho}(t) = \frac{1 - \exp\left[-\int_0^T a(s,x_m)ds\right]}{\exp\left[-\int_0^T a(s,x_m)ds\right]\int_t^{t+T}\exp\left[\int_t^s a(\theta,x_m)d\theta\right]ds}. \tag{1.4}$$

(ii) Moreover, $\dfrac{n(t,x)}{\rho(t)}$ *converges weakly in the sense of measures to* $\delta(x-x_m)$ *as* $t\to+\infty$*. As a consequence,*

$$n(t,x) - \widetilde{\varrho}(t)\delta(x-x_m) \rightharpoonup 0 \qquad \text{as } t\to+\infty,$$

in the sense of measures.

This result implies that the trait with the highest time average of the net growth rate over the time interval $[0,T]$, will be selected in long time, while the size of the population oscillates with environmental fluctuations.

To present our results for problem (1.1), we first introduce the following parabolic eigenvalue problems

$$\begin{cases} \partial_t p - \sigma\Delta p - a(t,x)p = \lambda p, & \text{in } [0,+\infty)\times\mathbb{R}^d, \\ 0 < p:\ T-\text{periodic}, \end{cases} \tag{1.5}$$

$$\begin{cases} \partial_t p_R - \sigma\Delta p_R - a(t,x)p_R = \lambda_R p_R, & \text{in } [0,+\infty)\times B_R, \\ p_R = 0, & \text{on } [0,+\infty)\times\partial B_R, \\ 0 < p_R:\ T-\text{periodic}, \end{cases} \tag{1.6}$$

where B_R is the ball in $\mathbb{R}^d$ centered at the origin with radius $R>0$. It is known that (see [53]) if $a\in L^\infty([0,+\infty)\times B_R)$, then there exists a unique principal eigenpair (λ_R, p_R) for (1.6) with $\|p_R(0,\cdot)\|_{L^\infty(B_R)} = 1$. Moreover, as $R\to+\infty$, $\lambda_R \searrow \lambda$ and p_R converges along subsequences to p, with (λ,p) solution of (1.5) (see for instance [56]).
We next assume a variant of hypothesis (H5), that is, there exist positive constants, δ and R_0 such that

$$a(t,x) + \lambda \le -\delta, \quad \text{for all } 0\le t, \text{ and } R_0 \le |x|. \tag{$H5_\sigma$}$$

Under the above additional assumption, which means that "a" takes small values at infinity, the eigenpair (λ,p) is also unique, (see Lemma 1.6).
We next define the $T-$periodic functions $Q(t)$ and $P(t,x)$ as follows

$$Q(t) = \frac{\int_{\mathbb{R}^d} a(t,x)p(t,x)dx}{\int_{\mathbb{R}^d} p(t,x)dx}, \quad P(t,x) = \frac{p(t,x)}{\int_{\mathbb{R}^d} p(t,x)dx}. \tag{1.7}$$

We deduce from previous Proposition that if and only if $\int_0^T Q(t) > 0$, then there exists a unique positive periodic solution $\widetilde{\rho}(t)$ for the problem

$$\begin{cases} \dfrac{d\widetilde{\rho}}{dt} = \widetilde{\rho}\left[Q(t) - \widetilde{\rho}\right], & t\in(0,T), \\ \widetilde{\rho}(0) = \widetilde{\rho}(T). \end{cases}$$

We can then describe the long time behavior of the solution of (1.1)

Proposition 1.2 *(case* $\sigma>0$*, long time behavior)*
Assume (H1), (H2), (H3) *and* ($H5_\sigma$)*. Let* n *be the solution of* (1.1)*, then*

(i) if $\lambda\ge 0$ *then the population will go extinct, i.e.* $\rho(t)\to 0$*, as* $t\to\infty$*,*

(ii) if $\lambda < 0$ *then* $|\rho(t) - \widetilde{\rho}(t)| \to 0$, *as* $t \to \infty$.

(iii) Moreover $\left\| \frac{n(t,x)}{\rho(t)} - P(t,x) \right\|_{L^\infty} \longrightarrow 0$, *as* $t \to \infty$. *Consequently we have, as* $t \to \infty$

$$\|n(t,\cdot) - \widetilde{\rho}(t)P(t,\cdot)\|_{L^\infty} \to 0, \text{ if } \lambda < 0 \quad \text{and} \quad \|n\|_{L^\infty} \to 0, \text{ if } \lambda \geq 0. \tag{1.8}$$

Remark 1.3 *Assuming* (H2) *implies that* $\lambda < 0$, *provided* σ *is small enough.*

We prove this remark in Lemma 1.9.

Proposition 1.2 guarantees, when $\lambda < 0$, the convergence in $L^\infty-$norm of the solution $n(t,x)$ of the equation (1.1) to the periodic function $\widetilde{n}(t,x) = \widetilde{\rho}(t)P(t,x)$ and it is not difficult to verify that $\widetilde{n}$ is in fact a solution of (1.1).
We next describe the periodic solution $\widetilde{n}$, asymptotically as the effect of mutations is small. To this end, with a change of notation, we take $\sigma = \varepsilon^2$ and study $(n_\varepsilon, \rho_\varepsilon)$, the unique periodic solution of the following equation

$$\begin{cases} \partial_t n_\varepsilon - \varepsilon^2 \Delta n_\varepsilon = n_\varepsilon[a(t,x) - \rho_\varepsilon(t)], \quad (t,x) \in [0,+\infty) \times \mathbb{R}^d, \\ \rho_\varepsilon(t) = \displaystyle\int_{\mathbb{R}^d} n_\varepsilon(t,x)dx, \\ n_\varepsilon(0,x) = n_\varepsilon(T,x). \end{cases} \tag{1.9}$$

We expect that $n_\varepsilon(t,x)$ concentrates as a Dirac mass as $\varepsilon \to 0$.
In order to study the limit of n_ε, as $\varepsilon \to 0$, we make the Hopf-Cole transformation

$$n_\varepsilon = \frac{1}{(2\pi\varepsilon)^{d/2}} \exp\left(\frac{u_\varepsilon}{\varepsilon}\right), \tag{1.10}$$

which allows us to prove

Theorem 1.4 *(case* $\sigma = \varepsilon^2$, *asymptotic behavior)*
Let n_ε *solve* (1.9) *and assume* (H1), (H2) *and* $(H5_\sigma)$. *Then*

(i) As $\varepsilon \to 0$, *we have*

$$\|\rho_\varepsilon(t) - \widetilde{\varrho}(t)\|_{L^\infty} \to 0, \quad \text{and} \quad n_\varepsilon(t,x) - \widetilde{\varrho}(t)\delta(x - x_m) \rightharpoonup 0, \tag{1.11}$$

point wise in time, weakly in x *in the sense of measures, with* $\widetilde{\varrho}(t)$ *given by* (2.65).

(ii) Moreover as $\varepsilon \to 0$, u_ε *converges locally uniformly to a function* $u(x) \in C(\mathbb{R})$, *the unique viscosity solution to the following equation*

$$\begin{cases} -|\nabla u|^2 = \dfrac{1}{T}\displaystyle\int_0^T (a(t,x) - \widetilde{\varrho}(t))dt, \quad x \in \mathbb{R}^d, \\ \max\limits_{x \in \mathbb{R}^d} u(x) = u(x_m) = 0. \end{cases} \tag{1.12}$$

In the case $x \in \mathbb{R}$, u *is indeed a classical solution and is given by*

$$u(x) = -\left| \int_{x_m}^x \sqrt{-\overline{a}(x') + \overline{\varrho}}\, dx' \right| \tag{1.13}$$

where $\overline{\varrho} = \frac{1}{T}\int_0^T \widetilde{\varrho}(t)dt$.

To prove Theorem 1.4, we first prove some regularity estimates on u_ε and then pass to the limit in the viscosity sense using the method of perturbed test functions. We finally show that (1.12) has a unique solution, and hence all the sequence converges. Note that in order to prove regularity estimates on u_ε, a difficulty comes from the fact that u_ε is

time-periodic and one cannot use, similarly to previous related works [10, 76], the bounds on the initial condition to obtain such bounds for all time and further work is required.

1.1.4 Some heuristics and the plan of the chapter

We next provide some heuristic computations which allow to better understand Theorem 1.4, but also suggest an approximation of the population's distribution n_ε, when ε is small but nonzero.
Replacing (1.10) in (1.9), we first notice that u_ε solves

$$\left\{\begin{array}{rcl} \frac{1}{\varepsilon}\partial_t u_\varepsilon - \varepsilon\Delta u_\varepsilon &=& |\nabla u_\varepsilon|^2 + a(t,x) - \rho_\varepsilon(t), \quad (t,x)\in[0,+\infty)\times\mathbb{R}^d, \\ u_\varepsilon(t=0,x) &=& u_\varepsilon^0(x) = \varepsilon \ln n_\varepsilon^0(x). \end{array}\right. \tag{1.14}$$

We then write formally an asymptotic expansion for u_ε and ρ_ε in powers of ε

$$u_\varepsilon(t,x) = u(t,x) + \varepsilon v(t,x) + \varepsilon^2 w(t,x) + o(\varepsilon^2), \quad \rho_\varepsilon(t) = \rho(t) + \varepsilon\kappa(t) + o(\varepsilon), \tag{1.15}$$

where the coefficients of the developments are time-periodic.
We substitute in (1.14) and organize by powers of ε, that is

$$\frac{1}{\varepsilon}\left(\partial_t u(t,x)\right) + \varepsilon^0\left[\partial_t v(t,x) - |\nabla u|^2 - a(t,x) + \rho(t)\right] + \varepsilon\left[\partial_t w - \Delta u - 2\nabla u\cdot\nabla v + \kappa(t)\right] + o(\varepsilon^2) = 0.$$

From here we obtain

$$\partial_t u(t,x) = 0 \Leftrightarrow u(x,t) = u(x),$$

and

$$\partial_t v(t,x) = |\nabla u|^2 + a(t,x) - \rho(t).$$

Integrating this latter equation in $t\in[0,T]$, we obtain that

$$0 = \int_0^T |\nabla u|^2 dt + \int_0^T a(t,x)dt - \int_0^T \rho(t)dt,$$

because of the $T-$periodicity of v. This implies that

$$-|\nabla u|^2 = \frac{1}{T}\int_0^T (a(t,x) - \rho(t))dt,$$

which is the first equation in (1.12). Keeping next the terms of order ε we obtain that

$$\partial_t w - \Delta u = 2\nabla u\cdot\nabla v - \kappa(t),$$

and again integrating in $[0,T]$ we find

$$-\Delta u = \frac{2}{T}\nabla u\int_0^T \nabla v dt - \overline{\kappa}, \qquad \text{with} \quad \overline{\kappa} = \frac{1}{T}\int_0^T \kappa(t)dt.$$

Evaluating the above equation at x_m we obtain that

$$\Delta u(x_m) = \overline{\kappa}.$$

Then, using the averaged coefficients $\overline{a}(x) = \frac{1}{T}\int_0^T a(t,x)dt$ and $\overline{\rho} = \frac{1}{T}\int_0^T \rho(t)dt$, we deduce, combining the above computations, that $v(t,x)$ satisfies

$$\left\{\begin{array}{rcl} \partial_t v &=& a(t,x) - \overline{a}(x) - \rho(t) + \overline{\rho}, \\ -\Delta u &=& \dfrac{2}{T}\displaystyle\int_0^T \nabla u \cdot \nabla v dt - \overline{\kappa}, \end{array}\right. \tag{1.16}$$

which allows to determine v.

We will use these formal expansions in Section 1.5, to estimate the moments of the population's distribution using the Laplace's method of integration. Note that such approximations were already used to study the phenotypical distribution of a population in a spatially heterogeneous environment [81, 45] (see also [82] where such type of approximation was first suggested). We next show, via two examples, how such results could be interpreted biologically. In particular, our work being motivated by a biological experiment in [60], we suggest a possible explanation for a phenomenon observed in this experiment.

The chapter is organized as follows. In Section 1.2 we deal with problem (1.2) and prove Proposition 1.1. In Section 1.3 we study the long time behavior of (1.1) and provide the proof of Proposition 1.2. Next, in Section 1.4 we study the asymptotic behavior of n_ε as $\varepsilon \to 0$, and prove Theorem 1.4. In Section 1.5, we use the above formal arguments to estimate the moments of the population's phenotypical distribution. Finally we use these results in Section 1.6 to study two biological examples considering two different growth rates.

1.2 The case with no mutations

In this section we study the qualitative behavior of (1.2), where $\sigma = 0$, and provide the proof of Proposition 1.1.
To this end, we define $N(t,x) = n(t,x)e^{\int_0^t \rho(s)ds}$ which solves

$$\partial_t N = a(t,x)N(t,x).$$

From the periodicity of a and the Floquet theory we obtain that N has the following form

$$N(t,x) = e^{\mu(x)t}p_0(t,x), \quad \text{with} \quad p_0(0,x) = p_0(T,x), \quad \text{and} \quad \mu(x) = \overline{a}(x) = \frac{1}{T}\int_0^T a(s,x)ds.$$

1.2.1 Long time behavior of ρ

In this subsection we prove Proposition 1.1 (i).
Integrating equation (1.2) with respect to x we obtain

$$\frac{d}{dt}\rho(t) = \int_{\mathbb{R}^d} n(t,x)a(t,x)dx - \rho(t)^2 = \rho(t)\left[\int_{\mathbb{R}^d} \frac{n(t,x)a(t,x)}{\rho(t)}dx - \rho(t)\right]. \tag{1.17}$$

Then we claim the following Lemma that we prove at the end of this subsection.

Lemma 1.5 *Assume* (H1)-(H3) *and* (H6) *then*

$$\left|\int_{\mathbb{R}^d} \frac{n(t,x)a(t,x)}{\rho(t)}dx - a(t,x_m)\right| \longrightarrow 0, \quad \text{as } t \to +\infty.$$

Proof. (Proposition 1.1)(i)
From Lemma 1.5, $\rho(t)$ satisfies

$$\frac{d}{dt}\rho(t) = \rho(t)[a(t, x_m) + \Sigma(t) - \rho(t)],$$

where $\Sigma(t) \to 0$ as $t \to \infty$. In order to prove the convergence to a periodic function, we adapt a method introduced in [73].
After a standard substitution $\kappa(t) = 1/\rho(t)$ in order to linearize the latter equation, and integration with the help of an integrating factor, the solution ρ can be written as follows

$$\frac{1}{\rho(t)} = \exp\left(-\int_0^t (a(s, x_m) + \Sigma(s))ds\right)\left(\frac{1}{\rho_0} + \int_0^t \exp\left(\int_0^s (a(\theta, x_m) + \Sigma(\theta))d\theta\right)ds\right).$$

We then write $\dfrac{1}{\rho((k+1)T)}$ as function of $\dfrac{1}{\rho(kT)}$, that is

$$\frac{1}{\rho((k+1)T)} = \exp\left(-\int_{kT}^{(k+1)T} (a(s, x_m) + \Sigma(s))ds\right)\left(\frac{1}{\rho(kT)} + \int_{kT}^{(k+1)T} e^{\int_{kT}^s (a(\theta, x_m)+\Sigma(\theta))d\theta}ds\right),$$

and we obtain a recurrent sequence for $\rho_k = \rho(kT)$ as follows

$$\frac{1}{\rho_{k+1}} = \xi_k + \frac{\eta_k}{\rho_k},$$

where

$$\eta_k = \exp\left(-\int_{kT}^{(k+1)T} (a(s, x_m) + \Sigma(s))ds\right), \quad \xi_k = \eta_k \int_{kT}^{(k+1)T} \exp\left(\int_{kT}^s (a(\theta, x_m) + \Sigma(\theta))d\theta\right)ds.$$

From the $T-$periodicity of a and the fact that $\Sigma(t) \to 0$ we obtain easily that $\eta_k \to \eta$ and $\xi_k \to \xi$ as $k \to \infty$, where

$$\eta = \exp\left(-\int_0^T a(t, x_m)dt\right), \quad \xi = \eta \int_0^T \exp\left(\int_0^t a(\theta, x_m)d\theta\right)dt.$$

From these convergences we have that for all $\epsilon > 0$, there exists K_ϵ such that

$$\xi - \epsilon \le \xi_k \le \xi + \epsilon, \qquad \eta - \epsilon \le \eta_k \le \eta + \epsilon, \quad \forall\, k \ge K_\epsilon,$$

which implies

$$\xi - \epsilon + \frac{\eta - \epsilon}{\rho_k} \le \frac{1}{\rho_{k+1}} \le \xi + \epsilon + \frac{\eta + \epsilon}{\rho_k}.$$

Note $\kappa_k = \dfrac{1}{\rho_k}$ then

$$\xi - \epsilon + (\eta - \epsilon)\kappa_k \le \kappa_{k+1} \le \xi + \epsilon + (\eta + \epsilon)\kappa_k. \tag{1.18}$$

From the inequality at the right hand side of (1.18), denoting $\kappa^* = \limsup_{k \to +\infty} \kappa_k$, we obtain

$$\kappa^* \le \xi + \epsilon + (\eta + \epsilon)\kappa^*, \qquad \forall \epsilon > 0.$$

Then thanks to assumption (H2), which implies $\eta < 1$, we have

$$\kappa^* \le \frac{\xi}{1 - \eta}.$$

Analogously, from the left hand side inequality in (1.18), and denoting $\kappa_* = \liminf_{k\to+\infty} \kappa_k$, we deduce that

$$\kappa_* \geq \frac{\xi}{1-\eta}.$$

Since $\kappa_* \leq \kappa^*$, we obtain

$$\kappa^* = \kappa_* = \lim_{k\to+\infty} \kappa_k = \frac{\xi}{1-\eta}.$$

Going back to variable ρ_k, it implies

$$\lim_{k\to\infty} \rho_k = \frac{1-\eta}{\xi}.$$

Finally we can make a translation from ρ_0 to obtain

$$\widetilde{\varrho}(t) = \lim_{k\to\infty} \rho(kT+t),$$

with $\widetilde{\varrho}(t)$ the unique periodic solution of equation (1.3) given by (2.65).

■

Finally we prove Lemma 1.5.

Proof. Let $K = \{x \in \mathbb{R}^d : |x| \leq R_0\}$ for R_0 as in assumption (H5) then

$$\int_{\mathbb{R}^d} \frac{n(t,x)a(t,x)}{\rho(t)}dx = \frac{\displaystyle\int_{\mathbb{R}^d} p_0(t,x)e^{t\mu(x)-\int_0^t \rho(s)ds}a(t,x)dx}{\displaystyle\int_{\mathbb{R}^d} p_0(t,x)e^{t\mu(x)-\int_0^t \rho(s)ds}dx} = \frac{\displaystyle\int_{K^c} p_0(t,x)e^{t\mu(x)}a(t,x)dx + \int_K p_0(t,x)e^{t\mu(x)}a(t,x)dx}{\displaystyle\int_{K^c} p_0(t,x)e^{t\mu(x)}dx + \int_K p_0(t,x)e^{t\mu(x)}dx}.$$

Thanks to (1.2) and assumptions (H1), (H3) and (H5) we can control the integral terms taken outside the compact set K as follows

$$\int_{K^c} p_0(t,x)e^{t\mu(x)}a(t,x)dx \leq \|a\|_{L^\infty} e^{-\delta t}\int_{K^c} n_0(x)dx \leq Ce^{-\delta t}\int_{K^c} e^{-C_2|x|}dx \longrightarrow 0, \quad \text{as } t\to\infty, \tag{1.19}$$

and an analogous inequality holds for $\int_{K^c} p_0(t,x)e^{t\mu(x)}dx$. Next for the remaining terms, we use Taylor expansions around the point $x = x_m$ until third order terms, for x_m given by (H2), that is,

$$\begin{aligned} I(t) &= \int_K p_0(t,x)e^{t\mu(x)}a(t,x)dx \\ &= \int_K \Big[a(t,x_m) + \nabla a(t,x_m)(x-x_m) + \frac{1}{2}\,{}^t(x-x_m)D^2a(t,x_m)(x-x_m) + O(|x-x_m|^3)\Big] \\ &\quad \cdot \Big[p_0(t,x_m) + \nabla p_0(t,x_m)(x-x_m) + \frac{1}{2}\,{}^t(x-x_m)D^2a(t,x_m)(x-x_m) + O(|x-x_m|^3)\Big] \\ &\quad \cdot\exp\Big\{\frac{t}{2}\,{}^t(x-x_m)D^2\mu(x_m)(x-x_m) + tO(|x-x_m|^3)\Big\}\,dx, \end{aligned}$$

where ${}^t x$ indicates the transpose vector of x.
We organize $I(t)$ by powers of $|x - x_m|$ as below

$$\begin{aligned}
I_0(t) &= a(t,x_m)p_0(t,x_m)\int_K e^{\frac{t}{2}\,{}^t(x-x_m)D^2\mu(x_m)(x-x_m)}dx,\\
I_1(t) &= \int_K \left[a(t,x_m)\nabla p_0(t,x_m) + p_0(t,x_m)\nabla a(t,x_m)\right](x-x_m)e^{\frac{t}{2}\,{}^t(x-x_m)D^2\mu(x_m)(x-x_m)}dx = 0,\\
I_2(t) &= \int_K \Big\{ {}^t(x-x_m)\left[\frac{1}{2}a(t,x_m)D^2p_0(t,x_m) + {}^t\nabla a(t,x_m)\nabla p_0(t,x_m) + \frac{1}{2}p_0(t,x_m)D^2a(t,x_m)\right](x-x_m)\\
&\qquad \cdot e^{\frac{t}{2}\,{}^t(x-x_m)D^2\mu(x_m)(x-x_m)}\Big\}dx,\\
I_3(t) &= \int_K (1+t)O(|x-x_m|^3)e^{\frac{t}{2}\,{}^t(x-x_m)D^2\mu(x_m)(x-x_m)}dx.
\end{aligned}$$

By performing a change of variables as $y = \sqrt{t}(x - x_m)$ we obtain for the non null integrals

$$I_0(t) = \frac{1}{t^{d/2}}a(t,x_m)p_0(t,x_m)\int_{\widetilde{K}_t} e^{\frac{1}{2}\,{}^t yD^2\mu(x_m)y}dy,$$

$$I_2(t) = \frac{1}{t^{d/2+1}}\int_{\widetilde{K}_t} {}^t y\left[\frac{1}{2}a(t,x_m)D^2p_0(t,x_m) + {}^t\nabla a(t,x_m)\nabla p_0(t,x_m) + \frac{1}{2}p_0(t,x_m)D^2a(t,x_m)\right]ye^{\frac{1}{2}\,{}^t yD^2\mu(x_m)y}dy,$$

$$I_3(t) = \frac{1+t}{t^{\frac{d+3}{2}}}\int_{\widetilde{K}_t} O(|y|^3)e^{\frac{1}{2}\,{}^t yD^2\mu(x_m)y}dy \approx O\left(\frac{1}{t^{\frac{d+1}{2}}}\right),$$

with $\widetilde{K}_t = \{x \in \mathbb{R}^d : |x| \le \sqrt{t}R_0\}$.
Note that $I_1(t) = 0$ because it is the integral of an odd function in a symmetric interval. Moreover we obtain the approximation for $I_3(t)$ thanks to assumption (H6), which implies that the derivatives of μ and a, and consequently p_0, up to order 3, are globally bounded.
Moreover, if we denote $A(t) = \Big(\alpha_{ij}(t)\Big)_{i,j}$ the periodic matrix inside the crochets in $I_2(t)$, i.e

$$A(t) = \frac{1}{2}a(t,x_m)D^2p_0(t,x_m) + {}^t\nabla a(t,x_m)\nabla p_0(t,x_m) + \frac{1}{2}p_0(t,x_m)D^2a(t,x_m),$$

we obtain, thanks to the periodicity of a and p_0, that all the coefficients of $A(t)$ are bounded as $t \to \infty$. Moreover,

$$\left|{}^t yA(t)y\right| = \left|\sum_{i,j=1}^d \alpha_{ij}(t)y_iy_j\right| \le \sum_{i,j=1}^d |\alpha_{ij}(t)||y_i||y_j| \le C|y|^2, \text{ for some } C > 0.$$

Then for I_2 we have, by using (H4)

$$|I_2(t)| \le \frac{C}{t^{d/2+1}}\int_{\widetilde{K}_t} |y|^2 e^{\frac{1}{2}\,{}^t yD^2\mu(x_m)y}dy \approx O\left(\frac{1}{t^{d/2+1}}\right) \qquad \text{as} \qquad t \to \infty.$$

By arguing in the same way we obtain for the denominator term

$$\int_K p_0(t,x)e^{t\mu(x)}dx = \frac{1}{t^{d/2}}p_0(t,x_m)\int_{\widetilde{K}_t} e^{\frac{1}{2}\,{}^t yD^2\mu(x_m)y}dy + O\left(\frac{1}{t^{\frac{d+1}{2}}}\right),$$

and we conclude multiplying by $t^{d/2}$ and using again (H4)

$$\int_{\mathbb{R}^d} \frac{n(t,x)a(t,x)}{\rho(t)}dx = \frac{a(t,x_m)p_0(t,x_m)\int_{\widetilde{K}_t} e^{\frac{y^2}{2}D^2\mu(x_m)}dy + O\left(\frac{1}{\sqrt{t}}\right)}{p_0(t,x_m)\int_{\widetilde{K}_t} e^{\frac{y^2}{2}D^2\mu(x_m)}dy + O\left(\frac{1}{\sqrt{t}}\right)} = a(t,x_m) + O\left(\frac{1}{\sqrt{t}}\right),$$

for t large enough.

■

1.2.2 Convergence to a Dirac mass

In this subsection we prove Proposition 1.1 (ii).

Proof. (ii)

We begin by defining

$$f(t,x) = \frac{n(t,x)}{\rho(t)} = \frac{p_0(t,x)e^{\mu(x)t}}{\int_{\mathbb{R}^d} p_0(t,x)e^{\mu(x)t}dx}.$$

Therefore, since $\int_{\mathbb{R}^d} f(t,x)dx = 1$, there exists a sub-sequence (f_{t_k}) that converges weakly to a measure ν, i.e.

$$\int_{\mathbb{R}^d} f_{t_k}\varphi dx \to \int_{\mathbb{R}^d} \nu\varphi dx \qquad \forall\, \varphi \in C_c(\mathbb{R}^d).$$

We first prove

$$\int_{\Omega_\zeta^c} \frac{n(t_k,x)}{\rho(t_k)}\varphi(x)dx \longrightarrow 0 \quad \text{as} \quad t_k \to \infty \quad \forall\, \varphi : \text{supp}\,\varphi \subset \Omega_\zeta^c, \quad \text{where} \quad \Omega_\zeta = \{x \in \mathbb{R}^d : |x - x_m| < \zeta\}. \tag{1.20}$$

We can rewrite the above integral as below

$$\int_{\Omega_\zeta^c} f(t,x)\varphi(x)dx = \frac{1}{\mathcal{I}(t)}\int_{\Omega_\zeta^c} p_0(t,x)e^{\mu(x)t}\varphi(x)dx,$$

where

$$\mathcal{I}(t) = \int_{\mathbb{R}^d} p_0(t,y)e^{\mu(y)t}dy.$$

We estimate $\mathcal{I}(t)$ using the Laplace's method for integration and the assumption (H4). It follows

$$\mathcal{I}(t) \sim \frac{e^{t\mu(x_m)}p_0(t,x_m)}{\sqrt{|\det H|}}\left(\frac{2\pi}{t}\right)^{d/2} \qquad \text{as} \quad t \to \infty,$$

with $\mu(x_m)$ the strict maximum that is attained at a single point thanks to assumption (H2), and H given by (H4). Since $p_0(t,x)$ is positive and periodic with respect to t, there exist positive constants K_1, K_2 such that

$$K_1\frac{e^{t\mu(x_m)}}{t^{d/2}} \le \mathcal{I}(t) \le K_2\frac{e^{t\mu(x_m)}}{t^{d/2}}.$$

Next we note that

$$t^{d/2}e^{-t\mu(x_m)}\int_{\Omega_\zeta^c} p_0(t,x)e^{\mu(x)t}\varphi(x)dx \longrightarrow 0, \quad \text{as } t \to +\infty,$$

since $\mu(x) - \mu(x_m) \leq -\beta$ for some $\beta > 0$, and φ has compact support, which immediately implies (1.20).
We deduce from (1.20) by letting $\zeta \to 0$, that as $t \to +\infty$ along subsequences

$$\frac{n(t,x)}{\rho(t)} \rightharpoonup \omega\delta(x - x_m).$$

We then prove that $\omega = 1$, and hence all the sequence converges to the same limit.

Let $K_R = \{x \in \mathbb{R}^d : |x| \leq R\}$, for $R > 0$.
We can write using (1.2) that

$$n(t,x) = n_0(x)e^{\int_0^t (a(s,x)-\rho(s))ds}. \tag{1.21}$$

Thanks to assumption (H3) and (H5), for $R_0 \leq R$, by making an analogous analysis to (1.19) we obtain

$$\int_{K_R^c} n(t,x)dx \to 0 \quad \text{as} \quad t \to +\infty.$$

Moreover, thanks to Section 1.2.1, we know that ρ converges to $\widetilde{\varrho}$, a periodic and positive function. Therefore, in long time, ρ is bounded from below and above by positive constants. We deduce that

$$\int_{K_R^c} f(t,x)dx = \int_{K_R^c} \frac{n(t,x)}{\rho(t)}dx \to 0 \quad \text{as} \quad t \to \infty.$$

Thanks to the above convergence and the fact that $\int_{\mathbb{R}^d} f(t,x)dx = 1$, we deduce that $\forall \zeta > 0$ there exists a compact set K and $t_0 > 0$ such that, for all $t \geq t_0$

$$1 - \zeta \leq \int_K f(t,x)dx.$$

Moreover, we know that f converges weakly to a measure $\omega\delta(x - x_m)$, thus choosing a smooth compactly supported function φ such that $\varphi(x) = 1$ if $x \in K$, $\varphi(x) = 0$ if $x \in (K')^c$ for another compact K' such that $K \subsetneq K'$ and $0 < \varphi(x) < 1$ for $x \in K' \setminus K$, we obtain

$$\int_{\mathbb{R}^d} f(t,x)\varphi(x)dx = \int_K f(t,x)dx + \int_{K^c} f(t,x)\varphi(x)dx \quad \longrightarrow \omega,$$

where the first term in the RHS is bigger than $1 - \zeta$ and the second one is positive. It follows that $1 - \zeta \leq \omega$, for all $0 < \zeta < 1$ and hence $\omega = 1$. We conclude that

$$\frac{n(t,x)}{\rho(t)} \rightharpoonup \delta(x - x_m) \quad \text{as} \quad t \to +\infty,$$

which implies, using the convergence result for ρ,

$$n(t,x) - \widetilde{\varrho}(t)\delta(x - x_m) \rightharpoonup 0 \quad \text{as} \quad t \to +\infty,$$

weakly in the sense of measures.

■

1.3 The case with mutations: long time behavior

In this section we study (1.1) with $\sigma > 0$ and provide the proof of Proposition 1.2.
To this end, we first introduce a linearized problem. Let n solve (1.1), we define $m(t,x) = n(t,x)e^{\int_0^t \rho(s)ds}$ which solves

$$\begin{cases} \partial_t m(t,x) - \sigma\Delta m(t,x) &= m(t,x)a(t,x), \quad (t,x) \in [0,+\infty) \times \mathbb{R}^d, \\ m(t=0,x) &= n_0(x), \end{cases} \tag{1.22}$$

and associate to (1.22) the parabolic eigenvalue problem (1.5). In Subsection 1.3.1, we provide a convergence result for (1.22). Next, using this property, we prove Proposition 1.2 in Subsection 1.3.2.

1.3.1 A convergence result for the linearized problem

In this section we provide a convergence result for the linearized problem.

Lemma 1.6 *Assume* (H1), (H3) *and* $(H5_\sigma)$. *Then,*

(i) there exists a unique principal eigenpair (λ, p) *for the problem* (1.5), *with* $p \in L^\infty(\mathbb{R} \times \mathbb{R}^d)$, *up to normalization of* p. *Moreover, the eigenfunction* $p(t,x)$ *is exponentially stable, i.e. there exist a constant* $\alpha > 0$ *such that the solution* $\overline{m}(t,x)$ *to problem* (1.22) *satisfies*

$$\|\overline{m}(t,x)e^{\lambda t} - \alpha p(t,x)\|_{L^\infty(\mathbb{R}^d)} \to 0 \quad \text{as } t \to \infty, \tag{1.23}$$

exponentially fast.

(ii) Moreover, let δ *and* R_0 *given by* $(H5_\sigma)$, *then we have*

$$p(t,x) \leq \|p\|_{L^\infty} e^{-\sqrt{\frac{\delta}{\sigma}}(|x|-R_0)}, \quad \forall (t,x) \in [0,+\infty) \times \mathbb{R}^d. \tag{1.24}$$

Proof. *The proof of (i).*
We will apply a result from [56] to equation

$$\partial_t \widetilde{m} - \sigma\Delta\widetilde{m} = \widetilde{m}[a(t,x) + \lambda + \delta], \quad (t,x) \in \mathbb{R} \times \mathbb{R}^d, \tag{1.25}$$

with δ given in assumption $(H5_\sigma)$. This result allows to show that there exists a unique principal eigenpair for the equation (1.25), with an eigenfunction which is exponentially stable.
Consider the problem

$$\begin{cases} \partial_t \widetilde{\phi}_R - \sigma\Delta\widetilde{\phi}_R &= \widetilde{\phi}_R[a + \lambda + \delta], \quad \text{in } \mathbb{R} \times B_R, \\ \widetilde{\phi}_R &= 0, \quad \text{on } \mathbb{R} \times \partial B_R. \end{cases} \tag{1.26}$$

Thanks to (H1) and $(H5_\sigma)$ we can choose R and $\delta > 0$ such that there exists $d_\delta > 0$

$$\|a(t,x) + \lambda + \delta\|_{L^\infty([0,+\infty)\times B_R)} < d_\delta, \quad a(t,x) + \lambda + \delta < 0, \quad \forall\, |x| \geq R_0.$$

Note that $\widetilde{\phi}_R = p_R e^{t(\delta - \lambda_R + \lambda)}$ is a positive entire solution to (1.26). Moreover, it satisfies the hypothesis (H1) of [56], that is

$$\frac{\|\widetilde{\phi}_R(t,\cdot)\|_{L^\infty(B_R)}}{\|\widetilde{\phi}_R(s,\cdot)\|_{L^\infty(B_R)}} = \frac{\|p_R(t,\cdot)\|_{L^\infty(B_R)}}{\|p_R(s,\cdot)\|_{L^\infty(B_R)}} e^{(\delta - \lambda_R + \lambda)(t-s)} \geq Ce^{(\delta - \lambda_R + \lambda)(t-s)}, \quad t \geq s,$$

with $\delta - \lambda_R + \lambda > 0$ for R large enough.
Therefore Theorem 2.1 (and its generalization Theorem 9.1) in [56] implies that there exists a unique positive entire solution $\widetilde{\phi}$ for problem (1.25), which is given by

$$\widetilde{\phi}(t,x) = \lim_{R\to\infty} \widetilde{\phi}_R(t,x).$$

Moreover, for $p = \widetilde{\phi}e^{-\delta t}$ we obtain

$$p(t,x) = \lim_{R\to\infty} p_R(t,x),$$

and since p_R is the solution of (1.6), then p is a positive periodic eigenfunction to (1.5).
Furthermore, Theorem 2.2 in [56] implies also that

$$\frac{\|\widetilde{m}(t,x) - \alpha\widetilde{\phi}(t,x)\|_{L^\infty(\mathbb{R}^d)}}{\|\widetilde{\phi}(t,\cdot)\|_{L^\infty(\mathbb{R}^d)}} \longrightarrow 0,$$

exponentially fast as $t \to \infty$.
Noting that every solution m of problem (1.22) can be written as $m = \widetilde{m}e^{-\lambda t - \delta t}$, we obtain

$$\|m(t,x)e^{\lambda t} - \alpha p(t,x)\|_{L^\infty(\mathbb{R}^d)} \longrightarrow 0 \quad \text{as} \quad t \to +\infty,$$

and this convergence is also exponentially fast.

The proof of (ii).
Next we prove (1.24) following similar arguments as in the proof of Lemma 2.4 in [89]. Let $\widetilde{a}(t,x) = a(t,x) + \lambda$ then p is a positive bounded solution of the following equation

$$\partial_t p - \sigma\Delta p = p\widetilde{a}(t,x), \quad \text{in } \mathbb{R}\times\mathbb{R}^d. \tag{1.27}$$

Note that we have defined p in $(-\infty, 0]$ by periodic prolongation. Let $\|p\|_{L^\infty(\mathbb{R}\times\mathbb{R}^d)} = M$. We define

$$\zeta(t,x) = Me^{-\delta(t-t_0)} + Me^{-\nu(|x|-R_0)},$$

where $\nu = \sqrt{\frac{\delta}{\sigma}}$ and R_0 is given by $(H5_\sigma)$. One can verify that

$$M \le \zeta(t,x) \quad \text{if } |x| = R_0 \text{ or } t = t_0.$$

Furthermore if $|x| > R_0$ or $t > t_0$ evaluating in (1.27) shows

$$\partial_t\zeta - \sigma\Delta\zeta - \zeta\widetilde{a}(t,x) = Me^{-\delta(t-t_0)}(-\delta - \widetilde{a}(t,x)) + Me^{-\nu(|x|-R_0)}\left(-\sigma\nu^2 - \widetilde{a}(t,x) + \sigma\nu\frac{d-1}{|x|}\right) \ge 0,$$

since $\widetilde{a}(t,x) \le -\delta$ thanks to assumption $(H5_\sigma)$. Thus ζ is a supersolution of (1.27) on

$$Q_0 = \{(t,x) \in (t_0,\infty)\times\mathbb{R}^d \,;\, |x| > R_0\},$$

which dominates p on the parabolic boundary of Q_0. Applying the maximum principle to $\zeta - p$, we obtain

$$p(t,x) \le Me^{-\delta(t-t_0)} + Me^{-\nu(|x|-R_0)}, \qquad |x| \ge R_0,\ t \in (t_0,\infty).$$

Taking the limit $t_0 \to -\infty$ yields

$$p(t,x) \leq Me^{-\nu(|x|-R_0)}, \qquad |x| \geq R_0,\ t \leq +\infty,$$

for $\nu = \sqrt{\frac{\delta}{\sigma}}$. We conclude that p satisfies (1.24).

■

1.3.2 The proof of Proposition 1.2

To prove Proposition 1.2 we first prove the following Lemmas.

Lemma 1.7 *Assume* (H1) *and* (H3) *and let* $C_3 = \sigma C_2^2 + d_0$ *then the solution* $n(t,x)$ *to equation* (1.1) *satisfies*

$$n(t,x) \leq \exp\left(C_1 - C_2|x| + C_3 t\right), \quad \forall (t,x) \in (0,+\infty) \times \mathbb{R}^d.$$

Proof. Define the function $\widetilde{n}(t,x) = \exp\left(C_1 - C_2|x| + C_3 t\right)$.
We prove that $n \leq \widetilde{n}$. To this end we proceed by a comparison argument. One can easily verify that for C_3 defined above, we have the following inequality

$$\partial_t \widetilde{n} - \sigma\Delta\widetilde{n} - \left[a(t,x) + \rho(t)\right]\widetilde{n} = e^{(C_1 - C_2|x| + C_3 t)}\left[C_3 - \sigma C_2^2 + \sigma\frac{C_2(d-1)}{|x|} - a(t,x) + \rho(t)\right] \geq 0, \quad \text{a.e in } \mathbb{R}\times\mathbb{R}^d.$$

Moreover, we have for $t = 0$, $n(0,x) \leq \widetilde{n}(0,x)$ thanks to assumption (H3). We can then apply a Maximum Principle, in the class of L^2 functions, and we conclude that

$$n(t,x) \leq \widetilde{n}(t,x), \quad \forall (t,x) \in (0,+\infty) \times \mathbb{R}^d.$$

■

Lemma 1.8 *Assume* (H1), (H3) *and* $(H5_\sigma)$ *then*

$$\left| \int_{\mathbb{R}^d} \frac{n(t,x)a(t,x)}{\rho(t)} dx - Q(t) \right| \longrightarrow 0, \quad \text{as } t \to +\infty,$$

with $Q(t)$ given by (1.7).
Proof. From (1.23), we obtain that

$$n(t,x)e^{\int_0^t \rho(s)ds + \lambda t} = \alpha p(t,x) + \Sigma(t,x),$$

with $\|\Sigma(t,x)\|_{L^\infty} \to 0$ exponentially fast, as $t \to \infty$.
We define the compact set $K_t = \{x \in \mathbb{R}^d : |x| \leq At\}$, for some $A >> 1$ large enough and compute

$$\frac{1}{\rho(t)}\int_{\mathbb{R}^d} n(t,x)a(t,x)dx = \frac{\displaystyle\int_{K_t} \alpha p(t,x)a(t,x)dx + \int_{K_t} \Sigma(t,x)a(t,x)dx + \int_{K_t^c} \left(\alpha p(t,x) + \Sigma(t,x)\right)a(t,x)\ dx}{\displaystyle\int_{K_t} \alpha p(t,x)dx + \int_{K_t} \Sigma(t,x)dx + \int_{K_t^c} \left(\alpha p(t,x) + \Sigma(t,x)\right)\ dx}.$$

We then notice that

$$\left| \int_{K_t} \Sigma(t,x)a(t,x)dx \right| \leq \|a\|_{L^\infty}\|\Sigma(t,\cdot)\|_{L^\infty}|K_t| \to 0 \quad \text{as } t \to \infty,$$

since $\|\Sigma(t,\cdot)\|_{L^\infty}$ converges exponentially fast to zero and the measure of K_t is at most algebraic in t. Making the same analysis for $\left|\int_{K_t}\Sigma(t,x)dx\right|$ it will just remain to prove that the integral terms taken outside the compact set K_t vanish as $t\to+\infty$.

We have, trivially

$$\left|\int_{K_t^c}(\alpha p(t,x)+\Sigma(t,x))a(t,x)dx\right|\leq\|a\|_{L^\infty}\left|\int_{K_t^c}n(t,x)e^{\int_0^t(\rho(s)+\lambda)ds}dx\right|.$$

Then we use Lemma 1.7 to obtain

$$\int_{K_t^c}n(t,x)e^{\int_0^t(\rho(s)+\lambda)ds}dx\leq\int_{K_t^c}e^{C_1-C_2|x|+Mt}dx\leq e^{C_1+Mt}\int_{K_t^c}e^{-C_2|x|}dx\to 0,\quad\text{as } t\to+\infty.$$

for $A>M$ large enough, where $M\geq\rho_M+\lambda+C_3$.

Combining the last two inequalities we obtain that the integral terms taken outside the compact, vanish as $t\to+\infty$. This concludes the proof.

■

Proof of Proposition 1.2

Convergence of ρ.

By integrating equation (1.1) in x, we obtain that

$$\int_{\mathbb{R}^d}\partial_t n(t,x)dx=\int_{\mathbb{R}^d}n(t,x)[a(t,x)-\rho(t)]dx,$$

and using Lemma 1.8 we deduce that

$$\frac{d\rho}{dt}=\rho(t)\left[\int_{\mathbb{R}^d}\frac{n(t,x)a(t,x)}{\rho(t)}dx-\rho(t)\right]=\rho(t)\left[Q(t)+\Sigma'(t)-\rho(t)\right],$$

where $\Sigma'(t)\to 0$ exponentially as $t\to\infty$, and $Q(t)$ is given by (1.7).

Following similar arguments as in the proof of Proposition 1.1 we obtain $|\rho(t)-\widetilde{\rho}(t)|\to 0$ as $t\to\infty$, with $\widetilde{\rho}$ the unique solution of

$$\begin{cases}\dfrac{d\widetilde{\rho}}{dt}=\widetilde{\rho}(t)\left[Q(t)-\widetilde{\rho}(t)\right],\\ \widetilde{\rho}(0)=\widetilde{\rho}(T),\end{cases}$$

provided $\displaystyle\int_0^T Q(t)dt>0$. Moreover if $\displaystyle\int_0^T Q(t)dt\leq 0$, then $\rho(t)\to 0$ as $t\to\infty$. Note also that

$$\lambda=-\frac{1}{T}\int_0^T Q(t)dt. \tag{1.28}$$

We consider, indeed, the eigenvalue problem (1.5) and integrate it in $x\in\mathbb{R}^d$

$$\partial_t\int_{\mathbb{R}^d}p(t,x)dx=\int_{\mathbb{R}^d}a(t,x)p(t,x)dx+\lambda\int_{\mathbb{R}^d}p(t,x)dx.$$

We divide by $\int_{\mathbb{R}^d} p(t,x)dx$ and integrate now in $t \in [0,T]$, to obtain

$$\int_0^T \frac{\partial_t \int_{\mathbb{R}^d} p(t,x)dx}{\int_{\mathbb{R}^d} p(t,x)dx} dt = \int_0^T Q(t)dt + \lambda T,$$

which implies that

$$0 = \ln\left(\int_{\mathbb{R}^d} p(T,x)dx\right) - \ln\left(\int_{\mathbb{R}^d} p(0,x)dx\right) = \int_0^T Q(t)dt + \lambda T,$$

and hence (1.28).
This ends the proof of statements $(i) - (ii)$ of Proposition 1.2.

Convergence of $\frac{n}{\rho}$.
Let $K_t = \{x \in \mathbb{R}^d : |x| < At\}$, for $A > R_0$, as in the proof of Lemma 1.8, we can write

$$\frac{n(t,x)}{\rho(t)} = \frac{\alpha p(t,x) + \Sigma(t,x)}{\int_{K_t} (\alpha p(t,x) + \Sigma(t,x))\, dx + \int_{K_t^c} (\alpha p(t,x) + \Sigma(t,x))\, dx}.$$

Following similar arguments as in Lemma 1.8 we obtain that

$$\left\| \frac{n(t,x)}{\rho(t)} - P(t,x) \right\|_{L^\infty} \longrightarrow 0,$$

with $P(t,x)$ as in (1.7).
Consequently, when $\lambda < 0$ we obtain that

$$\|n(t,\cdot) - \widetilde{\rho}(t)P(t,\cdot)\|_{L^\infty} \longrightarrow 0 \qquad \text{as } t \to \infty,$$

and this concludes the proof of (iii).

■

1.4 Case $\sigma << 1$. Small mutations

In this section we choose $\sigma = \varepsilon^2$ and we prove that for ε small enough, the principal eigenvalue λ given in (1.5) is negative. As a consequence, thanks to Proposition 1.2, any solution of (1.9) converges to the unique periodic solution $(n_\varepsilon, \rho_\varepsilon)$. Next, we prove Theorem 1.4, which allows to characterize n_ε, as $\varepsilon \to 0$.
Consider now the problem (1.9) and let $(\lambda_\varepsilon, p_\varepsilon)$ be the eigenelements of problem (1.5) for $\sigma = \varepsilon^2$, then we have the following result.

Lemma 1.9 *Under assumption* (H2) *there exists $\lambda_m > 0$ and $\varepsilon_0 > 0$ such that for all $\varepsilon < \varepsilon_0$ we have $\lambda_\varepsilon \leq -\lambda_m$.*

Proof. We follow the proof for the case of bounded domains, given in [53].
For $R > 0$ define $B_R := B(x_m, R)$ and $a_R(t) = \min_{x \in \overline{B}_R} a(t,x)$. Then we choose R_1 small enough such that

$$\int_0^T a_{R_1}(t)dt > 0. \tag{1.29}$$

This is possible thanks to (H2) and the continuity of a with respect to x.
We first consider the periodic-parabolic Dirichlet eigenvalue problem on $[0,+\infty)\times B_{R_1}$,

$$\begin{cases} \partial_t \underline{w} - \varepsilon^2 \Delta \underline{w} - a_{R_1}(t)\underline{w} = \underline{\mu_\varepsilon}\,\underline{w}, & \text{in } [0,+\infty)\times B_{R_1}, \\ \underline{w} = 0, & \text{on } [0,+\infty)\times \partial B_{R_1}, \\ \underline{w} :\ T-\text{periodic in } t. \end{cases} \tag{1.30}$$

We calculate $\underline{\mu_\varepsilon}$ by the Ansatz $\underline{w}(t,x)=\alpha(t)\varphi_1(x)$ where $\varphi_1>0$ is the principal eigenfunction of

$$\begin{cases} -\Delta\varphi_1 &= \gamma_1\varphi_1, & \text{in } B_{R_1}, \\ \varphi_1 &= 0, & \text{on } \partial B_{R_1}, \end{cases}$$

with principal eigenvalue $\gamma_1>0$. By substituting in (1.30) we deduce that

$$\alpha'(t)\varphi_1 + \gamma_1\varepsilon^2\alpha(t)\varphi_1 - a_{R_1}(t)\alpha(t)\varphi_1 = \underline{\mu_\varepsilon}\alpha(t)\varphi_1,$$

and consequently

$$\alpha(t) = \alpha(0)\exp\left(\int_0^t a_{R_1}(\tau)d\tau - (\gamma_1\varepsilon^2 - \underline{\mu_\varepsilon})t\right).$$

For $\underline{w}$ to be $T-$periodic we must have

$$\int_0^T a_{R_1}(\tau)d\tau - \gamma_1\varepsilon^2 T + T\underline{\mu_\varepsilon} = 0.$$

We deduce indeed that choosing

$$\underline{\mu_\varepsilon} = \gamma_1\varepsilon^2 - \frac{1}{T}\int_0^T a_{R_1}(t)dt,$$

we obtain the principal eigen-pair $(\underline{w},\underline{\mu_\varepsilon})$ for (1.30). Next we consider the periodic-parabolic eigenvalue problem

$$\begin{cases} \partial_t w - \varepsilon^2\Delta w - a(t,x)w = \lambda_{R_1} w, & \text{in } [0,+\infty)\times B_{R_1}, \\ w = 0, & \text{on } [0,+\infty)\times \partial B_{R_1}, \\ w :\ T-\text{periodic in } t. \end{cases}$$

Since $a_{R_1}(t)\le a(t,x)$ on $[0,+\infty)\times B_{R_1}$ we have $\lambda_{R_1}\le\underline{\mu_\varepsilon}$ (Lemma 15.5 [53]). By monotony of eigenvalues with respect to the domain we obtain $\lambda_\varepsilon\le\lambda_{R_1}\le\underline{\mu_\varepsilon}$. Finally, thanks to (1.29) we conclude that there exist $\lambda_m>0$, $\varepsilon_0>0$ such that for all $\varepsilon\le\varepsilon_0$, we have $\lambda_\varepsilon\le-\lambda_m$.

■

In the following subsections we provide the proof of Theorem 1.4. In Subsection 1.4.1, we give some global bounds for ρ_ε. Next, in Subsection 1.4.2, we prove that (u_ε) is locally uniformly bounded, Lipschitz with respect to x and locally equicontinuous in time. In the last subsection we conclude the proof of Theorem 1.4 letting ε goes to zero and describing the limits of u_ε, n_ε and ρ_ε.

1.4.1 Uniform bounds for ρ_ε

In this section we provide uniform bounds for ρ_ε.

Lemma 1.10 *Assume* (H1), $(H5_\sigma)$. *Then for every $\varepsilon>0$, there exist positive constants ρ_m and ρ_M such that*

$$0<\rho_m\le\rho_\varepsilon(t)\le\rho_M \quad \forall t\ge 0. \tag{1.31}$$

Proof. From equation (1.9) integrating in $x \in \mathbb{R}^d$ and using assumption (H1) we get

$$\frac{d\rho_\varepsilon}{dt} = \int_{\mathbb{R}^d} n_\varepsilon(t,x)[a(t,x) - \rho_\varepsilon(t)dx] \leq \rho_\varepsilon(t)[d_0 - \rho_\varepsilon(t)]. \tag{1.32}$$

This implies that

$$\rho_\varepsilon(t) \leq \rho_M := \max(\rho_\varepsilon^0, d_0).$$

To obtain the lower bound we recall that $n_\varepsilon(t,x) = \rho_\varepsilon(t)P_\varepsilon(t,x)$, with $\rho_\varepsilon(t)$ the unique periodic solution of

$$\frac{d\rho_\varepsilon}{dt} = \rho_\varepsilon(t)[Q_\varepsilon(t) - \rho_\varepsilon(t)],$$

and with $Q_\varepsilon(t)$ and $P_\varepsilon(t,x)$ given by (1.7). From (2.65) we know that

$$\rho_\varepsilon(t) = \frac{1 - \exp\left[-\int_0^T Q_\varepsilon(s)ds\right]}{\exp\left[-\int_0^T Q_\varepsilon(s)ds\right]\int_t^{t+T} \exp\left[\int_t^s Q_\varepsilon(\theta)d\theta\right]ds}. \tag{1.33}$$

From Lemma 1.9, we note that, $\lambda_\varepsilon = -\frac{1}{T}\int_0^T Q_\varepsilon(t)dt \leq -\lambda_m$, thus

$$\exp\left[-\int_0^T Q_\varepsilon(\theta)d\theta\right] \leq e^{-T\lambda_m}.$$

Also from (H1) and (1.7) we get

$$\int_t^{t+T} \exp\left[\int_t^s Q_\varepsilon(\theta)d\theta\right]ds \leq \int_t^{t+T} e^{d_0 T}ds = Te^{d_0 T}.$$

Combining the above inequalities with (1.33) we obtain

$$0 < \rho_m := \frac{1}{T}e^{-d_0 T}\left(e^{\lambda_m T} - 1\right) \leq \rho_\varepsilon(t), \quad \forall\, t \geq 0.$$

■

1.4.2 Regularity results for u_ε

In this section we study the regularity properties of $u_\varepsilon = \varepsilon \ln\left((2\pi\varepsilon)^{d/2}n_\varepsilon\right)$, where n_ε is the unique periodic solution of equation (1.9).

Theorem 1.11 *Assume* (H1), (H2) *and* $(H5_\sigma)$. *Then* u_ε *is locally uniformly bounded and locally equicontinuous in time in* $[0,T]\times\mathbb{R}^d$. *Moreover, for some* $D > 0$, $\omega_\varepsilon = \sqrt{2D - u_\varepsilon}$, *is Lipschitz continuous with respect to* x *in* $(0,\infty)\times\mathbb{R}^d$ *and there exists a positive constant* C *such that we have the following*

$$|\nabla\omega_\varepsilon| \leq C, \quad \textit{in } [0,+\infty)\times\mathbb{R}^d, \tag{1.34}$$

$$\forall R > 0, \quad \sup_{0\leq s\leq t\leq T,\ x\in B_R} |u_\varepsilon(t,x) - u_\varepsilon(s,x)| \to 0 \quad \text{as } \varepsilon \to 0. \tag{1.35}$$

We prove this theorem in several steps.

1.4.2.1 An upper bound for u_ε

We recall from (1.8) that $n_\varepsilon(t,x) = \rho_\varepsilon(t)\dfrac{p_\varepsilon(t,x)}{\int_{\mathbb{R}^d} p_\varepsilon(t,x)dx}$, where

$$\begin{cases} \partial_t p_\varepsilon - \varepsilon^2\Delta p_\varepsilon - a(t,x)p_\varepsilon = \lambda_\varepsilon p_\varepsilon, \quad \text{in } \mathbb{R}\times\mathbb{R}^d, \\ 0 < p_\varepsilon : \ T-\text{periodic}, \\ \|p_\varepsilon(0,x)\|_{L^\infty(\mathbb{R}^d)} = 1. \end{cases} \tag{1.36}$$

Define $q_\varepsilon(t,x) = p_\varepsilon(t,x\varepsilon)$, which satisfies

$$\begin{cases} \partial_t q_\varepsilon - \Delta q_\varepsilon = a_\varepsilon(t,x)q_\varepsilon, \quad \text{in } \mathbb{R}\times\mathbb{R}^d, \\ q_\varepsilon : \quad T-\text{periodic}, \end{cases} \tag{1.37}$$

for $a_\varepsilon(t,x) = a(t,x\varepsilon) + \lambda_\varepsilon$. Note that a_ε is uniformly bounded thanks to the $L^\infty-$norm of a, which together with Lemma 1.9 implies that $-d_0 \le \lambda_\varepsilon \le -\lambda_m$.
Since $\|p_\varepsilon(0,x)\|_{L^\infty(\mathbb{R}^d)} = 1$ we can choose x_0 such that $p_\varepsilon(0,x_0) = 1$. Moreover q_ε is a nonnegative solution of (1.37) in $(0,2T)\times B(\frac{x_0}{\varepsilon},1)$. Let δ_0, be such that $0 < \delta_0 < T$, then we apply the Theorem 2.5 [55] which is an elliptic-type Harnack inequality for positive solutions of (1.37) in a bounded domain, and we have $\forall\ t \in [\delta_0, 2T]$

$$\sup_{x\in B(\frac{x_0}{\varepsilon},1)} q_\varepsilon(t,x) \le C \inf_{x\in B(\frac{x_0}{\varepsilon},1)} q_\varepsilon(t,x),$$

where $C = C(\delta_0, d_0)$. Returning to p_ε this implies

$$p_\varepsilon(t_0,x_0) \le \sup_{y\in B(x_0,\varepsilon)} p_\varepsilon(t_0,y) \le Cp_\varepsilon(t_0,x), \quad \forall (t_0,x) \in [\delta_0,2T]\times B(x_0,\varepsilon). \tag{1.38}$$

Since p_ε is $T-$periodic we conclude that the last inequality is satisfied $\forall\ t \in [0,T]$. From (1.31), (1.38) and the upper bound (1.24) for p_ε with $\sigma = \varepsilon^2$, we obtain

$$n_\varepsilon(0,x) \le \rho_M \frac{p_\varepsilon(0,x)}{\int_{\mathbb{R}^d} p_\varepsilon(0,x)dx} \le \frac{C\rho_M p_\varepsilon(0,x)}{\int_{B(x_0,\varepsilon)} p_\varepsilon(0,x_0)dx} \le \rho_M \frac{Cp_\varepsilon(0,x)}{|B(x_0,\varepsilon)|} \le C'\varepsilon^{-d}\exp^{\frac{C_1'-C_2'|x|}{\varepsilon}},$$

for all $\varepsilon \le \varepsilon_0$, with ε_0 small enough, where the constant C' depends on ρ_M, $\|p\|_{L^\infty(R^d)}$ and the constant C in (1.38) and C_1' and C_2' depend on the constants of hypothesis $(H5_\sigma)$. Next we proceed with a Maximum Principle argument as in Lemma 1.7 to obtain for every $(t,x) \in [0,+\infty)\times\mathbb{R}^d$ and $C_3 = (C_2')^2 + d_0$,

$$n_\varepsilon(t,x) \le C'\exp^{\frac{C_1'-C_2'|x|}{\varepsilon}+C_3 t}.$$

From here and the periodicity of u_ε, with an abuse of notation for the constants, we can write, for all $\varepsilon \le \varepsilon_0$

$$u_\varepsilon(t,x) \le C_1' - C_2'|x|, \quad \forall (t,x) \in [0,+\infty)\times\mathbb{R}^d. \tag{1.39}$$

1.4.2.2 A lower bound for u_ε

Using the bounds for a in (H1) and for ρ_ε in (1.31) we obtain for $\widetilde{C} = d_0 + \rho_M$

$$\partial_t n_\varepsilon - \varepsilon^2\Delta n_\varepsilon \ge -\widetilde{C}n_\varepsilon.$$

Let n_ε^* be the solution of the following heat equation

$$\begin{cases} \partial_t n_\varepsilon^* - \varepsilon^2 \Delta n_\varepsilon^* + \widetilde{C} n_\varepsilon^* = 0, \\ n_\varepsilon^*(0,x) = n_\varepsilon^0, \end{cases}$$

given explicitly by the Heat Kernel K,

$$n_\varepsilon^*(t,x) = e^{-\widetilde{C}t}\left(n_\varepsilon^0 * K\right) = \frac{e^{-\widetilde{C}t}}{\varepsilon^d (4\pi t)^{d/2}} \int_{\mathbb{R}^d} n_\varepsilon^0(y) e^{-\frac{|x-y|^2}{4t\varepsilon^2}} dy, \quad t > 0.$$

By a comparison principle we have $n_\varepsilon^*(t,x) \leq n_\varepsilon(t,x)$. Moreover, from (1.38) and (1.24) we deduce that

$$\varepsilon^{-d} \widetilde{C}_0 e^{-\frac{\widetilde{C}_1}{\varepsilon}} \leq \rho_m \frac{p_\varepsilon(0,x)}{\int_{\mathbb{R}^d} p_\varepsilon(0,x)dx} \leq n_\varepsilon(0,x) \quad \forall x \in B(x_0,\varepsilon),$$

for some positive constants $\widetilde{C}_0$ and $\widetilde{C}_1$ depending on $\|p\|_{L^\infty}$, ρ_m, δ, d_0, d, and R_0, and x_0 the point where $p_\varepsilon(0,x_0) = 1$. Then

$$\begin{aligned} n_\varepsilon(t,x) &\geq \frac{\widetilde{C}_0}{\varepsilon^{2d}(4\pi t)^{d/2}} e^{-\frac{\widetilde{C}_1 + \varepsilon \widetilde{C} t}{\varepsilon}} \int_{B(x_0,\varepsilon)} e^{-\frac{|x-y|^2}{4t\varepsilon^2}} dy \\ &\geq \frac{\widetilde{C}_0 |B(x_0,\varepsilon)|}{\varepsilon^{2d}(4\pi t)^{d/2}} e^{-\frac{2|x|^2 + 2(|x_0|+\varepsilon)^2}{4t\varepsilon^2} - \frac{\widetilde{C}_1 + \widetilde{C} t\varepsilon}{\varepsilon}}. \end{aligned}$$

This, together with the definition of u_ε, implies that

$$\varepsilon \log\left(\frac{\widetilde{C}_0 |B(x_0,\varepsilon)|}{\varepsilon^{2d}(4\pi t)^{d/2}}\right) - \frac{|x|^2 + (|x_0|+\varepsilon)^2}{2t\varepsilon} - (\widetilde{C}_1 + \widetilde{C} t\varepsilon) \leq u_\varepsilon(t,x), \quad \forall t \geq 0.$$

In particular, we obtain that

$$\varepsilon \log\left(\frac{\widetilde{C}_0 |B(x_0,\varepsilon)|}{\varepsilon^{3d/2}(4\pi t)^{d/2}}\right) - \frac{|x|^2 + (|x_0|+\varepsilon)^2}{2t} - (\widetilde{C}_1 + \widetilde{C} t) \leq u_\varepsilon(\frac{t}{\varepsilon}, x), \quad \forall t \in [1, 1+\varepsilon T],$$

and again, using the periodicity of u_ε, we obtain a quadratic lower bound for u_ε for all $t \geq 0$; that is, there exist A_1, $A_2 \geq 0$ and ε_0 such that for all $\varepsilon \leq \varepsilon_0$,

$$-A_1 |x|^2 - A_2 \leq u_\varepsilon(t,x). \tag{1.40}$$

1.4.2.3 Lipschitz bounds

In this section we prove (1.34). To this end we use a Bernstein type method closely related to the one used in [10]. Let $\omega_\varepsilon = \sqrt{2C_1' - u_\varepsilon}$, for C_1' given by (1.39), thus ω_ε satisfies

$$\frac{1}{\varepsilon}\partial_t \omega_\varepsilon - \varepsilon \Delta \omega_\varepsilon - \left(\frac{\varepsilon}{\omega_\varepsilon} - 2\omega_\varepsilon\right) |\nabla \omega_\varepsilon|^2 = \frac{a(t,x) - \rho_\varepsilon(t)}{-2\omega_\varepsilon}.$$

Define $W_\varepsilon = \nabla \omega_\varepsilon$, which is also $T-$periodic. We differentiate the above equation with respect to x and multiply by $\frac{W_\varepsilon}{|W_\varepsilon|}$, i.e

$$\frac{1}{\varepsilon}\partial_t |W_\varepsilon| - \varepsilon \Delta |W_\varepsilon| - 2\left(\frac{\varepsilon}{\omega_\varepsilon} - 2\omega_\varepsilon\right) W_\varepsilon \cdot \nabla |W_\varepsilon| + \left(\frac{\varepsilon}{\omega_\varepsilon^2} + 2\right) |W_\varepsilon|^3 \leq \frac{(a(t,x) - \rho_\varepsilon(t))\,|W_\varepsilon|}{2\omega_\varepsilon^2} - \frac{\nabla a \cdot W_\varepsilon}{2\omega_\varepsilon |W_\varepsilon|}.$$

From (1.39) we know that $u_\varepsilon \le C_1'$, which together with (1.40) implies

$$\sqrt{C_1'} \le \omega_\varepsilon \le \sqrt{2C_1' + A_1|x|^2 + A_2}.$$

It follows that

$$\left|2\left(\frac{\varepsilon}{\omega_\varepsilon} - 2\omega_\varepsilon\right)\right| \le A_4|x| + C_4,$$

for some constants A_4 and C_4, from where, we have for θ large enough

$$\frac{1}{\varepsilon}\partial_t|W_\varepsilon| - \varepsilon\Delta|W_\varepsilon| - \big(A_4|x| + C_4\big)\big|W_\varepsilon \cdot \nabla|W_\varepsilon|\big| + 2\left(|W_\varepsilon| - \theta\right)^3 \le 0. \tag{1.41}$$

Let $T_M > 2T$ and A_5 to be chosen later, define now, for $(t,x) \in \left(0, \frac{T_M}{\varepsilon}\right] \times B_R(0)$

$$\overline{W}(t,x) = \frac{1}{2\sqrt{t\varepsilon}} + \frac{A_5R^2}{R^2 - |x|^2} + \theta.$$

We next verify that $\overline{W}$ is a strict supersolution of (1.41) in $\left(0, \frac{T_M}{\varepsilon}\right] \times B_R(0)$. To this end we compute

$$\partial_t\overline{W} = -\frac{1}{4t\sqrt{t\varepsilon}}, \quad \nabla\overline{W} = \frac{2A_5R^2x}{(R^2-|x|^2)^2}, \quad \Delta\overline{W} = \frac{2A_5R^2d}{(R^2-|x|^2)^2} + \frac{8A_5R^2|x|^2}{(R^2-|x|^2)^3},$$

and then replace in (1.41) to obtain

$$\begin{aligned}
&\tfrac{1}{\varepsilon}\partial_t\overline{W} - \varepsilon\Delta\overline{W} - \big(A_4|x| + C_4\big)|\overline{W}\nabla\overline{W}| + 2\left(\overline{W} - \theta\right)^3 \\
&= -\tfrac{1}{4\varepsilon t\sqrt{\varepsilon t}} - \varepsilon\left[\tfrac{2A_5R^2d}{(R^2-|x|^2)^2} + \tfrac{8A_5R^2|x|^2}{(R^2-|x|^2)^3}\right] - \big(A_4|x| + C_4\big)\left(\tfrac{1}{2\sqrt{\varepsilon t}} + \tfrac{A_5R^2}{R^2-|x|^2} + \theta\right)\tfrac{2A_5R^2|x|}{(R^2-|x|^2)^2} + 2\left(\tfrac{1}{2\sqrt{\varepsilon t}} + \tfrac{A_5R^2}{R^2-|x|^2}\right)^3 \\
&\ge -\varepsilon\left[\tfrac{2A_5R^2d}{(R^2-|x|^2)^2} + \tfrac{8A_5R^4}{(R^2-|x|^2)^3}\right] - \big(A_4R + C_4\big)\left(\tfrac{1}{2\sqrt{\varepsilon t}} + \tfrac{A_5R^2}{R^2-|x|^2} + \theta\right)\tfrac{2A_5R^3}{(R^2-|x|^2)^2} \\
&\quad + \tfrac{3A_5R^2}{R^2-|x|^2}\left(\tfrac{1}{2t\varepsilon} + \tfrac{A_5R^2}{\sqrt{\varepsilon t}(R^2-|x|^2)}\right) + \tfrac{2A_5^3R^6}{(R^2-|x|^2)^3},
\end{aligned}$$

where we have used that $|x| \le R$. One can verify that the RHS of the above inequality is strictly positive for $R > 1$, $\varepsilon \le 1$, and $A_5 > C\sqrt{T_M}$ for certain constant C large enough. Therefore, $\overline{W}$ is a strict supersolution of (1.41) in $\left(0, \frac{T_M}{\varepsilon}\right] \times B_R(0)$ and for $\varepsilon \le 1$.
We next prove that

$$|W_\varepsilon(t,x)| \le \overline{W}(t,x) \quad \text{in } \left(0, \frac{T_M}{\varepsilon}\right] \times B_R(0).$$

To this end, we notice that $\overline{W}(t,x)$ goes to $+\infty$ as $|x| \to R$ or as $t \to 0$. Therefore, $|W_\varepsilon|(t,x) - \overline{W}(t,x)$ attains its maximum at an interior point of $\left(0, \frac{T_M}{\varepsilon}\right] \times B_R(0)$. We choose $t_m \le \frac{T_M}{\varepsilon}$ the smallest time such that the maximum of $|W_\varepsilon|(t,x) - \overline{W}(t,x)$ in the set $(0,t_m] \times B_R(0)$ is equal to 0. If such t_m does not exist, we are done.

Let x_m be such that $|W_\varepsilon|(t,x) - \overline{W}(t,x) \le |W_\varepsilon|(t_m,x_m) - \overline{W}(t_m,x_m) = 0$ for all $(t,x) \in (0,t_m) \times B_R(0)$. At such point, we have

$$0 \le \partial_t\big(|W_\varepsilon| - \overline{W}\big)(t_m,x_m), \quad 0 \le -\Delta\big(|W_\varepsilon| - \overline{W}\big)(t_m,x_m), \quad |W_\varepsilon|(t_m,x_m)\nabla|W_\varepsilon|(t_m,x_m) = \overline{W}(t_m,x_m))\nabla\overline{W}(t_m,x_m).$$

Combining the above properties with the facts that $|W_\varepsilon|$ and $\overline{W}$ are respectively sub and strict supersolution of (1.41), we obtain that

$$(|W_\varepsilon|(t_m,x_m)-\theta)^3-(\overline{W}(t_m,x_m)-\theta)^3<0\Rightarrow|W_\varepsilon|(t_m,x_m)<\overline{W}(t_m,x_m),$$

which is in contradiction with the choice of (t_m,x_m). We deduce, then that

$$|W_\varepsilon(t,x)|\leq\frac{1}{2\sqrt{\varepsilon t}}+\frac{A_5R^2}{R^2-|x|^2}+\theta\quad\text{for }(t,x)\in\left(0,\frac{T_M}{\varepsilon}\right]\times B_R(0),\ \forall\ R>1.$$

We note that for $\varepsilon<\varepsilon_0$ small enough we have $\frac{T_M}{\varepsilon}>\frac{2T}{\varepsilon}>\frac{T}{\varepsilon}+T>\frac{T}{\varepsilon}$. Letting $R\to\infty$ we deduce that

$$|W_\varepsilon(t,x)|\leq\frac{1}{2\sqrt{\varepsilon t}}+A_5+\theta\leq\frac{1}{2\sqrt{T}}+A_5+\theta\quad\text{for }(t,x)\in\left[\frac{T}{\varepsilon},\frac{T}{\varepsilon}+T\right]\times\mathbb{R}^d.$$

Finally we use the periodicity of W_ε to extend the result for all $t\in[0,+\infty)$ and we obtain (1.34).

1.4.2.4 Equicontinuity in time

From the above uniform bounds and continuity results we can also deduce uniform equicontinuity in time for the family u_ε on compact subsets of $]0,+\infty]\times\mathbb{R}^d$ and prove (1.35). We follow a method introduced in [9].
We will prove that for any $\eta>0$, we can find constants A, B large enough such that: for any $x\in B(0,R/2)$, $s\in[0,T]$, and for all $\varepsilon<\varepsilon_0$ we have

$$u_\varepsilon(t,y)-u_\varepsilon(s,x)\leq\eta+A|x-y|^2+\varepsilon B(t-s),\forall(t,y)\in[s,T]\times B_R(0),\tag{1.42}$$

and

$$u_\varepsilon(t,y)-u_\varepsilon(s,x)\geq-\eta-A|x-y|^2-\varepsilon B(t-s),\forall(t,y)\in[s,T]\times B_R(0).\tag{1.43}$$

We provide the proof of (1.42). One can prove (1.43) following similar arguments.
Fix (s,x) in $[0,T[\times B_{R/2}(0)$. Define

$$\widehat{\xi}(t,y)=u_\varepsilon(s,x)+\eta+A|x-y|^2+\varepsilon B(t-s),\quad(t,y)\in[s,T[\times B_R(0),$$

where A and B are constants to be determined. We prove that, for A and B large enough, $\widehat{\xi}$ is a super-solution to (1.14) on $[s,T]\times B_R(0)$ and $\widehat{\xi}(t,y)>u_\varepsilon(t,y)$ for $(t,y)\in\{s\}\times B_R(0)\cup[s,T]\times\partial B_R(0)$.
According to the previous section, $\{u_\varepsilon\}_\varepsilon$ is locally uniformly bounded, so we can take a constant A such that for all $\varepsilon<\varepsilon_0$,

$$\frac{8\|u_\varepsilon\|_{L^\infty([0,T]\times B_R(0))}}{R^2}\leq A.$$

With this choice, $\widehat{\xi}(t,y)>u_\varepsilon(t,y)$ on $[s,T]\times\partial B_R(0)$, for all $\eta>0$, $B>0$ and $x\in B_{R/2}(0)$.
Next we prove that, for A large enough, $\widehat{\xi}(s,y)>u_\varepsilon(s,y)$ for all $y\in B_R(0)$. We argue by contradiction. Assume that there exists $\eta>0$ such that for all constants A there exists $y_{A,\varepsilon}\in B_R(0)$ such that

$$u_\varepsilon(s,y_{A,\varepsilon})-u_\varepsilon(s,x)>\eta+A|y_{A,\varepsilon}-x|^2.\tag{1.44}$$

This implies

$$|y_{A,\varepsilon}-x|\leq\sqrt{\frac{2M}{A}}\longrightarrow0,\quad\text{as }A\to\infty.$$

Here M is an uniform upper bound for $\|u_\varepsilon\|_{L^\infty([0,T]\times B_R(0))}$. Then for all $h>0$, there exist A large enough and ε_0 small enough, such that $\forall \varepsilon<\varepsilon_0$,

$$|y_{A,\varepsilon}-x|\leq h.$$

Therefore, from the uniform continuity in space of u_ε taking h small enough, we obtain

$$|u_\varepsilon(s,y_{A,\varepsilon})-u_\varepsilon(s,x)|<\eta/2 \quad \forall \varepsilon\leq\varepsilon_0,$$

but this is a contradiction with (1.44). Therefore $\widehat{\xi}(s,y)>u_\varepsilon(s,y)$ for all $y\in B_R(0)$.
Finally, noting that R is bounded we deduce that for B large enough, $\widehat{\xi}$ is a super-solution to (1.14) in $[s,T]\times B_R(0)$. Using a comparison principle, since u_ε is also a solution of (1.14) we have

$$u_\varepsilon(t,y)\leq\widehat{\xi}(t,y) \quad \forall (t,y)\in[s,T]\times B_R(0).$$

Thus (1.42) is satisfied for $t\geq s\geq 0$. Then we put $x=y$ and obtain that for all $\eta>0$ there exists $\varepsilon_0>0$ such that for all $\varepsilon<\varepsilon_0$

$$|u_\varepsilon(t,x)-u_\varepsilon(s,x)|\leq\eta+\varepsilon B(t-s),$$

for every $0\leq s\leq t\leq T,\ x\in B_R(0)$. This implies that u_ε is locally equicontinuous in time. Moreover letting $\varepsilon\to 0$ we obtain (1.35).

1.4.3 Asymptotic behavior of u_ε

Using the regularity results in the previous section we can now describe the behavior of u_ε and ρ_ε as $\varepsilon\to 0$ and prove Theorem 1.4.

Step 1 (Convergence of u_ε and ρ_ε) According to Section 1.4.2, $\{u_\varepsilon\}$ is locally uniformly bounded and equicontinuous, so by the Arzela-Ascoli Theorem after extraction of a subsequence, $u_\varepsilon(t,x)$ converges locally uniformly to a continuous function $u(t,x)$. Moreover from (1.35), we obtain that u does not depend on t, i.e $u(t,x)=u(x)$.
Moreover, from the uniform bounds on ρ_ε we obtain using (1.32) that $|\frac{d\rho_\varepsilon}{dt}|$ is bounded too. Thus applying again the Arzela-Ascoli Theorem we can assure that $\rho_\varepsilon(t)$ converges, along subsequences, to a function $\rho(t)$ as $\varepsilon\to 0$.

Step 2 ($\max_{x\in\mathbb{R}^d}u(x)=0$) Assume that for some x_0 we have $0<\alpha\leq u(x_0)$. Since u is continuous, we have $u(y)\geq\frac{\alpha}{2}$ on $B(x_0,r)$ for some $r>0$. Thus, using the convergence of u_ε there exists ε_0 such that for all $\varepsilon\leq\varepsilon_0$ we have $u_\varepsilon(y)\geq\frac{\alpha}{4}$ on $B(x_0,r)$, which implies that

$$|B(x_0,r)|\exp\left(\frac{\alpha}{2\varepsilon}\right)\leq\int_{B(x_0,r)}\exp\left(\frac{u_\varepsilon}{\varepsilon}\right)dx\leq\int_{\mathbb{R}^d}n_\varepsilon(t,x)dx=\rho_\varepsilon(t).$$

Therefore $\rho_\varepsilon\to\infty$ as $\varepsilon\to 0$. This is in contradiction with (1.31). Thus $u(x)$ cannot be strictly greater than zero.
Next we have thanks to (1.39) that

$$\lim_{\varepsilon\to 0}\int_{|x|>R}n_\varepsilon(t,x)dx\leq\lim_{\varepsilon\to 0}\int_{|x|>R}e^{\frac{C_1'-C_2'|x|}{\varepsilon}}=0,$$

for R large enough.
From this and Lemma (1.10) we deduce that

$$\rho_m \leq \lim_{\varepsilon \to 0} \int_{|x| \leq R} n_\varepsilon(t,x)dx. \tag{1.45}$$

If $u(x) < 0$ for all $|x| < R$, then $u(x) < -\beta$ for some $\beta > 0$, since we know that u_ε converges locally uniformly to u, then there exists ε_0 small enough such that for all $\varepsilon \leq \varepsilon_0$, we have $u_\varepsilon(t,x) < -\frac{\beta}{2}$, $\forall |x| < R$. Therefore

$$\int_{|x| \leq R} e^{\frac{u_\varepsilon(t,x)}{\varepsilon}} dx \leq \int_{|x| \leq R} e^{-\frac{\beta}{2\varepsilon}} dx = |B(x_0,R)| e^{-\frac{\beta}{2\varepsilon}} \longrightarrow 0 \quad \text{as} \quad \varepsilon \to 0.$$

Note that this is in contradiction with (1.45). It follows that $\max_{x \in \mathbb{R}} u(x) = 0$.

Step 3 (The equation on u) We claim that $u(x) = \lim_{\varepsilon \to 0} u_\varepsilon(t,x)$ is a viscosity solution of problem (1.12). Here, we prove that u is a viscosity subsolution of (1.12). One can prove, following similar arguments, that u is also a viscosity supersolution of (1.12).
Let us define the auxiliary "cell problem"

$$\begin{cases} \partial_t v = a(t,x) - \rho(t) - \overline{a}(x) + \overline{\rho}, \quad (t,x) \in [0,+\infty) \times \mathbb{R}^d, \\ v(0,x) = 0, \\ v : T - periodic. \end{cases} \tag{1.46}$$

This equation has a unique smooth solution, that we can explicitly write

$$v(t,x) = -t(\overline{a}(x) - \overline{\rho}) + \int_0^t (a(t,x) - \rho(t))dt.$$

Let $\phi \in C^\infty$ be a test function and assume that $u - \phi$ has a strict local maximum at some point $x_0 \in \mathbb{R}^d$, with $u(x_0) = \phi(x_0)$. We must prove that

$$-|\nabla \phi|^2(x_0) - \overline{a}(x_0) + \overline{\rho} \leq 0. \tag{1.47}$$

We define the perturbed test function $\psi_\varepsilon(t,x) = \phi(x) + \varepsilon v(t,x)$, such that $u_\varepsilon - \psi_\varepsilon$ attains a local maximum at some point $(t_\varepsilon, x_\varepsilon)$. We note that ψ_ε converges to ϕ as $\varepsilon \to 0$ since v is locally bounded by definition, and hence one can choose x_ε such that $x_\varepsilon \to x_0$ as $\varepsilon \to 0$, (see Lemma 2.2 in [8]). Then ψ_ε satisfies

$$\frac{1}{\varepsilon}\partial_t \psi_\varepsilon(t_\varepsilon, x_\varepsilon) - \varepsilon \Delta \psi_\varepsilon(t_\varepsilon, x_\varepsilon) - \left|\nabla \psi_\varepsilon(t_\varepsilon, x_\varepsilon)\right|^2 - a(t_\varepsilon, x_\varepsilon) + \rho_\varepsilon(t_\varepsilon) \leq 0,$$

since u_ε is a viscosity solution of (1.14). The above line implies that

$$\partial_t v(t_\varepsilon, x_\varepsilon) - \varepsilon \Delta \phi(x_\varepsilon) - \varepsilon^2 \Delta v(t_\varepsilon, x_\varepsilon) - \left|\nabla \phi(x_\varepsilon) + \varepsilon \nabla v(t_\varepsilon, x_\varepsilon)\right|^2 - a(t_\varepsilon, x_\varepsilon) + \rho_\varepsilon(t_\varepsilon) \leq 0.$$

Using (1.46), this last equation becomes

$$-\varepsilon \Delta \phi(x_\varepsilon) - \varepsilon^2 \Delta v(t_\varepsilon, x_\varepsilon) - \left|\nabla \phi(x_\varepsilon) + \varepsilon \nabla v(t_\varepsilon, x_\varepsilon)\right|^2 + (\rho_\varepsilon - \rho)(t_\varepsilon) - \overline{a}(x_\varepsilon) + \overline{\rho} \leq 0. \tag{1.48}$$

We can now pass to the limit as $\varepsilon \to 0$. We know from step 1 that $\rho_\varepsilon \to \rho$ as $\varepsilon \to 0$. Moreover v is smooth with respect to x, with locally bounded derivatives with respect to x, thanks to its definition. Using these arguments and letting $\varepsilon \to 0$ in (1.48) we obtain (1.47) which implies that u is a viscosity sub-solution of (1.12).

Step 4 (Uniqueness and regularity of u) We first note that, for the case $x \in \mathbb{R}$, that is $d = 1$, the solution given by (1.13) solves (1.12).
In general, Hamilton-Jacobi equations of type (1.12), may admit more than one viscosity solution. In this case the uniqueness is guaranteed thanks to Proposition 5.4 of Chapter 5 in [72], which assures that, since the RHS of the first equation in (1.12) is null at just one point ($x = x_m$), and the value of u in this point is known ($u = 0$), together with the fact that $\max_{x\in\mathbb{R}^d} u(x) \leq 0$ the solution of (1.12) is unique and is given by

$$u(z) = \sup\Big\{u(x_m) - \int_0^{T_0} \sqrt{\overline{\rho} - \overline{a}(\xi(s))}ds;\ (T_0, \xi) \text{ such that } \xi(0) = x_m,\ \xi(T_0) = z,\ \Big|\frac{d\xi}{ds}\Big| \leq 1,\ \text{a.e in } [0, T_0],$$
$$\text{with } \xi(t) \in \mathbb{R}^d, \forall t \in [0, T_0]\Big\}.$$

Moreover, in the case $x \in \mathbb{R}$, one can verify that the above formula is equivalent with (1.13) and such solution u is $C(\mathbb{R})$ since $\overline{a}(x) \in C(\mathbb{R})$.

Step 5 (Convergence of n_ε) We deal in this step with the result for the convergence of n_ε. To this end we proceed as in Section 1.2.2.
Call $f_\varepsilon(t, x) = \dfrac{n_\varepsilon(t, x)}{\rho_\varepsilon(t)}$, then f_ε is uniformly bounded in $L^\infty(\mathbb{R}^+, L^1(\mathbb{R}^d))$. Next, we fix $t \geq 0$, and we follow the arguments of Section 1.2.2 to prove that $f_\varepsilon(t, \cdot)$, as function of x, converges, along subsequences, to a measure, as follows

$$f_\varepsilon(t, \cdot) \rightharpoonup \delta(\cdot - x_m) \quad \text{as} \quad \varepsilon \to 0,$$

weakly in the sense of measures in x.
Indeed, from (1.13) we deduce that

$$\max_{x\in\mathbb{R}^d} u(x) = u(x_m) = 0.$$

Then note $\mathcal{O} = \mathbb{R}^d \setminus B_\zeta(x_m)$, for ζ small enough and $\psi \in C_c(\mathcal{O})$, such that supp $\psi \subset \mathcal{K}$, for a compact set $\mathcal{K}$

$$\Big|\int_{\mathcal{O}} f_\varepsilon(t, x)\psi(x)dx\Big| \leq \frac{1}{\rho_m}\int_{\mathcal{O}} e^{\frac{u_\varepsilon(t,x)}{\varepsilon}}|\psi(x)|dx \leq \frac{1}{\rho_m}\int_{\mathcal{K}} e^{\frac{u_\varepsilon(t,x)}{\varepsilon}}|\psi(x)|dx.$$

From the locally uniform convergence of u_ε, since $u(x) \leq -\beta$, $\forall x \in \mathcal{K}$, we obtain that there exists $\varepsilon_0 > 0$ such that $\forall \varepsilon < \varepsilon_0$, $u_\varepsilon(t, x) \leq -\frac{\beta}{2}$, $\forall x \in \mathcal{K}$, and hence

$$\int_{\mathcal{K}} e^{\frac{u_\varepsilon(t,x)}{\varepsilon}}|\psi(x)|dx \leq \int_{\mathcal{K}} e^{-\frac{\beta}{2\varepsilon}}|\psi(x)|dx \to 0 \quad \text{as } \varepsilon \to 0,$$

since ψ is bounded in $\mathcal{K}$. Therefore, thanks to the L^1 bound of f_ε, we obtain that f_ε converges weakly in the sense of measures and along subsequences to $\omega\delta(x - x_m)$ as ε vanishes. We can proceed as in Section 1.2.2 to prove that the convergence is in fact to $\delta(x - x_m)$.
Therefore using the convergence result for ρ_ε we deduce finally (1.11).

Step 6 (Identification of the limit of ρ_ε) We try now to identify ρ from the explicit expression for ρ_ε. To this end we need to compute the limit of Q_ε. Let p_ε be the periodic solution of (1.36), we know that $p_\varepsilon(t, x) = \dfrac{n_\varepsilon(t, x)}{\rho_\varepsilon(t)}\displaystyle\int_{\mathbb{R}^d} p_\varepsilon(t, y)dy$.

Substituting in Q_ε we obtain

$$Q_\varepsilon(t) = \frac{\displaystyle\int_{\mathbb{R}^d} a(t,x)p_\varepsilon(t,x)dx}{\displaystyle\int_{\mathbb{R}^d} p_\varepsilon(t,x)dx} = \frac{\displaystyle\int_{\mathbb{R}^d} a(t,x)\frac{n_\varepsilon(t,x)}{\rho_\varepsilon(t)}\int_{\mathbb{R}^d} p_\varepsilon(t,y)dydx}{\displaystyle\int_{\mathbb{R}^d} p_\varepsilon(t,x)dx} = \frac{\displaystyle\int_{\mathbb{R}^d} a(t,x)n_\varepsilon(t,x)dx}{\rho_\varepsilon(t)}.$$

From (1.11) and (H2) we deduce that

$$\lim_{\varepsilon\to 0} Q_\varepsilon(t) = \lim_{\varepsilon\to 0}\int_{\mathbb{R}^d} f_\varepsilon(t,x)a(t,x)dx = a(t,x_m).$$

Finally we can pass to the limit in the expression (1.33) for ρ_ε, to obtain (2.65), which is in fact the unique periodic solution of the equation (1.3).

1.5 Approximation of the moments

In this section we estimate the moments of the population's distribution with a small error, in the case $x \in \mathbb{R}$. To this end, we will use the formal arguments given in Section 1.
Using (1.13), one can compute a Taylor expansion of order 4 around the point of maximum x_m

$$u(x) = -\frac{A}{2}(x-x_m)^2 + B(x-x_m)^3 + C(x-x_m)^4 + O(x-x_m)^5. \tag{1.49}$$

Note also that one can obtain v formally from (1.16) and compute the following expansions

$$v(t,x) = v(t,x_m) + D(t)(x-x_m) + E(t)(x-x_m)^2 + O(x-x_m)^3, \quad w(t,x) = F(t) + O(x-x_m)^2.$$

The above approximations of u, v and w around the maximum point of u allow us to estimate the moments of the population's distribution with an error of at most order $O(\varepsilon^2)$ as $\varepsilon \to 0$.
Replacing u_ε by the approximation (1.15) and using the Taylor expansions of u, v and w given above, we can compute

$$\begin{aligned}\int_{\mathbb{R}^d} (x-x_m)^k n_\varepsilon(t,x)dx \quad &= \frac{e^{v(t,x_m)}\varepsilon^{\frac{k}{2}}}{\sqrt{2\pi}} \quad \int_{\mathbb{R}^d} y^k e^{\frac{-Ay^2}{2}}\left[1+\sqrt{\varepsilon}\left(By^3+D(t)y\right)\right.\\ &\left.+\varepsilon\left(Cy^4+E(t)y^2+F(t)+\tfrac{1}{2}(By^3+D(t)y)^2\right)+o(\varepsilon)\right]dy.\end{aligned}$$

Note that, to compute the above integral, we performed a change of variable $x-x_m = \sqrt{\varepsilon}\, y$. Therefore each term $x-x_m$ can be considered as of order $\sqrt{\varepsilon}$ in the integration. Note also that we have used the approximation

$$n_\varepsilon(t,x) = \frac{1}{\sqrt{2\pi\varepsilon}} e^{\frac{u(x)}{\varepsilon}+v(t,x)+\varepsilon w(t,x)}.$$

The above computation leads in particular to the following approximations of the population size, the phenotypical mean and the variance

$$\begin{cases} \rho_\varepsilon = \displaystyle\int_{\mathbb{R}^d} n_\varepsilon(t,x)dx = \frac{e^{v(t,x_m)}}{\sqrt{A}}\left[1+\varepsilon\left(\frac{15B^2}{2A^3}+\frac{3(C+BD(t))}{A^2}+\frac{E(t)+0,5D(t)^2}{A}+F(t)\right)\right]+O(\varepsilon^2),\\ \mu_\varepsilon = \dfrac{1}{\rho_\varepsilon(t)}\displaystyle\int_{\mathbb{R}^d} x\; n_\varepsilon(t,x)dx = x_m + \varepsilon\left(\frac{3B}{A^2}+\frac{D(t)}{A}\right)+O(\varepsilon^2),\\ \sigma_\varepsilon^2 = \dfrac{1}{\rho_\varepsilon(t)}\displaystyle\int_{\mathbb{R}^d}(x-\mu_\varepsilon)^2 n_\varepsilon(t,x)dx = \frac{\varepsilon}{A}+O(\varepsilon^2).\end{cases}$$

1.6 Some biological examples

In this section, we present two examples where two different growth rates $a(t,x)$ are considered. In particular, the fluctuations act on different terms in the two examples, (they act respectively on the optimal trait and on the pressure of the selection).

We are motivated by a biological experiment in [60], where a population of bacterial pathogen *Serratia marcescens* was studied. In this experiment several populations of Serratia marcescens were kept in environments with constant or fluctuating temperature for several weeks. Then, their growth rates were measured in different environments. In particular, it was observed that a population of bacteria that evolved in periodically fluctuating temperature (daily variation between 24°C and 38°C, mean 31°C) outperforms the strains that evolved in constant temperature (31°C), when both strains are allowed to compete in a constant environment with temperature 31°C. Note that this is a surprising effect, since one expects that the population evolved in a constant environment would select for the best trait in such environment.

Here, we estimate the moments of the population's distribution and the mean effective fitness of the population in a constant enviroment for our two examples. We will observe that the second example, where the fluctuations act on the pressure of selection, allows to capture the phenomenon observed in the experiment in [60]. Our analysis shows that, in presence of the mutations and while the fluctuations act on the pressure of the selection, a fluctuating environment can select for a population with the same mean phenotypic trait but with smaller variance and in this way lead to more performant populations.

Note that our analysis is very well adapted to the mentioned experiment, since we first study the long time behavior of the phenotypical distribution and we find that it is the periodic solution of a selection-mutation equation. This distribution corresponds to the phenotypical distribution of a population evolved in a periodic environment. Next, we characterize such distribution assuming small mutations. We remark that, although our analysis provides a possible explanation for the observed experience in [60], one should go back to the biological experiment and compare the population's distribution with our results to test this interpretation.

1.6.1 Oscillations on the optimal trait

In this subsection we study a case where the optimal trait fluctuates periodically. We show that in this case, the population's phenotypical mean follows the optimal trait with a delay.

We choose, as periodic growth rate

$$a(t,x) = r - g(x - c\sin bt)^2,$$

where r, g, c and b are positive constants. Here r represents the maximal growth rate, g models the selection pressure and the term $c\sin bt$ models the oscillations of the optimal trait with period $\frac{2\pi}{b}$ and amplitude c.

We compute the mean of $a(t,x)$

$$\overline{a}(x) = \frac{b}{2\pi}\int_0^{\frac{2\pi}{b}} a(t,x)dt = r - g\left(x^2 + \frac{c^2}{2}\right),$$

and we observe that the maximum of $\overline{a}(x)$ is attained at $x_m = 0$.

From here we can also compute the mean population size $\overline{\rho}_\varepsilon$. We do not provide an explicit formula for ρ_ε, but only for its mean value, in order to keep the simpler expression, however, for the higher order moments we give the exact value until order 1 in ε.

Let $u(x)$ be given by (1.13), which can be rewritten in this specific example as follows

$$u(x) = -\left|\int_0^x \sqrt{gy^2}dy\right| = -\frac{\sqrt{g}}{2}x^2,$$

then we obtain, from (1.12) and the second equation in (1.16)

$$\overline{\varrho} = \overline{a}(0) = r - \frac{gc^2}{2}, \qquad \overline{k} = \Delta u(0) = -\sqrt{g}.$$

On the other hand, by substituting $u(x)$ in (1.49) we find $A = \sqrt{g}$, $B = C = 0$, and also by substitution in (1.16) we obtain

$$\int_0^{\frac{2\pi}{b}} \partial_x v(t,x)dt = 0, \quad \partial_t\partial_x v = 2gc\sin bt.$$

We deduce that

$$\partial_x v(0,x) = \frac{-2cg}{b} \quad \text{and} \quad \partial_x v(t,x) = -\frac{2cg}{b}\cos bt.$$

Now we are able to compute the approximations of order one with respect to ε of the population mean size $\overline{\rho}_\varepsilon$, the phenotypical mean μ_p and the variance σ_p^2 of the population's distribution, following the computations we have done in the previous section, that is

$$\mu_p(t) \approx \frac{2\varepsilon c}{b}\sqrt{g}\sin\left(bt - \frac{\pi}{2}\right), \quad \sigma_p^2 \approx \frac{\varepsilon}{\sqrt{g}}, \quad \overline{\rho}_\varepsilon \approx r - \frac{gc^2}{2} - \varepsilon\sqrt{g}.$$

We observe, in fact, that the mean trait $\mu_p(t)$ oscillates with the same period as the optimal trait with a delay $\frac{\pi}{2b}$, and a small amplitude, as was suggested for instance in [69].
We also compute $\widetilde{F}_p(\tau)$ the mean fitness of the population (evolved in the periodic environment), in an environment with temperature τ, and hence with growth rate $a(\tau, x)$

$$\widetilde{F}_p(\tau) = \int_{\mathbb{R}^d} a(\tau,x)\frac{1}{T}\int_0^T \frac{n_\varepsilon(t,x)}{\rho_\varepsilon(t)}dtdx, \tag{1.50}$$

which can be approximated for this example at $\tau = \frac{\pi}{b}$ by

$$\widetilde{F}_p(\pi/b) \approx r - \varepsilon\sqrt{g}.$$

Note that (1.50) is the quantity which has been measured in the experiment in [60].

We next consider a population which has evolved in a constant environment with $t = \frac{\pi}{b}$, (mean time), that is when the growth rate is given by $a(\pi/b, x) = r - gx^2$. With such constant in time growth rate, the density of the population's distribution converges in long time to the unique solution of the following stationary equation

$$\begin{cases} -\varepsilon^2\partial_{xx}n_c = n_c\big(r - gx^2 - \rho_c\big), \\ \rho_c = \int_{\mathbb{R}} n_c dx. \end{cases}$$

The solution of the above equation can be computed explicitly and is given by

$$n_c = \rho_c\frac{g^{\frac{1}{4}}}{\sqrt{2\pi\varepsilon}}\exp\left(\frac{-\sqrt{g}x^2}{2\varepsilon}\right), \quad \rho_c = r - \varepsilon\sqrt{g}.$$

We can then compute the population mean size $\overline{\rho}_c$, the mean trait μ_c and the variance σ_c^2 for such population

$$\mu_c = 0, \quad \sigma_c^2 = \frac{\varepsilon}{\sqrt{g}}, \quad \overline{\rho}_c = r - \varepsilon\sqrt{g}.$$

Here we observe that the size of a population evolved in a constant environment $\overline{\rho}_c$ is greater than the mean size of a population evolved in a fluctuating environment $\overline{\rho}_\varepsilon$.
Moreover, the mean fitness of such population, in an environment with the same temperature ($t = \frac{\pi}{b}$), can be computed as below

$$\widetilde{F}_c = \int_{\mathbb{R}} a(\pi/b, x)\frac{n_c(x)}{\rho_c}dx = r - \varepsilon\sqrt{g}.$$

We hence obtain that, independently of the choice of constants r, g and c, both populations (the one evolved in a constant environment and the other evolved in a fluctuating environment) have the same mean fitness at the same constant environment, up to order ε. This result does not correspond to what was observed in the experiment of [60]. In the next subsection we consider another example where the oscillations act differently on the growth rate and where the outcome corresponds more to the experiment of [60].

1.6.2 Oscillations on the pressure of the selection

In this subsection, we study an example where the fluctuations act on the pressure of the selection. We show that in this case a population evolved in a fluctuating environment (for instance with fluctuating temperature), may outperform a population evolved in a constant environment, in such constant environment.

Here, we consider the following periodic growth rate

$$a(t, x) = r - g(t)x^2,$$

where $r > 0$ is the maximal growth rate as in the previous example in Section 6.1 and $g(t)$ is a $1-$periodic function which models the oscillating pressure of selection.
Then $\overline{a}$ is given by

$$\overline{a}(x) = r - \overline{g}x^2 \quad \text{with} \quad \overline{g} = \int_0^1 g(t)dt,$$

where again the maximum of $\overline{a}(x)$ is attained at $x_m = 0$.
We compute u and $\partial_x v$ as before and obtain

$$u(x) = -\frac{\sqrt{\overline{g}}}{2}x^2, \quad \partial_x v(t, x) = 2x\left(t\overline{g} - \int_0^t g(t')dt' + \int_0^1\int_0^t g(t')dt'dt - \frac{\overline{g}}{2}\right).$$

We compute again $\overline{\varrho}$ and $\overline{k}$, from (1.12) and (1.16), in order to approximate $\overline{\rho}_\varepsilon$, that is

$$\overline{\varrho} = \overline{a}(0) = r, \quad \overline{k} = \Delta u(0) = -\sqrt{\overline{g}}.$$

Then from the expression of u, again with the help of the formula from the previous section we obtain $A = \sqrt{\overline{g}}$, $B = C = 0$ and $D(t) = 0$.
We next compute the approximations of order one with respect to ε of the population mean size $\overline{\rho}_\varepsilon$, the phenotypical mean μ_p and the variance σ_p^2 of the population's distribution which are given by

$$\mu_p \approx 0, \quad \sigma_p^2 \approx \frac{\varepsilon}{\sqrt{\overline{g}}}, \quad \overline{\rho}_\varepsilon \approx r - \varepsilon\sqrt{\overline{g}}.$$

Analogously to the previous example, we also compute $\widetilde{F}_p(\tau)$ the mean fitness of the population (evolved in the periodic environment), in an environment with temperature $\tau = \frac{1}{2}$, and hence with growth rate $a(\frac{1}{2}, x)$, which can be approximated for this example as

$$\widetilde{F}_p(1/2) \approx r - \varepsilon \frac{g(1/2)}{\sqrt{\overline{g}}}.$$

We next consider, a population which has evolved in a constant environment with $t = \frac{1}{2}$, that is when the growth rate is given by $a(1/2, x) = r - g(1/2)x^2$. Again, the density of the population's distribution converges in long time to the unique solution of the following stationary solution

$$\begin{cases} -\varepsilon^2 \partial_{xx} n_c = n_c\big(r - g(1/2)x^2 - \rho_c\big), \\ \rho_c = \int_{\mathbb{R}} n_c dx. \end{cases}$$

The explicit solution of the above equation is given by

$$n_c = \rho_c \frac{g(1/2)^{\frac{1}{4}}}{\sqrt{2\pi\varepsilon}} \exp\big(\frac{-\sqrt{g(1/2)}x^2}{2\varepsilon}\big), \quad \rho_c = r - \varepsilon\sqrt{g(1/2)},$$

from where we obtain the following population mean size $\overline{\rho}_c$, mean μ_c and variance σ_c^2 for such population

$$\mu_c = 0, \quad \sigma_c^2 = \frac{\varepsilon}{\sqrt{g(1/2)}}, \quad \overline{\rho}_c = r - \varepsilon\sqrt{g(1/2)}.$$

Moreover, the mean fitness of such population, in an environment with the same temperature ($t = 1/2$), can be computed as below

$$\widetilde{F}_c = \int_{\mathbb{R}^d} a(1/2, x) \frac{n_c(x)}{\rho_c} dx = r - \varepsilon\sqrt{g(1/2)}.$$

We remark that if we choose $g(t)$ such that

$$\int_0^1 g(t)dt > g\,(1/2), \tag{1.51}$$

then we have

$$\overline{\rho}_\varepsilon < \overline{\rho}_c, \quad \sigma_p^2 < \sigma_c^2 \quad \text{and} \quad \widetilde{F}_c < \widetilde{F}_p(1/2).$$

Here we observe that, for this choice of g satisfying (1.51), the population evolved in a periodic environment has a larger fitness, in an environment with constant temperature ($\tau = 1/2$) than the one evolved in a constant temperature ($\tau = 1/2$). This property corresponds indeed to what was observed in the biological experiment in [60]. Note that both of these environments select for populations with the same phenotypic mean trait $x = 0$. However, the population evolved in a periodic environment has a smaller variance comparing to the one evolved in a constant environment. This makes the population evolved in the periodic environment more performant. This example shows that the phenomenon observed in the experiment of [60] can also be observed in mathematical models.

Chapter 2

Sélection et mutation dans un environnement avec changement à la fois directionel et fluctuant

***

Dans un environnement qui change, il n'y a pas de plus grand risque que de rester immobile–
Jacques CHIRAC

Résumé

Nous étudions la dynamique évolutive d'une population phénotypiquement structurée dans un environnement changeant, où les conditions environnementales varient avec une tendance linéaire mais de manière oscillatoire. De tels phénomènes peuvent être décrits par des équations paraboliques de type Lotka-Volterra avec une competition non locale et un taux de croissance dépendant du temps. Nous étudions d'abord le comportement à long terme de la solution à ce problème. Ensuite, en utilisant une approche basée sur les équations de Hamilton-Jacobi, nous étudions asymptotiquement ces solutions à long terme lorsque les effets des mutations sont petits. Nous prouvons que lorsque l'effet des mutations tend vers zero, la densité phénotypique de la population se concentre sur un seul trait qui varie linéairement dans le temps, tandis que la taille de la population oscille périodiquement. Contrairement au cas d'un environnement sans déplacement linéaire, ce trait dominant n'a pas le taux de croissance maximal dans l'environnement moyenné et il y a un coût sur le taux de croissance en raison du déplacement climatique. Nous fournissons également des développements asymptotiques pour la taille moyenne de la population et la vitesse critique au delà de laquelle la population s'éteint, ce qui est étroitement lié à la dérivation d'un développement asymptotique de la valeur propre du Floquet en termes du taux de diffusion. Ces développements permettent de montrer, à l'aide d'un exemple biologique que les fluctuations dans l'environnement peuvent aider la population à mieux suivre l'environnement. Les résultats dans ce chapitre feront l'objet d'une publication conjointe avec Sepideh Mirrahimi.

2.1 Introduction

2.1.1 Model and motivations

The goal of this chapter is to study the evolutionary dynamics of a phenotypically structured population in an environment which varies with a linear trend but in an oscillatory manner. We study the following non-local parabolic equation

$$\begin{cases} \partial_t \tilde{n} - \sigma \partial_{xx} \tilde{n} = \tilde{n}[a(t, x - \tilde{c}t) - \tilde{\rho}(t)], \quad (t, x) \in [0, +\infty) \times \mathbb{R}, \\ \tilde{\rho}(t) = \displaystyle\int_{\mathbb{R}} \tilde{n}(t, x) dx, \\ \tilde{n}(t = 0, x) = \tilde{n}_0(x). \end{cases} \tag{2.1}$$

This equation models the dynamics of a population which is structured by a phenotypic trait $x \in \mathbb{R}$. Here, n corresponds to the density of individuals with trait x. We denote by $a(t, x - \tilde{c}t)$ the intrinsic growth rate of an individual with trait x at time t. The term $-\tilde{c}t$ has been introduced to consider a variation of the optimal trait with a linear trend. The dependence of the term a on the first variable is assumed to be periodic to consider fluctuations of the environment, which may vary the optimal trait or other parameters of the selection as for instance the pressure of the selection. The term ρ which corresponds to the total size of the population represents a competition term. Here, we assume indeed a uniform competition between all the individuals. The diffusion term models the mutations, with σ the mutation rate.

A natural motivation to study such type of problem is the fact that many natural populations are subject both to directional change of phenotypic optimum and random fluctuations of the environment ([29]). Here, we consider a deterministic growth rate that varies with a linear trend but in an oscillatory manner as a first step to study such situations. Will the population be able to adapt to the environmental change? Is there a maximum speed above which the population will get extinct? How is such maximal speed modified due to the fluctuations?

2.1.2 Related works

Models closely related to (2.1), but with a local reaction term and no fluctuation, have been widely studied (see for instance [16, 14, 15, 13]). Such models are introduced to study dynamics of populations structured by a space variable neglecting evolution. It is shown in particular that there exists a critical speed of environment change c^*, such that the population survives if and only if the environment change occurs with a speed less than c^*. We also refer to [22] where an integro-difference model has been studied for the spatial dynamics of a population in the case of a randomly changing environment. Moreover, in [2], both spatial and evolutionary dynamics of a population in an environment with linearly moving optimum has been studied. While in the present work, we don't include any spatial structure, we take into account oscillatory change of environment in addition to a change with linear trend.
The evolutionary dynamics of structured population under periodic fluctuations of the environment has been recently studied by [83, 74, 41, 6]. The works in [74, 6] are focused on the study of a particular form of growth rate a and in particular some semi-explicit solutions to such equations are provided. In [83, 41] some asymptotic analysis of such equations for general growth rates are provided. The present chapter is closely related to Chapter 1 (see also [41]) where a periodically evolving environment was considered without the linear trend. The presence of such linear trend of environment change leads to new difficulties in the asymptotic analysis. Moreover, we go further than the results in [41] and provide an asymptotic expansion for the average size of the population in terms of the mutation rate. Such expansion is closely related to an asymptotic expansion of the Floquet eigenvalue for the linear problem.

In this chapter, we use an asymptotic approach based on Hamilton-Jacobi equations with constraint. This approach has been developed during the last decade to study the asymptotic solutions of selection-mutation equations, assuming small effect of the mutations. Such equations have the property that their solution concentrate as Dirac masses on the fittest traits. There is a large literature on this approach. We refer to [34, 88, 10] for the establishment of the basis of this approach for homogeneous environments.

2.1.3 Mathematical assumptions

To introduce our assumptions, we first define

$$\overline{a}(y) = \frac{1}{T}\int_0^T a(t,y)dt.$$

We then assume that $a \in L^\infty(\mathbb{R}^+, C^3(\mathbb{R}))$ is a time-periodic function with period T, such that:

$$a(t,\cdot) = a(t+T,\cdot),\ \forall\ t \in \mathbb{R}, \quad \text{and } \exists\ d_0 > 0 : \|a(t,\cdot)\|_{L^\infty(\mathbb{R})} \leq d_0 \quad \forall\ t \in \mathbb{R}, \tag{H1}$$

and that the averaged function $\overline{a}$ attains its maximum and

$$\max_{x\in\mathbb{R}}\ \overline{a}(x) > 0, \tag{H2a}$$

which means that there exist at least some traits with strictly positive average growth rate.
Moreover, for our second main result (Theorem 7) we assume that this maximum is attained at a single point x_m; that is

$$\exists!\ x_m : \max_{x\in\mathbb{R}} \overline{a}(x) = \overline{a}(x_m), \tag{H2b}$$

and also

$$\exists!\ \overline{x} \leq x_m;\ \overline{a}(\overline{x}) + \frac{\tilde{c}^2}{4\sigma} = \overline{a}(x_m). \tag{H3}$$

Finally, we make the following assumption on the initial data:

$$0 \leq \tilde{n}_0(x) \leq e^{C_1 - C_2|x|}, \quad \forall x \in \mathbb{R}, \tag{H4}$$

which indicates that the initial density of individuals with large traits is exponentially small.

2.1.4 Preliminary results

To avoid the shift in the growth rate a, we transform our problem with a change of variable. We introduce indeed $n(t,x) = \tilde{n}(t, x + \tilde{c}t)$ which satisfies:

$$\begin{cases} \partial_t n - \tilde{c}\partial_x n - \sigma\partial_{xx} n = n[a(t,x) - \rho(t)], \quad (t,x) \in [0,+\infty)\times\mathbb{R}, \\ \rho(t) = \displaystyle\int_{\mathbb{R}} n(t,x)dx, \\ n(t=0,x) = \tilde{n}_0(x). \end{cases} \tag{2.2}$$

Next, we introduce the linearized problem associated to (2.2). Let $m(t,x) = n(t,x)e^{\int_0^t \rho(s)ds}$, for n the solution of (2.2),

then m satisfies

$$\begin{cases} \partial_t m - \tilde{c}\partial_x m - \sigma\partial_{xx} m = a(t,x)m, & (t,x) \in [0,+\infty) \times \mathbb{R}, \\ m(t=0,x) = \tilde{n}_0(x), & x \in \mathbb{R}. \end{cases} \tag{2.3}$$

We also introduce the corresponding parabolic eigenvalue problem as follows

$$\begin{cases} \partial_t p_c - \tilde{c}\partial_x p_c - \sigma\partial_{xx} p_c - a(t,x)p_c = \lambda_{\tilde{c},\sigma} p_c, & (t,x) \in [0,+\infty) \times \mathbb{R}, \\ 0 < p_c;\ p_c(t,x) = p_c(t+T,x), & (t,x) \in [0,+\infty) \times \mathbb{R}. \end{cases} \tag{2.4}$$

For better legibility, we omit the tilde in the index of p_c, while we still refer to the problem with constant $\tilde{c}$. We also define the eigenvalue problem in the bounded domain $[-R,R]$, for some $R > 0$,

$$\begin{cases} \partial_t p_R - \tilde{c}\partial_x p_R - \sigma\partial_{xx} p_R - a(t,x)p_R = \lambda_R p_R, & (t,x) \in [0,+\infty) \times [-R,R], \\ p_R = 0, & (t,x) \in [0,+\infty) \times \{-R,R\}, \\ 0 < p_R;\ p_R(t,x) = p_R(t+T,x), & (t,x) \in [0,+\infty) \times [-R,R]. \end{cases} \tag{2.5}$$

It is known that problem (2.5) has a unique eigenpair (λ_R, p_R) with p_R a strictly positive eigenfunction such that $\|p_R(0,\cdot)\|_{L^\infty([-R,R])} = 1$, (see [53]). Another fundamental result (see for instance [56]), for our purpose is that the function $R \mapsto \lambda_R$ is decreasing and $\lambda_R \to \lambda_{\tilde{c},\sigma}$ as $R \to +\infty$.

To announce our first result we introduce another assumption. We assume that a takes small values at infinity in the following sense: there exist positive constants δ and R_0 such that

$$a(t,x) + \lambda_{\tilde{c},\sigma} \leq -\delta, \quad \forall t \geq 0 \text{ and } |x| \geq R_0. \tag{Hc}$$

Proposition 2.1 *Assume* (H1), (H4) *and* (Hc). *Then for problem* (2.4) *there exists a unique generalized principal eigenfunction p_c associated to $\lambda_{\tilde{c},\sigma}$, with $\|p_c(0,\cdot)\|_{L^\infty(\mathbb{R})} = 1$. Moreover, we have $p_c = \lim_{R\to\infty} p_R$ and*

$$p_c(t,x) \leq \|p_c\|_{L^\infty} e^{-\nu(|x|-R_0)}, \qquad \forall (t,x) \in [0,+\infty) \times \mathbb{R}, \tag{2.6}$$

for $\nu = -\frac{\tilde{c}}{2\sigma} + \sqrt{\frac{\delta}{\sigma} + \frac{1}{2}\left(\frac{\tilde{c}}{\sigma}\right)^2}$.

Finally, the eigenfunction $p_c(t,x)$ is exponentially stable, in the following sense; there exists $\alpha > 0$ such that:

$$\|m(t,x)e^{t\lambda_{\tilde{c},\sigma}} - \alpha p_c(t,x)\|_{L^\infty(\mathbb{R})} \to 0 \quad \textit{exponentially fast as } t \to \infty. \tag{2.7}$$

The proof of this proposition is based on the results in [41].

We next define the $T-$periodic functions $Q_c(t)$ and $P_c(t,x)$ as follows:

$$Q_c(t) = \frac{\int_{\mathbb{R}} a(t,x)p_c(t,x)dx}{\int_{\mathbb{R}} p_c(t,x)dx}, \quad P_c(t,x) = \frac{p_c(t,x)}{\int_{\mathbb{R}} p_c(t,x)dx}, \tag{2.8}$$

and we recall a result proved in [41].

Proposition 2.2 *There exists a unique periodic solution $\widehat{\rho}(t)$ to the problem*

$$\begin{cases} \dfrac{d\widehat{\rho}}{dt} = \widehat{\rho}\left[Q_c(t) - \widehat{\rho}\right], & t \in (0,T), \\ \widehat{\rho}(0) = \widehat{\rho}(T), \end{cases} \tag{2.9}$$

if and only if $\int_0^T Q_c(t)dt > 0$. *Moreover this solution can be explicitly expressed as follows:*

$$\widehat{\rho}(t) = \frac{1 - \exp\left[-\int_0^T Q_c(s)ds\right]}{\exp\left[-\int_0^T Q_c(s)ds\right]\int_t^{t+T} \exp\left[\int_t^s Q_c(\theta)d\theta\right]ds}. \tag{2.10}$$

2.1.5 The main results and the plan of the chapter

We are interested, in determining conditions on the environment shift speed $\tilde{c}$ which leads to extinction or survival of the population. In the case of the population survival we then try to characterize asymptotically the population density considering small effect of the mutations.

To present our result on the survival criterion, we define the "critical speed".

Definition 2.3 *We define the critical speed* $\tilde{c}^*_\sigma$ *as follows*

$$\tilde{c}^*_\sigma = \begin{cases} 2\sqrt{-\sigma\lambda_{0,\sigma}}, & \text{if } \lambda_{0,\sigma} < 0, \\ 0, & \text{otherwise}, \end{cases} \tag{2.11}$$

where $\lambda_{0,\sigma}$ *corresponds to the principal eigenvalue introduced by Proposition 2.1, in the case* $c = 0$.

The next result shows that $\tilde{c}^*_\sigma$ is indeed a critical speed of climate change above which the population goes extinct.

Proposition 2.4 *Let* $n(t,x)$ *be the solution of* (2.2). *Assume* (H1), (H2a), (H4) *and* (Hc). *Then the following statements hold:*

(i) if $\tilde{c} \geq \tilde{c}^*_\sigma$, *then the population will go extinct, i.e.* $\rho(t) \to 0$, *as* $t \to \infty$,

(ii) if $\tilde{c} < \tilde{c}^*_\sigma$, *then* $|\rho(t) - \widehat{\rho}(t)| \to 0$, *as* $t \to \infty$, *with* $\widehat{\rho}$ *the unique solution to* (2.9).

(iii) Moreover, $\left\| \frac{n(t,x)}{\rho(t)} - P_c(t,x) \right\|_{L^\infty} \longrightarrow 0$, *as* $t \to \infty$. *Consequently we have, as* $t \to \infty$*:*

$$\|n(t,\cdot) - \widehat{\rho}(t)P_c(t,\cdot)\|_{L^\infty} \to 0, \text{ if } \tilde{c} < \tilde{c}^*_\sigma \quad \text{and} \quad \|n\|_{L^\infty} \to 0, \text{ if } \tilde{c} \geq \tilde{c}^*_\sigma. \tag{2.12}$$

Remark 2.5 *Note that if* $\lambda_{0,\sigma} \geq 0$, *then* $\tilde{c}^*_\sigma = 0$, *which means that the population goes extinct even without climate change, that is* $\tilde{c} = 0$.

Proposition 2.4 allows to relate extinction/survival of the population to the climatic change speed and shows that if the change goes "too fast" the population will not be able to follow the environment change and will get extinct. However, if the change speed is "moderate" the phenotypic density n converges to the periodic function $n_c(t,x) = \widehat{\rho}(t)P_c(t,x)$, which is in fact the unique periodic solution of (2.2).

Next, we are interested in describing this periodic solution n_c, asymptotically as the effect of mutations is small. To this end, with a change of notation, we take $\sigma = \varepsilon^2$ and $\tilde{c} = \varepsilon c$, and we study asymptotically the solution $(n_{\varepsilon c}, \widehat{\rho}_{\varepsilon c})$ as ε vanish. Note that, in view of Proposition 2.4, to provide an asymptotic analysis considering $\sigma = \varepsilon^2$ small, a rescaling

of the climate shift speed as $\tilde{c} = \varepsilon c$ is necessary. In order to keep the notation simpler we denote $(n_{\varepsilon c}, \widehat{\rho}_{c\varepsilon}) = (n_\varepsilon, \rho_\varepsilon)$, which is the unique periodic solution of the problem:

$$\begin{cases} \partial_t n_\varepsilon - \varepsilon c \partial_x n_\varepsilon - \varepsilon^2 \partial_{xx} n_\varepsilon = n_\varepsilon [a(t,x) - \rho_\varepsilon(t)], \quad (t,x) \in [0,+\infty) \times \mathbb{R}, \\ \rho_\varepsilon(t) = \displaystyle\int_{\mathbb{R}} n_\varepsilon(t,x) dx, \\ n_\varepsilon(0,x) = n_\varepsilon(T,x). \end{cases} \tag{2.13}$$

To study asymptotically this problem we perform a Hopf-Cole transformation (or WKB ansatz), i.e we consider

$$n_\varepsilon = \frac{1}{\sqrt{2\pi\varepsilon}} \exp\left(\frac{\psi_\varepsilon}{\varepsilon}\right). \tag{2.14}$$

This change of variable comes from the fact that with such rescaling the solution n_ε will naturally have this form. While we expect that n_ε tends to a Dirac mass, as $\varepsilon \to 0$, ψ_ε will have a non singular limit.
For better legibility, we define $c^*_\varepsilon := \dfrac{\tilde{c}^*_{\varepsilon^2}}{\varepsilon}$ where $\tilde{c}^*_{\varepsilon^2}$ stands for the critical speed $\tilde{c}^*_\sigma$ with $\sigma = \varepsilon^2$. Here is our first main result:

Theorem 2.6 *Assume* (H1), (H2a) *and* (Hc) *and also that* $c < \liminf_{\varepsilon\to 0} c^*_\varepsilon$. *Then the following statements hold:*

(i) As $\varepsilon \to 0$, *we have* $\|\rho_\varepsilon(t) - \widetilde{\varrho}(t)\|_{L^\infty} \to 0$, *with* $\widetilde{\varrho}(t)$ *a* $T-$*periodic function.*

(ii) Moreover, as $\varepsilon \to 0$, $\psi_\varepsilon(t,x)$ *converges locally uniformly to a function* $\psi(x) \in C(\mathbb{R})$, *a viscosity solution to the following equation:*

$$\begin{cases} -\left|\partial_x \psi + \dfrac{c}{2}\right|^2 = \overline{a}(x) - \overline{\rho} - \frac{c^2}{4}, \quad x \in \mathbb{R}, \\ \max\limits_{x\in\mathbb{R}} \psi(x) = 0, \\ -A_1|x|^2 - \frac{c}{2}x - A_2 \leq \psi \leq c_1 - c_2|x|, \end{cases} \tag{2.15}$$

with

$$\bar{\rho} = \int_0^T \tilde{\varrho}(t) dt,$$

and some positive constants A_1, A_2, c_1 *and* $c_2 = -\frac{c}{2} + \sqrt{\delta + \frac{c^2}{2}}$.

The above theorem is closely related to Theorem 4 in [41]. A new difficulty comes from the drift term. To deal with the drift term we use a Liouville transformation (see for instance [14, 15]) that allows us to transform the problem to a parabolic problem without drift.
Finally, to present our last result, let us consider the eigenproblem (2.4) for $\sigma = \varepsilon^2$ and $\tilde{c} = c\varepsilon$, that is:

$$\begin{cases} \partial_t p_{c\varepsilon} - \varepsilon c \partial_x p_{c\varepsilon} - \varepsilon^2 \partial_{xx} p_{c\varepsilon} - a(t,x) p_{c\varepsilon} = p_{c\varepsilon} \lambda_{c,\varepsilon}, & (t,x) \in [0,+\infty) \times \mathbb{R}, \\ 0 < p_{c\varepsilon};\ p_{c\varepsilon}(t,x) = p_{c\varepsilon}(t+T,x), & (t,x) \in [0,+\infty) \times \mathbb{R}. \end{cases} \tag{2.16}$$

Here we denote $\lambda_{c,\varepsilon}$ the eigenvalue $\lambda_{\tilde{c},\sigma}$ with $\sigma = \varepsilon^2$ and $\tilde{c} = c\varepsilon$ for better legibility.

Theorem 2.7 *Let* $\lambda_{c,\varepsilon}$ *be the principal eigenvalue of problem* (2.16) *and assume* (H1), (H2b), (H3) *and* (Hc). *Assume in addition that* $c < \liminf_{\varepsilon\to 0} c^*_\varepsilon$, *then the following statements hold:*

(i) Let $\overline{\rho}_\varepsilon = \frac{1}{T}\int_0^T \rho_\varepsilon(t) dt$, *the following asymptotic expansions hold*

$$\overline{\rho}_\varepsilon = -\lambda_{c,\varepsilon} = \overline{a}(x_m) - \frac{c^2}{4} - \varepsilon\sqrt{-\overline{a}_{xx}(x_m)/2} + o(\varepsilon), \tag{2.17}$$

$$c_\varepsilon^* = 2\sqrt{\overline{a}(x_m)} - \varepsilon\sqrt{-\overline{a}_{xx}(x_m)/2} + o(\varepsilon). \tag{2.18}$$

(ii) Moreover the viscosity solution of (2.15) *is unique and it is indeed a classical solution given by*

$$\psi(x) = \frac{c}{2}(\overline{x} - x) + \int_{\overline{x}}^{x_m} \sqrt{\overline{a}(x_m) - \overline{a}(y)}dy - \left|\int_{x_m}^{x} \sqrt{\overline{a}(x_m) - \overline{a}(y)}dy\right|. \tag{2.19}$$

where $\overline{x} < x_m$ *is given in* (H3).

(iii) Furthermore, let n_ε *solve* (2.13)*, then*

$$n_\varepsilon(t,x) - \tilde{\varrho}(t)\delta(x - \overline{x}) \rightharpoonup 0, \quad \text{as } \varepsilon \to 0, \tag{2.20}$$

point wise in time, weakly in x *in the sense of measures, with* $\tilde{\varrho}$ *the unique periodic solution of the following equation*

$$\begin{cases} \dfrac{d\widetilde{\varrho}}{dt} = \widetilde{\varrho}\left[a(t,\bar{x}) - \widetilde{\varrho}\right], \quad t \in (0,T), \\ \widetilde{\varrho}(0) = \widetilde{\varrho}(T). \end{cases} \tag{2.21}$$

Remark 2.8 *The statement (iii) in Theorem 2.7 implies for the solution* $\tilde{n}_\varepsilon$ *to the initial problem* (2.1) *with* $\sigma = \varepsilon^2$ *and* $\tilde{c} = c\varepsilon$ *that*

$$\tilde{n}_\varepsilon(t,x) - \tilde{\varrho}(t)\delta(x - \overline{x} - ct) \rightharpoonup 0, \qquad \text{as } \varepsilon \to 0, \tag{2.22}$$

point wise in time, weakly in x *in the sense of measures. This implies that the phenotypic density of the population concentrates on a single Dirac mass which varies linearly with time, while the total size of the population oscillates periodically.*

Note that while in [41] the uniqueness of the viscosity solution to the corresponding Hamilton-Jacobi equation with constraint was immediate, here to prove such uniqueness more work is required. In particular, in order to prove such result the constraint is not enough and we use also the bounds on ψ, given in (2.15). More precisely we introduce a new function $u(x) = \psi(x) + \frac{c}{2}x$ which solves

$$\begin{cases} -|\partial_x u|^2 = \overline{a}(x) - \overline{\rho} - \frac{c^2}{4}, \quad x \in \mathbb{R}, \\ \\ -A_1|x|^2 - A_2 \le u(x) \le c_1 - c_2|x| + \frac{c}{2}x, \end{cases} \tag{2.23}$$

where the constants A_1, A_2, c_1, c_2 are the same as in (2.15).
The main idea comes from the fact that any viscosity solution to a Hamilton-Jacobi equation of type (2.23) but in a bounded domain Ω can be uniquely determined by its values on the boundary points of Ω and by its values at the maximum points of the RHS of the Hamilton-Jacobi equation, (see for instance [72]).
Note also that our results in Theorem 2.7-(i) goes further than the one in [41], since we provide additionally an asymptotic expansion for the Floquet eigenvalue which leads to an asymptotic expansion for the critical speed c_ε^* and the average size of the population $\bar{\rho}_\varepsilon$. Such expansion is indeed related to the harmonic approximation of the energy of the ground state of the Schrödinger operator ([49]). However, here we have a parabolic, non self-adjoint operator.

The chapter is organized as follows: in Section 2.2 we deal with the long time study of the problem and prove the preliminary results Proposition 2.1 and Proposition 2.4. Next in Section 2.3 we provide an asymptotic analysis of the problem considering small effect of mutations and we prove Theorem 2.6. In Section 2.4, we prove the uniqueness of the viscosity solutions for problem (2.15). Section 2.5 is devoted to obtain an approximation of the principal eigenvalue given

in Theorem 2.7. Finally in Section 2.6 we approximate the moments of the distribution of the population by mean of formal computations and discuss the results for a particular growth rate. At the end, in Appendix A and B, we provide some technical results and computations.

2.2 The convergence in long time

In this section we provide the proofs of Proposition 2.1 and Proposition 2.4. To this end, we make a change of variable which allows us to transform the problem into a parabolic equation without the drift term.
Let $m(t,x)$ satisfy the linearized problem (2.3), we denote $\mathcal{P}_0$ and $\mathcal{P}_c$ the linear operators associated to problem (2.3), for $\tilde{c}=0$ and $\tilde{c}>0$ respectively, that is:

$$\mathcal{P}_0\omega := \partial_t\omega - \sigma\partial_{xx}\omega - a(t,x)\omega, \qquad \mathcal{P}_c\omega := \partial_t\omega - \tilde{c}\partial_x\omega - \sigma\partial_{xx}\omega - a(t,x)\omega. \tag{2.24}$$

In Subsection 2.2.1, we introduce the Liouville transformation and provide a relation between $\mathcal{P}_0$ and $\mathcal{P}_c$ which allows us to obtain a relationship between $\tilde{c}$ and $\lambda_{\tilde{c},\sigma}$. Next in Subsection (2.2.2) and (2.2.3) we provide the proofs of Proposition 2.1 and Proposition 2.4 respectively.

2.2.1 Liouville transformation

Here, we reduce the parabolic equation (2.2) to a parabolic problem without the drift term via a Liouville transformation (see for instance [14, 15] where this transformation is used for an elliptic problem).
Let $M(t,x)$ be given by

$$M(t,x) := m(t,x)e^{\frac{\tilde{c}}{2\sigma}x}, \tag{2.25}$$

for $m(t,x)$ the solution of the linearized problem (2.3), then M satisfies:

$$\partial_t M - \sigma\partial_{xx}M = \left[a(t,x) - \frac{\tilde{c}^2}{4\sigma}\right]M. \tag{2.26}$$

We denote $\widetilde{\mathcal{P}}$ the linear operator associated to the above equation, i.e.

$$\widetilde{\mathcal{P}}\omega := \partial_t\omega - \sigma\partial_{xx}\omega - a_c(t,x)\omega,$$

where $a_c(t,x) = \left[a(t,x) - \frac{\tilde{c}^2}{4\sigma}\right]$.
We establish in the next lemma the relation between the principal eigenvalues associated to the operators $\mathcal{P}_0$, $\mathcal{P}_c$ and $\widetilde{\mathcal{P}}$.

Lemma 2.9 *Let $\lambda(\mathcal{P},\mathbb{D})$ denote the principal eigenvalue of the operator $\mathcal{P}$ in the domain $\mathbb{D}$, it holds*

$$\lambda_{\tilde{c},\sigma} = \lambda\left(\mathcal{P}_c, \mathbb{R}_+\times\mathbb{R}\right) = \lambda\left(\widetilde{\mathcal{P}}, \mathbb{R}_+\times\mathbb{R}\right).$$

Moreover, let $\lambda_{0,\sigma} = \lambda(\mathcal{P}_0, \mathbb{R}_+\times\mathbb{R})$, then $\lambda_{\tilde{c},\sigma} = \lambda_{0,\sigma} + \frac{\tilde{c}^2}{4\sigma}$.

Proof. The proof follows from the definition of the eigenfunction and eigenvalue and the fact that

$$\widetilde{\mathcal{P}}\omega = \left(\mathcal{P}_c\left(\omega e^{-\frac{\tilde{c}}{2\sigma}x}\right)\right)e^{\frac{\tilde{c}}{2\sigma}x}.$$

■

2.2.2 Proof of Proposition 2.1

Proposition 2.1 can be proved following similar arguments as in the proof of Lemma 6 in [41]. Note that the argument in [41] is based on an exponential separation result for linear parabolic equations in [56] that holds for general linear operators of the form

$$\omega_t = L(t,x)\omega, \quad \text{in } [0,+\infty)\times\mathbb{R},$$

with $L(t,x)$ being any time-dependent second-order elliptic operator in non-divergence form, i.e:

$$L(t,x)\omega = a_{ij}(t,x)\partial_i\partial_j\omega + B_i(t,x)\partial_i\omega + A(t,x)\omega,$$

where the functions $B_i, A \in L^\infty(\mathbb{R}^+\times\mathbb{R})$ and a_{ij} satisfies

$$a_{ij}(t,x)\xi_i\xi_j \geq \alpha_0|\xi|^2, \quad (t,x)\in\mathbb{R}^+\times\mathbb{R},$$

(see Section 9 in [56] for more details).
Here, we only provide the proof of the inequality (2.6) which is also obtained by an adaption of the proof of Lemma 6 in [41]. Let $\tilde{a}_c(t,x) = a_c(t,x) + \lambda_{\tilde{c},\sigma}$ then p_c is a positive periodic solution of the following equation:

$$\partial_t p_c - \tilde{c}\partial_x p_c - \sigma\partial_{xx}p_c = p_c\tilde{a}_c(t,x), \quad \text{in } \mathbb{R}\times\mathbb{R}. \tag{2.27}$$

Note that we have defined p_c in $(-\infty,0]$ by periodic prolongation. We denote $\|p_c\|_{L^\infty(\mathbb{R}\times\mathbb{R})} = \Gamma$ and define:

$$\zeta(t,x) = \Gamma e^{-\delta(t-t_0)} + \Gamma e^{-\nu(|x|-R_0)},$$

for some ν to be found later and δ, R_0 given in (Hc). One can verify that

$$\Gamma \leq \zeta(t,x) \quad \text{if } |x| = R_0 \text{ or } t = t_0.$$

Furthermore if $|x| > R_0$ or $t > t_0$ evaluating in (2.27) shows:

$$\partial_t\zeta - \tilde{c}\partial_x\zeta - \sigma\partial_{xx}\zeta - \zeta\tilde{a}_c(t,x) = \Gamma e^{-\delta(t-t_0)}(-\delta - \tilde{a}_c(t,x)) + \Gamma e^{-\nu(|x|-R_0)}\left(\tilde{c}\nu\frac{x}{|x|} - \sigma\nu^2 - \tilde{a}_c(t,x)\right) \geq 0,$$

since $\tilde{a}_c(t,x) + \frac{\tilde{c}^2}{4\sigma} = a(t,x) + \lambda_{\tilde{c},\sigma} \leq -\delta$ thanks to assumption (Hc) and choosing ν conveniently such that the inequality holds. Indeed, since $-1 \leq \frac{x}{|x|} \leq 1$, we have:

$$\tilde{c}\nu\frac{x}{|x|} - \sigma\nu^2 - \tilde{a}_c(t,x) \geq -\tilde{c}\nu - \sigma\nu^2 + \delta + \frac{\tilde{c}^2}{4\sigma} \geq 0 \quad \text{for} \quad \frac{-\tilde{c}-\sqrt{4\delta\sigma+2\tilde{c}^2}}{2\sigma} \leq \nu \leq \frac{-\tilde{c}+\sqrt{4\delta\sigma+2\tilde{c}^2}}{2\sigma}.$$

Thus ζ is a supersolution of (2.27) on:

$$Q_0 = \{(t,x)\in(t_0,\infty)\times\mathbb{R}\,;|x|>R_0\},$$

which dominates p_c on the parabolic boundary of Q_0. Applying the maximum principle to $\zeta - p_c$, we obtain

$$p_c(t,x) \leq \Gamma e^{-\delta(t-t_0)} + \Gamma e^{-\nu(|x|-R_0)}, \qquad |x|\geq R_0,\ t\in(t_0,\infty).$$

Taking the limit $t_0 \to -\infty$ yields

$$p_c(t,x) \leq \Gamma e^{-\nu(|x|-R_0)}, \qquad |x| \geq R_0,\ t < +\infty,$$

in particular, for $\nu = \dfrac{-\tilde{c} + \sqrt{4\delta\sigma + 2\tilde{c}^2}}{2\sigma}$. We conclude that p_c satisfies (2.6).

■

2.2.3 Proof of Proposition 2.4

The proof of Proposition 2.4, is closely related to the proof of Proposition 2 in [41] but we need to verify two properties before applying the arguments in [41]. To this end we prove the following lemmas. The rest of the proof follows from the arguments in [41].

Lemma 2.10 *Let $\lambda_{\tilde{c},\sigma}$ be the principal eigenvalue of problem (2.4). Then, $\lambda_{\tilde{c},\sigma} < 0$ if and only if $\tilde{c} < \tilde{c}^*_\sigma$.*

Proof. Follows directly from the definition of $\tilde{c}^*_\sigma$.

■

Lemma 2.11 *Assume (H1) and (H4) and let $C_3 = C_2(\sigma C_2 + \tilde{c}) + d_0$ then the solution $n(t,x)$ to equation (2.2) satisfies:*

$$n(t,x) \leq \exp\left(C_1 - C_2|x| + C_3 t\right), \quad \forall (t,x) \in (0,+\infty) \times \mathbb{R}.$$

Proof. We argue by a comparison principle argument. Define the function $\bar{n}(t,x) = \exp\left(C_1 - C_2|x| + C_3 t\right)$.
We prove that $n \leq \bar{n}$. One can verify that for C_3 defined as in the formulation of the Lemma, we have the following inequality a.e:

$$\partial_t \bar{n} - \tilde{c}\partial_x \bar{n} - \sigma \partial_{xx} \bar{n} - \left[a(t,x) - \rho(t)\right] \bar{n} = e^{(C_1 - C_2|x| + C_3 t)} \left[C_3 - \sigma C_2^2 + C_2 \frac{cx}{|x|} - a(t,x) + \rho(t) \right] \geq 0.$$

Moreover, we have for $t = 0$, $n(0,x) \leq \bar{n}(0,x)$ thanks to assumption (H4). We can then apply a maximum principle to $d(t,x) = \bar{n}(t,x) - n(t,x)$, in the class of L^2 functions, and we conclude that:

$$d(t,x) \geq 0 \Rightarrow n(t,x) \leq \bar{n}(t,x), \quad \forall (t,x) \in (0,+\infty) \times \mathbb{R}.$$

■

2.3 Regularity estimates

In this section, we prove Theorem 2.6. To this end we first provide some uniform bounds for $\rho_\varepsilon(t)$. Then, in Subsection 2.3.2, we prove that ψ is locally uniformly bounded, Lipschitz continuous with respect to x and locally equicontinuous in time. Finally in the last subsection we conclude the proof of Theorem 2.6 by letting ε go to zero and describing the limits of ψ_ε and ρ_ε.

2.3.1 Uniform bounds for ρ_ε

We have the following result on ρ_ε.

Proposition 2.12 *Assume* (H1), (Hc) *and let* $\tilde{c} = \varepsilon c$ *with* $c < \liminf_{\varepsilon\to 0} c_\varepsilon^*$. *Then for all* $0 < \varepsilon \le \varepsilon_0$, *there exist positive constants* ρ_m *and* ρ_M *such that:*

$$0 < \rho_m \le \rho_\varepsilon(t) \le \rho_M, \quad \forall t \ge 0. \tag{2.28}$$

The proof of this result follows similar arguments as in [41]. For the convenience of the reader, we provide this proof in Appendix 2.A.

2.3.2 Regularity results for ψ_ε

In this subsection we prove some regularity estimates on ψ_ε which give the basis to prove the convergence of ψ_ε and ρ_ε as $\varepsilon \to 0$ in Subsection 2.3.3. From the Hopf-Cole transformation (2.14) we deduce that ψ_ε solves:

$$\frac{1}{\varepsilon}\partial_t\psi_\varepsilon - \varepsilon\partial_{xx}\psi_\varepsilon = \left|\partial_x\psi_\varepsilon + \frac{c}{2}\right|^2 + a(t,x) - \frac{c^2}{4} - \rho_\varepsilon(t), \quad (t,x) \in [0,+\infty)\times\mathbb{R}. \tag{2.29}$$

We claim the following Theorem.

Theorem 2.13 *Assume* (H1), (H2a) *and* (Hc). *Let* ψ_ε *be a* $T-$*periodic solution to* (2.29). *Then the following items hold:*

(i) The sequence $(\psi_\varepsilon)_\varepsilon$ *is locally uniformly bounded; i.e.*

$$-A_1|x|^2 - \frac{c}{2}x - A_2 \le \psi_\varepsilon \le c_1 - c_2|x|, \quad \forall (t,x) \in \mathbb{R}_+\times\mathbb{R}, \tag{2.30}$$

for some positive constants A_1, A_2, c_1 *and* $c_2 = -\frac{c}{2} + \sqrt{\delta + \frac{c^2}{2}}$.

(ii) Moreover, the sequence $(\phi_\varepsilon = \sqrt{2c_1 - \psi_\varepsilon})_\varepsilon$, *is uniformly Lipschitz continuous with respect to* x *in* $(0,+\infty)\times\mathbb{R}$.

(iii) Also, $(\psi_\varepsilon)_\varepsilon$ *is locally equicontinuous in time in* $[0,T]\times\mathbb{R}$ *and satisfies*

$$|\psi_\varepsilon(t,x) - \psi_\varepsilon(s,x)| \to 0 \quad \text{as } \varepsilon \to 0. \tag{2.31}$$

In the next subsections we provide the proof of the lower bounds in (2.30) and the uniform Lipschitz continuity of ϕ_ε. The proof of the other properties can be obtained by an adaptation of the arguments in [41]. For the convenience of the reader we provide them in Appendix 2.A.

2.3.2.1 Lower bound for ψ_ε

To obtain the lower bound for ψ_ε we use the bounds for a in (H1) and for ρ_ε in (2.28) and we obtain for $D_0 = d_0 + \rho_M$

$$\partial_t n_\varepsilon - c\varepsilon\partial_x n_\varepsilon - \varepsilon^2\partial_{xx} n_\varepsilon \ge -D_0 n_\varepsilon.$$

Let n_ε^* be the solution of the following Cauchy problem

$$\begin{cases} \partial_t n_\varepsilon^* - c\varepsilon\partial_x n_\varepsilon^* - \varepsilon^2\partial_{xx} n_\varepsilon^* + D_0 n_\varepsilon^* = 0, \\ n_\varepsilon^*(0,x) = n_\varepsilon^0, \end{cases}$$

we define N_ε^* analogously to (2.25) by the Liouville transformation of n_ε^* as follows

$$N_\varepsilon^*(t,x) := n_\varepsilon^*(t,x)e^{\frac{c}{2\varepsilon}x}.$$

Then, N_ε^* solves the heat equation

$$\begin{cases} \partial_t N_\varepsilon^* - \varepsilon^2 \partial_{xx} N_\varepsilon^* + D_1 N_\varepsilon^* = 0, \\ N_\varepsilon^*(0,x) = n_\varepsilon^0(x) e^{\frac{c}{2\varepsilon}x}, \end{cases}$$

for $D_1 = D_0 + \frac{c^2}{4}$. The solution to the latter equation is given explicitly by the Heat Kernel K,

$$N_\varepsilon^*(t,x) = e^{-D_1 t}\,(N_\varepsilon^*(0,y) * K) = \frac{e^{-D_1 t}}{\varepsilon\sqrt{4\pi t}} \int_{\mathbb{R}} N_\varepsilon^*(0,y) e^{-\frac{|x-y|^2}{4t\varepsilon^2}} dy, \quad t > 0.$$

Note that $N_\varepsilon^*(0,x)$ from its definition can be written as follows

$$N_\varepsilon^*(0,x) := \frac{p_{c\varepsilon}(0,x)}{\int_{\mathbb{R}} p_{c\varepsilon}(0,x)dx} \rho_\varepsilon(0) e^{\frac{c}{2\varepsilon}x}. \tag{2.32}$$

We recall that $p_{c\varepsilon}$ is uniquely determined once $\|p_{c\varepsilon}(0,x)\|_{L^\infty(\mathbb{R})} = 1$ is fixed. Then, one can choose x_ε such that $p_{c\varepsilon}(0,x_\varepsilon) = 1$. From an elliptic-type Harnack inequality in a bounded domain we can obtain

$$p_{c\varepsilon}(t_0,x_\varepsilon) \le \sup_{y\in B(x_\varepsilon,\varepsilon)} p_{c\varepsilon}(t_0,y) \le C p_{c\varepsilon}(t_0,x), \quad \forall (t_0,x) \in [\delta_0, 2T] \times B(x_\varepsilon,\varepsilon), \tag{2.33}$$

where δ_0 is such that $0 < \delta_0 < T$ and C is a positive constant depending on δ_0 and d_0 (we refer to Appendix 2.A-Proof of upper bound, for more details on this inequality). We then use the $T-$periodicity of $p_{c\varepsilon}$ to conclude that the last inequality is satisfied $\forall\, t \in [0,T]$.
From (2.6), (2.32) and (2.33) we deduce that

$$\varepsilon^{-1} D_2 e^{-\frac{D_3}{\varepsilon} + \frac{c}{2\varepsilon}x} \le \rho_m \frac{p_\varepsilon(0,x) e^{\frac{c}{2\varepsilon}x}}{\int_{\mathbb{R}} p_\varepsilon(0,x)dx} \le N_\varepsilon^*(0,x) \quad \forall x \in B(x_\varepsilon,\varepsilon),$$

for some positive constants D_2 and D_3 depending on $\|p_\varepsilon\|_{L^\infty}$, ρ_m, δ, and the constants of hypothesis (Hc). Then, for all $(t,x) \in (0,+\infty)\times\mathbb{R}$

$$\begin{aligned} N_\varepsilon^*(t,x) &\ge \frac{D_2}{\varepsilon^2\sqrt{4\pi t}} e^{-\frac{D_3+\varepsilon D_1 t}{\varepsilon}} \int_{B(x_\varepsilon,\varepsilon)} e^{\frac{c}{2\varepsilon}y} e^{-\frac{|x-y|^2}{4t\varepsilon^2}} dy \\ &\ge \frac{D_2 |B(x_\varepsilon,\varepsilon)|}{\varepsilon^2\sqrt{4\pi t}} \exp\left\{ -\frac{|x|^2 + (|x_\varepsilon|+\varepsilon)^2}{2t\varepsilon^2} + \frac{c}{2}\left(\frac{x_\varepsilon}{\varepsilon} - 1\right) - \frac{D_3 + D_1 t\varepsilon}{\varepsilon} \right\}. \end{aligned}$$

By the definition of n_ε^* and the comparison principle we obtain that $n_\varepsilon^*(t,x) \le n_\varepsilon(t,x)$ and hence

$$n_\varepsilon(t,x) \ge \frac{D_2 |B(x_\varepsilon,\varepsilon)|}{\varepsilon^2\sqrt{4\pi t}} \exp\left\{ -\frac{|x|^2 + (|x_\varepsilon|+\varepsilon)^2}{2t\varepsilon^2} + \frac{c}{2}\left(\frac{x_\varepsilon - x}{\varepsilon} - 1\right) - \frac{D_3 + D_1 t\varepsilon}{\varepsilon} \right\}.$$

This, together with the definition of ψ_ε, implies that

$$\varepsilon \log\left(\frac{D_2 |B(x_\varepsilon,\varepsilon)|}{\varepsilon^2\sqrt{4\pi t}}\right) - \frac{|x|^2 + (|x_\varepsilon|+\varepsilon)^2}{2t\varepsilon} + \frac{c}{2}(x_\varepsilon - x - \varepsilon) - (D_3 + D_1 t\varepsilon) \le \psi_\varepsilon(t,x), \quad \forall t \ge 0.$$

In particular, we obtain that

$$\varepsilon \log\left(\frac{D_2 |B(x_\varepsilon,\varepsilon)|}{\varepsilon^{3/2}\sqrt{4\pi t}}\right) - \frac{|x|^2 + (|x_\varepsilon|+\varepsilon)^2}{2t} + \frac{c}{2}(x_\varepsilon - x - \varepsilon) - (D_3 + D_1 t) \le \psi_\varepsilon\left(\frac{t}{\varepsilon}, x\right), \quad \forall t \in [1, 1+\varepsilon T].$$

Note that x_ε is uniformly bounded in ε thanks to (2.6). Then we can conclude by using the periodicity of ψ_ε. We obtain a quadratic lower bound for ψ_ε for all $t \ge 0$; that is, there exist A_1, $A_2 \ge 0$ and ε_0 small enough such that for all $\varepsilon \le \varepsilon_0$,

$$-A_1|x|^2 - \frac{c}{2}x - A_2 \leq \psi_\varepsilon(t,x), \quad \forall t \geq 0. \tag{2.34}$$

2.3.2.2 Lipschitz bounds

In this section we prove the Lipschitz bounds for ψ_ε. To this end we use a Bernstein type method closely related to the one used in [10, 41]. Let $\phi_\varepsilon = \sqrt{2c_1 - \psi_\varepsilon}$, for c_1 given by (2.30), then ϕ_ε satisfies

$$\frac{1}{\varepsilon}\partial_t\phi_\varepsilon - c\partial_x\phi_\varepsilon - \varepsilon\partial_{xx}\phi_\varepsilon - \left(\frac{\varepsilon}{\phi_\varepsilon} - 2\phi_\varepsilon\right)|\partial\phi_\varepsilon|^2 = \frac{a(t,x) - \rho_\varepsilon(t)}{-2\phi_\varepsilon}.$$

Define $\Phi_\varepsilon = \partial_x\phi_\varepsilon$, which is also $T-$periodic. We differentiate the above equation with respect to x and multiply by $\frac{\Phi_\varepsilon}{|\Phi_\varepsilon|}$, i.e.,

$$\frac{1}{\varepsilon}\partial_t|\Phi_\varepsilon| - c\partial_x|\Phi_\varepsilon| - \varepsilon\partial_{xx}|\Phi_\varepsilon| - 2\left(\frac{\varepsilon}{\phi_\varepsilon} - 2\phi_\varepsilon\right)\Phi_\varepsilon\cdot\partial_x|\Phi_\varepsilon| + \left(\frac{\varepsilon}{\phi_\varepsilon^2} + 2\right)|\Phi_\varepsilon|^3 \leq \frac{(a(t,x) - \rho_\varepsilon(t))\,|\Phi_\varepsilon|}{2\phi_\varepsilon^2} - \frac{\partial_x a\cdot\Phi_\varepsilon}{2\phi_\varepsilon|\Phi_\varepsilon|}.$$

From (2.30) we deduce that

$$\sqrt{c_1} \leq \phi_\varepsilon \leq \sqrt{A_1|x|^2 + \frac{c}{2}x + A_3}, \qquad \forall\, t \geq 0,\ x \in \mathbb{R},$$

for $A_3 = A_2 + 2c_1$. It follows that

$$\left|2\left(\frac{\varepsilon}{\phi_\varepsilon} - 2\phi_\varepsilon\right)\right| \leq A_4|x| + A_5,$$

for some positive constants A_4 and A_5. From here, we deduce for ϑ large enough

$$\frac{1}{\varepsilon}\partial_t|\Phi_\varepsilon| - c\partial_x|\Phi_\varepsilon| - \varepsilon\partial_{xx}|\Phi_\varepsilon| - \big(A_4|x| + A_5\big)\big|\Phi_\varepsilon\cdot\partial_x|\Phi_\varepsilon|\big| + 2\left(|\Phi_\varepsilon| - \vartheta\right)^3 \leq 0. \tag{2.35}$$

Let $T_M > 2T$ and A_6 to be chosen later, define now, for $(t,x) \in \left(0, \frac{T_M}{\varepsilon}\right] \times [-R,R]$

$$\Theta_\varepsilon(t,x) = \frac{1}{2\sqrt{t\varepsilon}} + \frac{A_6R^2}{R^2 - |x|^2} + \vartheta.$$

We next verify that Θ_ε is a strict supersolution of (2.35) in $\left(0, \frac{T_M}{\varepsilon}\right] \times [-R,R]$. To this end we compute

$$\partial_t\Theta_\varepsilon = -\frac{1}{4t\sqrt{t\varepsilon}}, \quad \partial_x\Theta_\varepsilon = \frac{2A_6R^2x}{(R^2-|x|^2)^2}, \quad \partial_{xx}\Theta_\varepsilon = \frac{2A_6R^2}{(R^2-|x|^2)^2} + \frac{8A_6R^2|x|^2}{(R^2-|x|^2)^3},$$

and then replace in (2.35) to obtain

$$\begin{aligned}
&\tfrac{1}{\varepsilon}\partial_t\Theta_\varepsilon - c\partial_x\Theta_\varepsilon - \varepsilon\partial_{xx}\Theta_\varepsilon - \big(A_4|x| + A_5\big)|\Theta_\varepsilon\cdot\partial_x\Theta_\varepsilon| + 2\left(\Theta_\varepsilon - \vartheta\right)^3 \\
&= -\tfrac{1}{4\varepsilon t\sqrt{\varepsilon t}} - \tfrac{2cA_6R^2x}{(R^2-|x|^2)^2} - \varepsilon\left[\tfrac{2A_6R^2}{(R^2-|x|^2)^2} + \tfrac{8A_6R^2|x|^2}{(R^2-|x|^2)^3}\right] \\
&\quad -\big(A_4|x| + A_5\big)\left(\tfrac{1}{2\sqrt{\varepsilon t}} + \tfrac{A_6R^2}{R^2-|x|^2} + \vartheta\right)\tfrac{2A_6R^2|x|}{(R^2-|x|^2)^2} + 2\left(\tfrac{1}{2\sqrt{\varepsilon t}} + \tfrac{A_6R^2}{R^2-|x|^2}\right)^3 \\
&\geq -\varepsilon\left[\tfrac{2A_6R^2d}{(R^2-|x|^2)^2} + \tfrac{8A_6R^4}{(R^2-|x|^2)^3}\right] - \big(A_4R + A_5\big)\left(\tfrac{1}{2\sqrt{\varepsilon t}} + \tfrac{A_6R^2}{R^2-|x|^2} + \vartheta\right)\tfrac{2A_6R^3}{(R^2-|x|^2)^2} \\
&\quad + \tfrac{3A_6R^2}{R^2-|x|^2}\left(\tfrac{1}{2t\varepsilon} + \tfrac{A_6R^2}{\sqrt{\varepsilon t}(R^2-|x|^2)}\right) + \tfrac{2A_6R^3}{(R^2-|x|^2)^2}\left(\tfrac{A_6^2R^3}{R^2-|x^2|} - c\right),
\end{aligned}$$

where, for the inequality, we have used that $|x| \leq R$.
One can verify that the RHS of the above inequality is strictly positive for $R > 1$, $\varepsilon \leq 1$, and $A_6 >> \sqrt{T_M}$. Therefore, Θ_ε is a strict supersolution of (2.35) in $\left(0, \frac{T_M}{\varepsilon}\right] \times [-R, R]$ and for $\varepsilon \leq 1$.
We next prove that

$$|\Phi_\varepsilon(t,x)| \leq \Theta_\varepsilon(t,x) \quad \text{in } \left(0, \frac{T_M}{\varepsilon}\right] \times [-R, R].$$

To this end, we notice that $\Theta_\varepsilon(t,x)$ goes to $+\infty$ as $|x| \to R$ or as $t \to 0$. Therefore, $|\Phi_\varepsilon|(t,x) - \Theta_\varepsilon(t,x)$ attains its maximum at an interior point of $\left(0, \frac{T_M}{\varepsilon}\right] \times [-R, R]$. We choose $t_{\max} \leq \frac{T_M}{\varepsilon}$ the smallest time such that the maximum of $|\Phi_\varepsilon|(t,x) - \Theta_\varepsilon(t,x)$ in the set $(0, t_{\max}] \times [-R, R]$ is equal to 0. If such $t_{\max}$ does not exist, we are done.

Let $x_{\max}$ be such that $|\Phi_\varepsilon|(t,x) - \Theta_\varepsilon(t,x) \leq |\Phi_\varepsilon|(t_{\max}, x_{\max}) - \Theta_\varepsilon(t_{\max}, x_{\max}) = 0$ for all $(t,x) \in (0, t_{\max}) \times [-R, R]$. At such point, we have

$$0 \leq \partial_t \big(|\Phi_\varepsilon| - \Theta_\varepsilon\big)(t_{\max}, x_{\max}), \quad 0 \leq -\partial_{xx} \big(|\Phi_\varepsilon| - \Theta_\varepsilon\big)(t_{\max}, x_{\max}),$$

$$|\Phi_\varepsilon|(t_{\max}, x_{\max}) \partial_x |\Phi_\varepsilon|(t_{\max}, x_{\max}) = \Theta_\varepsilon(t_{\max}, x_{\max}) \partial_x \Theta_\varepsilon(t_{\max}, x_{\max}).$$

Combining the above properties with the facts that $|\Phi_\varepsilon|$ and Θ_ε are respectively sub- and strict super-solution of (2.35), we obtain that

$$\left(|\Phi_\varepsilon|(t_{\max}, x_{\max}) - \vartheta\right)^3 - \left(\Theta_\varepsilon(t_{\max}, x_{\max}) - \vartheta\right)^3 < 0 \Rightarrow |\Phi_\varepsilon|(t_{\max}, x_{\max}) < \Theta_\varepsilon(t_{\max}, x_{\max}),$$

which is in contradiction with the choice of $(t_{\max}, x_{\max})$. We deduce, then that

$$|\Phi_\varepsilon(t,x)| \leq \frac{1}{2\sqrt{\varepsilon t}} + \frac{A_6 R^2}{R^2 - |x|^2} + \vartheta \quad \text{for } (t,x) \in \left(0, \frac{T_M}{\varepsilon}\right] \times [-R, R], \ \forall\ R > 1.$$

We note that for $\varepsilon < \varepsilon_0$ small enough we have $\frac{T_M}{\varepsilon} > \frac{2T}{\varepsilon} > \frac{T}{\varepsilon} + T > \frac{T}{\varepsilon}$. Letting $R \to \infty$ we deduce that

$$|\Phi_\varepsilon(t,x)| \leq \frac{1}{2\sqrt{\varepsilon t}} + A_6 + \vartheta \leq \frac{1}{2\sqrt{T}} + A_6 + \vartheta \quad \text{for } (t,x) \in \left[\frac{T}{\varepsilon}, \frac{T}{\varepsilon} + T\right] \times \mathbb{R}.$$

Finally we use the periodicity of Φ_ε to extend the result for all $t \in [0, +\infty)$ and rewriting the result in terms of ϕ_ε we obtain for some positive constant A_7

$$|\partial_x \phi_\varepsilon| \leq A_7, \quad \text{in } [0, +\infty) \times \mathbb{R}. \tag{2.36}$$

2.3.3 Derivation of the Hamilton-Jacobi equation with constraint

In this section we derive the Hamilton-Jacobi equation with constraint (2.15) using the regularity estimates in Theorem 2.13.

2.3.3.1 Convergence along subsequences of ψ_ε and ρ_ε

According to Section 2.3.2, $\{\psi_\varepsilon\}$ is locally uniformly bounded and equicontinuous, so by the Arzela-Ascoli Theorem after extraction of a subsequence, $\psi_\varepsilon(t,x)$ converges locally uniformly to a continuous function $\psi(t,x)$. Moreover from (2.31), we obtain that ψ does not depend on t, i.e $\psi(t,x) = \psi(x)$.
Furthermore, from the uniform bounds on ρ_ε in (2.28) we obtain that $|\frac{d\rho_\varepsilon}{dt}|$ is also bounded. Then we apply the Arzela-Ascoli Theorem to guarantee the locally uniform convergence along subsequences of $\rho_\varepsilon(t)$, to a function $\tilde{\varrho}(t)$ as $\varepsilon \to 0$.

2.3.3.2 The Hamilton-Jacobi equation with constraint

Here we use a perturbed test function argument (see for instant [38]), in order to prove that, $\psi(x) = \lim_{\varepsilon\to 0}\psi(t,x)$ is in fact a viscosity solution of the following Hamilton-Jacobi equation.

$$-\left|\partial_x\psi + \frac{c}{2}\right|^2 = \overline{a}(x) - \overline{\rho} - \frac{c^2}{4}, \tag{2.37}$$

where $\overline{\rho} = \frac{1}{T}\int_0^T \tilde{\varrho}(t)dt$. We prove that ψ is a viscosity sub-solution and one can use the same type of argument to prove that it is also a super-solution.

Let us define the auxiliary "cell problem":

$$\begin{cases} \partial_t\phi = a(t,x) - \tilde{\varrho}(t) - \overline{a}(x) + \overline{\rho}, \quad (t,x) \in [0,+\infty)\times\mathbb{R}, \\ \phi(0,x) = 0, \\ \phi : \ T-periodic. \end{cases} \tag{2.38}$$

This equation has a unique smooth solution, that we can explicitly write:

$$\phi(t,x) = -t(\overline{a}(x) - \overline{\rho}) + \int_0^t (a(t,x) - \tilde{\varrho}(t))dt.$$

Let $\varphi \in C^\infty(\mathbb{R})$ be a test function and assume that $\psi - \varphi$ has a strict local maximum at some point $x_0 \in \mathbb{R}$, with $\psi(x_0) = \varphi(x_0)$. We must prove:

$$-\left|\partial_x\varphi(x_0) + \frac{c}{2}\right|^2 - \overline{a}(x_0) + \frac{c^2}{4} + \overline{\rho} \le 0. \tag{2.39}$$

We define the perturbed test function $\Psi_\varepsilon(t,x) = \varphi(x) + \varepsilon\phi(t,x)$, such that $\psi_\varepsilon - \Psi_\varepsilon$ attains a local maximum at some point $(t_\varepsilon, x_\varepsilon)$. We note that Ψ_ε converges locally uniformly to φ as $\varepsilon \to 0$ since ϕ is locally bounded by definition, and hence one can choose x_ε such that $x_\varepsilon \to x_0$ as $\varepsilon \to 0$, (see Lemma 2.2 in [8]). Then Ψ_ε satisfies:

$$\frac{1}{\varepsilon}\partial_t\Psi_\varepsilon(t_\varepsilon,x_\varepsilon) - \varepsilon\partial_{xx}\Psi_\varepsilon(t_\varepsilon,x_\varepsilon) - \left|\partial_x\Psi_\varepsilon(t_\varepsilon,x_\varepsilon) + \frac{c}{2}\right|^2 - a(t_\varepsilon,x_\varepsilon) + \frac{c^2}{4} + \rho_\varepsilon(t_\varepsilon) \le 0,$$

since ψ_ε is a solution of (2.29). The above line gives:

$$\partial_t\phi(t_\varepsilon,x_\varepsilon) - \varepsilon\partial_{xx}\varphi(x_\varepsilon) - \varepsilon^2\partial_{xx}\phi(t_\varepsilon,x_\varepsilon) - \left|\partial_x\varphi(x_\varepsilon) + \varepsilon\partial_x\phi(t_\varepsilon,x_\varepsilon) + \frac{c}{2}\right|^2 - a(t_\varepsilon,x_\varepsilon) + \frac{c^2}{4} + \rho_\varepsilon(t_\varepsilon) \le 0.$$

Using (2.38), this last equation becomes:

$$-\varepsilon\partial_{xx}\varphi(x_\varepsilon) - \varepsilon^2\partial_{xx}\phi(t_\varepsilon,x_\varepsilon) - \left|\partial_x\varphi(x_\varepsilon) + \varepsilon\partial_x\phi(t_\varepsilon,x_\varepsilon) + \frac{c}{2}\right|^2 + (\rho_\varepsilon - \tilde{\varrho})(t_\varepsilon) - \overline{a}(x_\varepsilon) + \overline{\rho} + \frac{c^2}{4} \le 0. \tag{2.40}$$

Next we pass to the limit as $\varepsilon \to 0$. We know from Subsection 3.3.1 that $\rho_\varepsilon \to \tilde{\varrho}$ locally uniformly as $\varepsilon \to 0$. Moreover ϕ is smooth with locally bounded derivatives with respect to x, thanks to its definition. Using these arguments and letting $\varepsilon \to 0$ in (2.40) we obtain (2.39) which implies that ψ is a viscosity sub-solution of (2.37).

Furthermore, note that ψ is also bounded from above, by taking the limit as $\varepsilon \to 0$ in (2.30), i.e.,

$$\psi(x) \le c_1 - c_2|x|, \tag{2.41}$$

and attains its maximum. We claim that

$$\max_{x\in\mathbb{R}} \psi(x) = 0.$$

Indeed, from the upper bound for ρ_ε in (2.28), the definition of ψ_ε in (2.14) and the continuity of ψ, we obtain that $\psi(x) \leq 0$. Moreover, from the locally uniform convergence of ψ_ε to ψ, as $\varepsilon \to 0$, and (2.30) we deduce that $\max_{x\in\mathbb{R}} \psi(x) < 0$ implies that $\psi_\varepsilon(x) < -\beta$, for all $x \in \mathbb{R}$ and $\varepsilon \leq \varepsilon_0$ and some positive constant β. This is in contradiction with the fact that ρ_ε is bounded by below by a positive constant ρ_m (we refer to section 4.3 of [41] for more details).

2.4 Uniqueness of the viscosity solution to (2.15) and explicit identification

In this section we deal with the uniqueness of the viscosity solution of equation (2.15). To this end, we first derive an equivalent Hamilton-Jacobi equation to (2.15) by mean of the Liouville transformation and prove some properties of the eigenvalue $\lambda_{c,\varepsilon}$. We then prove the uniqueness of the viscosity solution to such equivalent equation. This allows us to establish the uniqueness of the solution to (2.15) and to identify it explicitly.

2.4.1 Derivation of an equivalent Hamilton-Jacobi equation

In this subsection, analogously to Section 2.2.1 we make a Liouville transformation for the periodic solution n_ε of equation (2.13), followed by a Hopf-Cole change of variables, which lead to a modified Hamilton-Jacobi equation. That is, we call $N_\varepsilon(t,x) = n_\varepsilon(t,x)e^{\frac{c}{2\varepsilon}x}$ which solves:

$$\begin{cases} \partial_t N_\varepsilon - \varepsilon^2 \partial_{xx} N_\varepsilon &= N_\varepsilon \left[a(t,x) - \frac{c^2}{4} - \rho_\varepsilon(t) \right], \quad (t,x) \in [0,+\infty) \times \mathbb{R}, \\ N_\varepsilon(0,x) &= N_\varepsilon(T,x). \end{cases} \tag{2.42}$$

Now we make a Hopf-Cole transformation for N_ε, i.e:

$$N_\varepsilon(t,x) = \frac{1}{\sqrt{2\pi\varepsilon}} e^{\frac{u_\varepsilon(t,x)}{\varepsilon}}, \tag{2.43}$$

and we can verify easily that u_ε satisfies:

$$\frac{1}{\varepsilon}\partial_t u_\varepsilon - \varepsilon \partial_{xx} u_\varepsilon = |\partial_x u_\varepsilon|^2 + a(t,x) - \frac{c^2}{4} - \rho_\varepsilon(t). \tag{2.44}$$

Then, by combining (2.14), (2.43) and the definition of N_ε, we can write:

$$\psi_\varepsilon = u_\varepsilon - \frac{c}{2}x. \tag{2.45}$$

Therefore, following the convergence result proved for ψ, we obtain a limit function $u(x)$ such that

$$\lim_{\varepsilon\to 0} u_\varepsilon(t,x) = u(x) := \psi(x) + \frac{c}{2}x, \tag{2.46}$$

which solves the following Hamilton-Jacobi equation, also in the viscosity sense

$$-|\partial_x u|^2 = \overline{a}(x) - \overline{\rho} - \frac{c^2}{4}. \tag{2.47}$$

Moreover we have the following boundedness result for u.

Lemma 2.14 *The function $u(x)$ defined by (2.46) is bounded and satisfies*

$$-A_1|x|^2 - A_2 \leq u(x) \leq c_1 - c_2|x| + \frac{c}{2}x, \quad \forall\ x \in \mathbb{R}, \tag{2.48}$$

where the constants A_1, A_2, c_1 and c_2 are given in (2.30).

Proof. From Subsection 2.3.2 we got uniform bounds for ψ_ε in (2.30), which lead to bounds on ψ. That is

$$-A_1|x|^2 - \frac{c}{2}x - A_2 \leq \psi(x) \leq c_1 - c_2|x|.$$

Then, the upper bound (2.48) follows directly from the definition of $u(x)$ in (2.46).

■

Therefore, we conclude that the limit function u satisfies (2.23).

2.4.2 Some properties of the eigenvalue $\lambda_{c,\varepsilon}$

In this subsection we begin the proof of Theorem 2.7-(i) and prove the first equality in (2.17). We also establish the convergence along subsequences of the eigenvalue $\lambda_{c,\varepsilon}$ to some negative constant as $\varepsilon \to 0$.
From the equation (2.16) we can integrate in $\mathbb{R}$, divide by $\int_{\mathbb{R}} p_{c\varepsilon}(t,x)dx$ and integrate again in $t \in [0,T]$ (in that order) and obtain

$$\lambda_{c,\varepsilon} = -\frac{1}{T}\int_0^T Q_{c\varepsilon}(t)dt. \tag{2.49}$$

where $Q_{c\varepsilon}(t)$ is defined analogously to (2.8) from the periodic eigenfunction $p_{c\varepsilon}$. This implies thanks to (H1) that

$$-d_0 \leq \lambda_{c,\varepsilon}.$$

Moreover, since we are in the case $c < \liminf_{\varepsilon\to 0} c^*_\varepsilon$, there exists $\lambda_m > 0$ such that,

$$\lambda_{c,\varepsilon} \leq -\lambda_m < 0. \tag{2.50}$$

Indeed, since $c < \liminf_{\varepsilon\to 0} c^*_\varepsilon$ we can find a positive constant τ such that for every $\varepsilon \leq \varepsilon_0$, with ε_0 small enough we have $c < c^*_\varepsilon - \tau$. Then from the definition of c^*_ε we deduce:

$$c < 2\sqrt{-\lambda_{0,\varepsilon^2}} - \tau = 2\sqrt{-\lambda_{c,\varepsilon} + \frac{c^2}{4}} - \tau,$$

which leads to

$$\lambda_{c,\varepsilon} < -\frac{c\tau}{2} - \frac{\tau^2}{4} =: -\lambda_m.$$

Thus $(\lambda_{c,\varepsilon})_\varepsilon$ is a uniformly bounded sequence. This implies that we can extract a subsequence, still called $\lambda_{c,\varepsilon}$, which converges as $\varepsilon \to 0$ to some negative value λ_1. Moreover passing to the limit as $\varepsilon \to 0$ in assumption (Hc) we obtain, for all such limit values λ_1,

$$\overline{a}(x) \leq -\delta - \lambda_1, \quad \forall |x| \geq R_0. \tag{2.51}$$

We next use the relationship between the solution n_ε to (2.13) and the eigenfunction $p_{c\varepsilon}$ to obtain the first equality in

(2.17). Indeed, from equation (2.13) after an integration in $x \in \mathbb{R}$ we obtain:

$$\frac{d\rho_\varepsilon(t)}{dt} = \int_{\mathbb{R}} n_\varepsilon(t,x)a(t,x)dx - \rho_\varepsilon^2(t).$$

We divide by $\rho_\varepsilon(t)$ and use the relation between n_ε and $p_{c\varepsilon}$ inside of the integral, that is:

$$\rho_\varepsilon(t) + \frac{d}{dt}\ln\rho_\varepsilon(t) = \frac{\int_{\mathbb{R}} p_{c\varepsilon}(t,x)a(t,x)dx}{\int_{\mathbb{R}} p_{c\varepsilon}(t,y)dy}.$$

Note that the RHS is exactly $Q_{c\varepsilon}$. We then integrate in $[0,T]$ and using (2.49) and the $T-$periodicity of ρ_ε we deduce that

$$\bar{\rho}_\varepsilon = -\lambda_{c,\varepsilon}, \tag{2.52}$$

and passing to the limit as $\varepsilon \to 0$ along the same subsequence, we obtain that

$$\overline{\rho} = -\lambda_1. \tag{2.53}$$

2.4.3 Uniqueness and explicit formula for $u(x)$

In this subsection we prove the uniqueness of the viscosity solution of the Hamilton-Jacobi equation (2.23). To this end we consider the Hamilton-Jacobi equation as follows

$$-|\partial_x u|^2 = h(x), \quad x \in \Omega, \tag{2.54}$$

where $h \in C^1(\mathbb{R})$. Note that this corresponds to our problem for $h(x) = \bar{h}(x) := \overline{a}(x) - \overline{\rho} - \frac{c^2}{4}$.
We divide the proof of the uniqueness result into several steps. We first prove that, in the case where Ω is an open bounded domain and $h < 0$ in Ω, a viscosity solution to (2.54) can be uniquely determined from its values on the boundary of Ω. We then use this property and (2.48) to prove that in our problem it is not possible that $\bar{h}(x) < 0$ for all $x \in \mathbb{R}$. We prove indeed that $\max \bar{h}(x) = 0$ and this maximum is attained only at the point x_m. Finally we use these properties to conclude that u is indeed uniquely determined by an explicit formula.

Step 1: If $h < 0$ and Ω is bounded then the viscosity solution to (2.54) is unique. Suppose that $h(x) < 0$, for every $x \in \Omega$. For this problem we obtain uniqueness of the viscosity solution thanks to a monotone transformation of the function u. Indeed, for Ω bounded we define $L(x,y)$ as follows

$$L(x,y) = \sup\left\{\int_0^{T_0} -\sqrt{-h(\xi(t))}dt/(T_0,\xi) \text{ such that } \xi(0)=x,\ \xi(T_0)=y,\ \xi(t)\in\Omega, \forall t\in[0,T_0], \left|\frac{d\xi}{dt}\right| \le 1 \text{ a.e in } [0,T_0]\right\}, \tag{2.55}$$

and in Appendix 2.B we prove the following:

Proposition 2.15 *Assume that $h(x) < 0$, $\forall x \in \Omega$. The function*

$$u = \inf_{y\in\partial\Omega}[\varphi(y) + L(x,y)],$$

is the unique viscosity solution of

$$|Du| = \sqrt{-h(x)} \text{ in } \Omega; \quad u = \varphi \text{ on } \partial\Omega.$$

Step 2: $\max_{x\in\mathbb{R}} \bar{h}(x) = \bar{h}(x_m) = 0$ **and the maximum is only attained at this point.** We assume in the contrary that $\max_{x\in\mathbb{R}} \bar{h}(x) < 0$. We consider $\Omega = B_{R'} = (-R', R')$ for $R' > 0$, to be chosen later. According to step 1, we can write the viscosity solution of (2.54) for $\bar{h}(x)$ as follows:

$$u(x) = \max\left\{u(-R') - \left|\int_{-R'}^{x} \sqrt{-\bar{h}(y)}dy\right|; u(R') - \left|\int_{x}^{R'} \sqrt{-\bar{h}(y)}dy\right|\right\}.$$

Then, let $R > R_0$ and choose R' such that $R << R'$ and take $x \in B_R = [-R, R]$. Thanks to (2.51) and (2.53), we obtain that

$$\sqrt{\delta + \frac{c^2}{4}} \leq \sqrt{-\bar{h}(y)}, \quad \forall |y| \geq R_0.$$

We deduce that

$$\int_{-R'}^{x} \sqrt{-\bar{h}(y)}dy \geq \sqrt{\delta + \frac{c^2}{4}}(R' - R), \quad \text{and} \quad \int_{x}^{R'} \sqrt{-\bar{h}(y)}dy \geq \sqrt{\delta + \frac{c^2}{4}}(R' - R).$$

Next we combine the above inequalities with the second line of (2.23) to obtain

$$u(x) \leq \max\left\{c_1 - R'\sqrt{\delta + \frac{c^2}{2}} - \big(R' - R\big)\sqrt{\delta + \frac{c^2}{4}}; \quad c_1 + cR' - R'\sqrt{\delta + \frac{c^2}{2}} - \big(R' - R\big)\sqrt{\delta + \frac{c^2}{4}}\right\},$$

for c_1 given in (2.23). This implies that, taking R' arbitrarily large, $u(x)$ the limit as $\varepsilon \to 0$ of $u_\varepsilon(t, x)$ is arbitrarily small in $[-R, R]$ which is a contradiction. Therefore the assumption on $\bar{h}(x)$ of being strictly negative in Ω is false.
We have proved that $\bar{h}(x)$ vanishes at some point $x \in \mathbb{R}$. Note also from (2.47) that

$$\bar{a}(x) - \bar{\rho} - \frac{c^2}{4} \leq 0,$$

and $\max_{x\in\mathbb{R}} \bar{h}(x)$ is attained at the unique maximum point of $\bar{a}$, which is x_m.

Step 3: Identification of u in $\mathbb{R}$. We now prove that the solution u is uniquely determined by its value at the maximum point of $\bar{h}(x)$. That is, for all $x \in \mathbb{R}$

$$u(x) = -\left|\int_{x_m}^{x} \sqrt{-\bar{h}(y)}dy\right| + u(x_m). \tag{2.56}$$

To this end we choose $0 < R$, and $0 < R'$ such that $R << R'$ and we consider the domain $\overline{B_{R'}} = [-R', x_m] \cup [x_m, R']$ and we prove the following inequalities for R' large enough,

$$\left|\int_{x_m}^{x} \sqrt{-\bar{h}(y)}dy\right| - u(x_m) \leq \left|\int_{-R'}^{x} \sqrt{-\bar{h}(y)}dy\right| - u(-R'), \quad \forall x \in [-R, x_m],$$

$$\left|\int_{x_m}^{x} \sqrt{-\bar{h}(y)}dy\right| - u(x_m) \leq \left|\int_{x}^{R'} \sqrt{-\bar{h}(y)}dy\right| - u(R'), \quad \forall x \in [x_m, R].$$

Note that $\bar{h} < 0$ in the sets $(-R', x_m)$ and (x_m, R'). We can thus apply Proposition 2.15 in these domains and use the above inequalities to obtain (2.56) for all $x \in [-R, R]$. Since R is arbitrary we thus obtain (2.56). Note that at point $x = x_m$ the latter inequalities hold trivially. Suppose that $x_m < x < R$. We prove the second inequality (the first one

follows from an analogous argument). We claim that, for R' large enough

$$-\int_{x_m}^{x}\sqrt{-\bar{h}(y)}dy+u(x_m)+\int_{x}^{R'}\sqrt{-\bar{h}(y)}dy-u(R')\geq 0. \tag{2.57}$$

Indeed, for $x\in[x_m,R]$ we have

$$-\int_{x_m}^{x}\sqrt{-\bar{h}(y)}dy\geq-\int_{x_m}^{R}\sqrt{-\bar{h}(y)}dy. \tag{2.58}$$

Moreover, from the upper bound for u in (2.48) we obtain for all $x\in B_{R'}(x_m)$,

$$u(x)\leq c_1-c_2|x|+\frac{c}{2}x,\quad\Rightarrow u(R')\leq c_1+\frac{c}{2}R'. \tag{2.59}$$

Furthermore, it holds, following similar arguments as in the previous step that:

$$\sqrt{-\bar{h}(y)}\geq\sqrt{\delta+\frac{c^2}{4}},\quad\forall y\in(R_0,R'). \tag{2.60}$$

Finally, putting together(2.58), (2.59) and (2.60) we obtain:

$$-\int_{x_m}^{x}\sqrt{-\bar{h}(y)}dy+u(x_m)+\int_{x}^{R'}\sqrt{-\bar{h}(y)}dy-u(R')\geq-\int_{x_m}^{R}\sqrt{-\bar{h}(y)}dy+u(x_m)+(R'-R_0)\sqrt{\delta+\frac{c^2}{4}}-\frac{c}{2}R'-c_1\geq 0,$$

for R' large enough. We conclude that the solution u is indeed determined by its value at the maximum point of $\bar{a}$ and obtain the explicit formula (2.56).

2.4.4 Explicit formula for ψ

From the uniqueness of the viscosity solution to equation (2.23) for fixed $\bar{\rho}$ and the explicit representation (2.56), it follows:

$$u(x)=u(x_m)-\left|\int_{x_m}^{x}\sqrt{\overline{\rho}+\frac{c^2}{4}-\overline{a}(y)}dy\right|,\quad\forall x\in\mathbb{R}. \tag{2.61}$$

This directly implies that u is in fact a classical solution for $x\in\mathbb{R}$ which attains its maximum at $x=x_m$. Moreover from step 2 in Section 2.4.3 we have

$$\overline{a}(x_m)=\overline{\rho}+\frac{c^2}{4}, \tag{2.62}$$

and hence $\bar{\rho}$ and u are uniquely determined.

The formula (2.61) together with (2.46) also imply the uniqueness of the limit ψ, the viscosity solution to (2.15) and the following explicit representation,

$$\psi(x)=u(x_m)-\frac{c}{2}x-\left|\int_{x_m}^{x}\sqrt{\overline{a}(x_m)-\overline{a}(y)}dy\right|,\quad\forall x\in\mathbb{R}.$$

We denote the set of maximum points of ψ by X^*, i.e

$$X^*:=\{x^*\in\mathbb{R}\text{ such that }\psi(x^*)=0\}.$$

Let $x^*\in X^*$, we evaluate the above formula of ψ at x^* in order to obtain an expression for $u(x_m)$. This implies

$$\psi(x) = \frac{c}{2}(x^* - x) + \left| \int_{x_m}^{x^*} \sqrt{\overline{a}(x_m) - \overline{a}(y)}dy \right| - \left| \int_{x_m}^{x} \sqrt{\overline{a}(x_m) - \overline{a}(y)}dy \right|, \quad \forall x \in \mathbb{R}. \tag{2.63}$$

Moreover,

$$\psi(x_m) \leq \psi(x^*) \Rightarrow \frac{c}{2}(x^* - x_m) \leq 0,$$

then necessarily $x^* \leq x_m$. Note also from (2.15) that $\bar{a}(x^*) = \bar{\rho}$. Thus from (2.62) and assumption (H3) it follows that $x^* = \overline{x}$, and we can write $\psi(x)$ explicitly as in (2.19) for every $x \in \mathbb{R}$. This ends the proof of Theorem 2.7-(ii).

2.4.5 Convergence to the Dirac mass

We deal in this subsection with the result for the convergence of n_ε, that is Theorem 2.7-(iii).
Call $f_\varepsilon(t,x) = \dfrac{n_\varepsilon(t,x)}{\rho_\varepsilon(t)}$, then f_ε is uniformly bounded in $L^\infty(\mathbb{R}^+, L^1(\mathbb{R}))$. Next, we fix $t \geq 0$, and we prove that $f_\varepsilon(t,\cdot)$, converges, along subsequences, to a measure, as follows

$$f_\varepsilon(t,\cdot) \rightharpoonup \delta(\cdot - \bar{x}) \quad \text{as} \quad \varepsilon \to 0,$$

weakly in the sense of measures.
Indeed, we already know that

$$\max_{x\in\mathbb{R}} \psi(x) = \psi(\bar{x}) = 0 \quad \text{and} \quad \psi(x) \leq c_1 - c_2|x|,$$

for $\bar{x}$ given in Theorem 2.7. This implies that for any $\zeta > 0$, there exists $\beta > 0$ such that $\psi(x) \leq -\beta$ for every $x \in \mathbb{R} \setminus [\bar{x} - \zeta, \bar{x} + \zeta]$.
We denote $\mathcal{O} = \mathbb{R} \setminus [\bar{x} - \zeta, \bar{x} + \zeta]$ and choose $\chi \in C_c(\mathcal{O})$, such that supp $\chi \subset \mathcal{K}$, for some compact set $\mathcal{K}$, then it follows that

$$\left| \int_{\mathcal{O}} f_\varepsilon(t,x)\chi(x)dx \right| \leq \frac{1}{\rho_m} \int_{\mathcal{O}} e^{\frac{\psi_\varepsilon(t,x)}{\varepsilon}} |\chi(x)|dx \leq \frac{1}{\rho_m} \int_{\mathcal{K}} e^{\frac{\psi_\varepsilon(t,x)}{\varepsilon}} |\chi(x)|dx.$$

From the locally uniform convergence of ψ_ε, to $\psi(x)$, we obtain that there exists $\varepsilon_0 > 0$ such that $\forall \varepsilon < \varepsilon_0$, $\psi_\varepsilon(t,x) \leq -\frac{\beta}{2}$, $\forall x \in \mathcal{K}$, and hence

$$\int_{\mathcal{K}} e^{\frac{\psi_\varepsilon(t,x)}{\varepsilon}} |\chi(x)|dx \leq \int_{\mathcal{K}} e^{-\frac{\beta}{2\varepsilon}} |\chi(x)|dx \to 0 \quad \text{as } \varepsilon \to 0,$$

since χ is bounded in $\mathcal{K}$. Therefore, thanks to the uniform L^1 bound of f_ε, we obtain that f_ε converges weakly in the sense of measures and along subsequences to $\mu\delta(x - \bar{x})$ as $\varepsilon \to 0$. Then to prove that in fact, $\mu = 1$ we can proceed as in Section 4.3 in [41]. Therefore using the convergence result for ρ_ε we deduce finally (2.20) and this ends the proof of Theorem 2.7-(iii).

2.4.6 Identification of the limit of ρ_ε

We now identify $\tilde{\varrho}$ from the explicit expression for ρ_ε, that is:

$$\rho_\varepsilon(t) = \frac{1 - \exp\left[-\displaystyle\int_0^T Q_{c\varepsilon}(s)ds\right]}{\exp\left[-\displaystyle\int_0^T Q_{c\varepsilon}(s)ds\right] \displaystyle\int_t^{t+T} \exp\left[\int_t^s Q_{c\varepsilon}(\theta)d\theta\right] ds}, \tag{2.64}$$

where $Q_{c\varepsilon}$ is defined analogously to (2.8), using the periodic eigenfunction $p_{c\varepsilon}$ of problem (2.16).
We then compute the limit of $Q_{c\varepsilon}$ as $\varepsilon \to 0$. We know that $p_{c\varepsilon}(t,x) = \dfrac{n_\varepsilon(t,x)}{\rho_\varepsilon(t)} \displaystyle\int_{\mathbb{R}} p_{c\varepsilon}(t,y)dy$. Substituting in $Q_{c\varepsilon}$ we obtain

$$Q_{c\varepsilon}(t) = \frac{\displaystyle\int_{\mathbb{R}} a(t,x)p_{c\varepsilon}(t,x)dx}{\displaystyle\int_{\mathbb{R}} p_{c\varepsilon}(t,x)dx} = \frac{\displaystyle\int_{\mathbb{R}} a(t,x)\frac{n_\varepsilon(t,x)}{\rho_\varepsilon(t)}\int_{\mathbb{R}} p_{c\varepsilon}(t,y)dydx}{\displaystyle\int_{\mathbb{R}} p_{c\varepsilon}(t,x)dx} = \frac{\displaystyle\int_{\mathbb{R}} a(t,x)n_\varepsilon(t,x)dx}{\rho_\varepsilon(t)}.$$

From the previous subsection and hypotheses (H2b) and (H3) we deduce that:

$$\lim_{\varepsilon\to 0} Q_{c\varepsilon}(t) = \lim_{\varepsilon\to 0}\int_{\mathbb{R}} f_\varepsilon(t,x)a(t,x)dx = a(t,\bar{x}).$$

Finally we can pass to the limit in the expression (2.64) for ρ_ε, to obtain the following explicit formula for $\tilde{\varrho}$

$$\widetilde{\varrho}(t) = \frac{1-\exp\left[-\displaystyle\int_0^T a(s,\bar{x})ds\right]}{\exp\left[-\displaystyle\int_0^T a(s,\bar{x})ds\right]\displaystyle\int_t^{t+T}\exp\left[\int_t^s a(\theta,\bar{x})d\theta\right]ds}, \tag{2.65}$$

which is in fact the unique periodic solution of the equation (2.21).

2.5 Approximations of the eigenvalue

In this section we finish the proof of Theorem 2.7-(i) and prove the second equality in (2.17). To this end we develop an asymptotic approximation of the eigenvalue $\lambda_{c,\varepsilon}$ of order ε. We also prove (2.18). Let us come back to the eigenproblem (2.16).
To obtain such asymptotic expansion we construct an approximate eigenfunction $\tilde{p}_\varepsilon$ corresponding to an approximate eigenvalue $\tilde{\lambda}_\varepsilon$ which solves an equation close to (2.16). We then use Proposition 2.1 to prove that $\tilde{\lambda}_\varepsilon$ approximates $\lambda_{c,\varepsilon}$ with an error of order ε^2.
To construct an approximated eigenfunction, we first try to approximate w_ε, obtained from the Hopf-Cole transformation of $p_{c\varepsilon}$ as follows:

$$p_{c\varepsilon}(t,x) = \frac{1}{\sqrt{2\pi\varepsilon}}e^{\frac{w_\varepsilon(t,x)}{\varepsilon}}. \tag{2.66}$$

One can verify that w_ε solves:

$$\frac{1}{\varepsilon}\partial_t w_\varepsilon - \varepsilon\partial_{xx}w_\varepsilon = \left|\partial_x w_\varepsilon + \frac{c}{2}\right|^2 + a(t,x) + \lambda_{c,\varepsilon} - \frac{c^2}{4}. \tag{2.67}$$

We can obtain similar bounds for w_ε as for ψ_ε, which guarantee the convergence along subsequences of w_ε to certain function $w = w(x)$, which is in fact the limit of the whole sequence w_ε, and satisfies the following Hamilton-Jacobi equation in the viscosity sense

$$-\left|\partial_x w + \frac{c}{2}\right|^2 = \overline{a}(x) + \lambda_1 - \frac{c^2}{4}. \tag{2.68}$$

Remark 2.16 *Note that in order to obtain the limit equation* (2.68) *we can argue exactly as for ψ_ε in Section 2.3.3.2, by a "perturbed test function" argument, (see also [41]).*

Note that $\psi(x)$ is a solution to (2.68). We then, write (formally)

$$w_\varepsilon(t,x) = \psi(x) + \varepsilon\phi(t,x) + o(\varepsilon) \quad \text{and} \quad \lambda_{c,\varepsilon} = \lambda_1 + \varepsilon\lambda_2 + o(\varepsilon),$$

for ϕ a $T-$periodic function and we construct the following approximated eigenpair:

$$\tilde{\psi_\varepsilon} = \psi + \varepsilon\phi \quad \text{and} \quad \tilde{\lambda}_\varepsilon = \lambda_1 + \varepsilon\lambda_2. \tag{2.69}$$

We then substitute this pair $(\tilde{\psi_\varepsilon}, \tilde{\lambda}_\varepsilon)$ into (2.67) and obtain:

$$\partial_t\phi - c\psi_x - c\varepsilon\partial_x\phi - \varepsilon\psi_{xx} - \varepsilon^2\partial_{xx}\phi = |\psi_x + \varepsilon\partial_x\phi|^2 + a(t,x) + \lambda_1 + \varepsilon\lambda_2 + o(\varepsilon), \tag{2.70}$$

where the notations ψ_x and ψ_{xx} correspond respectively to the first and second derivative of ψ.
Regrouping in powers of ε we obtain the following system for ϕ,

$$\begin{cases} \partial_t\phi = \left|\psi_x + \dfrac{c}{2}\right|^2 + a(t,x) - \dfrac{c^2}{4} + \lambda_1, \\ \\ -\psi_{xx} = [2\psi_x + c]\dfrac{1}{T}\displaystyle\int_0^T \partial_x\phi(t,x)dt + \lambda_2. \end{cases} \tag{2.71}$$

We remark that the previous system has a unique solution ϕ up to addition by a constant. Indeed, from the equation (2.15) we obtain

$$\partial_t\phi = a(t,x) - \bar{a}(x).$$

Integrating in $[0,t]$ leads to

$$\phi(t,x) = \phi(0,x) + \int_0^t a(\tau,x)d\tau - t\bar{a}(x),$$

and the value of $\phi(0,x)$ can be obtained from the second equation in (2.71) once we fix $\phi(0,x_m)$. Note that here we use the fact that $2\psi_x + c$ vanishes only at the point x_m.
We now define $\widetilde{p}_\varepsilon(t,x) := \frac{1}{\sqrt{2\pi\varepsilon}} e^{\frac{\tilde{\psi}_\varepsilon(t,x)}{\varepsilon}}$, and use the system (2.71), to obtain the equality:

$$\mathcal{P}_\varepsilon\widetilde{p}_\varepsilon - \widetilde{\lambda}_\varepsilon\widetilde{p}_\varepsilon = -\varepsilon^2\left(|\partial_x\phi|^2 + \partial_{xx}\phi\right)\widetilde{p}_\varepsilon, \tag{2.72}$$

for $\mathcal{P}_\varepsilon$ the following parabolic operator

$$\mathcal{P}_\varepsilon p = \partial_t p - c\varepsilon\partial_x p - \varepsilon^2\partial_{xx}p - a(t,x)p.$$

We denote

$$\lambda_{\varepsilon^+} = \tilde{\lambda}_\varepsilon + \varepsilon^2 K, \quad \text{and} \quad \lambda_{\varepsilon^-} = \tilde{\lambda}_\varepsilon - \varepsilon^2 K,$$

with

$$K = \||\partial_x\phi|^2 + \partial_{xx}\phi\|_{L^\infty}, \tag{2.73}$$

where the well definition of K is guaranteed by the next lemma which is proved in the next subsection.

Lemma 2.17 *The constant K given in* (2.73) *is well defined. Moreover the function ϕ computed above solves* (2.71) *with $\lambda_1 = -\bar{a}(x_m) + \frac{c^2}{4}$ and $\lambda_2 = \sqrt{-\bar{a}_{xx}(x_m)/2}$.*

Therefore, it holds by substitution into (2.72)

$$\widetilde{p}_\varepsilon\lambda_{\varepsilon^-} \leq \partial_t\widetilde{p}_\varepsilon - c\varepsilon\partial_x\widetilde{p}_\varepsilon - \varepsilon^2\partial_{xx}\widetilde{p}_\varepsilon - a(t,x)\widetilde{p}_\varepsilon \leq \widetilde{p}_\varepsilon\lambda_{\varepsilon^+},$$

and we define the functions

$$\overline{q}_\varepsilon(t,x) = \widetilde{p}_\varepsilon(t,x)e^{-t\lambda_{\varepsilon^-}}, \quad \underline{q}_\varepsilon(t,x) = \widetilde{p}_\varepsilon(t,x)e^{-t\lambda_{\varepsilon^+}}.$$

One can verify that $\overline{q}_\varepsilon$ and $\underline{q}_\varepsilon$ are super- and sub-solution of the linear problem (2.3) with $\sigma = \varepsilon^2$ and $\tilde{c} = c\varepsilon$, that is

$$\partial_t \underline{q}_\varepsilon - c\varepsilon \partial_x \underline{q}_\varepsilon - \varepsilon^2 \partial_{xx} \underline{q}_\varepsilon \leq \underline{q}_\varepsilon a(t,x),$$

$$\partial_t \overline{q}_\varepsilon - c\varepsilon \partial_x \overline{q}_\varepsilon - \varepsilon^2 \partial_{xx} \overline{q}_\varepsilon \geq \overline{q}_\varepsilon a(t,x).$$

We then apply a Comparison Principle and obtain that the solution $q_\varepsilon(t,x)$ to the following linear problem

$$\begin{cases} \partial_t q_\varepsilon - c\varepsilon \partial_x q_\varepsilon - \varepsilon^2 \partial_{xx} q_\varepsilon = q_\varepsilon a(t,x), \\ q_\varepsilon(0,x) = \widetilde{p}_\varepsilon(0,x), \end{cases} \tag{2.74}$$

satisfies

$$\underline{q}_\varepsilon(t,x) \leq q_\varepsilon(t,x) \leq \overline{q}_\varepsilon(t,x), \quad \forall (t,x) \in \mathbb{R}_+ \times \mathbb{R}.$$

From the proof of Proposition 1 in Section 2.2 (see equation (2.7)), applied to the case $\sigma = \varepsilon^2$ and $c = c\varepsilon$ we know that q_ε converges exponentially fast as $t \to +\infty$ to the periodic eigenfunction in (2.16), (see also [56]); that is, we can write for some positive constants α and β,

$$\|q_\varepsilon e^{t\lambda_{c,\varepsilon}} - \alpha p_{c\varepsilon}\|_{L^\infty} \leq e^{-\beta t}. \tag{2.75}$$

We recall that $q_\varepsilon e^{t\lambda_{c,\varepsilon}}$ can indeed be written as

$$q_\varepsilon e^{t,\lambda_{c,\varepsilon}} = \tilde{q}_{\varepsilon,1} + \tilde{q}_{\varepsilon,2},$$

with $\tilde{q}_{\varepsilon,1}(t,\cdot) \in \text{span}\{p_{c\varepsilon}(t,\cdot)\}$, $\tilde{q}_{\varepsilon,2} \to 0$ exponentially fast and

$$\int_{\mathbb{R}} \tilde{q}_{\varepsilon,2}(t,x) p^*_{c\varepsilon}(t,x) dx = 0,$$

where $p^*_{c\varepsilon}$ is the principal eigenfunction to the adjoint problem

$$-\partial_t p^*_{c\varepsilon} + c\varepsilon \partial_x p^*_{c\varepsilon} - \varepsilon^2 \partial_{xx} p^*_{c\varepsilon} = (a(t,x) + \lambda_{c,\varepsilon}) p^*_{c\varepsilon}, \tag{2.76}$$

(see Theorem 2.2 [56] and the proof of Lemma 6 [41]). The positivity of α is then derived from the fact that $q_\varepsilon(0,x)$ and $p^*_{c\varepsilon}$ are positive functions.
On the one hand equation (2.75) implies that,

$$0 \leq \widetilde{p}_\varepsilon e^{(-\lambda_{\varepsilon^+} + \lambda_{c,\varepsilon})t} \leq \alpha p_{c\varepsilon} + e^{-\beta t}.$$

Since $p_{c\varepsilon}$ and $\widetilde{p}_\varepsilon$ are time-periodic functions, then necessarily

$$\lambda_{c,\varepsilon} - \lambda_{\varepsilon^+} \leq 0,$$

otherwise we get a contradiction as $t \to +\infty$. Therefore

$$\lambda_{c,\varepsilon} - \tilde{\lambda}_\varepsilon \leq K\varepsilon^2, \tag{2.77}$$

where K is defined in (2.73).
On the other hand, from (2.75) we obtain

$$\widetilde{p}_\varepsilon e^{(-\lambda_{\varepsilon^-} + \lambda_{c,\varepsilon})t} \geq \alpha p_{c\varepsilon} - e^{-\beta t}.$$

Note that if $\lambda_{c,\varepsilon} - \lambda_{\varepsilon^-} \leq 0$ we obtain from the $T-$periodicity of the eigenfunctions, as $t \to +\infty$, that $p_{c\varepsilon} \leq 0$, which is also a contradiction. Thus, it implies that

$$\lambda_{c,\varepsilon} - \lambda_{\varepsilon^-} \geq 0.$$

Therefore we have

$$\lambda_{c,\varepsilon} - \tilde{\lambda}_\varepsilon \geq -K\varepsilon^2. \tag{2.78}$$

Combining both inequalities (2.77) and (2.78) we write

$$\left|\lambda_{c,\varepsilon} - (\lambda_1 + \varepsilon\lambda_2)\right| \leq K\varepsilon^2, \tag{2.79}$$

which leads thanks to Lemma 2.17 to an approximation for the eigenvalue of order ε^2 as follows:

$$\lambda_{c,\varepsilon} = -\overline{a}(x_m) + \frac{c^2}{4} + \varepsilon\sqrt{-\bar{a}_{xx}(x_m)/2} + o(\varepsilon).$$

The approximation (2.18) for the critical speed c_ε^* can be derived from the above approximation and (2.11). Indeed, from (2.11) and the definition of c_ε^* we obtain

$$c_\varepsilon^* = 2\sqrt{\bar{a}(x_m) - \varepsilon\sqrt{-\frac{\bar{a}_{xx}(x_m)}{2}} + o(\varepsilon)} = 2\sqrt{\bar{a}(x_m)} - \varepsilon\sqrt{-\frac{\bar{a}_{xx}(x_m)}{2}} + o(\varepsilon).$$

2.5.1 Boundedness of K

In this subsection we prove Lemma 2.17. We provide the proof in several steps.

Step 1: $\lambda_1 = -\bar{a}(x_m) + \frac{c^2}{4}$**.** We integrate (2.71) with respect to t in $[0, T]$ and use the fact that $u_x(x_m) = \psi_x(x_m) + \frac{c}{2}$ to obtain the result.

Step 2: $|\partial_x\phi|$ **is bounded.** An integration in $[0, T]$ of the first equation in (2.71) gives us the already known equation for ψ in (2.37) with $\lambda_1 = -\bar{\rho}$. Then we can substitute and proceed as follows:

$$\partial_t\phi = a(t,x) - \overline{a}(x) \Rightarrow \partial_x\phi(t,x) = \partial_x\phi(0,x) + \int_0^t a_x(\tau,x)d\tau - t\overline{a}_x(x),$$

where a_x and $\overline{a}_x$ denote the derivatives with respect to x of $a(t,x)$ and $\overline{a}(x)$ respectively. This implies that in order to bound $\partial_x\phi$ we just need to bound the derivative of ϕ at point $t = 0$ since $a(t,x) \in L^\infty(\mathbb{R}_+, C^3(\mathbb{R}))$.
Then from the second equation in (2.71) we obtain:

$$\partial_x\phi(0,x) = \frac{-\psi_{xx}(x) + \psi_{xx}(x_m)}{2\psi_x(x) + c}, \tag{2.80}$$

if the last formula is well defined. We claim the following technical result.

Lemma 2.18 *The function $\psi(x)$ is twice differentiable for every $x \in \mathbb{R}$ and*

$$\psi_{xx}(x) = \begin{cases} -\dfrac{\overline{a}_x(x)}{2\sqrt{\overline{a}(x_m) - \overline{a}(x)}}, & x < x_m, \\ -\sqrt{-\overline{a}_{xx}(x_m)/2}, & x = x_m, \\ \dfrac{\overline{a}_x(x)}{2\sqrt{\overline{a}(x_m) - \overline{a}(x)}}, & x > x_m. \end{cases} \tag{2.81}$$

Proof of Lemma 2.18

Indeed, from the explicit formula (2.19) we differentiate and obtain:

$$\psi_x(x) = \begin{cases} -\frac{c}{2} + \sqrt{\overline{a}(x_m) - \overline{a}(x)}, & x < x_m, \\ -\frac{c}{2} & x = x_m, \\ -\frac{c}{2} - \sqrt{\overline{a}(x_m) - \overline{a}(x)}, & x > x_m. \end{cases} \tag{2.82}$$

We next compute

$$\lim_{x \to x_m^+} \frac{\psi_x(x) - \psi_x(x_m)}{x - x_m} = \lim_{x \to x_m^+} \frac{-\sqrt{\bar{a}(x_m) - \bar{a}(x)}}{x - x_m} = \lim_{x \to x_m^+} \frac{-\sqrt{f(x)}}{x - x_m},$$

where we have denoted $f(x) = \overline{a}(x_m) - \overline{a}(x)$. We write a Taylor expansion of f around $x = x_m$, i.e.:

$$f(x) = -\frac{1}{2}\bar{a}_{xx}(x_m)(x - x_m)^2 - \frac{1}{6}\bar{a}_{xxx}(x_m)(x - x_m)^3 + o((x - x_m)^3),$$

since $f(x_m) = 0$ and x_m is a maximum point. It implies that:

$$\lim_{x \to x_m^+} \frac{\psi_x(x) - \psi_x(x_m)}{x - x_m} = \lim_{x \to x_m^+} \frac{\bar{a}_x(x)}{2\sqrt{\bar{a}(x_m) - \bar{a}(x)}} = -\sqrt{-\overline{a}_{xx}(x_m)/2}.$$

Note that x_m being a maximum point, $\overline{a}(x_m) \geq \overline{a}(x)$, $\forall x \in \mathbb{R}$ and $\overline{a}_{xx}(x_m) \leq 0$. Following similar arguments one can prove that

$$\lim_{x \to x_m^-} \frac{\psi_x(x) - \psi_x(x_m)}{x - x_m} = \lim_{x \to x_m^-} \frac{-\bar{a}_x(x)}{2\sqrt{\bar{a}(x_m) - \bar{a}(x)}} = -\sqrt{-\overline{a}_{xx}(x_m)/2}.$$

■

We pursue with the proof of Lemma 2.17.

By substituting the derivatives of ψ in (2.80) we obtain for every $x \neq x_m$:

$$\partial_x \phi(0, x) = \begin{cases} \dfrac{\overline{a}_x(x) - \sqrt{-2\overline{a}_{xx}(x_m)(\overline{a}(x_m) - \overline{a}(x))}}{4(\overline{a}(x_m) - \overline{a}(x))}, & x < x_m, \\ \dfrac{\overline{a}_x(x) + \sqrt{-2\overline{a}_{xx}(x_m)(\overline{a}(x_m) - \overline{a}(x))}}{4(\overline{a}(x_m) - \overline{a}(x))}, & x > x_m. \end{cases} \tag{2.83}$$

We can bound $\partial_x\phi(0,x)$ near to $x = x_m$. We write the limits as $x \to x_m$ in (2.83) in terms of f and compute:

$$\lim_{x\to x_m^{\mp}} \partial_x\phi(0,x) = \lim_{x\to x_m^{\mp}} \frac{-f'(x) \mp 2\sqrt{A}\sqrt{f(x)}}{4f(x)}$$

$$= \lim_{x\to x_m^{\mp}} \frac{-2A(x-x_m) - 3B(x-x_m)^2 + o((x-x_m)^2) \mp 2A|x-x_m|\sqrt{1+\frac{B}{A}(x-x_m)+o(|x-x_m|)}}{4\left(A(x-x_m)^2 + B(x-x_m)^3 + o((x-x_m)^3)\right)}$$

$$= -\frac{B}{2A},$$

where $A = -\overline{a}_{xx}(x_m)/2$ and $B = -\overline{a}_{xxx}(x_m)/6$. From this last computation and formula (2.83) we deduce that $\partial_x\phi(t,x)$ is bounded for every $(t,x) \in \mathbb{R}_+ \times \mathbb{R}$.

Step 3: $|\partial_{xx}\phi|$ is bounded. Note that far from x_m this derivative exists and it is bounded because of the regularity of $a(t,x)$. To verify the boundedness near of x_m we follow the same arguments as above for the first derivative, that is, we want to compute the following limits

$$\lim_{x\to x_m^{\mp}} \frac{\partial_x\phi(0,x) - \partial_x\phi(0,x_m)}{x - x_m} = \lim_{x\to x_m^{\mp}} \frac{-f'(x) \mp 2\sqrt{A}\sqrt{f(x)} + \frac{2B}{A}f(x)}{4f(x)(x-x_m)}, \tag{2.84}$$

where $f(x) = \bar{a}(x_m) - \bar{a}(x)$ as before. Using the Taylor expansion for $f(x)$ around $x = x_m$ the above limit can be developed as follows

$$\begin{aligned} -f'(x) &= -2A(x-x_m) - 3B(x-x_m)^2 + o((x-x_m)^2), \\ 2\sqrt{A}\sqrt{f(x)} &= 2A|x-x_m|\sqrt{1+\tfrac{B}{A}(x-x_m)+o(x-x_m)} \\ &= 2A|x-x_m|\left(1+\tfrac{B}{2A}(x-x_m)+o(x-x_m)\right) \\ \tfrac{2B}{A}f(x) &= 2B(x-x_m)^2 + o((x-x_m)^2). \end{aligned}$$

We substitute into (2.84) and it holds that the terms remaining in the numerator are $o((x-x_m)^3)$, that is the same order of the denominator.

Step 4: $\lambda_2 = \sqrt{-\bar{a}_{xx}(x_m)/2}$. We next evaluate the second equation in (2.71) at $x = x_m$ to obtain $\lambda_2 = \sqrt{-\bar{a}_{xx}(x_m)/2}$.

■

2.6 An illustrating biological example

In this section we discuss the effect of the periodic fluctuations on the critical speed of survival and the dynamics for the following particular growth rate

$$a(t,x) = r - g(t)(x - \theta(t))^2, \tag{2.85}$$

where r is a positive constant which represents the maximal growth rate. The function $g(t)$ is a $1-$ periodic function representing the oscillations on the selection pressure and the $1-$periodic function $\theta(t)$ is representing the fluctuations

on the optimal trait. We introduce the effect of a climate shift on the trait x as follows

$$a(t, x - ct) = r - g(t)(x - ct - \theta(t))^2, \tag{2.86}$$

where $c > 0$ is the climate speed. Note that all the computations that follow have been done with $1-$periodic functions $g(t)$ and $\theta(t)$ for simplicity but they can be generalized to every period T without a great cost.
We then substitute into (2.13) after the change of variable $x' = x + ct$, it holds

$$\partial_t n_\varepsilon - c\varepsilon\partial_x n_\varepsilon - \varepsilon^2\partial_{xx} n_\varepsilon = n_\varepsilon \left[r - g(t)(x - \theta(t))^2 - \rho_\varepsilon(t)\right]; \quad \rho_\varepsilon(t) = \int_{\mathbb{R}} n_\varepsilon(t, x)dx.$$

We compute the mean of $a(t, x)$

$$\overline{a}(x) = \int_0^1 a(t, x)dt = r - x^2\bar{g} + 2xg_1 - g_2,$$

where

$$\bar{g} = \int_0^1 g(t)dt, \quad g_1 = \int_0^1 g(t)\theta(t)dt, \quad g_2 = \int_0^1 g(t)\theta^2(t)dt,$$

and we observe that the maximum of $\overline{a}(x)$ is attained at $x_m = \frac{g_1}{\bar{g}}$, with

$$\bar{a}(x_m) = r + \frac{g_1^2}{\bar{g}} - g_2.$$

Moreover from the Theorem 2.7-(ii) we obtain that $\psi(x)$ the solution of the Hamilton-Jacobi equation (2.15) attains its maximum at

$$\bar{x} = x_m - \frac{c}{2\sqrt{\bar{g}}} = \frac{g_1}{\bar{g}} - \frac{c}{2\sqrt{\bar{g}}}.$$

Let $\psi(x)$ be given by (2.19), then for this specific growth rate it can be written as follows

$$\begin{aligned}
\psi(x) &= \frac{c}{2}\left(x_m - \frac{c}{2\sqrt{\bar{g}}} - x\right) + \int_{x_m - \frac{c}{2\sqrt{\bar{g}}}}^{x_m} \sqrt{\bar{g}(y - x_m)^2}dy - \left|\int_{x_m}^{x} \sqrt{\bar{g}(y - x_m)^2}dy\right| \\
&= -\frac{\sqrt{\bar{g}}}{2}\left(x + \frac{c}{2\sqrt{\bar{g}}} - \frac{g_1}{\bar{g}}\right)^2 \\
&= -\frac{\sqrt{\bar{g}}}{2}(x - \bar{x})^2.
\end{aligned}$$

The results on Theorem 2.7-(i) also implies that for small values of ε we have

$$\overline{\rho}_\varepsilon \approx r + \frac{g_1^2}{\bar{g}} - g_2 - \frac{c^2}{4} - \varepsilon\sqrt{\bar{g}}, \quad c_\varepsilon^* \approx 2\sqrt{r + \frac{g_1^2}{\bar{g}} - g_2} - \varepsilon\sqrt{\bar{g}}.$$

Moreover by following the arguments in [41]-Section 5, we can also obtain an approximation of order ε for the phenotypic mean μ_ε and the variance σ_ε^2 of the population's distribution, that is:

$$\mu_\varepsilon(t) \approx \frac{g_1}{\bar{g}} - \frac{c}{2\sqrt{\bar{g}}} + \varepsilon D(t), \qquad \sigma_\varepsilon^2 \approx \frac{\varepsilon}{\sqrt{\bar{g}}},$$

where $D(t) = \partial_x\phi(\bar{x}, t)$ for ϕ the solution of the system (2.71). One can verify that for this growth rate we have

$$D(t) = -c\sqrt{\bar{g}}\left(t - \frac{1}{2}\right) + 2\int_0^1 \int_0^\tau g(s)(\bar{x} - \theta(s))dsd\tau - 2\int_0^t g(s)(\bar{x} - \theta(s))ds.$$

Note that the phenotypic mean is $1-$periodic since $D(0) = D(1)$. Moreover $\langle \mu_\varepsilon(t) \rangle = \frac{g_1}{g} - \frac{c}{2\sqrt{g}}$ since $\int_0^1 D(t)dt = 0$.

We are now interested in comparing these quantities with the case where there is no fluctuations. To do that we first consider a case where $g(t) = g > 0$ is constant and then a case where $\theta = 0$ is constant.

Case 1. $g(t) = g$ constant. Note that, in such a case $g_1 = g\bar{\theta}$ and $g_2 = g\int_0^1 \theta^2(t)dt$ with $\bar{\theta} = \int_0^1 \theta(t)dt$. We compute

$$\overline{\rho}_{\varepsilon,g(t)=g} \approx r + g\left[\bar{\theta}^2 - \int_0^1 \theta^2(t)dt\right] - \frac{c^2}{4} - \varepsilon\sqrt{g}, \qquad \left\langle \mu_{\varepsilon,g(t)=g}(t) \right\rangle = \bar{\theta} - \frac{c}{2\sqrt{g}},$$

$$c^*_{\varepsilon,g(t)=g} \approx 2\sqrt{r + g\left[\bar{\theta}^2 - \int_0^1 \theta^2(t)dt\right]} - \varepsilon\sqrt{g}.$$

We compare then, the sub-cases where θ is constant or periodic.

a) If $\theta(t) \equiv \theta_{1/2}$ is constant equal to its valueat $t = 1/2$, without lost of generality (i.e. $\theta_{1/2} := \theta(1/2)$), we obtain in particular $\bar{\theta}^2 = \int_0^1 \theta^2(t)dt$ and we have

$$\overline{\rho}_{\varepsilon,c} \approx r - \frac{c^2}{4} - \varepsilon\sqrt{g}, \quad \left\langle \mu_{\varepsilon,c}(t) \right\rangle = \theta_{1/2} - \frac{c}{2\sqrt{g}}, \quad c^*_{\varepsilon,c} \approx 2\sqrt{r} - \varepsilon\sqrt{g}.$$

b) If $\theta(t)$ is a $1-$periodic function then, $\bar{\theta}^2 < \int_0^1 \theta^2(t)dt$ and we obtain

$$\overline{\rho}_{\varepsilon,p} \lesssim r - \frac{c^2}{4} - \varepsilon\sqrt{g}, \quad \left\langle \mu_{\varepsilon,p}(t) \right\rangle = \bar{\theta} - \frac{c}{2\sqrt{g}}, \quad c^*_{\varepsilon,p} \lesssim 2\sqrt{r} - \varepsilon\sqrt{g}.$$

Thus, by keeping the pressure of selection constant, we deduce that

$$\overline{\rho}_{\varepsilon,p} \leq \overline{\rho}_{\varepsilon,c} \quad \text{and} \quad c^*_{\varepsilon,p} \leq c^*_{\varepsilon,c}.$$

This means that having an oscillating optimal trait is not beneficial for the population, in the sense that the mean total size of the population decreases with respect to the case with a constant optimal trait and the critical speed which leads the population to extinct is smaller in the periodic case.

Case 2. $\theta(t) = \theta$ constant. Note that, in such a case $g_1 = \bar{g}\theta$ and $g_2 = \bar{g}\theta^2$. We compute

$$\overline{\rho}_{\varepsilon,\theta(t)=\theta} \approx r - \frac{c^2}{4} - \varepsilon\sqrt{\bar{g}}, \qquad \left\langle \mu_{\varepsilon,\theta(t)=\theta}(t) \right\rangle = \theta - \frac{c}{2\sqrt{\bar{g}}}, \qquad c^*_{\varepsilon,g(t)=g} \approx 2\sqrt{r} - \varepsilon\sqrt{\bar{g}}.$$

We compare then, the sub-cases where g is constant or periodic.

a) If $g(t) \equiv g_{1/2}$ is constant equal to its value at $t = 1/2$, without lost of generality (i.e. $g_{1/2} := g(1/2)$), we obtain

$$\overline{\rho}_{\varepsilon,c} \approx r - \frac{c^2}{4} - \varepsilon\sqrt{g_{1/2}}, \quad \left\langle \mu_{\varepsilon,c}(t) \right\rangle = \theta - \frac{c}{2\sqrt{g_{1/2}}}, \quad c^*_{\varepsilon,c} \approx 2\sqrt{r} - \varepsilon\sqrt{g_{1/2}}.$$

b) If $g(t)$ is a $1-$periodic function then we obtain

$$\overline{\rho}_{\varepsilon,p} \approx r - \frac{c^2}{4} - \varepsilon\sqrt{\bar{g}}, \quad \left\langle \mu_{\varepsilon,p}(t) \right\rangle = \theta - \frac{c}{2\sqrt{\bar{g}}}, \quad c^*_{\varepsilon,p} \approx 2\sqrt{r} - \varepsilon\sqrt{\bar{g}}.$$

In this case by keeping the optimal trait constant we can deduce that if we choose an oscillating selection pressure function $g(t)$ which satisfies:

$$\bar{g} < g(1/2), \tag{2.87}$$

then we obtain that

$$\overline{\rho}_{\varepsilon,c} < \overline{\rho}_{\varepsilon,p} \quad \text{and} \quad c^*_{\varepsilon,c} < c^*_{\varepsilon,p}.$$

This means that the mean total size of the population increases with respect to the case with a constant selection pressure. Moreover, the critical speed above which the population goes extinct is larger in the periodic case. This means that the periodic fluctuations can help the population to follow the environment change.

Note that the condition (2.87) imposed to $g(t)$ is the opposite to the one imposed in Chapter 1, equation (1.51) (see also [41]), leading to more performant populations. There, it was proved that in presence of the mutations and while the fluctuations act on the pressure of the selection (that is with a similar growth rate, however with $c = 0$ and under the condition $\bar{g} > g(1/2)$), a fluctuating environment can select for a population with smaller variance and in this way lead to more performant populations. What is beneficial in a (in average) constant environment may indeed be disadvantageous in a changing environment.

Note also that in the present example under condition (2.87), we have

$$\Big|\big\langle \mu_{\varepsilon,p}(t)\big\rangle - \theta\Big| > \Big|\big\langle \mu_{\varepsilon,c}(t)\big\rangle - \theta\Big|.$$

This means that even if the population can follow the climatic change in a better way by considering a fluctuating environment, this population is less well adapted.

2.A The proofs of some regularity estimates

2.A.1 Uniform bounds for ρ_ε

Proof of Proposition 12.
From equation (2.13) integrating in $x \in \mathbb{R}$ and using assumption (H1) we obtain:

$$\frac{d\rho_\varepsilon}{dt} = \int_{\mathbb{R}} n_\varepsilon(t,x)[a(t,x) - \rho_\varepsilon(t)]dx \leq \rho_\varepsilon(t)[d_0 - \rho_\varepsilon(t)]. \tag{2.88}$$

This implies that

$$\rho_\varepsilon(t) \leq \rho_M := \max(\rho_\varepsilon^0, d_0).$$

For the lower bound we use the explicit expression for ρ_ε in (2.64), the solution of (2.9).
We come back to equation (2.49), which gives, thanks to (H1), (2.50) and (2.64) the following lower bound for ρ_ε

$$0 < \rho_m := \frac{1}{T} e^{-d_0 T}\left(e^{\lambda_m T} - 1\right) \leq \rho_\varepsilon(t), \quad \forall\, t \geq 0.$$

■

2.A.2 Upper bound for ψ_ε: the proof of the r.h.s of (3.3)

We prove that ψ_ε is bounded from above using the equation for n_ε. From (2.6), we have for $p_{c\varepsilon}$:

$$p_{c\varepsilon}(t,x) \leq \|p_{c\varepsilon}\|_{L^\infty} e^{-\frac{1}{\varepsilon}\left(-\frac{c}{2}+\sqrt{\delta+\frac{c^2}{2}}\right)(|x|-R_0)}, \quad \forall (t,x) \in [0,+\infty)\times\mathbb{R}. \tag{2.89}$$

Define $q_{c\varepsilon}(t,x) = p_{c\varepsilon}(t,x\varepsilon)$, which satisfies

$$\begin{cases} \partial_t q_{c\varepsilon} - c\partial_x q_{c\varepsilon} - \partial_{xx} q_{c\varepsilon} = a_\varepsilon(t,x) q_{c\varepsilon}, & \text{in } [0,+\infty)\times\mathbb{R}, \\ 0 < q_{c\varepsilon}(t,x) = q_{c\varepsilon}(t+T,x) \end{cases} \tag{2.90}$$

for $a_\varepsilon(t,x) = a(t,x\varepsilon) + \lambda_{c,\varepsilon}$. Note that a_ε is uniformly bounded thanks to the $L^\infty-$norm of a. Moreover we have the following bounds for $\lambda_{c,\varepsilon}$ coming from (2.49),

$$-d_0 \leq \lambda_{c,\varepsilon} \leq -\lambda_m. \tag{2.91}$$

We recall that $p_{c\varepsilon}$ is uniquely determined once $\|p_{c\varepsilon}(0,x)\|_{L^\infty(\mathbb{R})} = 1$ is fixed. Then, one can choose x_ε such that $p_{c\varepsilon}(0,x_\varepsilon) = 1$. Note also that q_ε is a nonnegative solution of (2.90) in the bounded domain $(0,2T)\times B(\frac{x_\varepsilon}{\varepsilon},1)$.
Here we apply an elliptic-type Harnack inequality for positive solutions of (2.90) in a bounded domain, (see for instance Theorem 2.5 [55]). Let δ_0, be such that $0 < \delta_0 < T$, then we have:

$$\sup_{x\in B(\frac{x_\varepsilon}{\varepsilon},1)} q_{c\varepsilon}(t,x) \leq C \inf_{x\in B(\frac{x_\varepsilon}{\varepsilon},1)} q_{c\varepsilon}(t,x), \quad \forall\, t \in [\delta_0, 2T],$$

where C is a positive constant depending on δ_0 and d_0. Coming back to $p_{c\varepsilon}$ this implies

$$p_{c\varepsilon}(t_0,x_\varepsilon) \leq \sup_{y\in B(x_\varepsilon,\varepsilon)} p_{c\varepsilon}(t_0,y) \leq C p_{c\varepsilon}(t_0,x), \quad \forall (t_0,x) \in [\delta_0,2T]\times B(x_\varepsilon,\varepsilon). \tag{2.92}$$

And we use the $T-$periodicity of $p_{c\varepsilon}$ to conclude that the last inequality is satisfied for $t \in [0,T]$.
From (2.28), (2.89) and (2.92) we obtain

$$n_\varepsilon(0,x) \leq \rho_M \frac{p_{c\varepsilon}(0,x)}{\int_{\mathbb{R}} p_{c\varepsilon}(0,x)dx} \leq \rho_M \frac{Cp_{c\varepsilon}(0,x)}{\int_{B(x_\varepsilon,\varepsilon)} p_{c\varepsilon}(0,x_\varepsilon)dx} = \rho_M \frac{Cp_{c\varepsilon}(0,x)}{|B(x_\varepsilon,\varepsilon)|} \leq C'\varepsilon^{-1} \exp^{\frac{c_1-c_2|x|}{\varepsilon}},$$

for all $\varepsilon \leq \varepsilon_0$, with ε_0 small enough, where the constant c_1 depends on ρ_M, δ, R_0 and c, and $c_2 = -\frac{c}{2} + \sqrt{\delta + \frac{c^2}{2}}$. Next we proceed with a maximum principle argument to obtain for every $(t,x) \in [0,+\infty) \times \mathbb{R}$ and $c_3 = c_2(c+c_2) + d_0$,

$$n_\varepsilon(t,x) \leq C' \exp^{\frac{c_1-c_2|x|}{\varepsilon}+c_3 t}.$$

From the latter inequality and the periodicity of ψ_ε, with an abuse of notation for constant c_1, we deduce that:

$$\psi_\varepsilon(t,x) \leq c_1 - c_2|x|, \quad \forall (t,x) \in [0,+\infty) \times \mathbb{R}. \tag{2.93}$$

2.A.3 Equicontinuity in time for ψ_ε

We will use the arguments in [41], which follow a method introduced in [9], in order to deduce uniform equicontinuity in time for the family ψ_ε on compact subsets of $(0,+\infty) \times \mathbb{R}$.
The goal will be to find for any $\eta > 0$, constants Λ_1, Λ_2 large enough such that: for any $x \in B(0,R/2)$, $s \in [0,T]$, and for all $\varepsilon < \varepsilon_0$ we have

$$\psi_\varepsilon(t,y) - \psi_\varepsilon(s,x) \leq \eta + \Lambda_1|x-y|^2 + \varepsilon\Lambda_2(t-s), \forall (t,y) \in [s,T] \times B_R(0), \tag{2.94}$$

and

$$\psi_\varepsilon(t,y) - \psi_\varepsilon(s,x) \geq -\eta - \Lambda_1|x-y|^2 - \varepsilon\Lambda_2(t-s), \forall (t,y) \in [s,T] \times B_R(0). \tag{2.95}$$

Because of the analogy between the both inequalities above we only prove (2.94).
We fix (s,x) in $[0,T[\times B_{R/2}(0)$ and define

$$\widehat{\xi}(t,y) = \psi_\varepsilon(s,x) + \eta + \Lambda_1|x-y|^2 + \varepsilon\Lambda_2(t-s), \quad (t,y) \in [s,T[\times B_R(0),$$

with Λ_1 and Λ_2 positive constants to be determined. We prove that, for Λ_1 and Λ_2 large enough, $\widehat{\xi}$ is a super-solution of the equation (2.29) on $[s,T] \times B_R(0)$ and $\widehat{\xi}(t,y) > \psi_\varepsilon(t,y)$ for $(t,y) \in \{s\} \times B_R(0) \cup [s,T] \times \partial B_R(0)$.

According to Section 3.2.1, $\{\psi_\varepsilon\}_\varepsilon$ is locally uniformly bounded, so we can find a constant Λ_1 such that for all $\varepsilon < \varepsilon_0$,

$$\frac{8\|\psi_\varepsilon\|_{L^\infty([0,T]\times B_R(0))}}{R^2} \leq \Lambda_1.$$

With this choice, $\widehat{\xi}(t,y) > \psi_\varepsilon(t,y)$ on $[s,T] \times \partial B_R(0)$, for all $\eta > 0$, $\Lambda_2 > 0$ and $x \in B_{R/2}(0)$.
Next we prove that, for Λ_1 large enough, $\widehat{\xi}(s,y) > \psi_\varepsilon(s,y)$ for all $y \in B_R(0)$. We argue by contradiction. Assume that there exists $\eta > 0$ such that for every constant Λ_1 there exists $y_{\Lambda_1,\varepsilon} \in B_R(0)$ such that

$$\psi_\varepsilon(s,y_{\Lambda_1,\varepsilon}) - \psi_\varepsilon(s,x) > \eta + \Lambda_1|y_{\Lambda_1,\varepsilon} - x|^2. \tag{2.96}$$

This implies

$$|y_{\Lambda_1,\varepsilon} - x| \leq \sqrt{\frac{2\Psi_M}{\Lambda_1}} \longrightarrow 0, \quad \text{as } \Lambda_1 \to \infty,$$

where we have denoted Ψ_M a uniform upper bound for $\|\psi_\varepsilon\|_{L^\infty([0,T]\times B_R(0))}$. Then for all $\delta_1 > 0$, there exist Λ_1 large enough and ε_0 small enough, such that $\forall \varepsilon < \varepsilon_0$,

$$|y_{\Lambda_1,\varepsilon} - x| \leq \delta_1.$$

Therefore, from the uniform continuity in space of ψ_ε taking δ_1 small enough, we obtain

$$|\psi_\varepsilon(s, y_{\Lambda_1,\varepsilon}) - \psi_\varepsilon(s,x)| < \eta/2 \quad \forall \varepsilon \leq \varepsilon_0,$$

but this is a contradiction with (2.96). Therefore $\widehat{\xi}(s,y) > \psi_\varepsilon(s,y)$ for all $y \in B_R(0)$.
Finally, noting that $R < +\infty$ we deduce that for Λ_2 large enough, $\widehat{\xi}$ is a super-solution to (2.29) in $[s,T] \times B_R(0)$. Using a comparison principle, we have

$$\psi_\varepsilon(t,y) \leq \widehat{\xi}(t,y) \quad \forall (t,y) \in [s,T] \times B_R(0).$$

Thus (2.94) is satisfied for $t \geq s \geq 0$. To conclude we put $x = y$ and obtain that for all $\eta > 0$ there exists $\varepsilon_0 > 0$ such that for all $\varepsilon < \varepsilon_0$

$$|\psi_\varepsilon(t,x) - \psi_\varepsilon(s,x)| \leq \eta + \varepsilon\Lambda_2(t-s),$$

for every $(t,x) \in [0,T] \times B_R(0)$. This implies that ψ_ε is locally equicontinuous in time. Moreover we obtain that

$$\forall R > 0, \sup_{t\in[0,T],\ x\in B_R} |\psi_\varepsilon(t,x) - \psi_\varepsilon(s,x)| \to 0 \quad \text{as } \varepsilon \to 0. \tag{2.97}$$

2.B Proof of Proposition 2.15

2.B.1 Some preliminary results for the uniqueness in a bounded domain

To provide the proof of Proposition 2.15, we first present a result given in [8].

Theorem 2.19 *Let $H : \Omega \times \mathbb{R} \times \mathbb{R} \to \mathbb{R}$ be of the form*

$$H(x,u,Du) = 0, \quad x \in \Omega \subset \mathbb{R}. \tag{2.98}$$

We assume that

$$\forall\ R > 0,\ H \text{ is uniformly continuous on } \overline{\Omega} \times [-R,R] \times \overline{B}_R, \tag{2.99}$$

$$\begin{cases} \forall\ R > 0\ \exists \gamma_R \text{ a positive constant such that,} \\ H(x,u,p) - H(x,v,p) \geq \gamma_R(u-v),\ \forall x \in \overline{\Omega},\ \forall p \in \mathbb{R},\ -R \leq v \leq u \leq R. \end{cases} \tag{2.100}$$

Let $u, v \in C(\Omega) \cap L^\infty(\Omega)$ being respectively viscosity sub-solution and super-solution of (2.98) and such that $u - v \leq 0$ on $\partial\Omega$. Then if $u, v \in W^{1,\infty}(\Omega)$ we have the following inequality:

$$\|(u-v)^+\|_{L^\infty(\Omega)} \leq \|(u-v)^+\|_{L^\infty(\partial\Omega)}. \tag{2.101}$$

In fact, for our problem in the bounded domain, we apply the following Corollary.

Corollary 2.20 *Let $H(x,t,p) \in C(\overline{\Omega} \times \mathbb{R} \times \mathbb{R})$ be convex in p. In addition we assume that*

$$\forall R > 0, \exists \alpha_R : \Big(H(x,t,p) - H(x,s,p)\Big)(t-s) \geq \alpha_R (t-s)^2. \tag{2.102}$$

Let $u, v \in W^{1,\infty}_{loc}(\Omega) \cap C(\overline{\Omega})$ satisfy

$$H(x,u,Du) = 0, \ \ a.e \ in \ \Omega \quad H(x,v,Dv) \leq 0, \ \ a.e \ in \ \Omega.$$

Then if Ω is bounded we have

$$\|(u-v)^+\|_{L^\infty(\Omega)} \leq \|(u-v)^+\|_{L^\infty(\partial\Omega)}.$$

We provide the proof of Theorem 2.19 but we skip the proof of this corollary since it is analogous to the proof of Theorem 2.19.

Proof.
We define $R = \max(\|u\|_\infty, \|v\|_\infty)$ and $\gamma = \gamma_R$. The goal of the proof will be to prove that $M = \max_{\overline{\Omega}}(u-v)$ is negative. We suppose by the contrary that $M > 0$, since $u \leq v$ on $\partial\Omega$, the maximum cannot be attained on the boundary. Since u and v are not necessary regular functions, the idea to resolve this difficulty is what is known as the *variable doubling*. We introduce the "test-function":

$$\Psi_\epsilon(x,y) := u(x) - v(y) - \frac{|x-y|^2}{\epsilon^2}.$$

Because of this *penalization* term $\frac{|x-y|^2}{\epsilon^2}$ which imposes to the points of maximum (x,y) of ψ_ϵ to verify that $x \sim y$ if ϵ is small, we can obtain that the maximum of Ψ_ϵ denoted as M_ϵ, is close to the maximum of $u-v$. In fact this idea is justified by the following:

Lemma 2.21 *The following properties are satisfied*

(i) $M_\epsilon \to M$ *as* $\epsilon \to 0$.

(ii) Si (x_ϵ, y_ϵ) *is a maximum point of* ψ_ϵ*, we have:*

$$\frac{|x_\epsilon - y_\epsilon|^2}{\epsilon^2} \to 0, \qquad as \ \epsilon \to 0,$$

$$u(x_\epsilon) - v(y_\epsilon) \to M, \qquad as \ \epsilon \to 0.$$

(iii) $x_\epsilon, y_\epsilon \in \Omega$ *if* ϵ *is small enough.*

(iv) Moreover, if u *or* v *is Lipschitz continuous in* x*, then the penalization term* $p_\epsilon = \frac{2(x_\epsilon - y_\epsilon)}{\epsilon^2}$*, is bounded by twice the Lipschitz constant of* u *or* v.

We refer to Lemma 2.3 in [8] for proof of this technical Lemma.
We use the statement (iii) assuming that ϵ is small. Note that (x_ϵ, y_ϵ) is a maximum point of the function:

$$x \mapsto u(x) - \varphi^1_\epsilon(x),$$

where

$$\varphi^1_\epsilon(x) = v(y_\epsilon) + \frac{|x-y_\epsilon|^2}{\epsilon^2}.$$

Since u is a viscosity sub-solution of (2.98) and $x_\epsilon \in \Omega$, then:

$$H(x_\epsilon, u(x_\epsilon), D\varphi^1_\epsilon(x_\epsilon)) = H\left(x_\epsilon, u(x_\epsilon), \frac{2(x_\epsilon - y_\epsilon)}{\epsilon^2}\right) \leq 0.$$

Analogously, y_ϵ is a maximum point of the function:

$$y \mapsto v(y) - \varphi_\epsilon^2(y),$$

where

$$\varphi_\epsilon^2(y) = u(x_\epsilon) + \frac{|x_\epsilon - y|^2}{\epsilon^2};$$

thus y_ϵ is a minimum point of the function $v - \varphi_\epsilon^2$; therefore v is a viscosity super-solution of (2.98) and $y_\epsilon \in \Omega$, then:

$$H(y_\epsilon, v(y_\epsilon), D\varphi_\epsilon^2(y_\epsilon)) = H\left(y_\epsilon, v(y_\epsilon), \frac{2(x_\epsilon - y_\epsilon)}{\epsilon^2}\right) \geq 0.$$

We subtract then both viscosity inequalities:

$$H\left(x_\epsilon, u(x_\epsilon), \frac{2(x_\epsilon - y_\epsilon)}{\epsilon^2}\right) - H\left(y_\epsilon, v(y_\epsilon), \frac{2(x_\epsilon - y_\epsilon)}{\epsilon^2}\right) \leq 0.$$

We add and subtract $H\left(x_\epsilon, v(y_\epsilon), p_\epsilon\right)$, then the inequality reads:

$$H\left(x_\epsilon, u(x_\epsilon), p_\epsilon\right) - H\left(x_\epsilon, v(y_\epsilon), p_\epsilon\right) \leq H\left(y_\epsilon, v(y_\epsilon), p_\epsilon\right) - H\left(x_\epsilon, v(y_\epsilon), p_\epsilon\right). \tag{2.103}$$

Now we use the statement about p_ϵ in Lemma 2.21(ii), to write

$$|p_\epsilon| \leq \|Du\|_\infty, \tag{2.104}$$

for $\|Du\|_\infty$ the Lipschitz constant of u.
We then conclude easily by applying hypothesis (2.100) to the LHS in (2.103) and by using the convergence to zero of the term in the RHS, as a consequence of the uniform continuity of H on a compact set, in assumption (2.99). That is,

$$\gamma(u(x_\epsilon) - v(y_\epsilon)) \leq O(\varepsilon),$$

and this implies, after letting $\epsilon \to 0$

$$\gamma M \leq 0,$$

which is a contradiction and the proof of uniqueness is complete.

■

Note that the above uniqueness result is proved under assumption (2.100).
In order to apply this theorem to the Hamiltonian in (2.54) we use a transformation suggested in the proof of Theorem 3.1 in [72].

We provide the proof of the uniqueness in the case $h(x) > \alpha > 0$ in $\overline{\Omega}$, with α a positive constant. The case with $h(x) > 0$ in Ω can be derived easily from this result.

2.B.2 Monotone transformation in a bounded domain

Let u solve

$$H(D_x u) = h(x),$$

in the viscosity sense, we make the following transformation

$$v = \frac{1}{\gamma}\left(e^{\gamma u_m} - e^{-\gamma u}\right), \tag{2.105}$$

where $\gamma > 0$ and $u_m = \max \|u\|_{L^\infty(\Omega)} + 1$, which is well defined since Ω is bounded and $u \in C(\Omega)$. Then it follows that v solves

$$(e^{\gamma u_m} - \gamma v)H\left(Dv(e^{\gamma u_m} - \gamma v)^{-1}\right) = (e^{\gamma u_m} - \gamma v)h(x),$$

in the viscosity sense, since v is a monotone transformation, (see for instance Corollary 2.1 (iii) [8]).
Therefore, if u_1, u_2 are two viscosity solutions for the Hamiltonian (2.54) it holds that v_1, v_2, defined from u_1 and u_2 as in (2.105) are two viscosity solutions for the Hamiltonian

$$\tilde{H}(x,t,p) = (e^{\gamma u_m} - \gamma t)H\left(p(e^{\gamma u_m} - \gamma t)^{-1}\right) - (e^{\gamma u_m} - \gamma t)h(x),$$

Note that v_1, v_2 lie in some $[\alpha, \beta]$, $0 < \alpha < \beta < \infty$ and for $t \in [\alpha, \beta]$, $\tilde{H}(x,t,p)$ is convex in p and

$$\frac{\partial \tilde{H}}{\partial t} = -\gamma H\left(p(e^{\gamma u_m} - \gamma t)^{-1}\right) + \gamma \frac{p}{e^{\gamma u_m} - \gamma t} \cdot H'\left(p(e^{\gamma u_m} - \gamma t)^{-1}\right) + \gamma h(x).$$

Note that for $S = \frac{p}{e^{\gamma u_m} - \gamma t}$, we have $H(S) - SH'(S) \leq 0$ since H is convex and $H(0) = 0$. This implies

$$\frac{\partial \tilde{H}}{\partial t} \geq \gamma h(x) > \alpha > 0, \quad \forall x \in \Omega.$$

Then it follows that

$$\left(\tilde{H}(x,t,p) - \tilde{H}(x,s,p)\right)(t-s) \geq \alpha(t-s)^2, \quad \forall x \in \Omega.$$

Now we apply Corollary 2.20 to $\tilde{H}$, to obtain for every two solutions u_1 and u_2 of equation (2.47) that

$$\|(u_1 - u_2)^+\|_{L^\infty(B_R)} \leq \|(u_1 - u_2)^+\|_{L^\infty(\partial B_R)}.$$

This concludes the proof of the uniqueness of a viscosity solution of (2.54) in a bounded domain.

Part II

EXEMPLES BIOLOGIQUES ET SIMULATIONS NUMERIQUES

Chapter 3

Modèles de mutation-sélection dans des environnements variables en temps; exemples de taux de croissance et simulations numériques

***

...dans la vie réelle, les erreurs sont susceptibles d'être irréversibles. La simulation par ordinateur, cependant, rend économiquement pratique de faire des erreurs à dessein–
John H. Mcleod

Résumé

Nous étudions plusieurs exemples de taux de croissance périodique en temps pour les équations paraboliques de Lotka-Volterra avec une compétition non locale. Ces équations modélisent la dynamique évolutive d'une population phénotypiquement structurée sous sélection et mutations dans un environnement changeant. Nous nous intéressons à la solution périodique qui peut être obtenue comme la limite en long temps d'un problème de Cauchy. Nous étudions d'abord deux taux de croissance dont les moyennes sur une période de temps prennent un seul maximum et fournissons des solutions analytiques ou semi-analytiques au modèle parabolique et calculons les moments de la distribution phénotypique de la population. Nous illustrons ensuite la solution lorsque les effets des mutations varient de petites à grandes valeurs. Nous montrons que, lorsque l'effet des mutations est petit, la densité phénotypique de la population se concentre sur un seul trait, alors que la taille de la population oscille périodiquement. De plus, étant motivés par une expérience biologique, nous comparons deux populations évoluées dans des environnements différents (constants ou périodiques). Ces résultats permettent d'une part de confirmer les résultats du Chapitre 1, et d'une autre part d'illustrer pour ces exemples, comment le comportement de la solution est modifié pour les taux de mutation grands. Enfin, nous étudions numériquement le cas où le taux de croissance moyen atteint son maximum deux fois dans une période de deux manières différentes (symétriques ou non) et montrons que dans un tel cas nous pouvons avoir une population dimorphe.

Introduction

In this chapter we are interested in the analytical and numerical resolution of the following equation

$$\begin{cases} \partial_t n_\varepsilon(t,x) - \varepsilon^2 \partial_{xx} n_\varepsilon(t,x) = n_\varepsilon(t,x)[a(t,x) - \rho_\varepsilon(t)], \quad (t,x) \in [0,+\infty) \times \mathbb{R}, \\ \rho_\varepsilon(t) = \displaystyle\int_{\mathbb{R}} n_\varepsilon(t,x)dx, \\ n(0,x) = n(T,x), \end{cases} \tag{3.1}$$

for some particular choices of the periodic growth rate a. Here $n_\varepsilon(t,x)$ represents the density of a phenotypically structured population in an environment which varies periodically in time with a period T. The biological meaning of the other quantities in the above model (3.1) are given below:

- $a(t,x)$ is a time-periodic function, corresponding to the net growth rate of individuals;
- $\varepsilon > 0$ is an effective size of the mutations;
- $\rho_\varepsilon(t)$ is the total population size, whose product with $n_\varepsilon(t,x)$ represents the death term due to the competition of the individuals.

We study several examples for particular growth rates a, construct explicit or semi-explicit solutions of (3.1), and illustrate the numerical solution of (3.1) considering different choices of ε. The existence and uniqueness of a periodic solution of (3.1) is guaranteed by Chapter 1. In each case, we first present an analytic study of an explicit or semi-explicit solution, obtained following the arguments in [6], (see also [30] and [31]) and then compute the moments of the population distribution to compare them with our approximations in Chapter 1. We next solve numerically (3.1) for different choices of a and different values of the mutation parameter ε. By the numerical resolution we confirm the results in Chapter 1 for the small values of ε, where the solution n_ε concentrates around a single Dirac mass while the population total size ρ_ε oscillates periodically in time. Moreover we illustrate the solution for these growth rates when the effect of mutations increases. Being motivated by the biological experience in [60] we also investigate in which situations a population evolved in a periodic environment outperfoms a population evolved in a constant environment when both populations are placed in the same constant enviroment. Finally, we study numerically the case where the function a attains its maximum twice in a period of time. Note that in this case the hypothesis in Chapter 1 are not valid anymore. We observe that, if the averaged growth rate takes two global maxima we can have dimorphic population, i.e, a phenotypic distribution with two peaks.

The plan of the chapter is as follows: In Section 3.1 we study a growth rate a where the oscillations act on the optimal trait, first by constructing an explicit solution and then numerically when the effect of mutations changes from small to larger values. Next in Section 3.2 we study the model with the function a having the oscillations on the pressure of selection, where in this case we construct a semi-explicit solution and then resolve numerically the problem, again for different values of the mutation rate ε. Finally, in Section 3.3 we study numerically the problem when the averaged growth rate takes more than one maximum in a period of time, first with these maxima being "symmetric", (in the sense that the second derivatives have the same behavior around both maximum points) and next in the case of "non-symmetric" maxima.

3.1 Oscillations on the optimal trait

In this section we study a particular growth rate a for the problem (3.1) where the oscillations act on the optimal trait and propose an explicit solution to the problem. In particular, we study the problem both analytically and numerically for two values of the mutation rate small and large.

3.1.1 Analytic study of the explicit solution

Let us consider the following growth rate:

$$a_1(t,x) = r - g(x - c\sin bt)^2. \tag{3.2}$$

Here r represents the maximal growth rate, g models the selection pressure and the term $c\sin bt$ models the oscillations of the optimal trait with period $\frac{2\pi}{b}$ and amplitude c. We substitute into (3.1) and obtain:

$$\partial_t n_\varepsilon(t,x) - \varepsilon^2 \Delta n_\varepsilon(t,x) = n_\varepsilon(t,x)[r - g(x - c\sin bt)^2 - \rho_\varepsilon(t)]. \tag{3.3}$$

We will show that the unique periodic solution of the above equation has the following form

$$\mathcal{N}(t,x) = \frac{\rho(t)}{\sqrt{2\pi\sigma^2(t)}} \exp\left[-\frac{(x-\mu(t))^2}{2\sigma^2(t)}\right], \tag{3.4}$$

with

$$\rho(t) = \int_{\mathbb{R}} \mathcal{N}(t,x)dx, \quad \mu(t) = \frac{1}{\rho(t)}\int_{\mathbb{R}} x\mathcal{N}(t,x)dx, \quad \sigma^2(t) = \frac{1}{\rho(t)}\int_{\mathbb{R}} (x-\mu(t))^2\mathcal{N}(t,x)dx. \tag{3.5}$$

From the results in Chapter 1 we know that problem (3.1) has a unique periodic solution, so it is enough to find a solution of the form (3.4). In fact we can prove that for this choice of a we have:

$$\rho(t) = \exp\left(I(t)\right)\left[K_2 + \int_0^t \exp\left(I(z)\right)dz\right]^{-1}, \quad \mu(t) = \frac{2c\varepsilon\sqrt{g}}{4\varepsilon^2 g + b^2}\left(2\varepsilon\sqrt{g}\sin bt - b\cos bt\right), \quad \sigma^2(t) = \frac{\varepsilon}{\sqrt{g}}, \tag{3.6}$$

where K_2 is a positive constant and

$$I(t) = (r - \varepsilon\sqrt{g})t - \frac{gc^2b^2}{(4g\varepsilon^2 + b^2)^2}\left[\frac{b^2}{2}\left(t - \frac{\sin 2bt}{2b}\right) + 2g\varepsilon^2\left(t + \frac{\sin 2bt}{2b}\right) + \varepsilon\sqrt{g}\left(1 - \cos 2bt\right)\right].$$

Moreover the mean fitness of this population (at value $\tau = \frac{\pi}{b}$) is given by

$$\overline{F}(\tau) = r - \varepsilon\sqrt{g} - \frac{2\varepsilon^2 g^2 c^2}{4\varepsilon^2 g + b^2}. \tag{3.7}$$

Note that, from this formula, the mean fitness decreases when the mutations have more important effect, that is, when the value of ε increases. The details of the computations for these expressions above are given in the last subsection of this section, namely sub-section 3.1.3.

It is interesting to compare these analytic results obtained from the explicit solution (3.4) with the analytic expressions given in Chapter 1 coming from an approximation of the solution of (3.1), as follows

$$n_\varepsilon(t,x) = \frac{1}{\sqrt{2\pi\varepsilon}} e^{\frac{u(x)}{\varepsilon} + v(t,x) + \varepsilon w(t,x)},$$

for certain functions $u(x)$, $v(t,x)$ and $w(t,x)$ computed in Chapter 1.

In Chapter 1, we approximate the following analytic formula for the moments and the mean fitness:

$$\begin{cases} \rho_\varepsilon(t) = \displaystyle\int_{\mathbb{R}^d} n_\varepsilon(t,x)dx, \quad \bar{\rho}_\varepsilon = \frac{1}{T}\int_0^T \rho_\varepsilon(t)dt, \\ \mu_\varepsilon(t) = \dfrac{1}{\rho_\varepsilon(t)} \displaystyle\int_{\mathbb{R}^d} x\ n_\varepsilon(t,x)dx, \\ \sigma^2_\varepsilon(t) = \dfrac{1}{\rho_\varepsilon(t)} \displaystyle\int_{\mathbb{R}^d} (x-\mu_\varepsilon)^2 n_\varepsilon(t,x)dx, \\ \widetilde{F}_\varepsilon(\tau) = \displaystyle\int_{\mathbb{R}^d} a(\tau,x)\frac{1}{T}\int_0^T \frac{n_\varepsilon(t,x)}{\rho_\varepsilon(t)}dtdx, \end{cases} \tag{3.8}$$

where $\rho_\varepsilon(t)$ denotes the total population size and $\bar{\rho}_\varepsilon$ its mean in a period of time, $\mu_\varepsilon(t)$, the mean phenotypic trait, $\sigma^2_\varepsilon(t)$, the variance and $\widetilde{F}_\varepsilon(\tau)$ the mean fitness computed in a constant environment. The following expressions were found coming from an approximation using the Hamilton-Jacobi approach

$$\bar{\rho}_{\varepsilon,approx}(t) \approx r - \frac{gc^2}{2} - \varepsilon\sqrt{g}, \quad \mu_{approx}(t) \approx \frac{2\varepsilon c}{b}\sqrt{g}\sin\left(bt - \frac{\pi}{2}\right), \quad \sigma^2_{approx} \approx \frac{\varepsilon}{\sqrt{g}}, \quad \widetilde{F}_{approx}(\tau) \approx r - \varepsilon\sqrt{g}. \tag{3.9}$$

Note that, our approximations in (3.9) match until order ε with the phenotypic mean μ and the mean fitness $\bar{F}$ obtained from the explicit solution, and the same variance σ^2 is obtained in both cases.

We are in particular motivated by a biological experiment in [60]. There the authors study the dynamics of a population of bacterial pathogen evolved in different environments with constant or fluctuating temperature and after several weeks they compare their growth rates at the same conditions. An interesiting outcome of the experiment was that a population evolved in periodically fluctuating temperature (daily variation between 24°C and 38°C, mean 31°C) was more performant that the strains evolved in constant temperature (31°C), when both strains were placed in a constant environment with temperature 31°C. This phenomenon is interesting since one could expect that the population evolved in a constant environment would select for the best trait in such environment. In Chapter 1 a well adapted analysis to the mentioned experiment was done and this phenomenon was analytically captured under some condition on the growth rate and considering small effect of mutations. Here we are interested in providing a numerical comparison between the moments and the mean fitness of two population evolved either in a periodic environment or in a constant one to illustrate the analytical results and to investigate the outcome for larger effect of the mutations.
To this end we first recall the expressions for the phenotypic density n_c and the total size ρ_c of a population which has evolved in a constant environment with $t = \frac{\pi}{b}$, (mean time), that is when the growth rate is given by $a(\pi/b, x) = r - gx^2$. These quantities can be computed explicitly and it holds that

$$n_c = \rho_c \frac{g^{\frac{1}{4}}}{\sqrt{2\pi\varepsilon}} \exp\left(\frac{-\sqrt{g}x^2}{2\varepsilon}\right), \quad \rho_c = r - \varepsilon\sqrt{g},$$

(see Chapter 1 for more details).
Moreover, the mean trait μ_c, the variance σ^2_c and the mean fitness $\widetilde{F}_c$ of such population, in an environment with the same temperature ($t = \frac{\pi}{b}$) are given below

$$\mu_c = 0, \quad \sigma^2_c = \frac{\varepsilon}{\sqrt{g}}, \quad \widetilde{F}_c = r - \varepsilon\sqrt{g}.$$

Here we observe that, independently of the choice of the constants r, g and c, both populations (the one evolved in a constant environment and the other evolved under periodic fluctuations) have the same mean fitness at the same constant environment, up to order ε. Indeed, we remark that for larger values of ε the mean fitness of a population evolved in a periodic environment $\overline{F}(\tau)$ given in (3.7) is smaller than the mean fitness of the population evolved in a constant regime $\widetilde{F}_c$.

3.1.2 Numerical simulations

In this subsection we consider again the growth rate a_1 in (3.2). For the numerical computations we consider $r = 2$, $g = c = 1$ and $b = 2\pi$; this implies that a_1 is a $1-$periodic function. Note that in order to obtain the numerical solution of (3.1) we consider an initial value problem whose solution converges to the unique periodic solution of (3.1) (see the appendix for more details). The initialization values for such a Cauchy problem are (n_0, ρ_0) as follows:

$$n_0(x) = e^{-|x-x_0|^2}, \quad \rho_0 = 1, \tag{3.10}$$

for some x_0 in the considered numerical domain. Along the whole section we use the notations μ_{approx}, σ^2_{approx} and $\overline{F}_{approx}$ to denote our analytic approximations in (3.9) and μ_ε, σ^2_ε and $\widetilde{F}_\varepsilon$ the respective quantities numerically computed from (3.8). We illustrate the results in two subsections for $\varepsilon = 10^{-2}$ and $\varepsilon = 1$.

3.1.2.1 Small effect of mutations

We first consider the case when the mutations are rare (that is, for $\varepsilon = 10^{-2}$), in order to compare the numerical results with those obtained analytically in Chapter 1, as the rate of mutations vanish.

The population's density and size

We illustrate in Figure 3.1 the density of the population and next in Figure 3.2 the dynamics of the total population size. We observe, as it was analytically proved in Chapter 1, that when the mutations are small, the solution concentrates on a single point with small oscillations, while the size of the population varies periodically in time.

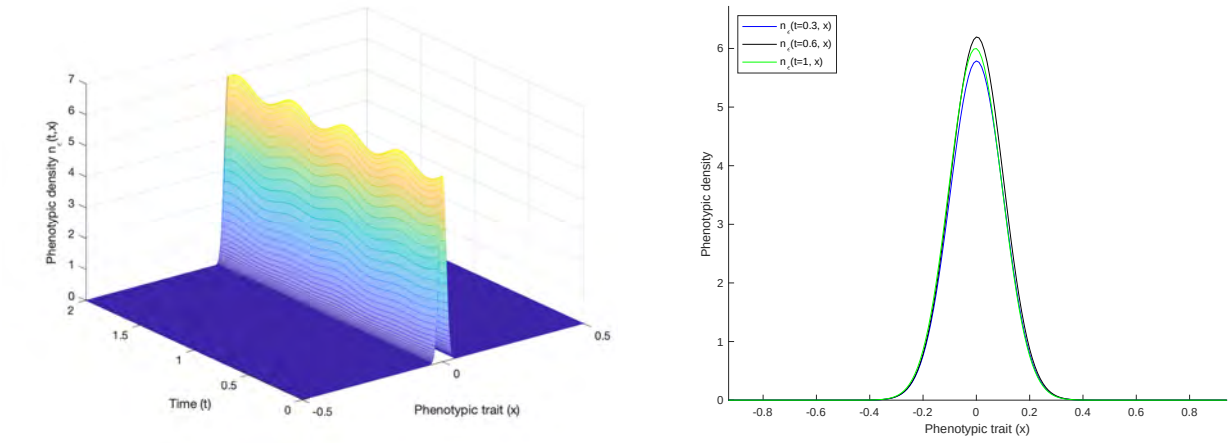

(a) (b)

Figure 3.1 – The phenotypic density $n_\varepsilon(t, x)$ of the population: (a) as a function of time and trait over two periods of time; (b) at three fixed times within one period. We observe that the population concentrates around a dominant trait which oscillates periodically in time with small amplitude. The dominant trait is $x = 0$, which is the maximum point of $\overline{a}_1$. Parameters: $\varepsilon = 10^{-2}$ and $a = a_1$ is given by (3.2), with $r = 2,\ c = g = 1,\ b = 2\pi$.

The moments and the fitness

Here we compare the numerical approximations for the moments of the population's distribution and the mean fitness in (3.8) with the analytic formula provided in (3.9).

Note that the analytical results in Chapter 1 provide an approximation of such moments with an error of order ε^2.

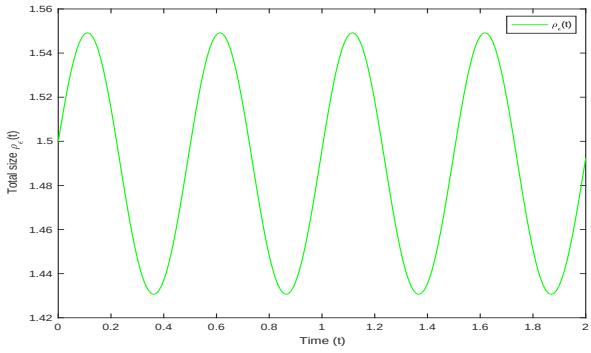

Figure 3.2 – The dynamics of the periodic total population size $\rho_\varepsilon(t)$ along two periods of time of n_ε. Parameters: $\varepsilon = 10^{-2}$ and $a = a_1$ is given by (3.2), with $r = 2,\ c = g = 1,\ b = 2\pi$.

By resolving numerically (3.1) in Figure 3.3 we compare the numerical and the analytic approximations of the mean phenotypic trait $\mu(t)$ and the variance $\sigma^2(t)$.

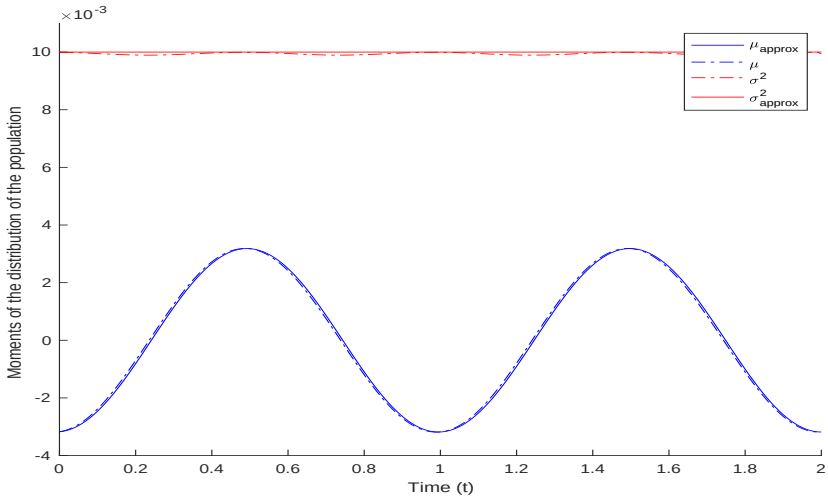

Figure 3.3 – Comparison of the moments of the population's distribution (variances in red and phenotypic means in blue). The numerical approximation in dashed lines Vs the analytic results in continuous lines. Parameters: $\varepsilon = 10^{-2}$ and $a = a_1$ is given in (3.2), with $r = 2,\ c = g = 1,\ b = 2\pi$.

Note that the curves look well approximated but in order to capture with more precision the order of the error, we compute explicitly in Table 3.1 the difference between the analytical and the numerical values. We observe that the error is in fact of order $\varepsilon^2 = 10^{-4}$ as expected from the analytic study. We remark that in Table 3.1 the third column correspond to the analytic difference between the expressions in (3.6)-(3.7) and the approximations in (3.9) for the values of the parameters given, while the fourth column refers to the difference between the same approximated values in (3.9) and the numerical computations of the formula (3.8).

Furthermore from the simulations we are able to observe a delay between the mean phenotypic trait $\mu_\varepsilon(t)$ and the

Error	Formula	Analytic Value	Numeric Value
Mean Phenotypical Trait	$\max_{t\in[0,T]}(\lvert\mu_\varepsilon(t)-\mu_{approx}(t)\rvert)$	$1.0132*10^{-5}$	$1.1234*10^{-4}$
Variance	$\max_{t\in[0,T]}(\lvert\sigma^2_\varepsilon(t)-\sigma^2_{approx}(t)\rvert)$	0	$5.639*10^{-5}$
Mean Fitness	$\lvert\widetilde{F}_\varepsilon-\widetilde{F}_{approx}\rvert$	$5.0660*10^{-6}$	$6.3555*10^{-5}$

Table 3.1 – Errors in the approximation of the moments of the population's distribution and the mean Fitness. The approximations are of order ε^2 and the numerical error corresponds to this order. Parameters: $\varepsilon = 10^{-2}$ and $a = a_1$ is given in (3.2), with $r = 2,\ c = g = 1,\ b = 2\pi$.

optimal trait $\theta(t) = c\sin bt$ (Figure 3.4). This phenomenon is well known in the biological litterature, the mean phenotypic trait oscillates with the same period as the optimal trait $\theta(t)$ but with a certain delay (see for instance [69, 23]). In this example the numerical delay corresponds to 0.24 which is close to the the analytic value $\frac{\pi}{2b}$, for $b = 2\pi$, found in Chapter 1.

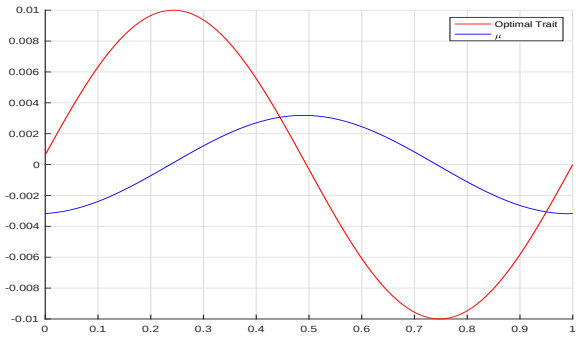

Figure 3.4 – Comparison between the numerical approximation of $\mu_\varepsilon(t)$ and the optimal trait $\theta(t)$. The time for which the population attains its optimal trait (that is $\sin bt = 1$) is $t \approx 0.25$ while the mean phenotypic trait attains this maximum value at time $t \approx 0.25 + 0.24$, which leads to an approximate delay of 0.24. Note that the amplitude of the oscillations of the mean phenotypic trait (blue) is smaller than the one of the optimal trait (red). Here we have re-normalized the optimal trait by multiplying by ε to keep similar scaling. Parameters: $\varepsilon = 10^{-2}$ and $a(t,x)$ is given in (3.2), with $r = 2,\ c = g = 1,\ b = 2\pi$.

Following our motivation from the biological experiment in [60], we compare the behavior of two populations evolved in different environments. We show in Table 3.2 the numerical values of the moments and the mean fitness of both cases: a population evolved in a constant environment and another one evolved under periodic fluctuations. Analogously to the results in Chapter 1, for this choice of the growth rate, the variance and the mean fitness do not change significantly from one environment to the other, but we remark that the averaged total population is smaller for the population evolved in a periodic environment, which is also consistent with our analytic computations ($\rho_c - \overline{\rho}_\varepsilon \approx \frac{gc^2}{2}$) given in Chapter 1. Note that for the numerical values of the mean phenotypic trait and the variance in the periodic environment shown in Table 3.2 we compute the maximum values over a period since they are periodic functions of t as shown in Figure 3.3.

Again the notations μ_ε, σ^2_ε and $\bar{\rho}_\varepsilon$ in Table 3.2 correspond to the numerical value of the quantities in (3.8), while the variables with sub-index c represent the similar quantities for a population evolved in the constant environment.

Values	Periodic environment	Constant environment
Averaged Total Size $[0,T]$	$\bar{\rho}_\varepsilon = 1,4893$	$\rho_c = 1,9900$
Mean Phenotypic Trait	$\max_{t\in[0,T]} \mu_\varepsilon = 0,00318$	$\mu_c \approx 10^{-19}$
Mean Variance	$\max_{t\in[0,T]} \sigma^2_\varepsilon = 0,01$	$\sigma^2_c = 0,0100$
Mean Fitness	$1,9901$	$1,9900$

Table 3.2 – Comparison between the moments of the population's distribution and mean fitness for populations evolved in periodic and constant environments. Parameters: $\varepsilon = 10^{-2}$ and $a = a_1$ given in (3.2), with $r = 2,\ c = g = 1,\ b = 2\pi$.

3.1.2.2 Large effect of Mutations

In order to observe the behavior of the population under a larger rate of mutations, we now consider a different value for the parameter ε, and keep the same growth function a_1.
Since we expect to have extinction for large values of ε we first compute the mean total size of the population as a function of the mutations rate, that is $\varepsilon \mapsto \bar{\rho}_\varepsilon$, to capture the maximum value of ε which avoids extinction. In Figure 3.5 we plot both the numerical value of the mean size $\bar{\rho}_\varepsilon$ in (3.8) and the approximated mean total size $\bar{\rho}_{\varepsilon,approx}$ computed in (3.9).

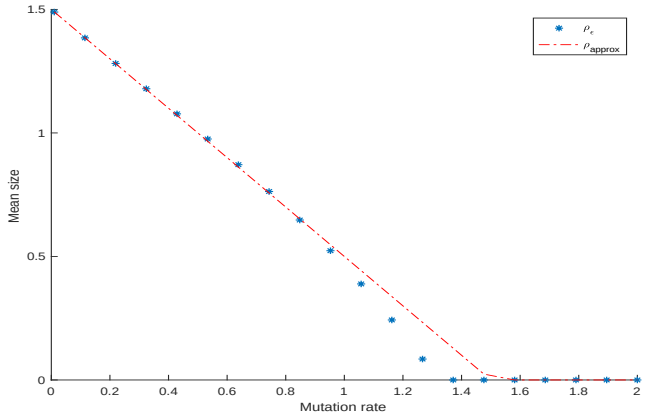

Figure 3.5 – Mean Total size of the population for different values of the mutation rate $\varepsilon \in [10^{-2}, 2]$. The red dashed line corresponds to the approximated value of $\bar{\rho}_{\varepsilon,approx}$ in (3.9) and the discontinuous blue points correspond to the numerical value of $\bar{\rho}_\varepsilon$ in (3.8) from the solution of (3.1) with the growth rate $a = a_1$ given in (3.2), for the parameter values $r = 2,\ c = g = 1,\ b = 2\pi$.

Note that, for the choice of the parameters (r, b, c, g) given in Figure 3.5 it is sufficient to take the rate of mutations smaller than $\varepsilon_{max} = 1.3$ to avoid the extinction of the population. Note also that the approximation given in (3.9) is better for the smaller values of ε which is coherent.
For the simulations in this subsection we consider $\varepsilon = 1$, to keep an acceptable total population size.

The population's density and size

In Figure 3.6 we first plot the distribution density of the population $n_\varepsilon(t,x)$ along two periods (Figure 3.6a) and then

for three fixed times in one period, i.e. $n_\varepsilon(t_i, x), i \in \{1, 2, 3\}$ (Figure 3.6b), similarly as we have done in the previous subsection. We observe that the solution has a distribution around the optimal trait, but this distribution is much less concentrated comparing to the case with ε small. In fact the maximum value of $n(t_{\text{fix}}, x)$, for t_{fix} a fixed value of time in a period, is attained nearly to but not exactly at the optimal trait $x = 0 = \max \overline{a}_1$. This is due to the effect of mutations. This distribution still has a time-periodic behavior as expected and the periodic oscillations are more remarkable for this larger ε. Indeed in Figure 3.7 we illustrate the dynamics of the periodic total population size along two periods of time.

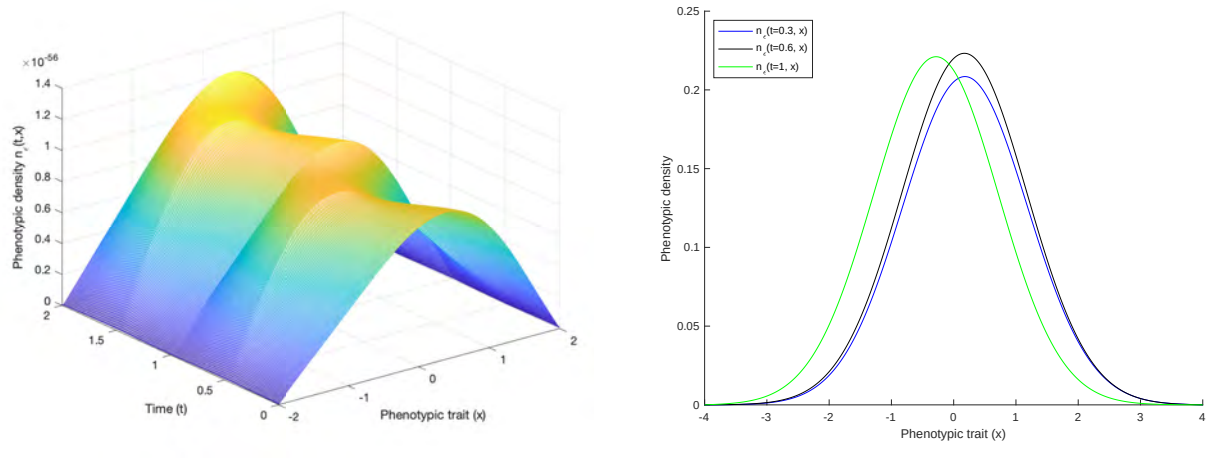

(a) (b)

Figure 3.6 – The phenotypic density $n_\varepsilon(t, x)$ of the population: (a) as a function of time and trait over two periods of time; (b) at three fixed times within one period. The population is distributed around a dominant trait which evolves periodically in time. Parameters: $\varepsilon = 1$ and $a = a_1$ given in (3.2), with $r = 2,\ c = g = 1,\ b = 2\pi$.

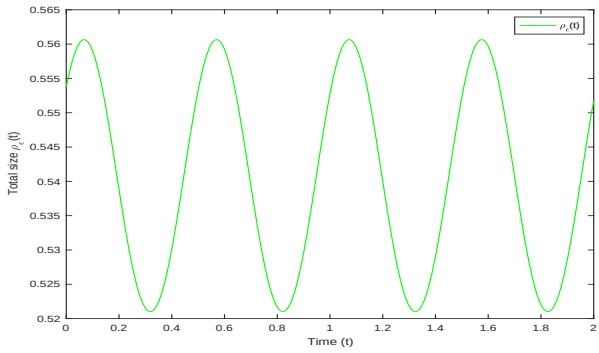

Figure 3.7 – The dynamics of the periodic total population size $\rho_\varepsilon(t)$ along two periods of time of n_ε. Parameters: $\varepsilon = 1$ and $a = a_1$ given in (3.2), with $r = 2,\ c = g = 1,\ b = 2\pi$.

The moments and the fitness

We next compare the numerical approximations obtained for the moments of the population's phenotypic distribution with their analytic expression provided in (3.9) with $\varepsilon = 1$, (see Figure 3.8). We observe that the variance (in red) is still well approximated by a constant, which is not surprising since our approximation in (3.9) coincides with the exact

value in (3.6). However, in the plot of the phenotypic means (in blue) we observe a larger error between both curves which comes from the fact that increasing ε leads to a larger difference between the values of $\mu(t)$ in (3.6) and (3.9).

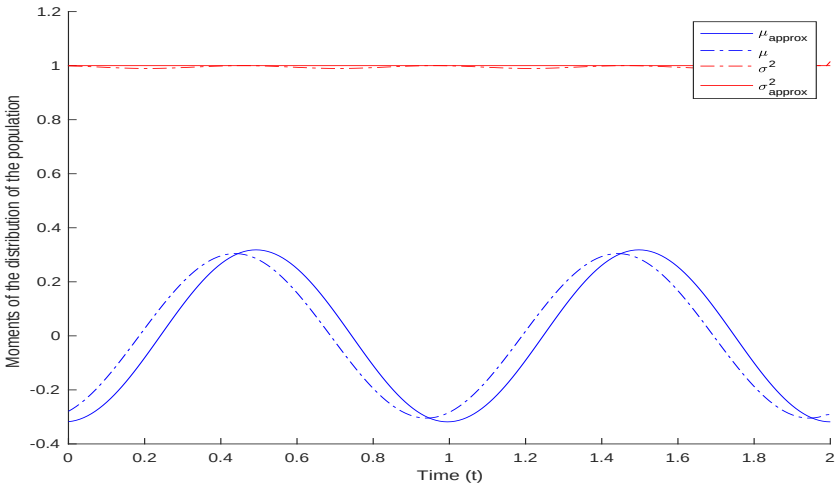

Figure 3.8 – Comparison of the moments of the population's distribution (variances in red and phenotypic means in blue). The numeric approximation in dashed lines Vs the analytic results in continuous lines. Parameters: $\varepsilon = 1$ and $a = a_1$ given in (3.2), with $r = 2,\ c = g = 1,\ b = 2\pi$.

Analogously as we have done in the previous subsection, we show in Table 3.3 the error in the approximations by taking the difference between the values of the analytic formula and the approximated values. The notations are similar as in the previous subsection. Again, note that the third column corresponds to the analytic difference between the expressions in (3.6) and the approximated values (3.9) for the values of the parameters given, while the fourth column refers to the difference of the same approximated values in (3.9) with the numerical computations of the formula in (3.8). It is interesting to point out that these errors are of order less than $\varepsilon^2 = 1$. In particular, we observe that these approximations are consistent with the explicit expressions in (3.6) and (3.7).

Error	Formula	Analytic value	Numeric Value
Mean Phenotypic Trait	$\max_{t\in[0,T]}(\lvert\mu_\varepsilon(t) - \mu_{approx}(t)\rvert)$	0.0920	0.1093
Variance	$\max_{t\in[0,T]}(\lvert\sigma^2_\varepsilon(t) - \sigma^2_{approx}(t)\rvert)$	0	$6.25 * 10^{-4}$
Fitness	$\lvert\widetilde{F}_\varepsilon(t) - \overline{F}_{approx}(t)\rvert$	0.0460	0.0409

Table 3.3 – Errors in the approximation of the moments of the population's distribution and mean Fitness. Parameters: $\varepsilon = 1$ and $a = a_1$ given in (3.2), with $r = 2,\ c = g = 1,\ b = 2\pi$.

Furthermore, for this value of ε we are able to catch "better" (without rescaling the optimal trait), the phenomenon of the delay that experiments the mean phenotypic trait of the population with respect to the optimal trait (Figure 3.9). In this case we obtain a delay of around 0.2 which is smaller than the one in the previous case (delay = 0.24 for $\varepsilon = 10^{-2}$). This shows that the mutations may help the population to follow the environmental changes.

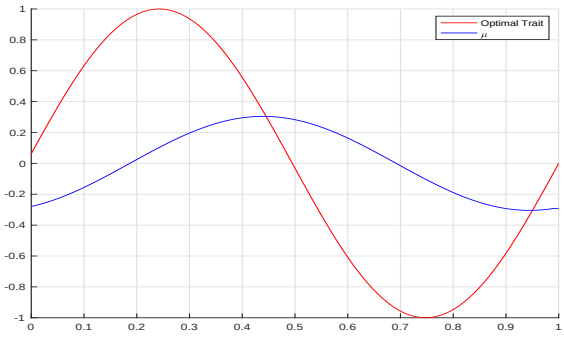

Figure 3.9 – Comparison between the numerical approximation of $\mu_\varepsilon(t)$ with the optimal trait $\theta(t)$. The time for which the population attains its optimal trait (that is $\sin bt = 1$) is $t \approx 0.25$ while the mean phenotypic trait attains this maximum value at time $t \approx 0.25 + 0.2$, which leads to an approximate delay of 0.2. Parameters: $\varepsilon = 1$ and $a = a_1$ given in (3.2), with $r = 2,\ c = g = 1,\ b = 2\pi$.

Again we compare the behavior of two populations evolved in different environments. We show in Table 3.4 the numerical values of the moments and the mean fitness for two populations: one evolved in a constant environment and the other evolved under periodic oscillations. The notations are similar to the Table 3.2.

Values	Periodic environment	Constant environment
Averaged Total Size $[0, T]$	$\bar{\rho}_\varepsilon = 0,5406$	$\rho_c = 1$
Mean Phenotypic Trait	$\max_{t\in[0,T]} \mu_\varepsilon = 0,3043$	$\mu_c \approx 10^{-17}$
Mean Variance	$\max_{t\in[0,T]} \sigma^2_\varepsilon = 0,9999$	$\sigma^2_c = 0,9988$
Mean Fitness	$0,9590$	$1,0009$

Table 3.4 – Comparison between the moments of the population's distribution and mean fitness for populations evolved in periodic and constant environments. Parameters: $\varepsilon = 1$ and $a = a_1$ given in (3.2), with $r = 2,\ c = g = 1,\ b = 2\pi$.

Note that in contrast with the case for $\varepsilon = 10^{-2}$, here the mean fitness of the population evolved in a periodic environment is smaller than the mean fitness of the population evolved in a constant environment. Larger rate of mutations increases indeed the cost of fluctuations.

3.1.3 Derivation of the explicit solution $\mathcal{N}(t, x)$ and the moments of the distribution

We now present the arguments to obtain the given expression for ρ, μ and σ in (3.6). Here, for the simplicity in the forward notations we introduce the function $f(t) = \left(\frac{\varepsilon}{\sigma^2(t)}\right)^2$ such that the anzats in (3.4) read as follows

$$\mathcal{N}(t,x) = \frac{\rho(t)}{\sqrt{\pi}} \left(\frac{f(t)}{4\varepsilon^2}\right)^{1/4} \exp\left[-\left(\frac{f(t)}{4\varepsilon^2}\right)^{1/2} (x-\mu(t))^2\right], \tag{3.11}$$

and from here we compute

$$\log(\mathcal{N}) = \log(\rho(t)) + \frac{1}{4}\log\left(\frac{f(t)}{4\varepsilon^2}\right) - \left(\frac{f(t)}{4\varepsilon^2}\right)^{1/2}(x-\mu(t))^2 + cst,$$

$$\frac{1}{\mathcal{N}}\frac{\partial \mathcal{N}}{\partial t} = \frac{\rho'(t)}{\rho(t)} + \frac{1}{4}\frac{f'(t)}{f(t)} - \frac{1}{4}\frac{f'(t)}{(\varepsilon^2 f(t))^{1/2}}(x-\mu(t))^2 + \left(\frac{f(t)}{\varepsilon^2}\right)^{1/2}(x-\mu(t))\mu'(t),$$

$$\frac{1}{\mathcal{N}}\frac{\partial \mathcal{N}}{\partial x} = -\left(\frac{f(t)}{\varepsilon^2}\right)^{1/2}(x-\mu(t)), \quad \frac{1}{\mathcal{N}}\frac{\partial^2 \mathcal{N}}{\partial x^2} = -\left(\frac{f(t)}{\varepsilon^2}\right)^{1/2} + \frac{f(t)}{\varepsilon^2}(x-\mu(t))^2.$$

We now substitute the above formula of $\mathcal{N}$ and its derivatives into (3.3), and find

$$\begin{aligned}&\frac{\rho'(t)}{\rho(t)} + \frac{1}{4}\frac{f'(t)}{f(t)} - \frac{1}{4}\frac{f'(t)}{\varepsilon f(t)^{1/2}}(x-\mu(t))^2 + \frac{f(t)^{1/2}}{\varepsilon}(x-\mu(t))\mu'(t)\\ &= \varepsilon^2\left[-\frac{f(t)^{1/2}}{\varepsilon} + \frac{f(t)}{\varepsilon^2}(x-\mu(t))^2\right] + \left[r - g(x - c\sin bt)^2 - \rho(t)\right].\end{aligned}$$

We then obtain the following ODE system by a factorization in powers of x:

$$\begin{cases} f'(t) = 4\varepsilon f(t)^{1/2}(g - f(t)), \\ \mu'(t) = \dfrac{2g\varepsilon}{f(t)^{1/2}}(c\sin bt - \mu(t)), \\ \rho'(t) = (Q(t) - \rho(t))\,\rho(t), \end{cases} \tag{3.12}$$

where

$$Q(t) = r - g(c\sin bt - \mu(t))^2 - g\frac{\varepsilon}{f(t)^{1/2}}.$$

Note that, the above system, is "uncoupled" in the sense that we can find the solution $f(t)$ from its own equation (Ricatti type equation with constant coefficients) and then substitute it in the equation for $\mu(t)$, which has also an explicit known solution. Finally we can substitute $f(t)$ and $\mu(t)$ in the expression of $Q(t)$ which allows us to obtain an explicit formula for $\rho(t)$. We will do this in the following paragraphs.

Solving equation for $f(t)$

From the first equation in (3.12) we make the change of variables $h(t) = (f(t))^{1/2}$ and obtain the following Ricatti type equation:

$$h'(t) = 2\varepsilon(g - h^2(t)).$$

Since $g > 0$ this equation can be analytically solved by the method of separable variables and we obtain the following solution:

$$h(t) = \sqrt{g}\frac{1 + Ke^{-4t\varepsilon\sqrt{g}}}{1 - Ke^{-4t\varepsilon\sqrt{g}}},$$

where K is the integrating constant.

We recall that we are looking for periodic solutions of the parabolic system. The periodicity condition implies that $h(0) = h(T)$ since f has to be $T-$periodic. It holds that

$$h(T) = \sqrt{g}\frac{1 + Ke^{-4T\varepsilon\sqrt{g}}}{1 - Ke^{-4T\varepsilon\sqrt{g}}} = \sqrt{g}\frac{1+K}{1-K} = h(0) \Rightarrow K = 0,$$

since $g, \varepsilon, T > 0$. Thus the $T-$periodicity condition leads to $f(t) = g$. This implies also that the variance is constant, $\sigma^2(t) = \frac{\varepsilon}{\sqrt{g}}$.

Solving equation for $\mu(t)$

We first substitute the solution $f(t) = g$ into the second equation of (3.12), it gives:

$$\mu'(t) = 2\varepsilon\sqrt{g}(c\sin bt - \mu(t)).$$

This equation can be solved by integrating factor method. The solution can be expressed as follows

$$\mu(t) = \frac{2c\varepsilon\sqrt{g}}{4\varepsilon^2 g + b^2}\left(2\varepsilon\sqrt{g}\sin bt - b\cos bt\right) + K_1 e^{-2\varepsilon t\sqrt{g}},$$

where K_1 is the integrating constant. Since we look for solutions with the same period of the optimal trait, it holds that $K_1 = 0$ in order to have $\mu(0) = \mu(2\pi/b)$. This gives for $\mu(t)$ the expression in (3.9).

Solving equation for $\rho(t)$

After a standard substitution $\kappa(t) = 1/\rho(t)$ in order to linearize the third equation in (3.12), we can integrate it and the function κ can be written as follows:

$$\kappa(t) = \exp\left(-\int_0^t Q(s)ds\right)\left(K_2 + \int_0^t \exp\left(\int_0^s Q(\theta)d\theta\right)ds\right),$$

where K_2 can be computed by using the $T-$peridicity of $\kappa(t)$ and we obtain:

$$K_2 = \frac{\int_0^T \exp\left(\int_0^t Q(s)ds\right)dt}{\exp\left(\int_0^T Q(s)ds\right) - 1}.$$

This gives, after substitution of the expression for $f(t)$ and $\mu(t)$, the following formula for $\rho(t)$:

$$\rho(t) = \exp\left(I(t)\right)\left[K_2 + \int_0^t \exp\left(I(z)\right)dz\right]^{-1}, \tag{3.13}$$

where

$$I(t) = (r - \varepsilon\sqrt{g})t - \frac{gc^2b^2}{(4g\varepsilon^2 + b^2)^2}\left[\frac{b^2}{2}\left(t - \frac{\sin 2bt}{2b}\right) + 2g\varepsilon^2\left(t + \frac{\sin 2bt}{2b}\right) + \varepsilon\sqrt{g}\left(1 - \cos 2bt\right)\right],$$

and

$$K_2 = \frac{\exp\left(\int_0^T I(s)ds\right)}{\exp\left(I(T)\right) - 1}.$$

The computation of the mean fitness

With these results we are able to compute also the mean fitness for the phenotypic density $\mathcal{N}(t, x)$. Indeed we compute

$$\overline{F}(\tau) = \int_{\mathbb{R}} a_1(\tau, x)\frac{1}{T}\int_0^T \frac{\mathcal{N}(t, x)}{\rho(t)}dtdx.$$

We consider the mean value $\tau = \frac{\pi}{b}$ since the function a_1 is $\frac{2\pi}{b}-$periodic. We compute then

$$\overline{F}\left(\frac{\pi}{b}\right) = \int_{\mathbb{R}}(r - gx^2)\frac{b}{2\pi}\int_0^{2\pi/b} \frac{\frac{\rho(t)}{\sqrt{2\pi\varepsilon}}f(t)^{1/4}\exp\left[-\frac{f(t)^{1/2}}{2\varepsilon}(x - \mu(t))^2\right]}{\rho(t)}dtdx.$$

After a simplification and a substitution of the known expressions for $f(t)$ and $\mu(t)$ we obtain:

$$\overline{F}\left(\frac{\pi}{b}\right) = \frac{b\sqrt[4]{g}}{(2\pi)^{3/2}\varepsilon^{1/2}} \int_0^{2\pi/b} \int_{\mathbb{R}} (r - gx^2) \exp\Big[- \frac{\sqrt{g}}{2\varepsilon}(x - \mu(t))^2\Big] dtdx,$$

which is an analytically integrable function giving (3.7).

3.2 Oscillations on the pressure of selection

In this section we study another particular growth rate a for the problem (3.1) where the oscillations act on the pressure of selection and obtain a semi-explicit solution to the problem. Again, we study the problem both analytically and numerically for two values of the mutation rate small and large. In particular, with this analysis we arrive to capture the phenomenon observed in the biological experiment in [60].

3.2.1 Analytic study of the semi-explicit solution

Let us consider now a growth rate function as follows:

$$a_2(t, x) = r - g(t)x^2. \tag{3.14}$$

In this example r represents again the maximal growth rate and $g(t)$ the pressure of selection, which we consider not constant anymore as in the previous example but a positive $1-$periodic function. Note that the optimal trait in this example is constant equal to 0. We substitute into (3.1) and obtain:

$$\partial_t n_\varepsilon(t, x) - \varepsilon^2 \Delta n_\varepsilon(t, x) = n_\varepsilon(t, x)[r - g(t)x^2 - \rho_\varepsilon(t)]. \tag{3.15}$$

We show that the unique solution to (3.15) has the following form, analogous to the first example, i.e.,

$$\mathcal{N}(t, x) = \frac{\rho(t)}{\sqrt{2\pi\sigma^2(t)}} \exp\left[-\frac{(x - \mu(t))^2}{2\sigma^2(t)}\right], \tag{3.16}$$

with $\rho(t)$, $\mu(t)$ and $\sigma^2(t)$ as in (3.5). Again from the results in Chapter 1 we know that problem (3.1) has a unique periodic solution, so it is enough to find a solution in this form. We also prove that for this choice of a we have:

$$\rho(t) = \exp\left(I_2(t)\right)\left[K_3 + \int_0^t \exp\left(I_2(z)\right) dz\right]^{-1}, \quad \mu(t) = 0, \quad \sigma^2(t) = \frac{\varepsilon}{\sqrt{f(t)}} \tag{3.17}$$

with

$$I_2(t) = rt - \varepsilon \int_0^t \frac{g(s)}{f(s)^{1/2}} ds, \tag{3.18}$$

and f the solution to the following equation

$$\frac{df}{dt} = 4\varepsilon\sqrt{f(t)}(g(t) - f(t)). \tag{3.19}$$

In particular we note that

$$\int_0^T f(t)dt = \int_0^T g(t)dt.$$

Moreover the mean fitness of this population (at value 1/2) is given by

$$\overline{F}(1/2) = r - \varepsilon g(1/2) \int_0^1 f(t)^{-1/2} dt. \tag{3.20}$$

It is interesting to compare these analytic results obtained from the explicit solution (3.16) with the analytic expressions given in Chapter 1 coming from an approximation using the Hamilton-Jacobi approach, that is:

$$\mu_\varepsilon(t) \approx 0, \quad \sigma_\varepsilon^2 \approx \frac{\varepsilon}{\sqrt{\overline{g}}}, \quad \widetilde{F}_\varepsilon(1/2) \approx r - \varepsilon \frac{g(1/2)}{\sqrt{\overline{g}}}. \tag{3.21}$$

with

$$\overline{g} = \int_0^1 g(t) dt.$$

Note that our approximations in (3.21) are coherent, in the sense that, once we know the function f then the expressions for the variance and the mean fitness coincide until order ε with the values given in (3.17) and (3.20). Note also, that the phenotypic mean remains constant equal to one for any value of ε. This is not surprising since all the environmental states select for the trait $x = 0$.

Following our motivation from the biological experiment, we consider again a population evolved in a constant environment with $t = \frac{1}{2}$, (mean time) and recall the phenotypic density n_c and the total size ρ_c. That is when the growth rate is given by $a(1/2, x) = r - g(1/2)x^2$ the solution can be computed explicitly and is given by

$$n_c = \rho_c \frac{g(1/2)^{\frac{1}{4}}}{\sqrt{2\pi\varepsilon}} \exp\big(\frac{-\sqrt{g(1/2)}x^2}{2\varepsilon}\big), \quad \rho_c = r - \varepsilon\sqrt{g(1/2)},$$

from where we obtain the following phenotypic mean μ_c, variance σ_c^2 and mean fitness $\widetilde{F}_c$ of such population, in an environment with the same temperature ($t = 1/2$)

$$\mu_c = 1, \quad \sigma_c^2 = \frac{\varepsilon}{\sqrt{g(1/2)}}, \quad \widetilde{F}_c = r - \varepsilon\sqrt{g(1/2)}.$$

Note from here that, as was analytically proved if we choose g such that its average in one period is smaller than its mean value, i.e, $\frac{g(1/2)}{\sqrt{\overline{g}}} < 1$, then the mean fitness of the population evolved under periodic fluctuations is larger than the one of the population evolved in a constant environment. This is also observed from the semi-explicit formula in (3.20) if $\int_0^1 f(t)^{-1/2} dt < 1$.

3.2.2 Numerical simulations

In this subsection, for the numerical resolution of (3.1) we consider the growth rate in (3.14), that is the optimal trait is constant equal to 0.
We take $g(t)$ the following positive $1-$periodic function

$$g(t) = \cos bt + 1.5,$$

for $b = 2\pi$. For the numerical computations we take the same values of the algorithm's parameters (ρ_0, n_0) as in the previous section, and the parameter $r = 2$. Again, we develop the numerical analysis for both values of the mutations rate $\varepsilon = 10^{-2}$ and $\varepsilon = 1$.

3.2.2.1 Small effect of Mutations

We first study the case when the mutations are rare (that is, $\varepsilon = 10^{-2}$) and resolve numerically the equation (3.1) for a given in (3.14).

The population's density and size

In Figure 3.10, we illustrate the phenotypic density $n_\varepsilon(t, x)$, first along two periods of time (Figure 3.10a) and then for three different fixed times in one period $n_\varepsilon(t_i, x)$ (Figure 3.10b). Note that for this small value of the mutations rate, the solution concentrates on a single point ($x = 0$), as expected from the analytic results. We remark that, while the time-periodic behavior of n_ε is not observable because the oscillations are quite small, in Figure 3.11 we observe the periodic fluctuations of the total size of the population.

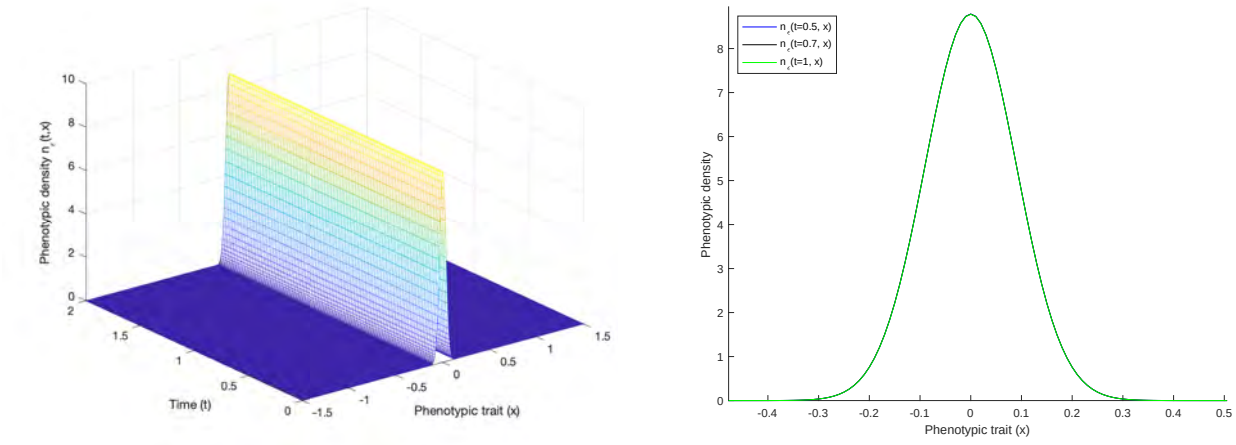

(a) (b)

Figure 3.10 – The phenotypic density $n_\varepsilon(t, x)$ of the population: (a) as a function of time and trait over two periods of time; (b) at three fixed times within one period. The population is distributed around a dominant trait, which is $x = 0$, the maximum point of $\overline{a}_2$. Parameters: $\varepsilon = 10^{-2}$ and $a = a_2$ given in (3.14), with $r = 2, b = 2\pi$.

The moments and the fitness

We follow the structure in the previous section and we compare the analytic approximations obtained for the moments of the population's distribution and the mean fitness in (3.21), with the numerical computation of the exact value in (3.17)-(3.20), in order to compute the error of approximation (see Figure 3.12).

To be more precise, we next compute, the approximate values for the errors, shown in Table 3.5. Again we point out that these errors are less than order $\varepsilon^2 = 10^{-4}$. The notations in Table 3.5 are similar to those in Table 3.1. We remark that, on the contrary that for Table 3.1 we only show the difference between the approximated values in (3.21) and the numerical computations of the formula (3.8), since we do not have the explicit expressions of the variance and the mean fitness in (3.17)-(3.20).

Analogously to the previous example, we follow the motivation coming from the biological experiment in [60] to compare the values of the moments of the distribution and the mean Fitness of two populations evolving in differ-

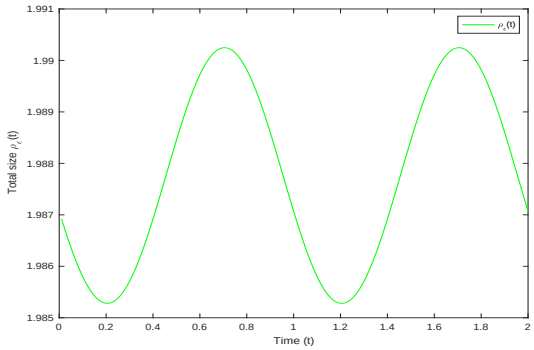

Figure 3.11 – The dynamics of the periodic total population size $\rho_\varepsilon(t)$ along two periods of time of n_ε. Parameters: $\varepsilon = 10^{-2}$ and $a = a_2$ in (3.14), with $r = 2,\ b = 2\pi$.

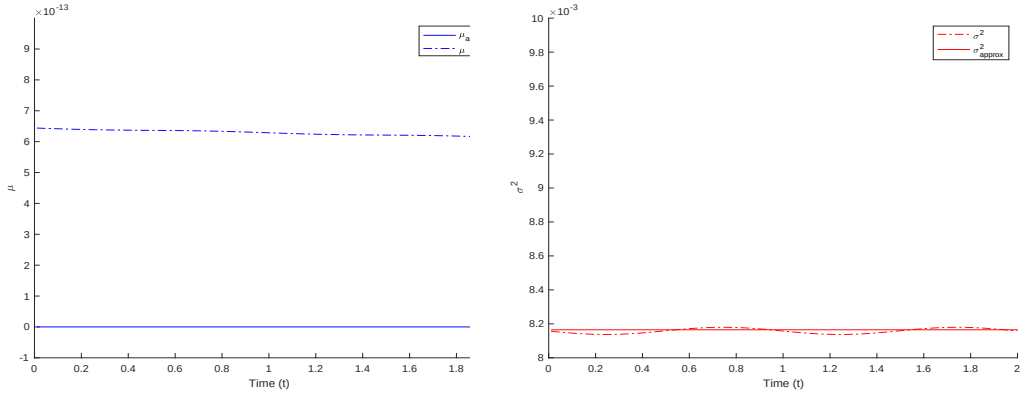

(a) Mean phenotipic trait $\mu(t)$ (b) Variance σ^2

Figure 3.12 – Comparison of the moments of the population's distribution (phenotypic means in (a) and variances in (b)). The numerical approximations of the moments are in dashed lines and the analytical approximations, given by (3.21), are in continuous lines. Parameters: $\varepsilon = 10^{-2}$ and $a = a_2$ in (3.14), with $r = 2,\ b = 2\pi$.

ent environments: constant versus periodic. We show in Table 3.6 this comparison. Note that again the mean total size of the population evolved in a periodic environment is smaller than the one evolved in a constant regime. Moreover, these results show that the population evolved in a periodic environment has a larger fitness than the one evolved in a constant environment, when they are both placed in a constant environment (with $t = 1/2$). This is consistent with our analytic results in Chapter 1. Note indeed that, with the pressure of the selection $g(t)$ given in (3.14), we have

$$\int_0^1 g(t)dt = 1,5 > 0,5 = g(1/2).$$

This satisfies the necessary condition $\overline{g} > g(T/2)$ given in the analytic study, (see Chapter 1) which implies that the population evolved in a periodic environment outperforms the population evolved in a constant environment. Note that both of these environments select for populations with the same phenotypic mean trait $x = 0$. However, the population evolved in a periodic environment has a smaller variance comparing to the one evolved in a constant environment. This makes the population evolved in the periodic environment more performant.

Error	Formula	Value
Mean Phenotypic Trait	$\max_{t\in[0,T]}(\lvert\mu_\varepsilon(t)-\mu_{approx}(t)\rvert)$	$6,4399*10^{-13}$
Variance	$\max_{t\in[0,T]}(\lvert\sigma^2_\varepsilon(t)-\sigma^2_{approx}(t)\rvert)$	$2,7650*10^{-5}$
Fitness	$\lvert\widetilde{F}_\varepsilon(t)-\widetilde{F}_{approx}(t)\rvert$	$3,2302*10^{-6}$

Table 3.5 – Errors in the approximation of the moments of the population's distribution and mean Fitness. Parameters: $\varepsilon = 10^{-2}$ and $a = a_2$ given in (3.14), with $r = 2,\ b = 2\pi$.

Values	Periodic environment	Constant environment
Averaged Total Size $[0,T]$	$\overline{\rho} = 0,9938$	$\overline{\rho}_c = 1,9858$
Mean Phenotypic Trait	$\max_{t\in[0,T]}\mu_\varepsilon \approx 10^{-13}$	$\mu_c \approx 10^{-18}$
Mean Variance	$\max_{t\in[0,T]}\sigma^2_\varepsilon = 0,0081$	$\sigma^2_c = 0,0141$
Mean Fitness	$1,9959$	$1,9929$

Table 3.6 – Comparison between the moments of the population's distribution and mean Fitness for populations evolved in periodic and constant environments. Parameters: $\varepsilon = 10^{-2}$ and $a = a_2$ given in (3.14), with $r = 2,\ b = 2\pi$.

3.2.2.2 Large effect of Mutations

In this subsection we study the behavior of the phenotypic density of a population with the same growth rate (3.14) under larger effect of mutations. First, it is convenient to know the maximum value of ε that we can consider such that the population does not get extinct. We plot $\varepsilon \mapsto \overline{\rho}_\varepsilon$ in Figure 3.13. Analogously as for the previous growth rate, in Figure 3.13 we plot both the numerical value of the mean size $\bar{\rho}_\varepsilon$ in (3.8) and the approximated mean total size $\bar{\rho}_{\varepsilon,approx}$ computed in (3.21).

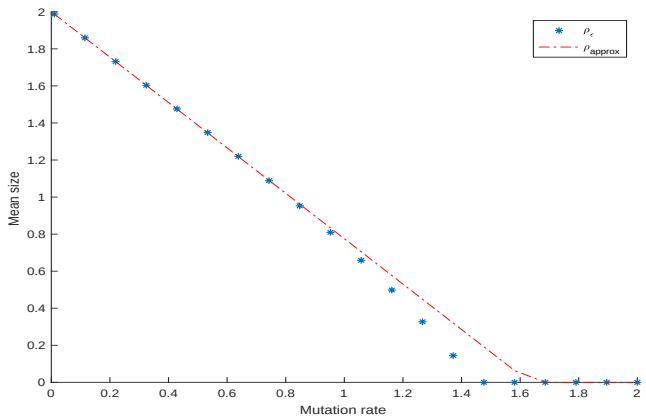

Figure 3.13 – Mean Total size of the population for different values of the mutation rate $\varepsilon \in [10^{-2}, 2]$. The red dashed line corresponds to the approximated value of $\bar{\rho}_{\varepsilon,approx}$ in (3.21) and the discontinuous blue points correspond to the numerical value of $\bar{\rho}_\varepsilon$ in (3.8) from the solution of (3.1) with the growth rate $a = a_2$ given in (3.14), for the parameter values $r = 2,\ b = 2\pi$.

We observe in Figure 3.13 that, with this choice of the parameters (r, b) it is enough to take a rate of mutations to be

smaller than $\varepsilon_{max} = 1.5$ which is the threshold above which the population goes extinct. Moreover, the approximation remains better for smaller values of ε as for the previous example.
Again we will consider $\varepsilon = 1$, to keep an acceptable total population size.

The population's density and size

In Figure 3.14 we illustrate the phenotypic density of the population for $\varepsilon = 1$. Similarly as we have done in the previous subsection we split the analysis into two subfigures: Figure 3.14a shows the behavior of $n_\varepsilon(t, x)$ along two periods of time and in Figure 3.14b it is shown $n(t_i, x), i \in \{1, 2, 3\}$ for t_i a fixed time within one period.

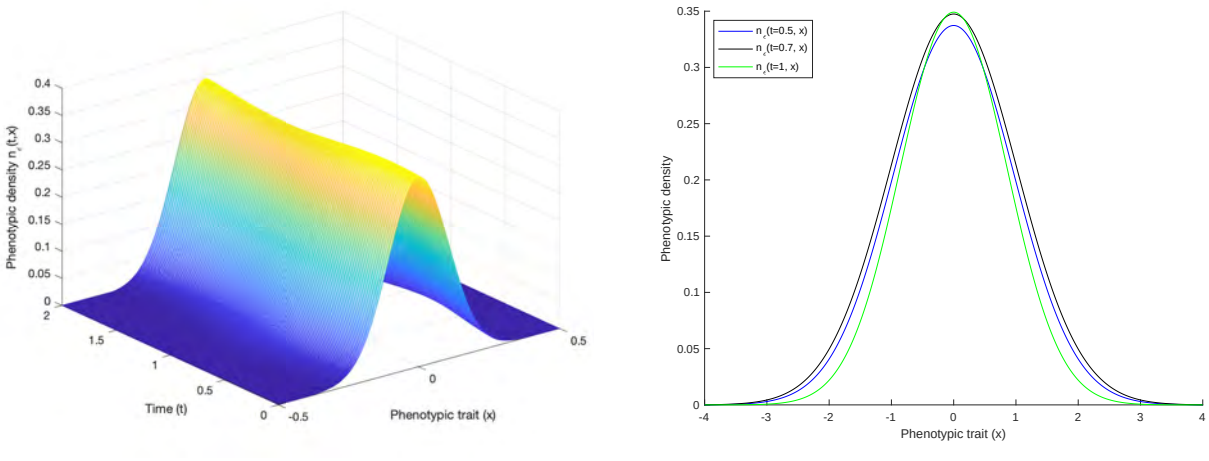

(a) (b)

Figure 3.14 – The phenotypic density $n_\varepsilon(t, x)$ of the population: (a) as a function of time and trait over two periods of time; (b) at three fixed times within one period. The population is distributed around a fixed dominant trait, while the variance and the amplitude of the population distribution varies periodically in time. Parameters: $\varepsilon = 1$ and $a = a_2$ given in (3.14), with $r = 2,\ b = 2\pi$.

It is not surprising that the population is distributed around the optimal trait, but as in the previous example the population distribution is less concentrated than in the case with $\varepsilon = 10^{-2}$. As well, it is worth noticing that the time-periodicity of n_ε is more observable for this value of ε than for the smaller value $\varepsilon = 10^{-2}$ in Figure 3.10.
Next in Figure 3.15 we show the periodic oscillations of the total size of the population.

The moments and the fitness

Next we compare again the analytic expressions of the moments of the population's distribution in (3.21) with the numerical approximations of (3.8), this time for larger effect of mutations, (see Figure 3.16).

We observe that, the mean phenotypic trait (in blue) is still well approximated by a constant which is in accordance with the analytic results in (3.17). The variance (in red) however has important oscillations when the mutations are frequent ($\varepsilon = 1$). Such oscillations were not captured in our first order approximations for ε small. Such second order oscillations were however predicted by (3.17)-(3.19).

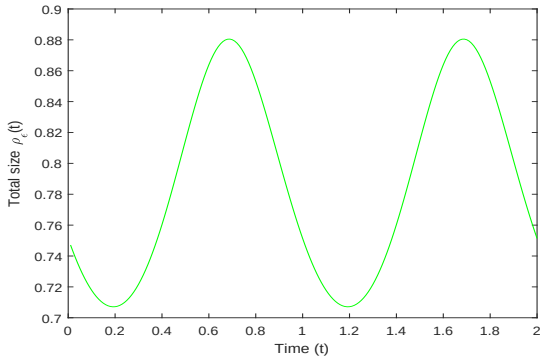

Figure 3.15 – The dynamics of the periodic total population size $\rho_\varepsilon(t)$ along two periods of time of n_ε. Parameters: $\varepsilon = 1$ and $a = a_2$ given in (3.14), with $r = 2,\ b = 2\pi$.

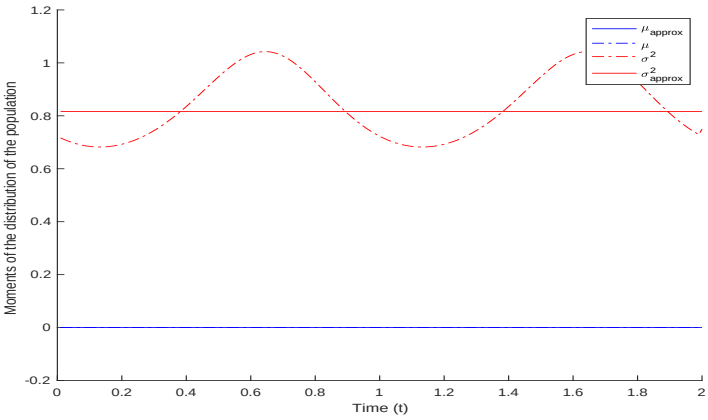

Figure 3.16 – Comparison of the moments of the population's distribution (variances in red and phenotypic means in blue). The numeric approximations of the moments are in dashed lines and the analytic approximations given in (3.21) are in continuous lines. Parameters: $\varepsilon = 1$ and $a = a_2$ given in (3.14), with $r = 2,\ b = 2\pi$.

We follow the structure in the previous subsections, and show in Table 3.7 the error in the approximations by taking the difference between the analytical and the numerical values. Note that the order of the error in these approximations is smaller than $\varepsilon^2 = 1$ as expected.

We next, compare the behavior of two populations evolved either in a constant environment or under periodic oscillations. We show in Table 3.8 the numerical values of the moments and the mean fitness for these two populations. The notations are similar to Table 3.4.

Note that, the conclusion here is analogous to the one for the smaller effect of mutations, that is, the population evolved in a periodic environment has a larger fitness, than the one evolved in a constant temperature. Again the environment select for a population with the same phenotypic mean and a smaller variance. Note indeed that the difference between the mean fitness of the two populations is more important comparing to the case with $\varepsilon = 10^{-2}$ (Table 3.6). Larger effect of mutations is in this case more favorable to the population evolved in a periodic environment. We deduce

Error	Formula	Value
Mean Phenotypical Trait	$\max_{t\in[0,T]}(\lvert\mu_\varepsilon(t)-\mu_{approx}(t)\rvert)$	$8.756*10^{-6}$
Variance	$\max_{t\in[0,T]}(\lvert\sigma^2_\varepsilon(t)-\sigma^2_{approx}(t)\rvert)$	0.169
Fitness	$\lvert\overline{F}_\varepsilon(t)-\overline{F}_{approx}(t)\rvert$	$9.980*10^{-4}$

Table 3.7 – Errors in the approximation of the moments of the population's distribution and mean Fitness. Parameters: $\varepsilon=1$ and $a=a_2$ given in (3.14), with $r=2,\ b=2\pi$.

Values	Periodic environment	Constant environment
Averaged Total Size $[0,T]$	$\bar{\rho}_\varepsilon=0,3937$	$\bar{\rho}_c=0,5857$
Mean Phenotypic Trait	$\max_{t\in[0,T]}\mu_\varepsilon\approx 10^{-7}$	$\mu_c\approx 10^{-17}$
Mean Variance	$\max_{t\in[0,T]}\sigma^2_\varepsilon=1,0424$	$\sigma^2_c=1,4000$
Mean Fitness	$1,5788$	$1,2984$

Table 3.8 – Comparison between the moments of the population's distribution and mean fitness for populations evolved in periodic and constant environments. Parameters: $\varepsilon=1$ and $a=a_2$ given in (3.14), with $r=2,\ b=2\pi$.

in particular that the phenomenon observed in the experiment in [60] can occur in a case where the fluctuations act on the pressure of selection and with large or small effect of the mutations.

3.2.3 Derivation of the explicit solution $\mathcal{N}(t,x)$ and the moments of the distribution

In this section we present the arguments to obtain the expressions in (3.17). Again for simplicity in the forward notations we introduce $f(t)=\left(\frac{\varepsilon}{\sigma^2(t)}\right)^2$ so that the anzats (3.16), reads as in (3.11). After a substitution into (3.15) we obtain an ODE system similar to (3.12). It reads as follows:

$$\begin{cases} f'(t)=4\varepsilon f(t)^{1/2}(g(t)-f(t)), \\ \mu'(t)=2\varepsilon f(t)^{-1/2}(1-\mu(t))g(t), \\ \rho'(t)=[Q_2(t)-\rho(t)]\rho(t), \end{cases} \tag{3.22}$$

where

$$Q_2(t)=r-g(t)(1-\mu(t))^2-\varepsilon g(t)f(t)^{-1/2}.$$

We remark that, on the contrary to the previous example, in this case we cannot resolve analytically the whole above system, the equation for $f(t)$ being a Ricatti type differential equation, with variable coefficients. However we can still obtain some information from the last ODE system.

Solving equation for $f(t)$

By analogous arguments for solving the equation satisfied by f in (3.12) we obtain the following Ricatti equation for

$h(t) = f(t)^{1/2}$:

$$h'(t) = 2\varepsilon(g(t) - h^2(t)).$$

We integrate in $[0, T]$ and use the periodicity of h; it holds

$$\int_0^T f(t)dt = \int_0^T g(t)dt,$$

which implies that the function f has the same mean in one period of time that the given $T-$periodic function $g(t)$. Note that this **does not** imply that $f(t) = g(t)$; indeed this latter equality is satisfied if and only if $g(t) = g$ constant.

Solving equation for $\mu(t)$

From the second equation in (3.22) we obtain

$$\mu(t) = \mu(0) \exp\left(-2\varepsilon \int_0^t \frac{g(s)}{(f(s))^{1/2}} ds\right).$$

The $T-$periodicity of μ leads to the only possible solution $\mu(t) = 0$.

Solving equation for $\rho(t)$

Finally from the explicit formula computed for $\rho(t)$ in the previous example (3.23), we obtain after substituting the value of μ that:

$$\rho(t) = \exp\left(I_2(t)\right) \left[K_3 + \int_0^t \exp\left(I_2(z)\right)\right]^{-1}, \tag{3.23}$$

where I_2 is given in (3.18) and

$$K_3(t) = \frac{\exp\left(\int_0^T I_2(s)ds\right)}{\exp\left(I_2(T)\right) - 1}.$$

The computation of the mean fitness

We consider the mean value $\tau = \frac{1}{2}$ since the function a_1 is $1-$periodic and compute the mean fitness at this point; that is

$$\overline{F}(1/2) = \int_{\mathbb{R}} \left(r - g(1/2)x^2\right) \int_0^1 \frac{\frac{\rho(t)}{\sqrt{2\pi\varepsilon}} f(t)^{1/4} \exp\left[-\frac{f(t)^{1/2}x^2}{2\varepsilon}\right]}{\rho(t)} dtdx,$$

which gives after a simplification and integration

$$\overline{F}(1/2) = r - \varepsilon g(1/2) \int_0^1 f(t)^{-1/2} dt.$$

3.3 Numerical examples with several maxima for $\bar{a}$

In the analytic study in Chapter 1, we have assumed that there exists a single maximum point for the averaged growth rate $\bar{a}(x) = \frac{1}{T}\int_0^T a(t, x)dt$. However, in order to go further, in this subsection we consider the averaged growth rate, having two maximum points, and study numerically the behavior of the solution.

Our first example consists in an averaged growth rate having two "symmetric" maxima, i.e. the second derivatives at these points are the same. Next we go further and consider another function with "non symmetric" maxima.

We follow the structure of the previous subsections and study the numerical solutions for both values of $\varepsilon = 10^{-2}$ and $\varepsilon = 1$.

3.3.1 Symmetric maxima

We consider here the following growth rate

$$a_S(t,x) = \begin{cases} 1-(x-x_1)^2(x-x_2)^2(1-x), & \text{if} \quad t \in [0,1/2], \\ 1-(x-x_1)^2(x-x_2)^2 x, & \text{if} \quad t \in (1/2,1], \end{cases} \tag{3.24}$$

where x_1 and x_2 are real numbers. Note that the second derivatives of $\bar{a}(x)$ at maximum points are equals, indeed:

$$\bar{a}_S''(x) = -2(x-x_1)^2 - 2(x-x_2)^2) - 8(x-x_1)(x-x_2),$$

which implies that $\bar{a}_S''(x_1) = \bar{a}_S''(x_2) = -2(x_1-x_2)$.
For the numerical computations we vary the values of x_1 and x_2.

Small effect of mutations
In Figure 3.17 we show different behaviors of the population density depending on the position of the maximum points of $\overline{a}$ considering a small effect of mutation $\varepsilon = 10^{-2}$.
We split the graphics into three groups depending on the distance between x_1 and x_2. Along the three sub-figures (Figure 3.17 (a)-(b)-(c)) we show at the left and center column the density of the population $n_\varepsilon(t,x)$ respectively as function of trait and time along two periods of time and at three fixed time within one period. Then the right column illustrates the oscillations of the total population size. In sub-figure 3.17a we consider that x_1, x_2 take the closer values, next in 3.17b we consider them fairly close and finally in 3.17c they are illustrated for the relatively far values. Along this figures we can observe a transition from a unimodal trait distribution into a bimodal one.
The dominant trait in the first case (Figure 3.17a) is around $x \approx 0.5 = (x_1+x_2)/2$. For the next maximum points considered ($x_1 = 0.2$ and $x_2 = 0.8$ in Figure 3.17b) the population oscillates between two dominant traits: $x \approx 0.35$ and $x \approx 0.65$. Finally in the dimorphic picture (Figure 3.17c) the population distribution has two peaks at $x \approx 0.15$ and at $x \approx 0.85$.
Moreover, in the three cases the total population size oscillates periodically in time. Note that as we are considering a non regular growth rate we obtain a population size function which is also non regular.

Large effect of mutations
In order to study the situation with a large effect of mutations, we first compute the maximum value of ε, such that the population does not get extinct. We show in Figure 3.18 the plot $\varepsilon \mapsto \overline{\rho}_\varepsilon$.

We note in Figure 3.18 that for $\varepsilon < 1.7$ the population does not get extinct. However we observe, contrarily to the previous examples that the dependence of the mean total size on ε is not monotonous and the maximal population size is given for the intermediate values of ε. Here, we consider $\varepsilon = 1$, and maximum points $x_1 = 0.1$ and $x_2 = 0.9$. Note that for this value of ε the plots have more or less the same behavior and do not depend significantly on the values of x_1, x_2. We show in Figure 3.19 the phenotypic density as a function of time and trait over two periods of time (3.19a) and at three fixed times within one period (3.19b); and the total population size is illustrated in (3.19c).
We illustrate the periodic oscillations of the dominant trait around the maximum points of a_S. Note that, the dominant traits are not exactly located at $x_1,\ x_2$; in fact we observe as the effect of mutations increases, that the dominant traits (oscillating between $x \approx -0.26$ and $x \approx 0.75$)) are further from these optimal traits.

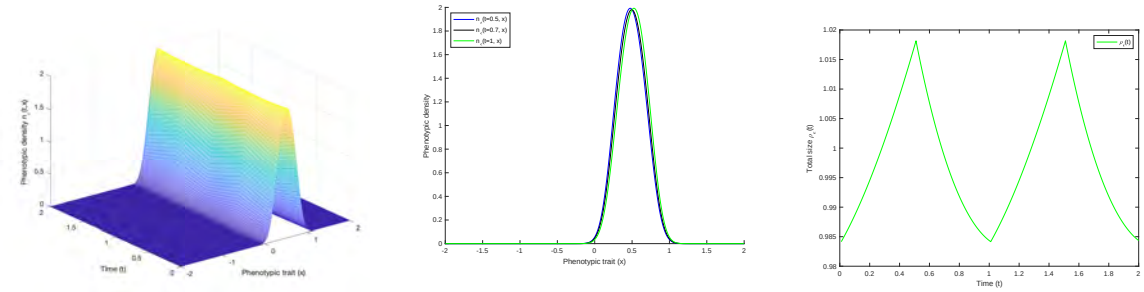

(a) $x_1 = 0.4$ and $x_2 = 0.6$

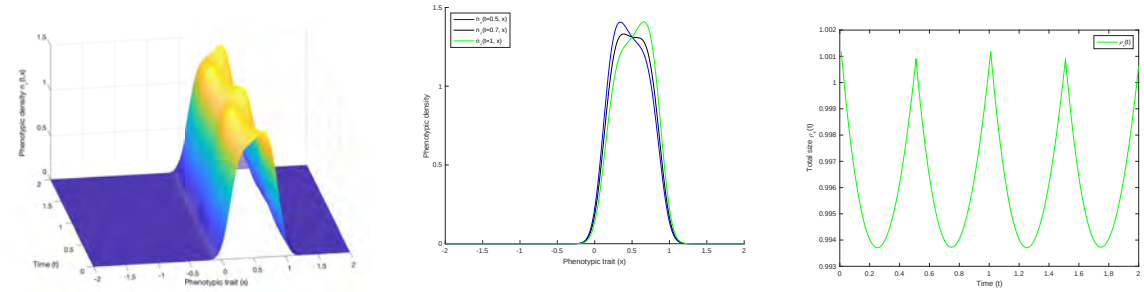

(b) $x_1 = 0.2$ and $x_2 = 0.8$

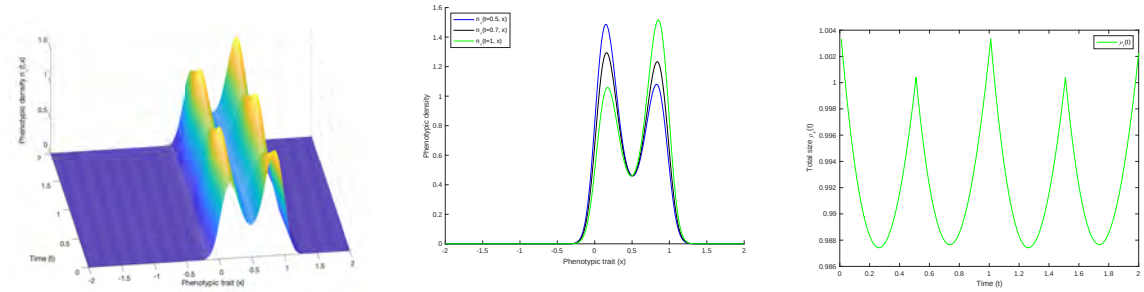

(c) $x_1 = 0.1$ and $x_2 = 0.9$

Figure 3.17 – The phenotypic density $n_\varepsilon(t,x)$ and the total size $\rho_\varepsilon(t)$ of the population for different values of the maximum points of $\bar{a}_S$ with $\varepsilon = 10^{-2}$. From left to right the density function $n_\varepsilon(t,x)$ is plotted in the first column as a function of time and trait over two periods of time and in the second column at three fixed times within one period; in the last column the function $\rho_\varepsilon(t)$ is illustrated along two periods of time. The population evolves periodically in time and it is concentrated around the mean of the maximum points if they are near enough but when they become distant the phenotypic density concentrates periodically on two dominant traits. Moreover the total population size oscillates periodically with a different non-regular behaviour in each case.

3.3.2 Non Symmetric maxima

Finally, in this example we consider a growth rate with two maximum points which are non symmetric in the sense that the behaviors around the maxima are not analogous, that is, the second derivatives are not the same. We consider the following function

$$a_{NS}(t,x) = \begin{cases} 1-(x-1)^4(x+1)^2(1-x), & \text{if} \quad t \in [0,1/2], \\ 1-(x-1)^4(x+1)^2 x, & \text{if} \quad t \in (1/2,1]. \end{cases} \tag{3.25}$$

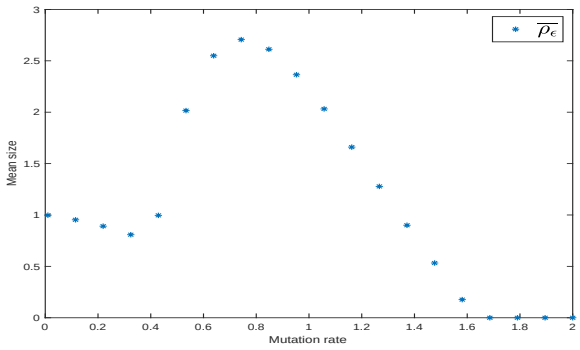

Figure 3.18 – Mean Total size of the population for different values of mutations rate $\varepsilon \in [10^{-2}, 2]$. Parameters: $a = a_S$ in (3.24) with $x_1 = 0.1$ and $x_2 = 0.9$.

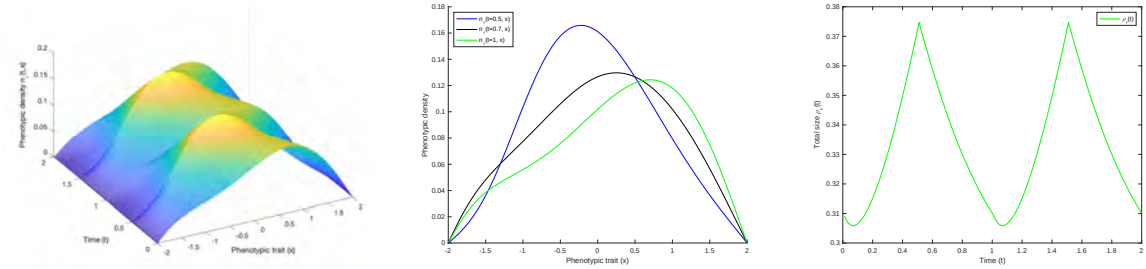

(a) $n_\varepsilon(t, x)$ (b) $n_\varepsilon(T, x)$, T fixed (c) $\rho_\varepsilon(t)$

Figure 3.19 – The phenotypic density of population $n_\varepsilon(t, x)$ and the total population size $\rho_\varepsilon(t)$. In (a) the phenotypic density $n_\varepsilon(t, x)$ is plotted as a function of time and trait over two periods of time and in (b) at three fixed times within one period. The function $\rho_\varepsilon(t)$ is illustrated in (c) along two periods of time. The population density evolves periodically in time with an oscillating dominant trait. Moreover the total population size oscillates periodically. Parameters: $\varepsilon = 1$, $a = a_S$ given in (3.24) with $x_1 = 0.1$ and $x_2 = 0.9$.

In this example we have chosen a_{NS} such that:

$$\bar{a}''_{NS} = 12(x-1)^2(x+1)^2 + 8(x-1)^3(x+1) + 8(x-1)^3(x+1)^2 + 2(x-1)^4,$$

which implies that the second derivatives of $\bar{a}_{NS}$ at maximum points $(x_1 = 1, x_2 = -1)$ are different, in fact

$$\bar{a}''_{NS}(1) = 0 \neq 32 = \bar{a}''_{NS}(-1).$$

For the numerical simulations, we make also both analysis for $\varepsilon = 10^{-2}$ and $\varepsilon = 1$.

Small effect of mutations

For the growth rate a_{NS} we illustrate in Figure 3.20 that the maximum point $x_0 = 1$ is selected as point of concentration of the population; in fact the numerical value of the dominant trait is always $x \approx 0.9\overline{9}$. The total size of population is still periodically oscillating, with a non-regular behaviour since the function a_{NS} is also non regular. Note that in this case we do not take several values of maximum points since the behavior remains the same.

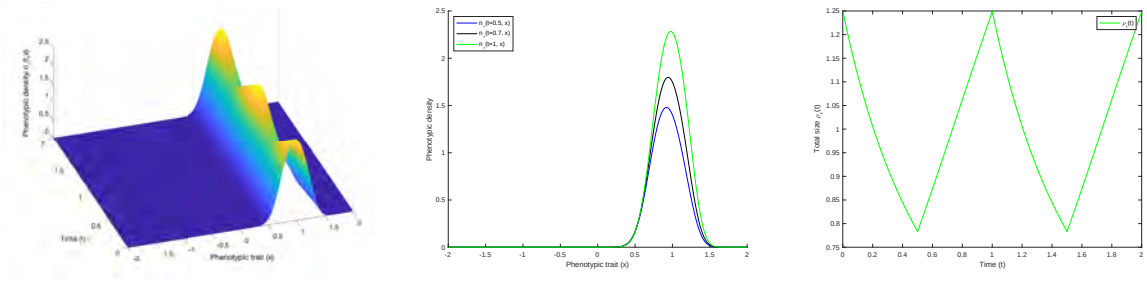

(a) $n_\varepsilon(t,x)$ (b) $n_\varepsilon(T,x)$ (c) $\rho_\varepsilon(t)$

Figure 3.20 – The phenotypic density of population $n_\varepsilon(t,x)$ and the total population size $\rho_\varepsilon(t)$. In (a) the density function $n_\varepsilon(t,x)$ is plotted as a function of time and trait over two periods of time and in (b) at three fixed times within one period. The function $\rho_\varepsilon(t)$ is illustrated in (c) along two periods of time. The population evolves periodically in time and it is distributed around the flatter maximum. Moreover the total population size oscillates periodically. Parameters: $\varepsilon = 10^{-2}$, $a = a_{NS}$ in (3.25).

It is worth noticing that in this example the population concentrates around the flatter maximum point of $\overline{a}$. This phenomenon is related to the fact that the ground state of a Schrödinger operator concentrates on the flattest global minimum point of the potential [50, 51]. Note also that in [5] a related model of replicator-mutator type in the case of a constant environment has been studied where the authors investigate the uni-modal or multi-modal nature of the phenotypic distribution of the population as a function of both the growth rate and the mutation rate.

Large effect of mutations

We compute one more time the critical ε which leads the population to extinction (see Figure 3.21) and according to this graph we consider again $\varepsilon = 1$ which allows to keep a reasonable population size.

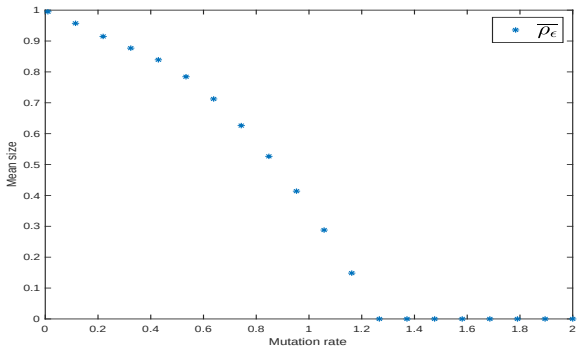

Figure 3.21 – Mean Total size of the population for different values of mutations rate $\varepsilon \in [10^{-2}, 2]$. Parameters: $a = a_{NS}$ in (3.25).

We plot in Figure 3.22 the numerical solution of (3.1) with growth rate $a = a_{NS}$ for $\varepsilon = 1$. We illustrate, as before, the phenotypic density $n_\varepsilon(t,x)$ (Figures 3.22a and 3.22b) and the total population size $\rho_\varepsilon(t)$ (Figure 3.22c). The first thing to note is that we do not have anymore a real concentration around a unique maximum point but a periodically oscillation between several traits. Furthermore we observe, analogously to the symmetric case for this large value of ε,

that the dominant traits are not exactly located at $x_1 = -1,\ x_2 = 1$; as the effect of mutations increases, the dominant traits are further from these optimal traits. We obtain, in particular, that the dominant traits oscillate in the interval $[-0.5, 0.7]$. Finally, the total population size is periodically oscillating with non-regular behavior, analogously to the previous case for $a = a_S$.

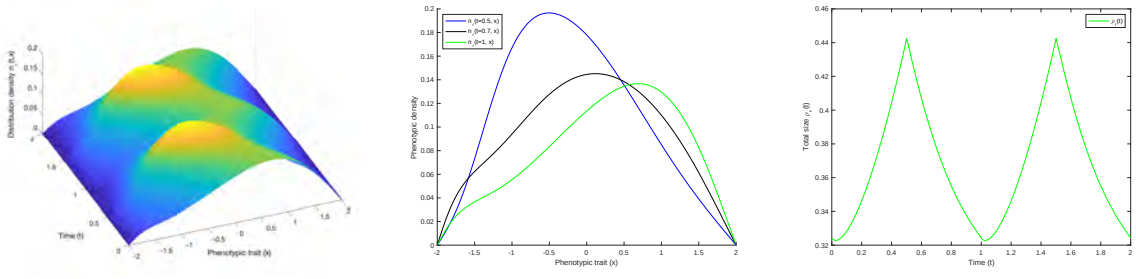

(a) $n_\varepsilon(t,x)$ (b) $n_\varepsilon(T,x)$ (c) $\rho_\varepsilon(t)$

Figure 3.22 – The phenotypic density of population $n_\varepsilon(t,x)$ and the total population size $\rho_\varepsilon(t)$. In (a) the density function $n_\varepsilon(t,x)$ is plotted as a function of time and trait over two periods of time and in (b) at three fixed times within one period. The function $\rho_\varepsilon(t)$ is illustrated in (c) along two periods of time. The population evolves periodically in time while the total population size oscillates periodically. Parameters: $\varepsilon = 1$, $a = a_{NS}$ in (3.25).

Appendix: Numerical scheme

In this section we present the numerical scheme used to resolve the periodic problem (3.1). To this end we first resolve the following Cauchy problem

$$\begin{cases} \partial_t n(t,x) - \varepsilon^2 \partial_{xx} n(t,x) = n(t,x)[a(t,x) - \rho(t)], \quad (t,x) \in [0,+\infty) \times \mathbb{R}, \\ \rho(t) = \displaystyle\int_{\mathbb{R}} n(t,x)dx, \\ n(t=0,x) = n_0(x), \end{cases} \tag{3.26}$$

where we consider the initial condition given in (3.10).

We use the results of Chapter 1 which provides the convergence of the solution of (3.26) to the unique periodic solution of (3.1). Then we study the numerical solution of (3.26) in long time when it becomes periodic.

We describe below the numerical scheme used to resolve (3.26). We discretize $n(t,x)$ around the mesh $x = \{x_i\}$ and $t = \{t_k\}$, where:

- we assume a bounded numerical space domain, denoted by $\Omega = (-L, L)$. The number of nodes is denoted N_x, so that we have the space step $\Delta x = \frac{2L}{N_x - 1}$. We write $\{x_i\}_{1 \le i \le N_x}$ for the nodes coordinates,
- the time step is denoted Δt and defined by $\Delta t = \frac{T_{final}}{N_t}$ where T_{final} is the final time and N_t is the number of iterations N_t. We write $\{t_k\}_{1 \le k \le N_t}$ for the time discretization,
- the discretized solution of the problem (3.26) writes now $\{(n_i^k, \rho^k)\}_{1 \le k \le N_t,\, 1 \le i \le N_x}$, with $n_i^k = n(t_k, x_i)$ and $\rho^k = \rho(t_k)$.

The initial density ρ^0 is a given value ($\rho^0 = 1$) and we initialize the solution in $t = 0$ as follows

$$n^0 = \frac{\rho_0 n_0(x_i)}{\Delta x \sum_{i=1}^{N_x} n_0(x_i)}, \tag{3.27}$$

for $n_0(x_i)$ defined in (3.10).

We use a classical Euler scheme, which reads for the main equation (for nodes away from the boundary, i.e. $k \geq 1$ and $1 \leq i \leq N_x - 1$)

$$\begin{cases} \dfrac{n_i^{k+1} - n_i^k}{\Delta t} - \dfrac{\varepsilon^2 \left(n_{i+1}^{k+1} - 2n_i^{k+1} + n_{i-1}^{k+1} \right)}{\Delta x^2} = n_i^{k+1} a_-(t_{k+1}, x_i) + n_i^k \left(a_+(t_k, x_i) - \rho^k \right), \\ \\ \rho^k = \displaystyle\sum_{i=1}^{N_x} n_i^k \Delta x, \end{cases} \tag{3.28}$$

where

$$a_- = \min\{a, 0\} \quad \text{and} \quad a_- = \max\{a, 0\}.$$

Since we expect the solution to concentrate as a Dirac mass, following the analytic results, we consider the Dirichlet boundary conditions; that is:

$$n(t, -L) = n(t, L) = 0 \quad \forall t \in \mathbb{R}^+.$$

This is an implicit scheme for n where the only explicit terms are coming from the positive part of a and the population density ρ.

Chapter 4

Approche numérique pour décrire le Transfert Horizontal de Gènes : comparaison entre le modèles stochastique et déterministe

***

Le début de la santé est de connaître la maladie –
proverbe espagnol

Résumé

Nous faisons ici une étude numérique comparative entre les équations stochastiques et déterministes modelisant le transfert horizontal de gènes (HT). Le HT est défini comme la transmission de matériel génétique entre deux organismes vivants, contrairement à la transmission verticale qui désigne le transfert d'ADN d'un parent à sa progéniture. Ce phénomène joue un rôle important dans l'évolution de certaines bactéries, notamment pour le développement d'une résistance aux antibiotiques. Nous considérons ici un processus stochastique à saut individu-centré, et l'équation intégro-differentielle non linéaire obtenue comme limite pour une population de grande taille. En supposant que les mutations sont petites, après un changement de variable et un passage à la limite, nous obtenons une équation d'Hamilton-Jacobi. La comparaison de ces différents modèles à l'aide de simulations numériques permet de prouver que l'équation d'Hamilton-Jacobi parvient à mieux capturer les phénomènes qualitatifs du modèle stochastique par rapport au modèle en EDP, notamment le sauvetage évolutif. Le travail dans ce chapitre à été realisé en colaboration avec Anna Melnykova, Samuel Nordmann, Hélène Hivert, Vincent Calvez et Sylvie Méléard dans le cadre de CEMRACS'18, et a été soumis pour future publication au journal ESAIM: Proceedings and Surveys, 2018.

4.1 Introduction

4.1.1 Motivations and state of the art

The mathematical description of the transmission of pathogens, or antibiotic resistance of bacteria is an open question in biology and medicine. This is directly linked to the ability of the bacteria population to mutate and exchange genetic material either vertically (from parents to offspring), or horizontally (from the interaction between non-parental individuals). This resistance occurs when one bacterial cell becomes resistant to an antibiotic due to mutation, and then transfers resistance genes to other species of bacteria. This latter phenomenon is known as Horizontal Transfer (HT). Some artificial applications of the HT include forms of genetic engineering which are particularly useful in some experimental procedure that may help treat or prevent genetic disorders and some types of cancer. The primary goal of this work is to describe the mechanism of the transfer itself and the different models which characterize it, stochastic and deterministic. We then provide a numerical comparison between those models in order to know which one is better to catch the biological phenomenon.

Several mathematical models for describing the impact of HT on ecological dynamics were proposed in literature with two different types of models. A first class of models is referred to the 1970's and is attributed to Anderson and May on host-pathogen population dynamics [7] where the authors investigate whether and how a pathogen might drive its host to extinction. The models constructed using the May-Anderson's framework (e.g.[77, 71]) are deterministic and make highly simplified ecological assumptions, in particular the competition between hosts is often completely ignored. A second class of models was developed within the framework of population genetics [11] to address the question of the effect of HT on the emergence of beneficial mutations ([86]). However, these models also make strong simplifying assumptions, again on the competition between individuals but also by keeping the size of the population constant.

More recently in [20, 19] the authors develop a mathematically rigorous stochastic model of population dynamics by relaxing most of the previous limitations, and consider both vertical transmission and HT of traits. This model describes the dynamics of reproduction, competition, and exchange of genetic material between individuals in a population. The phenotype of each individual is described by a numerical parameter, called trait. Numerical experiments show that the effect of a unilateral horizontal gene transfer may lead to a cyclic behavior of the population. That is, while HT drives individuals towards a non-fit phenotype and, consequently, to extinction, very few not affected by transfer fit individuals may eventually repopulate the environment, before being driven again to deleterious phenotypes. This phenomenon is called an *evolutionary rescue of a small population*.

However, within a framework of stochastic jump processes, it is hard to define and study the observed cycling phenomena accurately. The second drawback of the stochastic system is that it is costly to compute, especially for a large time scale and population size. Thus, in the case of a large population, it is more practical to work with a deterministic PDE model, obtained as the limit of a stochastic system [19, 40]. In certain settings, the population dynamics involve concentration phenomena (i.e., the convergence of the population density to singular solutions, such as Dirac masses, see for instance [88, 76]). In that case, the PDE formulation is not suitable. Thus, applying a limiting procedure for small mutations and time rescaling to the PDE model, one can pass to a Hamilton-Jacobi type equation (see also [10, 82, 41] where a rigorous analysis on this limit procedure is done).

4.1.2 The goal and the plan of the chapter

The primary goal of our work is thus to conduct a numerical analysis of the population dynamics on a macroscopic individual-based model and to compare it with the deterministic system which is obtained as a limit for a large population. We are especially interested in determining to which extent the limiting Hamilton-Jacobi equation can grasp qualitative

properties of the stochastic model. This framework has already been successfully used to understand the concentration phenomena, and the location of the dominant trait. We aim to understand if the Hamilton-Jacobi approach is also well suited to describe the evolutionary rescue phenomena which crucially rely on an accurate description of the small populations.

On this step, the choice of an approximation scheme for simulating solutions of the PDE model is of tremendous importance. As we further explain in Section 4.4, classical explicit schemes do not preserve the asymptotic behavior of the solution if the time rescaling step goes to 0. From a numerical point of view, it involves operations with exponentially big values, which lead to non-negligible errors for explicit numerical schemes. We address this question by proposing an asymptotic preserving scheme for a Hamilton-Jacobi equation, adapting an approach proposed in [32]. More generally, the numerical approximation problem for solutions of Hamilton-Jacobi equations is treated in [1].

This chapter is structured as follows: in Section 4.2 we introduce the models both in a stochastic and deterministic setting, and formally derive the limiting Hamilton-Jacobi equation. Then, we simulate a jump process, describing the bacteria population, and study its properties for different values of parameters. Numerical experiments are gathered in Section 4.4. We aim to numerically determine the critical HT rate, which leads to an almost sure extinction of the whole population. On the next step, we conduct the same analysis for a Hamilton-Jacobi equation with the help of an asymptotic preserving scheme and compare it with the stochastic model on an appropriate timescale, and explain why the classical scheme fails to work. We end our study with conclusions and discussion of yet unsolved numerical and theoretical questions.

4.2 Presentation of the models

We split this section into three subsection where we first introduce the stochastic model describing the bacteria population, and then the PDE model for a limit of large population. Finally in the last subsection we formally derive the limiting Hamilton-Jacobi equation.

4.2.1 Stochastic model

We consider a stochastic model describing the evolution of a population structured by phenotype, which is described at each time t by the point measure

$$\nu_t^K(dx) = \frac{1}{K}\sum_{i=0}^{N_t^K} \delta_{X_i(t)}(dx), \tag{4.1}$$

where parameter K is a scaling parameter, referred to as the *carrying capacity*. It stands for the maximal number of individuals that the underlying environment is able to host (K can represent, for example, the amount of available resources). $N_t^K = K\int \nu_t^K(dx)$ is the size of the population at time t, and $X_i(t) \in \mathbb{R}^n$ is the trait of i-th individual living at time t, which summarizes all the informations on phenotype.

The demography of the population is regulated, first of all, by birth and death. An individual with trait x gives birth to a new individual with rate $b(x)$. The trait y of the offspring is chosen from a probability distribution $m(x-y)dy$, referred to as the mutation kernel. An individual with trait x dies according to an intrinsic death rate $d(x)$ plus an additional death rate $C\dfrac{N_t^K}{K}$ (independent of x) which stands for the competition between individuals.

Finally, an individual with trait x can induce a *unilateral* Horizontal Transfer to an individual with trait y at rate $h_K(x,y,\nu)$, such that the pair (x,y) becomes (x,x). This kind of transfer is sometimes referred to as *conjugation* in the

biological literature. For simplicity, we assume $h_K(x,y,\nu)$ to be in the particular form

$$h_K(x,y,\nu) = h_K(x-y,N) = \tau_0 \frac{\alpha(x-y)}{N/K}, \tag{4.2}$$

where $N = K\int_{\mathbb{R}^n}\nu(dx)$ is the number of individuals, $\tau_0 > 0$ is a constant and α is either a Heaviside, or a smooth bounded function, such that for a small $\delta > 0$:

$$\alpha(z) = \begin{cases} 0 & \text{if } z < -\delta \\ 1 & \text{if } z > +\delta \end{cases}, \quad \alpha'(0) = \frac{1}{2\delta}, \tag{4.3}$$

where δ is the stiffness parameter. We introduce δ to have the advantage of working with smooth function (which will be useful in the following parts), while mimicking the binary nature of the Heaviside function.

For a population $\nu = \frac{1}{K}\sum_{i=1}^N \delta_{x_i}$ and a generic measurable bounded function F, the generator of the process is then given by:

$$\begin{aligned} L^K F(\nu) = \sum_{i=1}^N b(x_i)\int_{\mathbb{R}^n}\left(F\left(\nu + \frac{1}{K}\delta_y\right) - F(\nu)\right) m(x_i,dy) \\ + \sum_{i=1}^N \left(d(x_i) + C\frac{N}{K}\right)\left(F\left(\nu - \frac{1}{K}\delta_{x_i}\right) - F(\nu)\right) \\ + \sum_{i,j=1}^N h_K(x_i,x_j,\nu)\left(F\left(\nu + \frac{1}{K}\delta_{x_i} - \frac{1}{K}\delta_{x_j}\right) - F(\nu)\right). \end{aligned}$$

It is standard to construct the measure-valued process ν^K as the solution of a stochastic differential equation driven by Poisson point measures and to derive moment and martingale properties (see for instance [43]).

4.2.2 The PDE model

It is proven (see, in particular [18, 25]) that for $K \to +\infty$ the stochastic process defined by a sequence of point measures given by (4.1) converges in probability to a non-linear integro-differential equation, whose solution exists and is unique. This equation is given by:

$$\begin{cases} \partial_t f(t,x) = -(d(x) + C\rho_1(t))f(t,x) + \displaystyle\int_{\mathbb{R}^n} m(x-y)b(y)f(t,y)dy + f(t,x)\int_{\mathbb{R}^n}\tau(x-y)\frac{f(t,y)}{\rho_1(t)}dy, \text{ in } \mathbb{R}_+\times\mathbb{R}^n, \\ \rho_1(t) = \displaystyle\int_{\mathbb{R}^n} f(t,x)dx, \\ f(0,x) = f^0(x) > 0, \end{cases}$$

where $f(t,x)$ is the macroscopic density of the population with trait x at time t and, accordingly to the previous section, $b(x)$, $d(x)$ and C are the birth, death and competition rate respectively, m is the mutation kernel, and

$$\tau(y-x) := \tau_0\left[\alpha(x-y) - \alpha(y-x)\right] \tag{4.4}$$

is the horizontal transfer flux, with τ_0 and α defined as in (4.2)-(4.3).

Now our goal is to pass from micro- to a macroscopic scale with the help of a rescaling. On the one hand, we consider

the case of small mutations: for a small parameter $\varepsilon > 0$ we define

$$m_\varepsilon(x-y) = \frac{1}{\varepsilon^n} m\left(\frac{x-y}{\varepsilon}\right).$$

With a change of variable $z = \frac{x-y}{\varepsilon}$ we can rewrite the mutation term at (t,x) as

$$\int_{\mathbb{R}^n} m_\varepsilon(x-y)b(y)f(t,y)dy = \int_{\mathbb{R}^n} m(z)b(x+\varepsilon z)f(t,x+\varepsilon z)dz.$$

On the other hand, when ε is small, the effect of mutations can only be observed in a larger time scale. Thus, we rescale time with $t \mapsto \frac{t}{\varepsilon}$.

We end up with the following system, for $\varepsilon > 0$, and $(t,x) \in \mathbb{R}_+ \times \mathbb{R}^n$:

$$\begin{cases} \varepsilon \partial_t f_\varepsilon(t,x) = -(d(x) + C\rho_\varepsilon(t))f_\varepsilon(t,x) + \displaystyle\int_{\mathbb{R}^n} m(z)b(x+\varepsilon z)f_\varepsilon(t,x+\varepsilon z)dz + f_\varepsilon(t,x)\int_{\mathbb{R}^n} \tau(x-y)\frac{f_\varepsilon(t,y)}{\rho_\varepsilon(t)}dy, \\ \rho_\varepsilon(t) = \displaystyle\int_{\mathbb{R}^n} f_\varepsilon(t,x)dx, \\ f_\varepsilon(0,x) = f_\varepsilon^0(x) > 0. \end{cases} \tag{4.5}$$

4.2.3 The Hamilton-Jacobi limit

We now derive the limiting problem (4.5) when $\varepsilon \to 0$. As we will see, the limiting problem allows us to give a rigorous mathematical framework and to perform useful formal calculations.

Equations in the form of (4.5) often give rise to concentration phenomena, i.e the convergence of f_ε towards a Dirac mass when $\varepsilon \to 0$ (see [88, 34]). The usual way to deal with these asymptotics is to perform a Hopf-Cole transformation (or WKB ansatz), i.e to consider

$$u_\varepsilon(t,x) := \varepsilon \ln(f_\varepsilon(t,x)). \tag{4.6}$$

This change of variable comes from the fact that with such rescaling the solution f_ε will naturally have this form. Accordingly, we expect u_ε to have a non singular limit when $\varepsilon \to 0$. Incidentally, this substitution also gives insights on the convenient scheme to use for numerical simulations, as we will see in the following section.

Now, let us explain how to identify and derive some properties about the asymptotics of u_ε when $\varepsilon \to 0$, which will be used for discussions in the sequel. The following computations are only formal, since rigorous proofs are often intricate in this context and it is not our goal in this chapter. Substituting (4.6) into (4.5) we deduce that u_ε satisfies:

$$\partial_t u_\varepsilon = -(d(x) + C\rho_\varepsilon(t)) + \int_{\mathbb{R}^n} m(z)b(x+\varepsilon z)\exp\left\{\frac{u_\varepsilon(t,x+\varepsilon z) - u_\varepsilon(t,x)}{\varepsilon}\right\}dz + \int_{\mathbb{R}^n} \tau(x-y)\frac{f_\varepsilon(t,y)}{\rho_\varepsilon(t)}dy. \tag{4.7}$$

Formally, at the limit $\varepsilon \to 0$, u_ε converges to a continuous function u which satisfies the following Hamilton-Jacobi equation in the *"viscosity"* sense:

$$\partial_t u = -(d(x) + C\rho(t)) + b(x)\int_{\mathbb{R}^n} m(z)e^{z\cdot\nabla_x u}dz + \tau(x-\overline{x}(t)), \tag{4.8}$$

where $\rho(t) \geq 0$ is the weak limit of $\rho_\varepsilon(t)$ and

$$\bar{x}(t) = \text{argmax } u(t,\cdot). \tag{4.9}$$

We formally assume here and in the following that the definition of $\bar{x}(t)$ is unambiguous, i.e that u reaches its maximum

on a single point. Note that the limiting function u is not expected to be C^1 for all time. We thus need to deal with a generalized notion of solutions, namely *viscosity solution* (see [8]).

4.3 Formal analysis on the Hamilton-Jacobi equation

Hamilton-Jacobi equations are particularly known in mathematical biology to be a good model to describe how a population concentrates around the dominant trait(s) when the mutations are small. However, here we are interested to use this model to describe a phenomenon of *evolutionary rescue*. Here, we make some formal analysis on the equation. We point out that the calculations are only formal, since rigorous proofs are intricate and beyond the scope of this paper.

4.3.1 Generality

From an integration of (4.5) with respect to x and classical computations (under the assumptions of bounded functions for the birth, death and transfer rates), we deduce that our model satisfies a *saturation property*, i.e. $\rho_\varepsilon(t)$ is bounded from above, uniformly in $t \geq 0$ and $\varepsilon > 0$.

From this, and $\rho_\varepsilon(t) = \int_{\mathbb{R}^n} e^{\frac{u_\varepsilon(t,x)}{\varepsilon}} dx$, we deduce that for all $t > 0$, $\sup_{x\in\mathbb{R}^n} u(t,x) \leq 0$ and the following constraint holds:

$$\sup_{x\in\mathbb{R}^n} u(t,x) = 0 \quad \text{when} \quad \rho(t) > 0. \tag{4.10}$$

Note that our model allows the population to get extinct, thus we cannot expect ρ to be positive at all times. As a byproduct, we derive the *concentration property*, i.e the formal weak convergence of measures

$$f_\varepsilon(t,x) \rightharpoonup \rho(t)\delta_{\bar{x}(t)}(dx), \quad \text{when } \varepsilon \to 0,$$

where $\delta_{\bar{x}(t)}$ denotes, as usually, the Dirac measure centered in $\bar{x}(t)$. From (4.10), it is possible to formally derive a formula for ρ. Indeed, either $\rho(t) = 0$ or $\rho(t) > 0$ and

$$\partial_t u(t, \bar{x}(t)) = 0,$$

which implies

$$\rho(t) = \frac{b(\bar{x}(t)) - d(\bar{x}(t)) + \tau(0)}{C} = \frac{b(\bar{x}(t)) - d(\bar{x}(t))}{C}, \tag{4.11}$$

for τ defined in (4.4).

Having above definitions in hand, we can now perform a formal analysis on the dynamics of $\bar{x}(t)$, defined below in (4.15). Our aim is to show how the behaviour of the system can be analyzed within the framework of a Hamilton-Jacobi equation (4.8). To fix ideas, we fix all constants but τ_0 and we assume (4.12)-(4.14) as follows:

$$b(x) = b_r > 0, \tag{4.12}$$

$$d(x) = d_r x^2, \quad d_r > 0, \tag{4.13}$$

$$m(z) = \frac{1}{\sqrt{2\pi}\sigma} e^{-\frac{z^2}{2\sigma^2}}, \tag{4.14}$$

and the transfer function $h_K(x, y, \nu)$ is defined in (4.2). Moreover we work under the following assumptions:

$$\begin{aligned} &u(t,\cdot) \text{ reaches its maximum on a single point } \bar{x}(t), \\ &\bar{x}(t) \text{ is a non-degenerate maximum, i.e } \nabla_x^2 u(t,x) < 0, \\ &\bar{x}(t) \text{ is smooth with respect to } t. \end{aligned} \tag{4.15}$$

Finally we assume that the initial condition f^0 is a given function of x which reads

$$f_\varepsilon^0(x) = \frac{1}{\sqrt{\varepsilon}} e^{-\frac{x^2}{2\varepsilon}}. \tag{4.16}$$

4.3.2 Smooth dynamics $\bar{x}(t)$

The following statement deals with the smooth dynamics of $\bar{x}(t)$, i.e in the regime where no jump occurs in the dynamics of $\bar{x}(t)$.

Statement 4.1 *Under assumptions* (4.12)-(4.15)*, the function $t \mapsto \bar{x}(t)$ is an increasing function which satisfies the following inequality for every $t \geq 0$,*

$$0 \leq \bar{x}(t) \leq \frac{\tau_0}{2d\delta}.$$

More precisely, $\bar{x}(t)$ satisfies the canonical equation

$$\frac{\mathrm{d}}{\mathrm{d}t}\bar{x}(t) = \left[-\nabla_x^2 u(t, \bar{x}(t))\right]^{-1} \cdot \left(\nabla_x r(\bar{x}(t)) + \nabla_x \tau(0)\right), \tag{4.17}$$

where

$$r(x) := b(x) - d(x), \tag{4.18}$$

and $\nabla_x^2 u$ denotes the Hessian of u with respect to the x variable.

Proof.
Under the above assumptions we can derive the dynamics of $\bar{x}(t)$, referred to as the *canonical equation* in the literature (see for instance [82]). Indeed, starting from

$$\nabla_x u(t, \bar{x}(t)) = 0,$$

a differentiation with respect to t gives (4.17).

Equation (4.17) has a unique singular point $x_\star$, which satisfies $r'(x_\star) + \tau'(0) = 0$, with τ defined in (4.2) and r in (4.18). We find

$$x_\star = \frac{\tau_0}{2d_r\delta}. \tag{4.19}$$

Note that $t \mapsto \bar{x}(t)$ is increasing when $\bar{x}(t) < x_\star$ and decreasing when $\bar{x}(t) > x_\star$. Besides, from the initial condition (4.16), we have $\bar{x}(0) = 0$, and consequently $0 \leq \bar{x}(t) \leq x_\star \quad$ for all t.

■

4.3.3 Evolutionary rescue

In general, the canonical equation (4.17) does not hold in every point of time. Indeed, a new maximum of u can arise in finite time, which would cause a "jump" in the dynamics of $\bar{x}(t)$: this is what we call an *evolutionary rescue*. Formally, this is what happens (periodically in time) in the case of cycles, see Figure 4.4b. We thus expect $\bar{x}(t)$ to possibly jump periodically, and to follow (4.17) between two jumps. We now try to characterize the possible jumps. For $T > 0$, we denote

$$\bar{x}(T^-) := \lim_{\substack{t \to T \\ t < T}} \bar{x}(t), \quad \bar{x}(T^+) := \lim_{\substack{t \to T \\ t > T}} \bar{x}(t).$$

Statement 4.2 *We assume that* (4.12)-(4.15) *hold until a time $T > 0$, such that $u(T, \cdot)$ reaches its maximum on $\bar{x}(T^-)$ and on another point $\tilde{x}$. Then $\tilde{x} = 0$ and $\bar{x}(t)$ will jump towards 0 at time T, i.e $\bar{x}(T^+) = 0$.*

Proof.
From assumption (4.15), we have for all $t \in [0,T]$ that $u(t,\cdot)$ is concave non-degenerate on $[\bar{x}(t) \pm \theta]$, with $\theta > 0$. For simplicity, we further assume $\delta \leq \theta$, where δ is defined in (4.3).

First, let us show that $\tilde{x} = 0$. We define the fitness function of trait x in a population concentrated in $\bar{x}$:

$$F_{\bar{x}}(x) := r(x) + \tau(x - \bar{x}), \tag{4.20}$$

where r and τ are respectively defined in (4.18) and (4.4). Note that we have $\partial_t u(t,x) = F_{\bar{x}(t)}(x) - C\rho(t)$, for $t < T$. But $\tilde{x} \notin [\bar{x}(t) \pm \delta]$ and the choice of parameters (4.12)-(4.13)-(4.3) implies $\tilde{x}$ must maximize $F_{\bar{x}(T^-)}(\cdot)$, hence $\tilde{x} = 0$.

The second step is to prove that there will be an actual jump towards 0, i.e $\bar{x}(T^+) = 0$. First, note that there exists a small $\eta > 0$ such that $\forall t \in (T-\eta, T)$, $u(t, \bar{x}(t)) = 0$ and $u(t,0) < 0$. Let us fix $t \in (T-\eta, T)$. We have $F_{\bar{x}(t)}(0) \geq F_{\bar{x}(t)}(\bar{x}(t))$, and we claim that the inequality is strict. Indeed, since $t \mapsto x(t)$ is increasing, $F_{\bar{x}(t)}(\bar{x}(t))$ is decreasing, whereas $F_{\bar{x}(t)}(0)$ is constant (as long as η is small enough such that $\bar{x}(T-\eta) > \delta$). We end up with

$$F_{\bar{x}(t)}(0) > F_{\bar{x}(t)}(\bar{x}(t)). \tag{4.21}$$

The above inequality expresses the fact that 0 is fitter than $\bar{x}(t)$ in a population with trait $\bar{x}(t)$. In general, this does not allow to conclude that 0 will invade and become the new dominant trait (i.e., that the jump will occur) because it does not imply that 0 will remain fitter during all the process of invasion. But the particular form of our problem, especially the fact that τ is an odd function, implies

$$F_0(0) > F_0(\bar{x}(t)). \tag{4.22}$$

Indeed we have from the definition of $F_{\bar{x}}(x)$ that

$$F_0(0) - F_0(\bar{x}(t)) = r(0) - r(\bar{x}(t)) + \tau(\bar{x} - \bar{x}) - \tau(0) = d_r \bar{x}(t)^2 > 0.$$

Consequently that for all $\lambda \in [0,1]$

$$\lambda F_0(0) + (1-\lambda) F_{\bar{x}(t)}(0) > \lambda F_0(\bar{x}(t)) + (1-\lambda) F_{\bar{x}(t)}(\bar{x}(t)).$$

It shows that 0 remains the fittest trait during all the process of invasion, and therefore that 0 will actually invade, i.e that $\bar{x}(t)$ will actually jump towards 0 at time T^+.

■

4.3.3.1 Threshold for cycles

In the previous subsection, we described the possible *evolutionary rescue*, i.e the possible jumps in the dynamics of $\bar{x}(t)$ towards $x = 0$. When a jump occurs, a new cycle begins: it leads to a periodical behavior of $\bar{x}(t)$, hence the cycling phenomena.

We recall that a jump corresponds to a rescue of the population concentrated at $\bar{x}(t)$ by the small population with trait $x = 0$. It is possible only if $\bar{x}(t) > \delta$ and if 0 is fitter than $\bar{x}(t)$ during a sufficiently large interval of time (which is

the time needed for the small population at $x = 0$ to regrow). Note that 0 is fitter than $\bar{x}(t)$ if and only if

$$F_{\bar{x}(t)}(0) \geq F_{\bar{x}(t)}(\bar{x}(t)) \quad \text{iff} \quad b_r - \tau_0 \geq b_r - d_r \bar{x}(t)^2, \tag{4.23}$$

$$\text{iff} \quad \bar{x}(t) \geq x_{resc} := \sqrt{\frac{\tau_0}{d_r}}. \tag{4.24}$$

But if no jump occurs, $\bar{x}(t)$ formally follows (4.17), thus $\bar{x}(t) < x_\star$ and $\bar{x}(t)$ converges to $x_\star$ when $t \to +\infty$ (with $x_\star$ is defined in (4.19)). The next statement allows to determine a critical τ leading to cycles.

Statement 4.3 *Under assumptions* (4.12)-(4.15)*, the evolutionary rescue phenomena occurs if and only if*

$$\tau_0 > \tau_{cyc} := 4 d_r \delta^2. \tag{4.25}$$

4.3.3.2 Threshold for extinction

The population is said to be "extinct" at time t if $\rho(t) = 0$. According to (4.11), we define x_{ext} as to solve $r(x_{ext}) = 0$, i.e

$$x_{ext} := \sqrt{\frac{b_r}{d_r}}, \tag{4.26}$$

that is, a population concentrated at trait $\bar{x}$ is extinct iff $\bar{x} \geq x_{ext}$.

The picture is simple in the case of stabilization without cycles, i.e when $\tau_0 \leq \tau_{cyc}$ (see (4.25)). In this case, we recall that $\bar{x}(t)$ formally follows (4.17) for all $t > 0$, thus $\bar{x}(t) < x_\star$ and $\bar{x}(t)$ converges to $x_\star$ when $t \to +\infty$ (where $x_\star$ is defined in (4.19)). Thus, if $x_\star \leq x_{ext}$, we have $\rho(t) > 0$ for all $t > 0$; on the contrary, if $x_\star > x_{ext}$, there exists a time $t_{ext} > 0$ for which $\rho(t) = 0$ for all $t \geq t_{ext}$. It gives a sharp threshold for extinction of the population: indeed, the population eventually gets extinct if and only if $x_\star > x_{ext}$, which is equivalent to

Statement 4.4 *Under assumptions* (4.12)-(4.15)*, if $\tau_0 \leq \tau_{cyc}$, then the population eventually gets extinct if and only if*

$$\tau_0 > \tau_{ext} := 2\sqrt{b_r d_r}\delta. \tag{4.27}$$

We point out that, surprisingly enough, τ_{ext} is an increasing function of the death rate d_r, meaning that under a higher death rate, the population can survive to a higher HT rate. The interpretation we propose is that if d_r is high, the population driven outward $x = 0$ dies rapidly, thus the population that remained closer to 0 undergoes a milder HT, which makes the overall population more resistant to a high HT rate.

Let us now focus on the case where the cycling phenomenon occurs, i.e when $\tau_0 > \tau_{cyc}$. In this case, $\bar{x}(t)$ will follow (4.17) and will periodically jump to $x = 0$. First, note that if $x_\star < x_{ext}$, $\bar{x}(t)$ remains below x_{ext} for all t and the population does not get extinct:

$$\text{if} \quad \tau \leq \tau_{ext}, \quad \text{then} \quad \rho(t) > 0, \quad \forall t > 0. \tag{4.28}$$

The most intricate case is when $x_\star > x_{ext}$, which contains case of extinction and non-extinction, depending on whether the jump of $\bar{x}(t)$ towards 0 happens before or after $\bar{x}(t)$ has passed beyond x_{ext}. In other words, extinction can be avoided if the evolutionary rescue happens before the dominant trait is led to extinction, i.e if $\bar{x}(T^-) \leq x_{ext}$, where T is the time where the jump of $\bar{x}(t)$ towards 0 occurs. However, we are not able to give a satisfactory formula or estimate on T.

Besides, when the jump of $\bar{x}(t)$ occurs, it can happen that the trait $x = 0$ is not fit enough to avoid extinction: in this case the evolutionary rescue does not manage to sustain the population. It corresponds to the case $x_{resc} > x_{ext}$. We have the following threshold: the evolutionary rescue is able to sustain the population iff $r(0) + \tau_0 > 0$, which is

equivalent to

$$\tau_0 < \tau_{sus} := b_r. \tag{4.29}$$

If $\tau \geq \tau_{sus}$, the population eventually gets extinct. If $\tau < \tau_{sus}$, the population is effectively rescued by the evolutionary rescue, even in the case where it passed through an episode of extinction during the previous cycle: in some cases the population is able to regrow after being extinct, which can be seen on Figure 4.4c. We think this is an interesting feature that the Hamilton-Jacobi approach is able to grasp. Regarding the stochastic model, an episode of extinction on Hamilton-Jacobi corresponds to an interval of time where the population reaches extremely small values (of order $e^{-\frac{1}{\varepsilon}}$, with ε the variance of the mutation kernel), and thus on which there is a nonzero probability that every individual dies.

Statement 4.5 *Assume* (4.12)-(4.15) *and* $\tau_0 > \tau_{cyc}$.

- *if* $\tau_0 \leq \tau_{ext}$, *the population never gets extinct.*
- *the evolutionary rescue effectively manages to sustain the population if and only if* $\tau_0 < \tau_{sus} := b_r$.

4.4 Numerical tests

In this section we perform several numerical tests for the presented models considering different values of the parameters, replicating different scenarios: stabilization around an optimal value, cycles (occurring through the evolutionary rescue phenomena) and the extinction. We then compare the numerical results obtained for the stochastic and deterministic approaches, using in particular an asymptotic-preserving scheme which allows us to observe the population dynamics on the passage from the integro-differential equation (4.5) to a limit (4.7). Throughout this section we define the birth, death rates and the mutation kernel to those given in (4.12)-(4.14) respectively, with the parameters fixed throughout all the experiments to $b \equiv 1$, $d_r \equiv 1$, $C \equiv 0.5$ respectively (unless otherwise stated).

4.4.1 The algorithm and the simulation for the Stochastic model

Our aim is to simulate the population dynamics over a fixed interval $[0, T]$. We begin by simulating an initial population of size N^0. We assume that the population is normally distributed around a mean trait x^0_{mean} with a standard deviation σ^0 so that the resulting vector $X^0 \in \mathbb{R}^{N^0}$. We know that in a time step Δ, an individual can die, give birth, or be a subject to HT. Each event happens according to a certain probability that we compute from the rates. More detailed description of the simulations is provided in Algorithm 1.

Note that in our setting it is possible that $1, 2$ or 3 events happen within the time step. Keeping a discretization time step small helps us to keep a biological sense in our simulation: even if the event of horizontal transfer with an "already dead" individual is possible in our setting (if $T_d \leq T_{HT} \leq \Delta$), this event is extremely rare. We simulate the population of initial size $N_0 = 10000$ up to time $T = 1000$ with $\Delta = 0.01$, with the parameters being defined at the beginning of the section, and α — a Heaviside function. Even if a Heaviside function is not the most easy to analyze when we pass to the deterministic limit of the system (see Subsections 4.2.2 and 4.2.3), we use it for the stochastic simulation, since it is the most straightforward model for HT in biological context, and is much faster to compute that a smooth function. We fix all constants but τ_0, which regulates the Horizontal Transfer, and study how it affects the dynamics.

Then we plot the density of the population at each moment of time (left side of each Figure): brighter colors on plot mean that there is a big amount of individuals with very similar traits. On the right top and right bottom we plot the normalized population size (ratio between the actual size and the carrying capacity of the system), and the mean trait.

Depending on the parameters we may observe three types of behavior, (see Figure 4.1). First possibility, for small values of τ_0, is the stabilization (Figure 4.1a). In this case the population rapidly reaches the equilibrium and concentrates

Algorithm 1: Population dynamics on time interval $[0, T]$

Random initialization of a population $X^0 := \mathcal{N}(x^0_{mean}, \sigma^0) \times N^0$;
while $i\Delta \leq T$ **do**
  $X^i = X^{i-1}$, $N^{i-1} = size(X^{i-1})$;
  for $\forall x \in X^i$ **do**
    $R_b := b(x)$, $R_d := d(x)+CN^{i-1}$, $R_{HT} := \sum_{y\in X^i} h_K(x-y, N^{i-1})$;
    $T_b := \lambda(R_b)$, $T_d := \lambda(R_d)$, $T_{HT} := \lambda(R_{HT})$, where λ denotes an exponential random law;
    if $T_b \leq \Delta$ **then**
      pick up a new trait z from $\mathcal{N}(x, \sigma)$;
      add a new individual with trait z to X^i;
    end
    if $T_{HT} \leq \Delta$ **then**
      pick a trait $y \in X^{i-1}$ according to the law $\frac{h_K(x-y,N^{i-1})}{\sum_{y\in X^i} h_K(x-y,N^{i-1})}$;
      remove individual with trait x and add individual with trait y;
    end
    if $T_d \leq \Delta$ **then**
      remove the individual with trait x from X^i
    end
  end
  return X^i
end

around the optimal trait, which is close to 0.1 (with stochastic fluctuations). Note that in this case, the mean trait is shifted in comparison to the optimal trait without HT (which is $x = 0$).

Second option, for intermediate values of τ_0, is the cycling behavior (Figure 4.1b). Since the transfer rate is sufficiently large, the population is driven towards a deleterious trait, which is eventually less fit than the trait $x = 0$. If the drift is not too strong, the very few individuals which were not affected by HT and remained fit (with x close to 0) manage to regrow and eventually repopulate the environment, which launches the cycle again.

The last possibility, for large values of the horizontal transfer rate τ_0, is extinction of the population (Figure 4.1c). It occurs because too many individuals were affected by deleterious traits of their neighbors, so that they die faster than is needed for replicating the population.

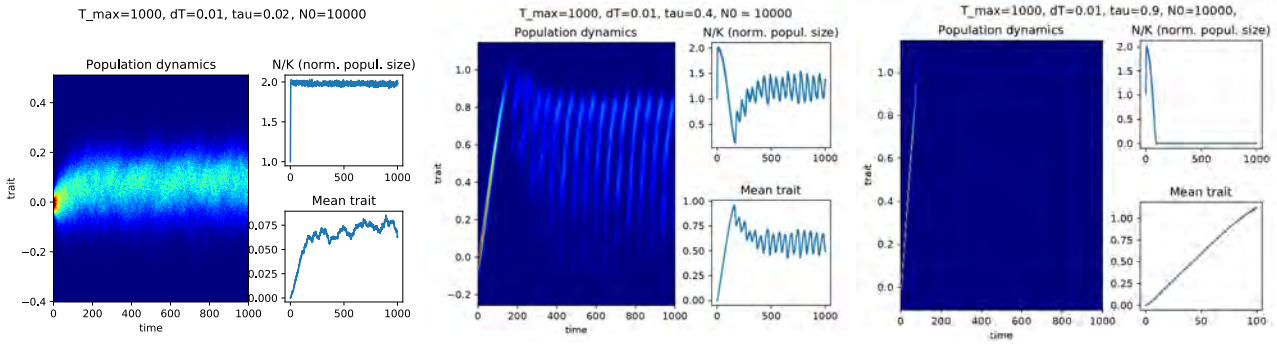

(a) Stabilization: $\tau_0 = 0.02$ (b) Cycles: $\tau_0 = 0.4$ (c) Extinction: $\tau_0 = 0.9$

Figure 4.1 – Behavior of the population dynamics as the mutation rate τ_0 is changing, ($b_r = d_r = 1$, $\sigma = 10^{-2}$, $K = 10^4$, $\sigma^0 = 10^{-2}$, $x^0_{mean} = 0$, $N^0 = 10^4$).

To understand better this phenomenon, we have to give a precise definition of what do we actually refer to, when we say "the critical value" of the transfer rate? In stochastic setting the answer is not trivial, and that is where the individual-based model reaches its limit. What we observe experimentally is the following when we change the value of HT rate starting from zero, the cycles in the population dynamics become more clearly visible, the fluctuations of the mean trait and the population size become more ample, until at some point the probability of extinction overweights the probability of survival and, finally, at the value of τ_0, which we call "critical" we obtain an almost sure extinction.

But since we are working with a point process, giving a strict definition of "critical value for an extinction" in terms of probability measures seems to be out of reach. Even in the experimental setting this notion is ambiguous: when the value of τ_0 is getting closer to a "critical" (numerically we observe an almost sure extinction at $\tau_0 = 0.49$), in different repetitions of the same experiment we may observe different types of behavior: either cycles, or extinction, which occurs after several cycles. It is illustrated on Figure 4.2, where the computations are launched with exactly the same set of parameters give very different results. Furthermore, it is not always clear how to differentiate between the stabilization and cycles, especially when the variance of the mutation kernel is large. To the best of our knowledge, there is no straightforward way to analytically measure the probability of each outcome under given initial conditions, which makes it difficult to analyse.

This constraint of an individual-based model naturally leads us to studying a limiting system described in Subsection 4.2.2.

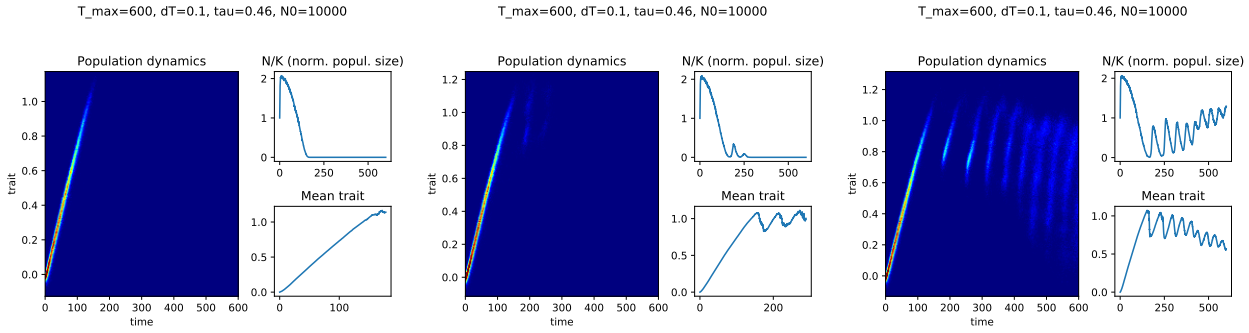

(a) Extinction (b) Cycle and extinction (c) Cycles

Figure 4.2 – Different behaviors for $\tau_0 = 0.46$ (and the other parameters as in Figure 4.1).

4.4.2 Numerical scheme and simulation for the PDE model

In this subsection, a numerical scheme for (4.5) is presented, and its properties are numerically investigated. For the discretization of (4.5), we consider a bounded space of traits $[X_{\min}, X_{\max}]$, discretized with N_x points. Denoting N_x the number of discretization points of the interval $[X_{\min}, X_{\max}]$, we define

$$\Delta x = \frac{X_{\min} - X_{\max}}{N_x - 1},$$

and

$$x_i = X_{\min} + i\Delta x, \quad 0 \leq i \leq N_x - 1.$$

We consider the time interval $[0, T_{\max}]$, discretized with N_t points $t_n = n\Delta t$, for $0 \leq n \leq N_t - 1$, and where Δt is defined as

$$\Delta t = \frac{T_{\max}}{N_t - 1}.$$

The approximations of the solution f of (4.5) at (t_n, x_i), and of its density ρ at t_n are denoted f_i^n and ρ^n respectively.

We recall that the initial condition f^0 is a smooth function of x given in (4.16) and the initial density ρ^0 is computed using a left-point quadrature rule for f^0 as follows:

$$\rho^0 = \Delta x \sum_{i=0}^{N_x-1} f^0(x_i).$$

The scheme is written with an explicit Euler scheme, in which the integrals are computed with a left-point quadrature rule. For $n \geq 1$ and $0 \leq i \leq N_x - 1$, it reads

$$\varepsilon \frac{f_i^{n+1} - f_i^n}{\Delta t} = (d(x_i) + C\rho^n)\, f_i^n + [m * (bf)]_i^n + f_i^n \Delta x \sum_{j=0}^{N_x-1} \tau(x_i - x_j) \frac{f_j^n}{\rho^n}. \tag{4.30}$$

In (4.30), the convolution product $[m * (bf)]_i^n$ is computed with a left-point quadrature rule, as well of the other integrals. To do so, a grid in the z variable is defined as for the x variable. Let $Z_{\min}$ and $Z_{\max}$, and the number N_z of discretization points be given. The grid in z is defined as

$$\forall 0 \leq k \leq N_z - 1, z_k = Z_{\min} + k\Delta z,$$

where $\Delta z = (Z_{\max} - Z_{\min}) / (N_z - 1)$. This leads to two possibles cases: $x_i + \varepsilon z_k \in [X_{\min}, X_{\max}]$ or not. We proceed in each case as follows:

- When $x_i + \varepsilon z_k \in [X_{\min}, X_{\max}]$, the value of $f(t_n, x_i + \varepsilon z_k)$ is approximated by linear interpolation of the $(f_i^n)_{0 \leq i \leq N_x - 1}$.
- When $x_i + \varepsilon z_k < X_{\min}$, or $x_i + \varepsilon z_k > X_{\max}$, it is computed with a linear extrapolation of the $(f_i^n)_{0 \leq i \leq N_x - 1}$, using the slope at the corresponding end of the X domain.

Using the notation $f^n(x_i + \varepsilon z_k)$ for the approximation of $f(t_n, x_i + \varepsilon z_k)$, we then approximated the convolution product $\int m(z) b(x + \varepsilon z) f(x + \varepsilon z) \mathrm{d}z$ by

$$[m * (bf)]_i^n = \Delta z \sum_{k=0}^{N_z-1} m(z_k) b(x_i + \varepsilon z_k) f^n(x_i + \varepsilon z_k).$$

4.4.2.1 Case $\varepsilon = 1$: comparison with stochastic model

First thing that we are interested in is whether under identical parameters and initial conditions we may reproduce the same behavior as in the stochastic model. Thus, we conduct several experiments, fixing parameter ε to 1 (thus, we do not rescale time, nor mutation rate), leaving all the other parameters fixed to the same values as in stochastic simulation case.

As we may see on Figure 4.3, simulations in overall correspond to those of the stochastic model. Indeed, when the HT rate τ_0 is small enough the population rapidly stabilizes around its equilibrium state (see Figure 4.3a), as in the stochastic simulations. Further similarity between two models is that in both cases the optimal trait is shifted a bit above 0. It is caused by HT phenomena.

For larger values of τ_0, where we would expect to have distinguishable cycles, we observe indeed damped oscillations, see Figure 4.3b. Again, we stress out that for the stochastic model it is not the case, see Figure 4.1b. The way we understand the damping in the oscillations is that the PDE model and the numerical algorithm that we use are not

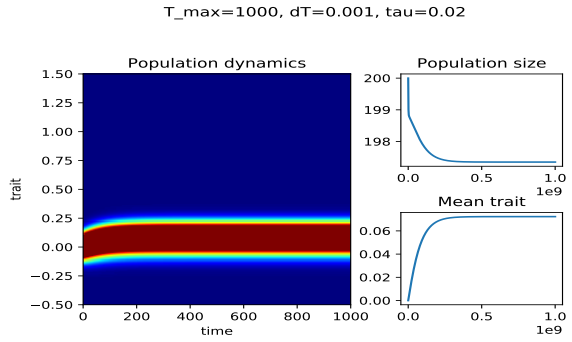

(a) Stabilization: $\tau_0 = 0.02$

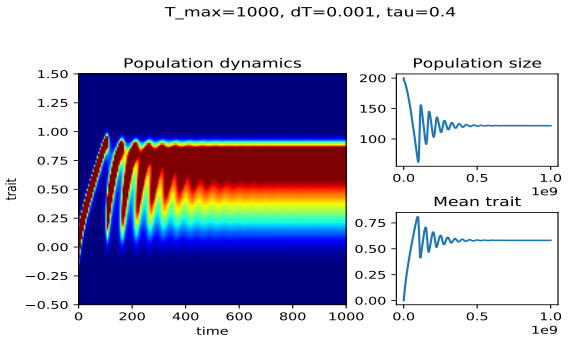

(b) Cycles: $\tau_0 = 0.4$

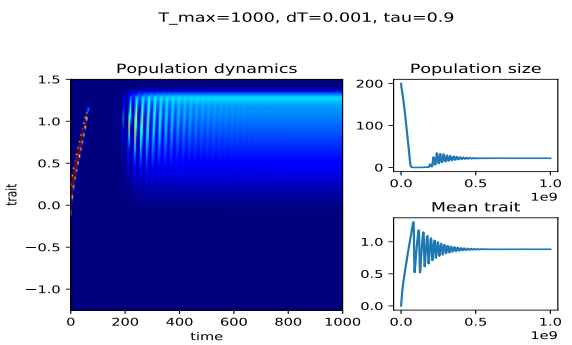

(c) Extinction and cycles: $\tau_0 = 0.9$

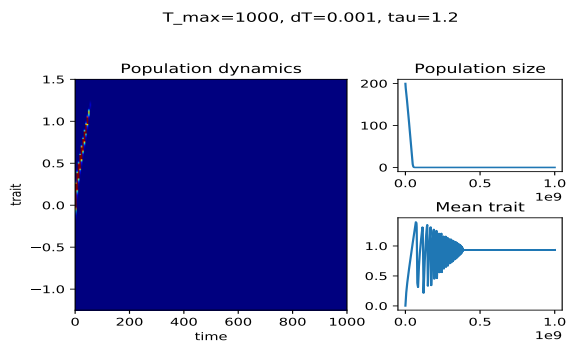

(d) Full Extinction $\tau_0 = 1.2$

Figure 4.3 – Behavior of the population dynamics described by a PDE model as the mutation rate τ_0 is changing, ($b_r = d_r = 1$, $\sigma = 0.01$, $\varepsilon = 1$).

designed to have a precise grasp on the exponential small values of f, on which the cycling phenomenon relies. This limitation suggests to perform the change of variable (4.6), and to write a numerical scheme which converges uniformly when $\varepsilon \to 0$. This is what the next section is devoted to.

On Figure 4.3c, we observe that as τ_0 becomes larger the population gets extinct, and then, surprisingly enough, "reborns" after a period of extinction. This scenario can only be reproduced on density-based models, since in individual-based model any extinction is definitive. On Figure 4.3d we observe a full extinction of the population without report. We will give further insights on those two cases in the next section.

4.4.3 The scheme for the Hamilton-Jacobi equation

4.4.3.1 Case $\varepsilon \to 0$: description of the numerical scheme

As the rescaling parameter ε goes to 0, the model given by (4.7) gets closer to its limiting state (4.8). However, numerical approximation of the (4.5) for $\varepsilon << 1$ is not a trivial task. Indeed, for small ε, the solution f_ε of (4.5), is expected to concentrate at a dominant trait. To be able to catch its stiffness numerically, one then has to refine the grid in x, to ensure enough precision in the computation of f. As a consequence, the computational cost of the numerical simulations increases when $\varepsilon \to 0$, and reaching the asymptotic regime with this scheme is not possible. In this part, we present a numerical scheme for (4.5) which enjoys stability properties in the limit $\varepsilon \to 0$.

To avoid the increase of computational cost when reaching the asymptotics, and to ensure the scheme approaches the limit Hamilton-Jacobi equation for small ε, a scheme for the solution u_ε of (4.7) which enjoys the Asymptotic Preserving

(AP) property is proposed here. Such schemes have been introduced in [64, 65, 58], their properties are often summarized by the following diagram

$$\begin{array}{ccc} P_\varepsilon & \xrightarrow{\varepsilon\to 0} & P_0 \\ \uparrow{\scriptstyle h\to 0} & & \uparrow{\scriptstyle h\to 0} \\ S_\varepsilon^h & \xrightarrow{\varepsilon\to 0} & S_0^h \end{array}$$

that should be understood as follows: when the parameter $\varepsilon > 0$ is fixed, the scheme S_ε^h is consistent with the ε-dependent problem P_ε. When ε goes to 0, the solution of P_ε converges to the solution of the limit problem P_0. The AP scheme S_ε^h is stable along the transition to the asymptotic regime. It means that, when ε goes to 0 with fixed discretization parameters h, the scheme becomes a limit scheme S_0^h, which is consistent with the limit problem P_0.

As an AP scheme is required to enjoy stability properties when ε is going to 0, one has to ensure that all the quantities that have to be computed enjoy this property. In the case we are considering, the main concerns are the computation of the integral containing the birth term, the computation of the integral containing the transfer term and the computation of ρ. If all of them are correctly defined, the scheme proposed reads

$$\frac{u_i^{n+1} - u_i^n}{\Delta t} = -(d(x_i) + C\rho^{n+1}) + B_i^n + T_i^n, \tag{4.31}$$

where B_i^n stands for an approximation of

$$\int_{\mathbb{R}} m(z) b(x_i + \varepsilon z) \mathrm{e}^{(u_\varepsilon(t^n, x_i+\varepsilon z) - u_\varepsilon(t^n, x_i))/\varepsilon} \mathrm{d}z, \tag{4.32}$$

and T_i^n is for

$$\int_{\mathbb{R}} \tau(x_i - y) \frac{f(t^n, y)}{\rho(t^n)} \mathrm{d}y. \tag{4.33}$$

Here, we used the notations and discretization grids defined in the beginning of Section 4.4.2, and the dependences in ε are omitted to simplify the notations. In what follows, we present how T_i^n, B_i^n and ρ^{n+1} can be computed in a way that ensures they are consistent with their definition for fixed ε, that they can be computed with a constant computational cost with respect to ε, and that their asymptotic behavior when ε goes to 0 is meeting the continuous one (4.8).

- **Computation of T_i^n.** The direct approximation of (4.33) with a quadrature rule is consistent for $\varepsilon \sim 1$. However, since f is expected to concentrate when $\varepsilon \to 0$, it lacks precision in the asymptotic regime. Especially, the convergence of f/ρ to a Dirac is not ensured when the integral is approximated directly. Remarking that

$$\frac{f_\varepsilon(t^n, y)}{\rho_\varepsilon(t^n)} = \frac{\mathrm{e}^{u_\varepsilon(t^n,y)/\varepsilon}}{\displaystyle\int_{\mathbb{R}} \mathrm{e}^{u_\varepsilon(t^n,z)/\varepsilon}\mathrm{d}z} = \frac{\mathrm{e}^{(u_\varepsilon(t^n,y) - \max\limits_x u_\varepsilon(t^n,x))/\varepsilon}}{\displaystyle\int_{\mathbb{R}} \mathrm{e}^{(u_\varepsilon(t^n,z) - \max\limits_x u_\varepsilon(t^n,x))/\varepsilon}\mathrm{d}z},$$

  (4.33) is computed with a left-point quadrature rule in the integrals of the previous expression. It reads

$$T_i^n = \Delta x \sum_{j=1}^{N_x-1} \tau(x_i - y_j) \frac{\mathrm{e}^{(u_j^n - \max\limits_l u_l^n)/\varepsilon}}{\Delta x \displaystyle\sum_{k=0}^{N_x-1} \mathrm{e}^{(u_k^n - \max\limits_l u_l^n)/\varepsilon}} = \frac{\displaystyle\sum_{j=1}^{N_x-1} \tau(x_i - x_j) \mathrm{e}^{(u_j^n - \max\limits_l u_l^n)/\varepsilon}}{\displaystyle\sum_{k=0}^{N_x-1} \mathrm{e}^{(u_k^n - \max\limits_l u_l^n)/\varepsilon}}. \tag{4.34}$$

For fixed ε, (4.34) is consistent with (4.33). Since all the arguments of the exponentials are nonpositive, the limit of (4.34) for small ε can be read on that expression. Denoting j_0 the index such that

$$u^n_{j_0} = \max_l u^n_l,$$

and supposing that there exists a unique such j_0, the limit of (4.34) for small ε is

$$\tau(x_i - x_{j_0}).$$

This is consistent with the last term in the limit Hamilton-Jacobi equation (4.8).

- **Computation of B^n_i.** Once again, the numerical approximation of (4.32) is done with a quadrature in the integral. Using the notations of Section 4.4.2, a grid in z is defined. The functions m and b are respectively evaluated at z_k and $x_i + \varepsilon z_k$, but the interpolation of u^n at $x_i + \varepsilon z_k$ has to be done with special care to make the scheme enjoy the expected asymptotic behavior. Using a left-point quadrature rule, (4.32) is approximated by

$$\Delta z \sum_{\substack{k=0 \\ \varepsilon|z_k|\leq dx}}^{N_z-1} m(z_k) b(x_i + \varepsilon z_k) \mathrm{e}^{z_k \nabla^{\varepsilon,small}_{n,i,k}} + \Delta z \sum_{\substack{k=0 \\ \varepsilon|z|>dx}}^{N_z-1} m(z_k) b(x_i + \varepsilon z_k) \mathrm{e}^{z_k \nabla^{\varepsilon,large}_{n,i,k}}, \tag{4.35}$$

where $\nabla^{\varepsilon}_{n,i,k}$ stands for an approximation of

$$\frac{u^\varepsilon(t^n, x_i + \varepsilon z_k) - u^\varepsilon(t^n, x_i)}{\varepsilon z_k}.$$

In both cases, it is computed with a linear interpolation of the values u^n_i. Hence, $\nabla^{\varepsilon,large}_{n,i,k}$ is given by

$$\nabla^{\varepsilon,large}_{n,i,k} = \frac{\tilde{u}^n_{i,k} - u^n_i}{\varepsilon z_k},$$

where $\tilde{u}^n_{i,k}$ is computed as the linear interpolation of $(u^n_i)_{1\leq i\leq N_x}$ at $x_i + \varepsilon z_k$. If $x_i + \varepsilon z_k < X_{\min}$ or $x_i + \varepsilon z_k > X_{\max}$, the extrapolation is done linearly using the slope at the first or last point of the interval. Since $\varepsilon z_k > \Delta x$, no stability issue is faced in this computation. Still using a linear interpolation, when $0 < \varepsilon z_k \leq \Delta x$, it is worth noticing that

$$\frac{\tilde{u}^n_{i,k} - u^n_i}{\varepsilon z_k} = \frac{u^n_{i+1} - u^n_i}{\Delta z},$$

and when $0 > \varepsilon z_k \geq -\Delta x$,

$$\frac{\tilde{u}^n_{i,k} - u^n_i}{\varepsilon z_k} = \frac{u^n_i - u^n_{i-1}}{\Delta x}.$$

as a consequence, we define:

$$\nabla^{\varepsilon,small}_{n,i,k} = \begin{cases} \dfrac{u^n_{i+1} - u^n_i}{\Delta x}, & \text{if } 0 < \varepsilon z_k \leq \Delta x \\ \dfrac{u^n_i - u^n_{i-1}}{\Delta x}, & \text{if } -\Delta x \leq \varepsilon z_k < 0 \\ 0, & \text{if } z_k = 0. \end{cases}$$

This definition of B^n_i is consistent with (4.32). Moreover, when ε goes to 0 with fixed numerical parameters, such

as $Z_{\min}$ and $Z_{\max}$, the expression $\nabla_{n,i,k}^{\varepsilon,large}$ is not used at all, and

$$B_i^n \underset{\varepsilon\to 0}{=} B_i^{n,0} = \Delta z \sum_{\substack{k=0\\ z_k<0}}^{N_z-1} m(z_k)b(x_i)\mathrm{e}^{z_k\frac{u_i^n-u_{i-1}^n}{\Delta x}} + \Delta z m(0)b(x_i) + \Delta z \sum_{\substack{k=0\\ z_k>0}}^{N_z-1} m(z_k)b(x_i)\mathrm{e}^{z_k\frac{u_{i+1}^n-u_i^n}{\Delta x}}. \tag{4.36}$$

- **Computation of ρ^{n+1}.** In (4.31), ρ^{n+1} is considered in an implicit way, to make the limit scheme be consistent with the limit equation (4.8). Since

$$\rho(t) = \int_{\mathbb{R}} \mathrm{e}^{u(t,x)/\varepsilon}\mathrm{d}x,$$

for $\varepsilon > 0$, we define

$$\rho^{n+1} = \Delta x \sum_{i=0}^{N_x-1} \mathrm{e}^{u_i^{n+1}/\varepsilon}.$$

A closed equation on ρ^{n+1} can be deduced from (4.31). Indeed, (4.31) yields

$$\mathrm{e}^{u_i^{n+1}/\varepsilon} = \mathrm{e}^{-\Delta t\rho^{n+1}/\varepsilon}\mathrm{e}^{(u_i^n+\Delta t\left[-d(x_i)+B_i^n+T_i^n\right])/\varepsilon},$$

and so

$$\rho^{n+1} = \Delta x\ \mathrm{e}^{-\Delta t\rho^{n+1}/\varepsilon} \sum_{i=0}^{N_x-1} \mathrm{e}^{A_i^n/\varepsilon}, \tag{4.37}$$

where A_i^n denotes $u_i^n + \Delta t\left(-d(x_i) + B_i^n + T_i^n\right)$ to simplify the notations. Eventually, ρ^{n+1} is solution of $h(y) = 0$, with

$$h(y) = y\mathrm{e}^{\Delta t y/\varepsilon} - \Delta x \mathrm{e}^{A_{i_0}^n/\varepsilon} \sum_{i=0}^{N_x-1} \mathrm{e}^{(A_i^n-A_{i_0}^n)/\varepsilon}, \tag{4.38}$$

where $A_{i_0}^n = \max_i A_i^n$ has been taken apart to get an uniform estimate with respect to ε on the remaining sum. It is also solution of the equivalent equation $g(y) = 0$, with

$$g(y) = -\varepsilon\ln(y) - \Delta t y + \varepsilon\ln(\Delta x) + A_{i_0}^n + \varepsilon\ln\left(\sum_{i=0}^{N_x-1} \mathrm{e}^{(A_i^n-A_{i_0}^n)/\varepsilon}\right). \tag{4.39}$$

To find ρ^{n+1}, a Newton's method is applied on expression (4.38) or on (4.39). Both expressions are smooth convex functions of ρ, and are equivalent. Hence, the Newton's method converges whatever is used. Nevertheless, it must be chosen with care. Indeed, because of numerical phenomena, i.e. the continuous accumulation of error, (4.38) is to be chosen when ρ^{n+1} is close to 0, whereas (4.39) is more adapted when ρ^{n+1} is not small. In the effective implementation of the method, either one formulation or the other is chosen, depending on the values reached during the iterations of the algorithm. Eventually, to ensure the stability of the numerical resolution of (4.37) when $\varepsilon \to 0$, the inverse of the derivatives of h and g are analytically computed and implemented as

$$\frac{1}{h'(y)} = \frac{\varepsilon}{\varepsilon + \Delta t}\mathrm{e}^{-\Delta t y/\varepsilon}, \quad \frac{1}{g'(y)} = -\frac{y}{\varepsilon+\Delta t}.$$

Since $y > 0$, these two expressions are uniformly bounded with respect to ε when Δt is fixed. As a consequence, the cost of the numerical resolution of (4.37) does not increase with ε.

When $\varepsilon > 0$ is fixed, the scheme (4.31) is consistent with (4.7), since only quadrature formula and interpolation methods have been used to write it. The way all the terms are computed, as well as the numerical resolution of the non-linear equation (4.37), ensures the stability of the numerical computations in the small ε regime. Hence, when $\varepsilon \to 0$

with fixed discretization parameters, the scheme (4.31) becomes

$$\frac{u_i^{n+1} - u_i^n}{\Delta t} = -\left(d(x_i) + C\rho^{n+1}\right) + B_i^{n,0} + \tau(x_i - x_{j_0}), \tag{4.40}$$

where j_0 is such that $u_{j_0}^n = \max_i u_i^n$, and $B_i^{n,0}$ has been defined in (4.36).

We do not give a strict proof of consistency of this scheme with respect to the limiting Hamilton-Jacobi equation (4.8), since it is out of scope of the chapter. However, we draw the attention to few important points which need to be taken into account while working with the scheme. In particular, the behaviour of the quantity $\rho(t)$ is not well understood in the case of an extinction. The problem is that intuitively, $\rho(t)$ must represent the density of the population — so that when it goes to zero, we expect an extinction. However, in a Hamilton-Jacobi case even when the $\rho(t)$ reaches zero, the population can still regrow after some time. This can be explained by the fact that after two limiting procedures (passing first to infinite system size, and then to the infinite time horizon), the "size" of the population can not be described straightforwardly. Accurate link between the quantities obtained as a result of stochastic and PDE simulation is also a question which requires further investigation when $\rho(t) << 1$.

4.4.3.2 Case $\varepsilon \to 0$: the numerical results

In this subsection we simulate the dynamics of the population by considering a small value of ε and discuss the obtained results in order to compare them with previous simulations. Note that, in order to compare both, the stochastic and the Hamilton-Jacobi behaviours, the first thing to do is to obtain the simulations for the stochastic model also in the case where the HT rate is a smooth function as we do for the Hamilton-Jacobi case. We recall that, in Subsection 4.4.1 simulations for stochastic model are done with a Heaviside function as HT rate since it is a more natural choice for simulation of a jump process.

On Figure 4.4 we simulate the population dynamics for $\varepsilon = 0.01$. Upon rescaling time (for chosen ε time scale $T = 10$ correspond, in fact, to $\frac{T}{\varepsilon} = 1000$ in previous simulations) and the variance parameter, we see the same patterns, with few differences.

On Figure 4.4a, we observe a stabilization of the mean trait, as in Figure 4.1a. Similarly, on Figure 4.4b, we observe cycles, but on the contrary to PDE model, oscillations are not damped. Moreover, it is worth pointing out that the duration of a cycle here corresponds to what we observe in the corresponding stochastic plot (on Figure 4.1b) multiplied by $\varepsilon = 0.01$. On Figure 4.4c, we also observe a cycling behavior, but the population goes periodically extinct (i.e the population reaches exponentially small value, of order $e^{1/\varepsilon}$), and then reborn. On the stochastic model, it corresponds to what is illustrated in Figure 4.2. It is not surprising that this behavior is difficult to observe on the stochastic model, since very small populations are likely to go extinct.

On Figure 4.4d, we can see that the population goes completely extinct. The most interesting case to comment is probably "partial" extinction seen on 4.4c. Note that despite the fact that ρ remains at 0 for some time, the population regrows. The point is that, as it was already mentioned above, this numerical parameter has no 1:1 correspondence to the population size parameter $\frac{N_t}{K}$ used in stochastic model. Also note that similar behaviour of stochastic and HJ model are reproduced under a bit different values of parameters. It is caused by the rescaled time and mutation kernel, so that the rigorous link between two models is still to be developed.

Another interesting thing to comment is that on Figure 4.4b we may notice that due to the fact that the system is deterministic and we see no stochasticity on curves, describing the mean trait and the density of the population, it is easy to estimate the periods of the system, computing distances between local maxima on each curve. For the stochastic system this task is more difficult, especially for a small population, because it includes filtering problem of a noisy signal. To get more accurate results in stochastic model we have to increase the time scale and number of individuals, which is

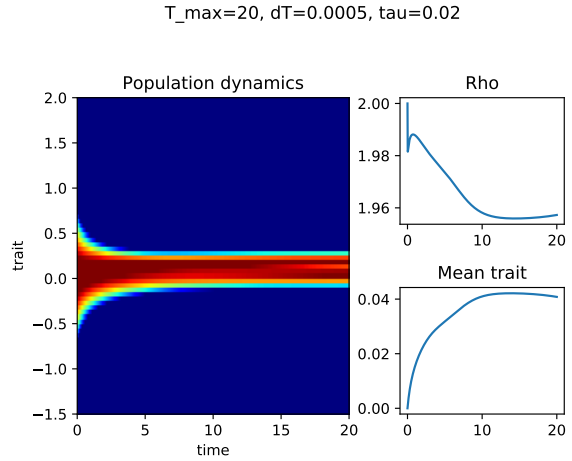

(a) Stabilization: $\tau_0 = 0.02$

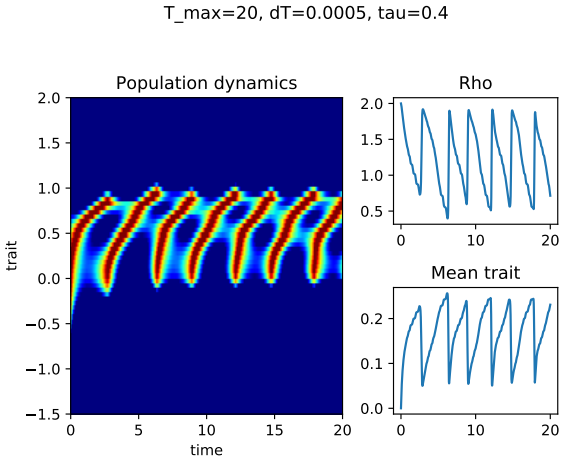

(b) Cycles: $\tau_0 = 0.4$

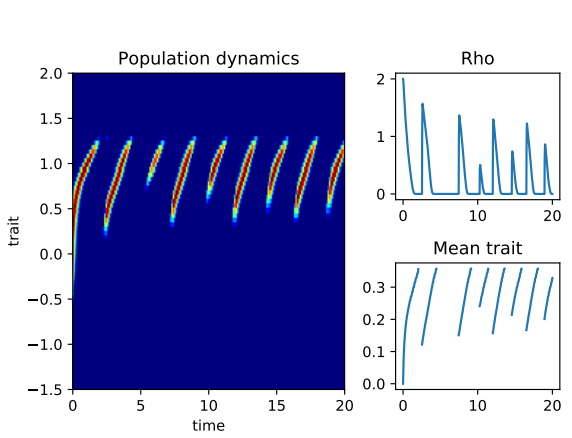

(c) Cyclic extinction: $\tau_0 = 0.9$

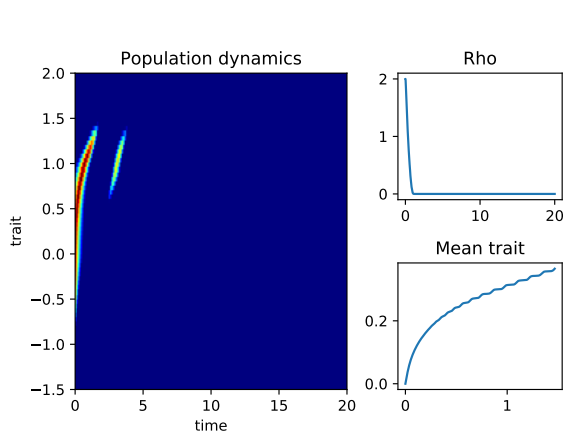

(d) Full extinction: $\tau_0 = 1.2$

Figure 4.4 – Behavior of the population dynamics described by a PDE model for $\varepsilon = 0.01$ as the mutation rate τ is changing, ($b_r = d_r = 1$, $\sigma = 1$).

costly from computational point of view.

To finish with, let us give some flavor on the computational cost of the simulations for each type. In Table 4.1 we give a short overview of the elapsed time for the same values of parameters, but for different schemes. As expected, individual-based model is the most expensive to compute. All the computations were performed in `numpy` library of Python on MacBook Pro (Intel Core i5 processor, 2,7GHz).

	$\Delta = 0.1,\ T = 10$	$\Delta = 0.01,\ T = 10$
SM ($N = 1000$)	3.883s	38.145s
SM ($N = 10000$)	15.805s	153.255s
PDE ($\varepsilon = 1$)	0.186s	1.673s
HJ ($\varepsilon = 10^{-2}$)	0.191s	1.636s
HJ ($\varepsilon = 10^{-6}$)	0.195s	1.656s

Table 4.1 – Elapsed time for simulation of population dynamics for different models (other parameters are fixed to values used throughout all the other simulations, $\tau = 0.5$).

4.5 Comparison between the theoretical analysis of the Hamilton-Jacobi equation and the numerical simulations of the stochastic model

4.5.1 Formal computations

In this section, we propose some formal computations on the stochastic model, based on the analysis of the Hamilton-Jacobi equation performed in the previous section. To fix ideas, we assume $n = 1$ and (4.3)-(4.12)-(4.13), and we fix all constants but τ_0, as in the previous section. However, we choose the function α as a Heaviside function (this is what has been used in the simulations), which is not a smooth function, and thus will lead to minor modifications compared to the previous section.

We make a strong formal assumption: taking $K \gg 1$, we assume that the population behaves like a normally distributed random variable all the time, i.e

$$\nu_t^K(dx) = \rho(t)\frac{1}{\sqrt{2\pi}s(t)}e^{-\frac{|x-\bar{x}(t)|^2}{2s(t)^2}}dx, \tag{4.41}$$

for some standard deviation $s(t)$ and for $\bar{x}(t)$ defined in (4.9). We expect $s(t)$ to be of the same order as σ, but giving a general estimate for $s(t)$ in function of $\bar{x}(t)$ seems intricate. The normalized size of the population $\rho(t) := \frac{N_t^K}{K}$ is approximately given by (see (4.11))

$$\rho(t) = \frac{1}{C}r(\bar{x}(t)), \tag{4.42}$$

where r is defined in (4.18).

We now formally compute the evolutionary singular state $x_\star$. But as α is a Heaviside function (which formally corresponds to the case when $\delta \to 0$ in (4.19)), our derivations must be slightly adapted. In particular, $\tau(x - \bar{x}(t))$ in (4.8) has to be replaced by

$$\int_{\mathbb{R}} \tau(x-y)\frac{\nu_t^K(dy)}{\rho(t)}, \tag{4.43}$$

and accordingly, recalling that the weak derivative of a Heaviside is a Dirac mass at 0, $\tau'(0)$ in (4.19) has to be replaced by

$$\int_{\mathbb{R}} \tau'(\bar{x}(t)-y)\frac{\nu(dy)}{\rho(t)} = \frac{2\tau_0}{\sqrt{2\pi}s(t)}.$$

We find

$$x_\star = \frac{\tau_0}{\sqrt{2\pi}s_\star d_r}, \tag{4.44}$$

where $s_\star$ is an unknown corresponding to the standard deviation of the population at equilibrium concentrated at $x = x_\star$. Note that it corresponds to (4.19) with $\tilde{\delta} := s_\star\sqrt{\pi/2}$.

We now try to estimate $s_\star$. Formally, $s_\star$ should be such that $u_\star(x) := \frac{-(x-x_\star)^2}{2s_\star^2}$ is a stationary solution of (4.8). Differentiating twice, and applying at $x = x_\star$ we find

$$0 = b_r\sigma^2 \left(u_\star''(x_\star)\right)^2 - 2d_r,$$

(with the reasonable assumption $\tau''(0) = 0$), which gives

$$s_\star = \sqrt{\sigma\sqrt{\frac{b_r}{2d_r}}}.$$

Numerically, we find $s_\star = 0.12$. We end up with the following formula:

$$x_\star = \frac{\tau_0}{\sqrt{2\pi\sigma}d_r}\sqrt[4]{\frac{2d_r}{b_r}}. \tag{4.45}$$

Stabilization

We run a numerical test on the stochastic model corresponding to stabilization, for $\tau_0 = 0.02$, and the other parameters as in Figure (4.1a). In this case, $x_\star$ correspond to the mean trait of the population for large time. From, (4.45) we find $x_\star = 0.067$, and from (4.42), we obtain $\rho_\star = 1.99$, which corresponds to what we can see on Figure (4.1a).

Threshold for cycles

Since equation (4.23) remains unchanged, we obtain the following threshold for cycles (corresponding to (4.25)):

$$\tau_{cyc} = 2\pi d_r\sigma\sqrt{\frac{b_r}{2d_r}}. \tag{4.46}$$

With our choice of parameters, we obtain $\tau_{cyc} = 0.09$. This threshold corresponds to the numerical simulations (however, characterizing precisely whether cycles occurs or not on the numerical simulations is not easy when τ_0 is close to the threshold).

Threshold for extinction

Using (4.26), we can also find a threshold for extinction:

$$\tau_{ext} := \sqrt{2\pi b_r d_r\sigma}\sqrt[4]{\frac{b_r}{2d_r}}.$$

For our choice of parameters, we obtain $\tau_{ext} = 0.30$.

We now compare this formula with numerical experiments on individual-based model. They are organized as follows: we fix the birth b_r or the death rate d_r, and save the first value of τ_0 under which the extinction occurs. Then, we increase the rate and save the next HT rate under which we have an extinction. Resulting curve for the birth rate is saved on Figure 4.5a (for death rate: Figure 4.5b). Non-concerned parameters remain fixed as in Subsection 4.4.1.

The numerical results, in particular, justify at the first glance surprising fact that the extinction threshold depends on the birth and death rate in the same manner. It seems logical to assume that while the higher birth rate contributes to a bigger survival probability even with a relatively big horizontal transfer rate, higher death rate must have an opposite effect. However, in conditions of a very "harsh" environment individuals with non-fit traits die out before they manage

to transfer their genetic information to the other individuals. As a consequence, value of the critical τ increases as the value of the birth (or death) rate constant increase.

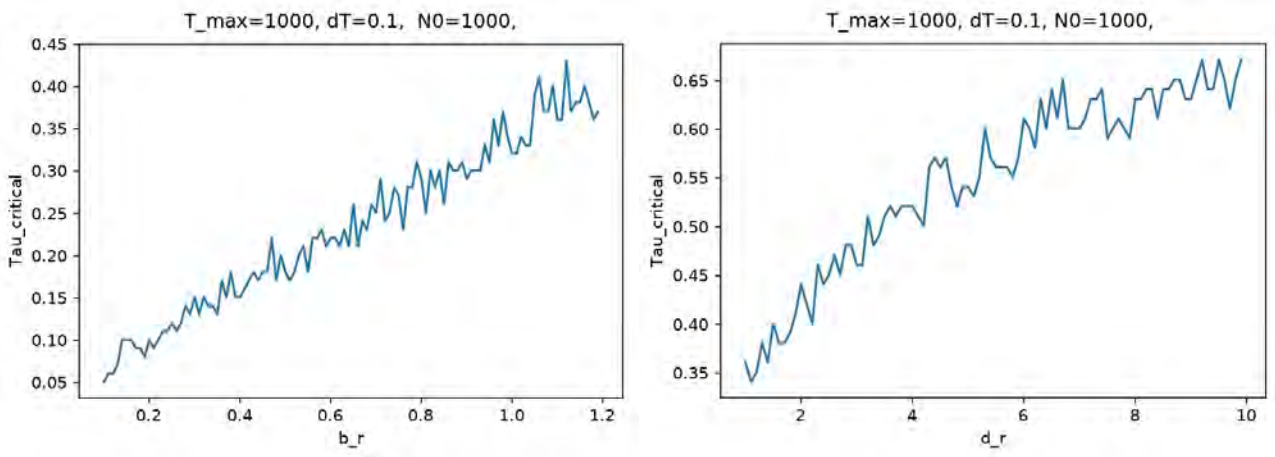

(a) Birth dependency

(b) Death dependency

Figure 4.5 – Dependency on the threshold for extinction τ_{ext} with respect to the birth rate b_r and death rate d_r

4.6 Discussion

First achievement of the study consists in an accurate numerical study conducted on the stochastic model given by a point measure (4.1). To the best of our knowledge, in-depth analysis of the influence of the HT rate on the evolutionary dynamics has not been yet attempted. Along with its accuracy, the stochastic model reveals its limitation: an accurate theoretical description of what actually happens in each observed scenario from a mathematical point of view seems to be out of reach.

On the next step, in a numerical comparative study between the stochastic (individual based) and the PDE (density) model both models exhibit the same behavior for a given set of parameters, which justifies theoretical results from [18, 20]. Minor differences — in particular, presence of damping oscillations – can be explained by a choice of a numerical scheme. However, further analysis shows that the classical PDE model defined by (4.2.2) leads to instabilities if we try to pass to an asymptotic setting under the small mutation assumption. Those instabilities are then resolved by a transformation of an initial model to a Hamilton-Jacobi type equation and using an asymptotic-preserving scheme. Further advantage of this approach is that the resulting equation (4.7) makes an easier subject of a theoretical analysis.

Finally, in a Hamilton-Jacobi setting we manage to numerically replicate the evolutionary rescue of a small population which we observe in the stochastic model. This phenomena is illustrated for stochastic, PDE and HJ simulation on Figure 4.6. On Figures 4.6a-4.6c we trace the moment of the regrowth for different models. Figure 4.6a show the state of the population at certain moment of time: we see how the individuals are centered around a mean trait. For PDE and HJ model (red and green line respectively) we simply plot the density function, and on the first (blue) plot we approximate a histogram which describes ratio $\frac{N_t}{K}$ sorted by traits in stochastic model. Stochastic simulations show the evolutionary rescue in more distinct manner: we see how the very small number of non-mutated individuals rescues the whole population from extinction (transition from 4.6b to 4.6c). On the contrary, the transition on the PDE model is dumped, and the regrowth is not clearly visible. It is due to, again, numerical instability of the PDE scheme for small values of the density function. Finally, HJ explicitly shows how the cycle occurs: the regrow of the ”fit” individuals we

see in stochastic plot is reproduced by a change of the maximum point (see again 4.6b to 4.6c).

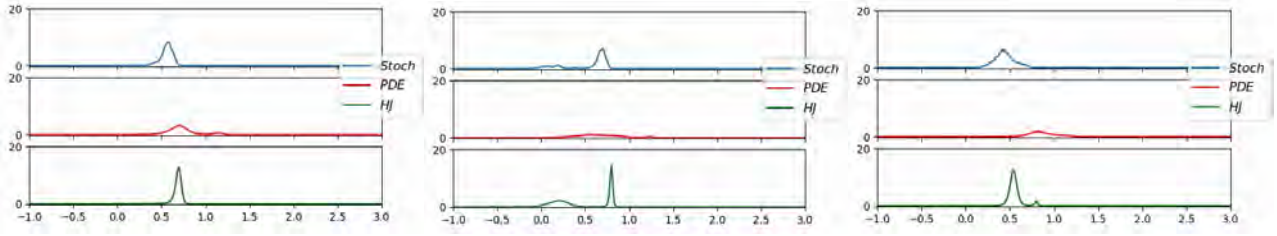

(a) $t = 167$ (b) $t = 198$ (c) $t = 216$

Figure 4.6 – Comparison of numerical simulations between the different models. $\tau_0 = 0.4$, $\varepsilon = 0.1$, $\delta = 0.001$ and other parameters as in Figure 4.1.

We highlight again that in order to compare the models on a more applied level, we have to give a formal definition of a quantity represented by ρ in a Hamilton-Jacobian case. Even though establishing a rigorous mathematical link between the behavior observed in the individual-based model and the Hamilton-Jacobi equation is out of scope of this thesis, the obtained analytical results already give a flavor of how the analysis of the evolutionary dynamics can be simplified in the future.

Bibliography

***

[1] Achdou, Y., Barles, G., Ishii, H. and Litvinov, G-L. *Hamilton-Jacobi equations: approximations, numerical analysis and applications*, volume 2074 of *Lecture Notes in Mathematics*. Springer, Heidelberg; Fondazione C.I.M.E., Florence, 2013. Lecture Notes from the CIME Summer School held in Cetraro, August 29–September 3, 2011, Edited by Paola Loreti and Nicoletta Anna Tchou, Fondazione CIME/CIME Foundation Subseries.

[2] Alfaro, M. and Berestycki, H. and Raoul, G. The effect of climate shift on a species submitted to dispersion, evolution, growth, and nonlocal competition. *SIAM Journal on Mathematical Analysis*, 49(1):562–596, 2017.

[3] Alfaro, M. and Carles, R. Explicit solutions for replicator-mutator equations: extinction versus acceleration. *SIAM J. Appl. Math.*, 74(6):1919–1934, 2014.

[4] Alfaro, M. and Carles, R. Replicator-mutator equations with quadratic fitness. *Proc. Amer. Math. Soc.*, 145(12):5315–5327, 2017.

[5] Alfaro, M. and Veruete, M. Evolutionary branching via replicator-mutator equations. (to appear in J. Dynamics Differential Equations).

[6] Almeida, L., Bagnerini, P., Fabrini, G., Hughes, B.D. and Lorenzi, T. Evolution of cancer cell populations under cytotoxic therapy and treatment optimisation: insight from a phenotype-structured model. *ESAIM: Mathematical Modelling and Numerical Analysis (ESAIM: M2AN)*, In press, 1 2019.

[7] Anderson, R. and May, R. Population biology of infectious diseases: Part i. *Nature*, 280:361–7, 09 1979.

[8] Barles, G. Solutions de viscosité des équations de Hamilton-Jacobi. *Mathématiques & Applications*, vol 17, 1994.

[9] Barles, G., Biton, S. and Ley, O. A geometrical approach to the study of unbounded solutions of quasilinear parabolic equations. *Arch. Rational Mech. Anal*, vol. 162, :287–325, 2002.

[10] Barles, G., Mirrahimi, S. and Perthame, B. Concentration in Lotka-Volterra parabolic or integral equations: A general convergence result. *Methods & Applications of Analysis*, vol. 16, (No. 3):321–340, 2009.

[11] Baumdicker, F. and Pfaffelhuber, P. The infinitely many genes model with horizontal gene transfer. *Electron. J. Probab.*, 19:27 pp., 2014.

[12] Beardmore, RE., Pena-Miller, R., Gori, F. and Iredell, J. Antibiotic cycling and antibiotic mixing: which one best mitigates antibiotic resistance? *Molecular Biology and Evolution*, 2017-01-17 00:00:00.0.

[13] Berestycki, H. and Fang, J. Forced waves of the Fisher-KPP equation in a shifting environment. *Journal of Differential Equations*, 264(3):2157 – 2183, 2018.

[14] Berestycki, H. and Rossi, L. Reaction-diffusion equations for population dynamics with forced speed i - the case of the whole space, disc. *Discrete and Continuous Dynamical Systems*, 21, 05 2008.

[15] Berestycki, H. and Rossi, L. Reaction-diffusion equations for population dynamics with forced speed ii - cylindrical-type domains. *Discrete and Continuous Dynamical Systems - A*, 25(1078-0947):19, 2009.

[16] Berestycki, H., Diekmann, O., Nagelkerke, C. J. and Zegeling, P. A. Can a species keep pace with a shifting climate? *Bulletin of Mathematical Biology*, 71(2):399, Dec 2008.

[17] Berestycki, H., Nadin, G., Perthame, B. and Ryzhik, L. The non-local fisher–KPP equation: travelling waves and steady states. *Nonlinearity*, 22(12):2813–2844, oct 2009.

[18] Billiard, S. and Collet, P. and Ferrière, R. and Méléard, S. and Tran, V. Stochastic dynamics for adaptation and evolution of microorganisms. *arXiv preprint arXiv:1610.00983*, 2016.

[19] Billiard, S., Collet, P., Ferrière, R. and Méléard, S. and Tran, V. The effect of competition and horizontal trait inheritance on invasion, fixation, and polymorphism. *J. Theoret. Biol.*, 411:48–58, 2016.

[20] Billiard, S., Ferrière, R., Méléard, S. and Tran, V. Stochastic dynamics of adaptive trait and neutral marker driven by eco-evolutionary feedbacks. *J. Math. Biol.*, 71(5):1211–1242, 2015.

[21] Bolker and Pacala. Using moment equations to understand stochastically driven spatial pattern formation in ecological systems. *Theoretical population biology*, 52 3:179–97, 1997.

[22] Bouhours, J. and Lewis, M. A. Climate change and integrodifference equations in a stochastic environment. *Bulletin of Mathematical Biology*, 78(9):1866–1903, Sep 2016.

[23] Burger, R. and Lynch, M. Evolution and extinction in a changing environment: A quantitative-genetic analysis. *Evolution*, 49(1):151–163, 1995.

[24] Calsina, A. and Cuadrado, S. Small mutation rate and evolutionarily stable strategies in infinite dimensional adaptive dynamics. *J. Math. Biol.*, 48(2):135–159, 2004.

[25] Champagnat, N. and Ferrière, R. and Méléard S. From individual stochastic processes to macroscopic models in adaptive evolution. *Stochastic Models*, 24(sup1):2–44, 2008.

[26] Champagnat, N. and Lambert, A. Evolution of discrete populations and the canonical diffusion of adaptive dynamics. *Ann. Appl. Probab.*, 17(1):102–155, 2007.

[27] Champagnat, N., Ferrière, R., and Méléard, S. Individual-based probabilistic models of adaptive evolution and various scaling approximations. 59:75–113, 2008.

[28] Chevin, L-M., Lande, R. and Mace, G.M. Adaptation, plasticity, and extinction in a changing environment: Towards a predictive theory. 2010.

[29] Chevin, L-M., Visser, M.E. and Tufto, J. Estimating the variation, autocorrelation, and environmental sensitivity of phenotypic selection. *Evolution*, 69(9):2319–2332, 2015.

[30] Chisholm, RH. and Lorenzi, T. and Desvillettes, L. and Hughes, BD. Evolutionary dynamics of phenotype-structured populations: from individual-level mechanisms to population-level consequences. *Z. Angew. Math. Phys.*, 67(4):Art. 100, 34, 2016.

[31] Chisholm, RH. and Lorenzi, T. and Lorz, A. and Larsen, AK. and de Almeida, LN. and Escargueil, A., and Clairambault, J. Emergence of drug tolerance in cancer cell populations: An evolutionary outcome of selection, nongenetic instability, and stress-induced adaptation. *Cancer Research*, 75(6):930–939, March 2015.

[32] Crandall, M. G. and Lions, P. L. Two approximations of solutions of Hamilton-Jacobi equations. *Mathematics of Computation*, 43(167):1–19, 1984.

[33] Desvillettes, L., Jabin, P-E., Mischler, S. and Raoul, G. On selection dynamics for continuous structured populations. *Commun. Math. Sci.*, 6(3):729–747, 2008.

[34] Dieckmann, O., Jabin, P-E., Mischler, S., and Perthame, B. The dynamics of adaptation: An illuminating example and a Hamilton-Jacobi approach. *Theoretical Population Biology*, 67(4):257–271, 2005.

[35] Dieckmann, Ulf. and Law, R. The dynamical theory of coevolution: a derivation from stochastic ecological processes. *Journal of Mathematical Biology*, 34:579–612, 1996.

[36] Diekmann, O. *A beginner's guide to adaptive dynamics*, volume 63. Banach Center Publication, 2004.

[37] Doebeli, M. and Dieckmann, U. Evolutionary branching and sympatric speciation caused by different types of ecological interactions. *The American Naturalist*, 156(S4):S77–S101, 2000. PMID: 29592583.

[38] Evans, L.C. Periodic homogenisation of certain fully nonlinear partial differential equations. *Proceedings of the Royal Society of Edinburgh*, 120A(1):245–265, 1992.

[39] Evans, L.C. and Souganidis, P.E. A PDE approach to geometric optics for certain semilinear parabolic equations. *Indiana Univ. Math. J.*, 38(1):141–172, 1989.

[40] Ferrière, R. and Tran, V. Stochastic and deterministic models for age-structured populations with genetically variable traits. In *CANUM 2008*, volume 27 of *ESAIM Proc.*, pages 289–310. EDP Sci., Les Ulis, 2009.

[41] Figueroa Iglesias, S. and Mirrahimi, S. Long time evolutionary dynamics of phenotypically structured populations in time-periodic environments. *SIAM Journal on Mathematical Analysis*, 50(5):5537–5568, 2018.

[42] Fleming, WH. Equilibrium distributions of continuous polygenic traits. *SIAM Journal on Applied Mathematics*, 36(1):148–168, 1979.

[43] Fournier, N. and Méléard, S. A microscopic probabilistic description of a locally regulated population and macroscopic approximations. *Ann. Appl. Probab.*, 14(4):1880–1919, 2004.

[44] Freidlin, M. Limit theorems for large deviations and reaction-diffusion equations. *Ann. Probab.*, 13(3):639–675, 1985.

[45] Gandon, S. and Mirrahimi, S. A Hamilton-Jacobi method to describe the evolutionary equilibria in heterogeneous environments and with non-vanishing effects of mutations. *Comptes Rendus Mathematique*, 355(2):155 – 160, 2017.

[46] Genieys, S. and Volpert, V. and Auger, P. Pattern and waves for a model in population dynamics with nonlocal consumption of resources. *Mathematical Modelling of Natural Phenomena*, 1(1):63–80, 2006.

[47] Gil, M-E. and Hamel, F. and Martin, G. and Roques, L. Mathematical properties of a class of integro-differential models from population genetics. *SIAM Journal on Applied Mathematics*, 77:1536–1561, 01 2017.

[48] Gourley, S. Travelling front solutions of a nonlocal fisher equation. *Journal of mathematical biology*, 41:272–284, 10 2000.

[49] Helffer, B. Introduction to semi-classical methods for the Schrödinger operator with magnetic field. *Séminaires et Congrés*, 05 2004.

[50] Helffer, B. and Sjöstrand, J. Multiple wells in the semiclassical limit. I. *Comm. Partial Differential Equations*, 9(4):337–408, 1984.

[51] Helffer, B. and Sjöstrand, J. Multiple wells in the semiclassical limit. III. Interaction through nonresonant wells. *Math. Nachr.*, 124:263–313, 1985.

[52] Henry, LM., Peccoud J., Simon JC., Hadfield JD., Maiden MJ., Ferrari J. and Godfray HC. Horizontally transmitted symbionts and host colonization of ecological niches. *Current biology : CB*, 23, 08 2013.

[53] Hess, P. *Periodic-Parabolic Boundary Value Problems and Positivity*. Series 247. Longman Scientific & Technical, Harlow, Essex, UK, 1991.

[54] Hofbauer, J. and Sigmund, K. *The theory of evolution and dynamical systems*, volume 7 of *London Mathematical Society Student Texts*. Cambridge University Press, Cambridge, 1988. Mathematical aspects of selection, Translated from the German.

[55] Húska, J. Harnack inequality and exponential separation for oblique derivative problems on Lipschitz domains. *J. Differential Equations*, vol. 226, :541–557, 2006.

[56] Húska, J. and Polácik, P. Exponential separation and principal Floquet bundles for linear parabolic equations on $\mathbb{R}^N$. 2008.

[57] Jenouvrier, S. and Visser, M. Climate change, phenological shifts, eco-evolutionary responses and population viability: Toward a unifying predictive approach. *International journal of biometeorology*, 55:905–19, 06 2011.

[58] Jin, S. Efficient asymptotic-preserving (AP) schemes for some multiscale kinetic equations. *SIAM J. Sci. Comput.*, 21(2):441–454, 1999.

[59] Kamimura, K., Suda, T., Zhang, G. and Liu, D. Advances in gene delivery systems. *Pharmaceut Med.*, 25(5):293–306, 2011.

[60] Ketola, T., et al. Fluctuating temperature leads to evolution of thermal generalism and preadaptation to novel environments". *Evolution*, 2013.

[61] Kimura, M. A stochastic model concerning the maintenance of genetic variability in quantitative characters. *Proceedings of the National Academy of Sciences*, 54(3):731–736, 1965.

[62] Kimura, M. and Crow, JF. The theory of genetics loads. *Proc. XI Int. Congr. Genetics*, 2:495–505, 1964.

[63] Kisdi, A. Evolutionary branching under asymmetric competition. *Journal of Theoretical Biology*, 197(2):149 – 162, 1999.

[64] Klar, A. An asymptotic-induced scheme for nonstationary transport equations in the diffusive limit. *SIAM J. Numer. Anal.*, 35(3):1073–1094, 1998.

[65] Klar, A. An asymptotic preserving numerical scheme for kinetic equations in the low mach number limit. *SIAM J. Numer. Anal.*, 36(5):1507–1527, 1999.

[66] Kopp, M. and Matuszewski, S. Rapid evolution of quantitative traits: theoretical perspectives. *Evolutionary Applications*, 7(1):169–191, 2014.

[67] Kussell, E., et al. Bacterial persistence: A model of survival in changing environments. *Genetics Society of America*, vol. 169, :1807–1814, 2005.

[68] Lande, R. The maintenance of genetic variability by mutation in a polygenic character with linked loci. *Genetical Research*, 26(3):221–235, 1975.

[69] Lande, R. and Shannon S. The role of genetic variation in adaptation and population persistence in a changing environment. *Evolution*, vol. 50, (No. 1):434–437, 1996.

[70] Law, R. and Dieckmann, U. . Moment approximations of individual-based models. Iiasa interim report, IIASA, Laxenburg, Austria, December 1999.

[71] Lili, L-N., Britton, N-F. and Feil, E-J. The persistence of parasitic plasmids. *Genetics*, 177(1):399–405, 2007.

[72] Lions, P.L. *Generalized solutions of Hamilton-Jacobi equations*, volume 69 of *Research notes in mathematics*. Pitman Advanced Publishing Program, Boston, 1982.

[73] Lopez, R.M., Morin, B.R. and Suslov, S. Logistic models with time-dependent coefficients and some of their applications. arXiv.org>q-bio>arXiv:1008.2534v1, 2010.

[74] Lorenzi, T. and Chisholmm R.H. and Desvillettes, L. and Hughes, B.D. Dissecting the dynamics of epigenetic changes in phenotype-structured populations exposed to fluctuating environments. *Journal of Theoretical Biology, Elsevier*, 386:166–176, 2015.

[75] Lorz, A. and Lorenzi, T.and Hochberg, ME. and Clairambault, J. and Perthame, B. Populational adaptive evolution, chemotherapeutic resistance and multiple anti-cancer therapies. *ESAIM: Mathematical Modelling and Numerical Analysis - Modélisation Mathématique et Analyse Numérique*, 47(2):377–399, 2013.

[76] Lorz, A., Mirrahimi, S. and Perthame, B. Dirac mass dynamics in multidimensional non local parabolic equations. *Commun. Partial Differ. Equ.*, vol. 36, (No. 6):1071–1098, 2011.

[77] M. Stewart, F and Levin, B. The population biology of bacterial plasmids: A priori conditions for the existence of conjugationally transmitted factors. *Genetics*, 87:209–28, 11 1977.

[78] Magal, P. and Webb, G. F. Mutation, selection, and recombination in a model of phenotype evolution". *Discrete Contin. Dynam. Systems*, 6(1):221–236, 2000.

[79] Méléard, S. and Tran, V. Trait substitution sequence process and canonical equation for age-structured populations. *Journal of Mathematical Biology*, 58(6):881, Jul 2008.

[80] Mirrahimi, S. *Phénomènes de concentration dans certaines EDPs issues de la biologie.* PhD thesis, Université Pierre et Marie Curie, http://www.math.univ-toulouse.fr/ smirrahi/manuscrit.pdf., 2011.

[81] Mirrahimi, S. A Hamilton-Jacobi approach to characterize the evolutionary equilibria in heterogeneous environments. *Mathematical Models and Methods in Applied Sciences*, 27(13):2425–2460, 2017.

[82] Mirrahimi, S. and Roquejoffre, J. A class of Hamilton-Jacobi equations with constraint: uniqueness and constructive approach. *J. Differential Equations*, 260(5):4717–4738, 2016.

[83] Mirrahimi, S., Perthame, B. and Souganidis, P. Time fluctuations in a population model of adaptive dynamics. *Ann. I.H.Poincaré*, vol. 32, (No. 1):41–58, 2015.

[84] Nadin, G. The principal eigenvalue of a space–time periodic parabolic operator. *Annali di Matematica Pura ed Applicata*, 188(2):269–295, Apr 2009.

[85] Nadin, G. Existence and uniqueness of the solution of a space-time periodic reaction-diffusion equation. *Journal of Differential Equations*, 249(6):1288 – 1304, 2010.

[86] Novozhilov, A-S. and Koonin, E-V. and Karev, G-P. Mathematical Modeling of Evolution of Horizontally Transferred Genes. *Molecular Biology and Evolution*, 22(8):1721–1732, 05 2005.

[87] Parmesan, C. Ecological and evolutionary responses to recent climate change. *Annual Review of Ecology, Evolution, and Systematics*, 37:637–669, 2006.

[88] Perthame, B. and Barles, G. Dirac concentrations in Lotka-Volterra parabolic PDEs. *Indiana Univ. Math. J.*, vol. 7, :3275–3301, 2008.

[89] Poláčik, P. Symmetry properties of positive solutions of parabolic equations on $\mathbb{R}^N$: II. Entire solutions. *Communications in Partial Differential Equations*, 31:11,:1615–1638, 2006.

[90] Raoul, G . *Etude qualitative et numérique d'équations aux dérivées partielles issues des sciences de la nature.* PhD thesis, ENS Cachan, 2009.

[91] Salignon, J., Richard, M., Fulcrand, E., Duplus-Bottin, H. and Yvert, G. Genomics of cellular proliferation in periodic environmental fluctuations. *Molecular Systems Biology*, 14(3), 2018.

[92] Smith, J.M. *Evolution and the Theory of Games.* Cambridge University Press, 1982.